Lecture Notes

Signals, Systems, and Transform Methods

Roland Hostettler

Department of Electrical Engineering
Uppsala University, Sweden

October 22, 2021

Contents

Preface

These lecture notes are the main text for the course Signals and Transforms at Uppsala University. Writing the lecture notes started out with the aim of creating a text that is entirely tailored to the audience of the course; third-year information technology students. The manuscript is inspired by several lecture notes and text books, which individually did not meet the goal of providing a concise text that highlights the important concepts without going into too many theoretical details. The main sources of inspiration are the lecture notes for the course Embedded Signal Processing Systems by Steffi Knorn (Knorn, 2019), which in turn is inspired by Mandal and Asif (2007), and the textbooks by von Grünigen (2002) (in particular the parts on discrete Fourier transform and digital filtering) and McClellan et al. (2003) (in particular the parts on sines and the sine-in, sine-out principles).

These lecture notes are updated every year to fix errors and address other issues. Hence, I would like to thank all my students and colleagues for providing feedback and comments. In particular, I would like to thank (in alphabetical order) Abbas Araghavi, Johan Lövgren, Christoffer Nyberg, David Svedberg, Matlida Tamm, and Fredrik Yngve for their valuable input.

Roland Hostettler

Chapter 1

Introduction

1.1 Background

The theory of signals and systems is fundamental in many everyday technologies. For example, applications such as (wireless) communication systems, media encoding in television and streaming services, or driver assistance systems in cars heavily rely on the theory of signals and dynamic systems and make use of transform methods in their inner workings.

The common denominator of all of these are that we can think of them in an abstract way: The process of interest (e.g., the communication system) takes a set of input signals (e.g., the data to be transmit), processes these signals according to some rules, and outputs other signals that carry a different type of information (e.g., a radio signal to be transmit through the air). We can thus think of a system as a black box with input and output signals that performs some operations (Figure 1.1). The operations are of course very specific for the particular application, but it turns out these can be described using the same kind of framework of *signals and systems*. Naturally, a system can often be broken down into smaller components to reveal its inner working. This can again often by done by using the same kind of framework, which thus provides several layers of abstraction down to the component level.

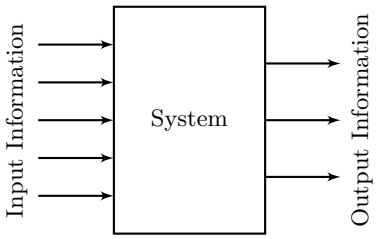

Figure 1.1. A general black box view of technical systems that process incoming information (input signals) and output another type of processed information (output signals).

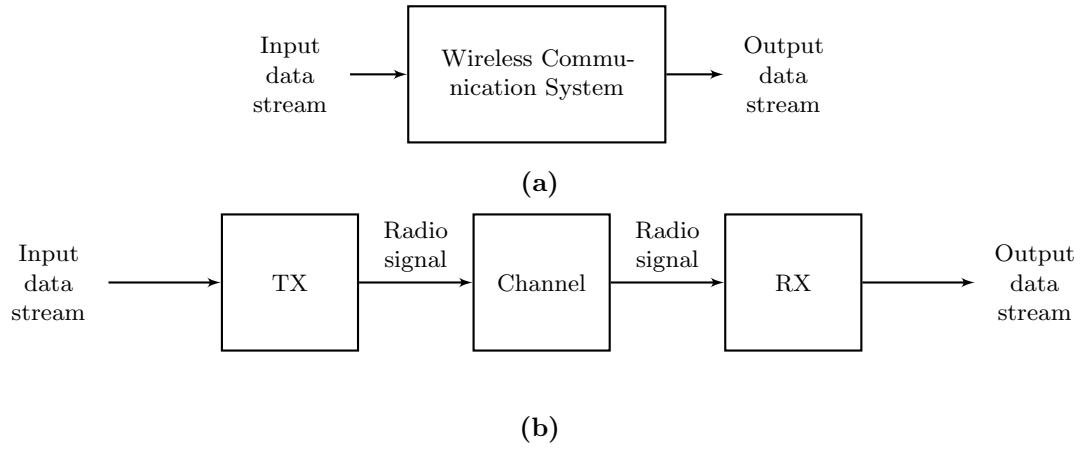

Figure 1.2. (a) High-level view of a wireless communication system with a data stream as the input and (hopefully) the same data stream as the output. (b) Intermediate-level view of the same system with the three subsystems (transmitter, channel, and receiver).

Example 1.1: Wireless communication system

The aim of a wireless communication system is to transmit some data from a transmitter to a receiver. The data may, for example, be a stream of digital data such as a network signal in WiFi but it could also be a signal such as speech (e.g., in a walkie talkie). On a high level, the wireless communication system should thus aim for the input and output signal to be the same such that no data is lost (Figure 1.2a). Breaking down the system, however, we can identify at least three subsystems (Figure 1.2b):

- The transmitter (TX),
- the communication channel, and
- the receiver (RX).

Naturally, these three subsystems can be decomposed further until the full architecture becomes visible.

In the context of signals and systems, *transform methods* are a set of tools to a) simplify the mathematics used to describe the input-output relationships of systems, and b) analyze the properties of signals and dynamic systems and predict their behavior. Transform methods also play an important role in, for example, data compression (e.g., audio, image, and video compression), pattern recognition, or representation theory. These topics are, however, not discussed in this course.

1.2 Signals

A signal is understood as a quantity that carries some kind of information. The quantity may be physical or virtual and typical examples of signals are human speech, WiFi

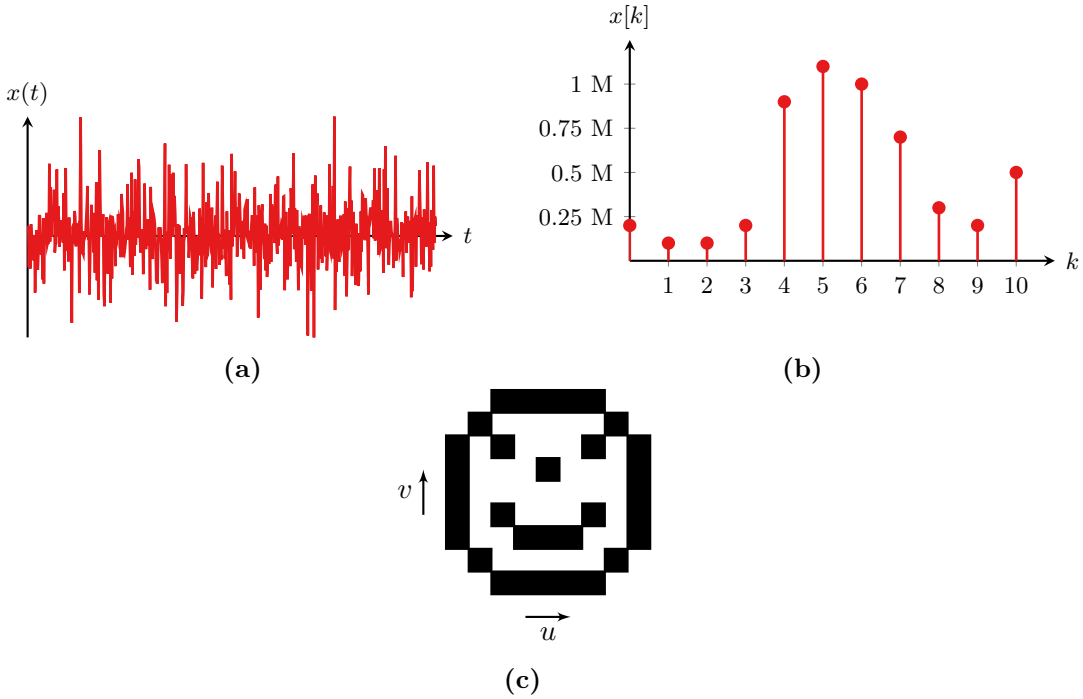

Figure 1.3. Examples of typical signals: (a) An audio signal, (b) the number of hits for a particular website as a function of the day, and (c) a digital black-and-white bitmap picture.

signals, images, the number of clicks in a search engine, or streaming music. Formally, a signal is defined as a function of a free variable. The free variable is typically the time t (or a time index k), in which case a signal is written as

$$x(t),$$

where $x(t)$ is the signal and t free variables[1] For an image, the signal is a function of two free variables and may take on the form

$$x(u, v),$$

where $x(u, v)$ is the signal, and u and v are the image coordinates. A video signal is a function of three free variables: The image coordinates u and v as well as time t. Thus, a video signal can be described as

$$x(u, v, t).$$

We are mainly concerned with time signals, that is signals with one free variable (time). However, the theory covered can be extended to other, more complex signals, but this is beyond the scope of this course. A few signal examples are shown in Figure 1.3.

Signals can furthermore be classified according to their properties and the most elementary signal classes follow below.

[1]Note that this is in contrast to mathematics, where often the variables x and y are used as free variables and $f(\cdot)$, $g(\cdot)$, or $h(\cdot)$ for functions.

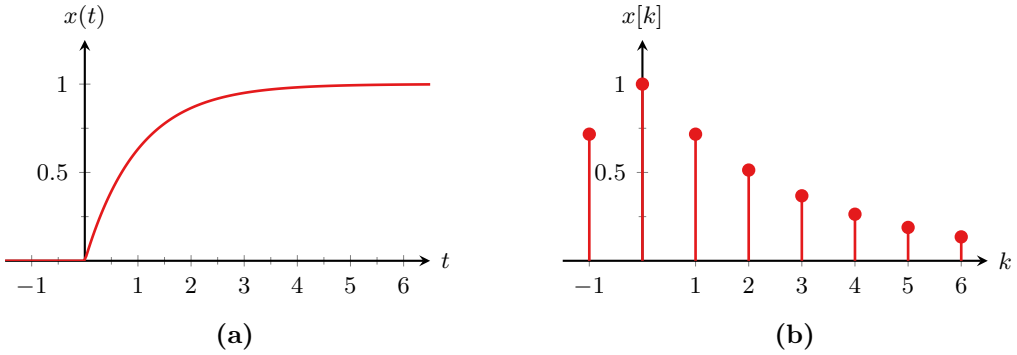

Figure 1.4. Illustration of a (a) continuous time signal and (b) discrete time signal.

Continuous and discrete time signals. In general, we can distinguish between *continuous time* and *discrete time* signals. Continuous time signals are signals that are defined for all times t, where t is a continuous variable (formally, $t \in \mathbb{R}$), that is, defined for all real numbers such as $t = 0$, $t = \frac{3}{2}$, or $t = \pi$. Such a signal is denoted

$$x(t).$$

Figure 1.4a illustrates a continuous time signal.

A discrete time signal on the other hand is only defined for *discrete*, integer time instants $k = -2, -1, 0, 1, 2, \ldots$ (formally, $k \in \mathbb{Z}$). A discrete time signal is denoted as

$$x[k],$$

where the square brackets replace the ordinary parentheses to signify that the signal is a discrete time signal (Figure 1.4b). Note that when illustrating a discrete time signal in a plot, the signal is undefined in-between any two points k and $k+1$ in time. Furthermore, the signal is plotted as a "stem" or "comb" plot with teeth at the discrete time indexes k and a knot at the signal value.

A discrete time signal is often obtained by *sampling* a continuous time signal. Sampling is the process of regularly measuring the value of a continuous time signal and storing the value in a digital computer. Formally, a sampled signal can be defined as

$$x[k] \triangleq x(kT_s),$$

where T_s is the *sampling time*. This is to be interpreted as follows. The discrete time signal $x[k]$ at time instant k is equal to the continuous time signal $x(t)$ at time $t = kT_s$. The sampling time T_s determines how long time that passes between two consecutive measurements of $x(t)$. An example of a continuous time signal and its sampled version is shown in Figure 1.5a. Sampling (and its counterpart operation reconstruction) is the link between the continuous and discrete time worlds and is discussed in detail in Chapter 6.

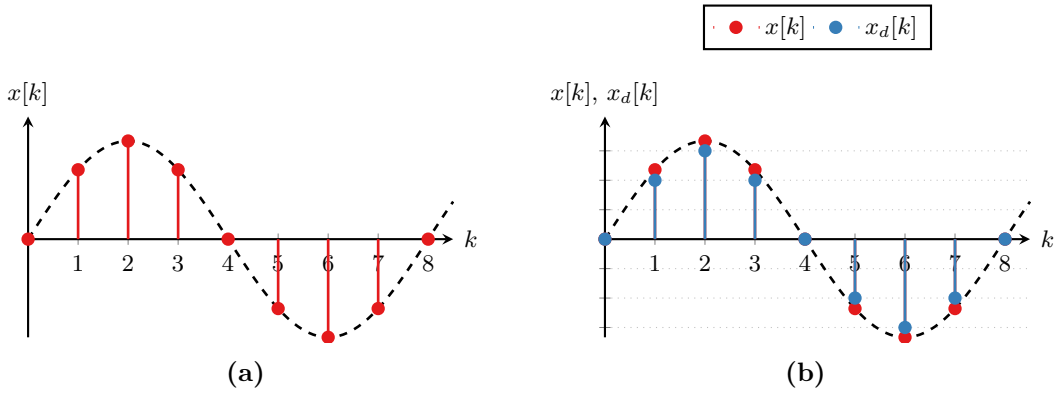

Figure 1.5. Illustration of the sampling process. (a) Sampling picks the signal values at $x(kT_s)$, which yields the discrete time signal $x[k]$. (b) Sampling picks the signal values at $x(kT_s)$, followed by quantization (mapping to a finite set of y-values indicated by dotted grid lines), which yields the digital signal $x_d[k]$.

Analog and digital signals. An analog signal is characterized by not only being a continuous time signal, but also having a continuous, unbounded range of signal values $y(t)$. That means, the amplitude of an analog signal can take on any value (i.e., $y(t) \in \mathbb{R}$ for real-valued signals). An analog signal may also be bounded, for example such that $|y(t)| \leq M_y$ for some constant M_y, but such a signal is still analog as it can take on any arbitrary value in the interval between $-M_y$ and M_y.

A digital signal on the other hand is a discrete time signal that only can take on a limited range of discrete signal amplitudes $y[k]$. All signals processed by a digital computer are digital signals since computers do not have infinite numerical precision. For example, the bitmap in Figure 1.3c is a digital signal with discrete independent variables u and v (the image coordinates) as well as the two signal levels "black" and "white".

Sampling turns a continuous time signal into a discrete time signal. In order for the discrete time signal to become a digital signal, it also has to be *quantized*. Quantization is the process of assigning a specific level of a range of different *quantization levels* to each analog value as illustrated in Figure 1.5b. Since infinitely many continuous signal levels are mapped to one and the same quantization level, quantization is an irreversible operation that causes data loss. Hence, it is important that there are sufficiently many quantization levels available for the signal that is being digitized. Sampling and quantization often go hand in hand when converting analog signals to digital ones in an *analog to digital converter* (A/D converter or ADC). ADCs are an important building block in digital signal processing systems, described in more detail in Section 1.5.

Deterministic and stochastic signals. A deterministic signal can be described analytically for all times t (or k). Conversely, a signal that can not be described analytically is called a *stochastic signal* and stochastic signals are typically characterized by their statistical properties such as their mean and covariance functions. Deterministic signals can often be expressed as mathematical formulas or as graphs. In engineering

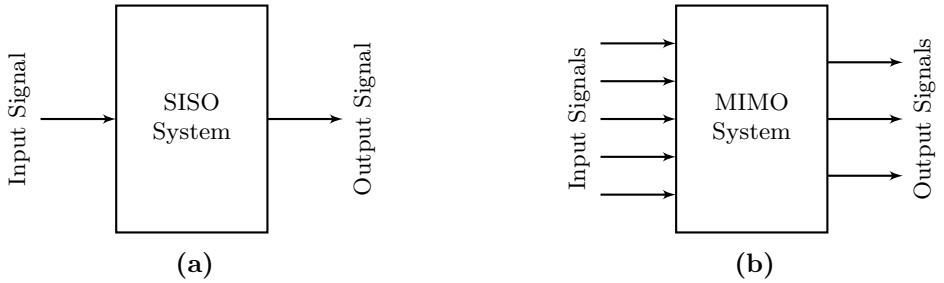

Figure 1.6. Illustration of a single input single output system (SISO) and a multiple input multiple output (MIMO) system as *blockdiagrams*. The systems are represented as blocks, whereas the input and output signals are represented by arrows into (input signals) and out of (output signals) the block.

most signals are stochastic signals to some degree as they cannot be fully and accurately described. However, often they are modeled as a sum of a well defined deterministic signal and a stochastic signal. In some cases the additional stochastic signal (often referred to as noise) can be neglected and the signal can be approximated by a deterministic signal. In this course, we assume the latter case and do not discuss stochastic signals.

1.3 Systems

A system is a physical, technical, biological, or social process that in some way affects a signal. In particular, a system typically has one or more input signals and one or more output signals. If the system has exactly one input and output signal, it is called a single input single output (SISO) system. Conversely, if the system has multiple inputs and multiple outputs, it is called a multiple input multiple output (MIMO) system (Figure 1.6). Here, we consider SISO systems where the input signal typically is denoted as $x(t)$ (or $x[k]$ for discrete time systems) and the output signal is denoted $y(t)$ (or $y[k]$).

Formally, a system is defined as a mapping of an input signal to an output signal as

$$x(t) \mapsto y(t)$$

for continuous time systems and

$$x[k] \mapsto y[k]$$

for discrete time systems. The notation $x(t) \mapsto y(t)$ is to be read as "The input $x(t)$ produces the output $y(t)$". Depending on how this mapping affects the input, the system can be classified according to the following four elementary classes (Figure 1.7):

1. Linear, time-invariant (LTI) systems,
2. linear, time-varying systems
3. nonlinear, time-invariant systems, and
4. nonlinear, time-varying systems.

In this course, we are concerned with the first class of systems, LTI systems. For a system to be linear, the *superposition principle* must hold: If an input $x_1(t)$ gives rise to

Linear, time-invariant	Linear, time-varying
Nonlinear, time-invariant	Nonlinear, time-varying

Figure 1.7. Illustration of the four elementary system classes.

the output $y_1(t)$ and if $x_2(t)$ gives rise to the output $y_2(t)$, then, for a system to be linear, their scaled superposition must give rise to the scaled superposition of the outputs, that is,

$$\alpha x_1(t) + \beta x_2(t) \mapsto \alpha y_1(t) + \beta y_2(t).$$

Example 1.2: Linearity of systems

Consider the system where the output is defined as a scaled version of the input $x(t)$ plus a time-delayed version of it $x(t-T)$, that is, the input-output relationship can be written as

$$y(t) = c_0 x(t) + c_1 x(t-T).$$

Applying the input $x_1(t)$ yields the output

$$y_1(t) = c_0 x_1(t) + c_1 x_1(t-T)$$

and applying $x_2(t)$ yields

$$y_2(t) = c_0 x_2(t) + c_1 x_2(t-T).$$

Applying the input $x_3(t) = \alpha x_1(t) + \beta x_2(t)$ yields

$$\begin{aligned} y_3(t) &= c_0 x_3(t) + c_1 x_3(t-T) \\ &= c_0(\alpha x_1(t) + \beta x_2(t)) + c_1(\alpha x_1(t-T) + \beta x_2(t-T)) \\ &= \alpha c_0 x_1(t) + \beta c_0 x_2(t) + \alpha c_1 x_1(t-T) + \beta c_1 x_2(t-T) \\ &= \alpha c_0 x_1(t) + \alpha c_1 x_1(t-T) + \beta c_0 x_2(t) + \beta c_1 x_2(t-T) \\ &= \alpha \left[c_0 x_1(t) + c_1 x_1(t-T)\right] + \beta \left[c_0 x_2(t) + c_1 x_2(t-T)\right] \\ &= \alpha y_1(t) + \beta y_2(t). \end{aligned}$$

Hence, the system must be linear, since the superposition principle holds.

Time invariance refers to the property of how a system responds to the same input at different times. If the system responds the same way, no matter when the input is

applied, the system is called time-invariant. In other words, if a specific signal $x_1(t)$ gives $y_1(t)$, then the system is time-invariant if and only if the time-shifted version $x_1(t - \Delta t)$ gives the time-shifted output $y_1(t - \Delta t)$. This leads to the definition of continuous time LTI systems in Definition 1.1.

Definition 1.1: Continuous time linear, time-invariant system

A continuous time system is linear and time-invariant if it fulfills the following two properties:

1. *Linearity:* If the input $x_1(t)$ gives rise to the output $y_1(t)$,

$$x_1(t) \mapsto y_1(t),$$

and the input $x_2(t)$ gives rise to the output $y_2(t)$,

$$x_2(t) \mapsto y_2(t),$$

then a system is called linear if and only if

$$\alpha x_1(t) + \beta x_2(t) \mapsto \alpha y_1(t) + \beta y_2(t)$$

for any complex constants α and β.

2. *Time invariance:* If the input $x_1(t)$ gives rise to the output $y_1(t)$,

$$x_1(t) \mapsto y_1(t),$$

then a system is called time-invariant if and only if

$$x_1(t - \Delta t) \mapsto y_1(t - \Delta t)$$

for any real Δt.

Example 1.3 illustrates the time-invariance property for the linear system in Example 1.2.

Example 1.3: Time-invariance of systems

Consider again the system from Example 1.2 with input-output relationship

$$y(t) = c_0 x(t) + c_1 x(t - T).$$

Applying the signal $x_1(t)$ yields

$$y_1(t) = c_0 x_1(t) + c_1 x_1(t - T).$$

Applying the delayed signal $x_2(t) = x_1(t - \Delta t)$ yields

$$\begin{aligned} y_2(t) &= c_0 x_1(t - \Delta t) + c_1 x_1(t - \Delta t - T) \\ &= y_1(t - \Delta t), \end{aligned}$$

which shows that the system is time-invariant.
Hence, the system defined by the input-output relationship above is a continuous time LTI system.

The same elementary system classification (Figure 1.7) applies for discrete time systems. Hence, the definition of a discrete time LTI system is analog to the one for continuous time LTI systems and is given in Definition 1.2 below.

Definition 1.2: Discrete time linear, time-invariant system

A discrete time system is linear and time-invariant if it fulfills the following two conditions:

1. *Linearity:* If the input $x_1[k]$ gives rise to the output $y_1[k]$,

   $$x_1[k] \mapsto y_1[k],$$

   and the input $x_2(t)$ gives rise to the output $y_2(t)$,

   $$x_2[k] \mapsto y_2[k],$$

   then a system is called linear if and only if

   $$\alpha x_1[k] + \beta x_2[k] \mapsto \alpha y_1[k] + \beta y_2[k]$$

   for any complex constants α and β.

2. *Time invariance:* If the input $x_1[k]$ gives rise to the output $y_1[k]$,

   $$x_1[k] \mapsto y_1[k],$$

   then a system is called time-invariant if and only if

   $$x_1[k - k_0] \mapsto y_1[k - k_0]$$

   for any integer k_0.

Another important property of a system is whether it is a static or dynamic system. In a static system, the current output of the system only depends on the current input. On the other hand, a dynamic system depends on both the current input as well as past and possibly future inputs and outputs. Furthermore, if a dynamic system only depends

on past and current inputs, it is called *causal*. In practice, all systems must be causal as it is not possible for a system to look into the future and anticipate future inputs or outputs.

A causal system is a system that only depends on the current input $x(t)$ ($x[k]$) as well as past inputs $x(t-T_1)$ ($x[k-k_1]$) for $T_1 \geq 0$ ($k_1 \geq 0$) and past outputs $y(t-T_2)$ ($x[k-k_2]$) for $T_2 > 0$ ($k_2 > 0$), but not any future inputs or outputs.

1.4 Transform Methods

Transform methods can be viewed as a set of tools that simplify the analysis of LTI systems and help us to gain insight in the composition of signals as well as how LTI systems affect different signals. Formally, a transform method can be defined as an operation $\mathcal{T}\{\cdot\}$ that transforms a signal $x(t)$ into a *transform domain* or *image domain* $X(\varsigma)$. Here, ς is the free variable in the transform domain (the ς-domain) and the transformation can be written as

$$X(\varsigma) = \mathcal{T}\{x(t)\}.$$

The pair $\{x(t), X(\varsigma)\}$ is called a transform pair, which we denote as

$$x(t) \circ\!\!-\!\!\bullet\, X(\varsigma).$$

Note that sometimes, transform pairs are also denoted using arrows such as "$\Leftrightarrow$" or "$\leftrightarrow$".

The inverse transform that brings a signal's transform $X(\varsigma)$ back from the transform domain to the time domain is denoted as $\mathcal{T}^{-1}\{\cdot\}$ and it must hold that

$$x(t) = \mathcal{T}^{-1}\{X(\varsigma)\}.$$

Note that if there is no unique inverse transform, the transform is irreversible.

In this course, we are going to discuss the Fourier transforms, the Laplace transform, and the z-transform. As it will be shown, these transform methods are very closely related to each other and very useful when working with LTI systems.

1.5 Digital Signal Processing

Nowadays, modern signal processing systems are implemented as much as possible in digital computers rather than analog electronics. This has several advantages such as less hardware that can fail or much more flexibility when developing and implementing the signal processing algorithms. Furthermore, with emerging technologies such as cloud and edge computing, or internet of things, the added flexibility also allows for remotely improving signal processing systems by over the air updates. The trade-offs are, of course, the vulnerability of software bugs and, in the case of connected devices, the risk of cyberattacks.

Thus, in a modern signal processing chain, signals are sampled as early as possible, processed in a digital computer, and reconstructed as late as possible. A block diagram of a typical digital signal processing system is shown in Figure 1.8. Typically, there is

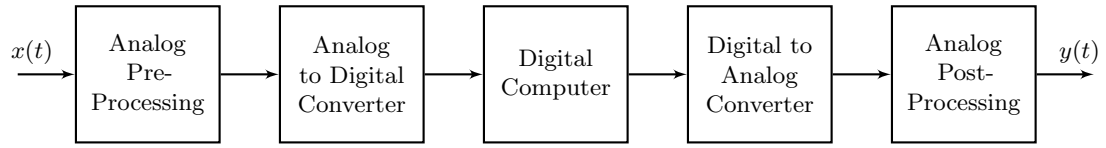

Figure 1.8. Block diagram of a typical digital signal processing architecture.

at least some analog pre-processing required. This may include signal amplification or band limitation and this is implemented using analog electronics. Then, the signal is converted from an analog signal to a digital one using an analog to digital converter (ADC or A/D converter). This involves sampling the signal as well as quantizing it to a finite number of quantization levels. The signal sample is then loaded from the ADC's registers into the digital computer, where the desired operations are performed on the signal. Once the sample is processed, the result is sent to the digital to analog converter (DAC or D/A converter), where a continuous-time output signal is reconstructed. The analog post-processing again includes operations such as amplification (e.g., in a radio frequency front-end) and band-limitation. The sampling-processing-reconstruction steps are typically executed on a periodic schedule with sampling time T_s.

Naturally, the key components in a digital signal processing system are the ADC, the digital computer itself, and the DAC. The theoretical properties as well as the function of the ADC and DAC are discussed in Chapter 6. As for the digital computer, this may be a general purpose computer such as a desktop computer (e.g., for streaming services), a virtual machine in the cloud, an edge computing device, or a tailored application-specific processor. In embedded systems, the digital computer is often a digital signal processor, which is a microprocessor system specifically for signal processing applications. In addition to general purpose computing and interfacing capabilities, these digital signal processors also come with special features such as multiply-and-accumulate units that perform typical signal processing tasks within a single processor cycle.

Chapter 2

Continuous Time Signals and Systems

2.1 Continuous Time Signals

In this section, elementary signals as well as some important signal properties are introduced. While signals can never entirely be described by these theoretical signal types, they will help us analyze and construct signal processing systems. Hence, good understanding of the signals and their properties is crucial.

2.1.1 Sine and Cosine Signals

Sinusoidal signals, that is, sine and cosine signals, play a key role in the analysis of dynamic systems. Hence, it is important to gain perfect understanding of their properties and parameters. Recall that the sine and cosine functions are trigonometric functions of some angle α, that is, $x = \sin(\alpha)$ or $x = \cos(\alpha)$ (Figure 2.1a). Furthermore, we can also think of $\sin(\alpha)$ and $\cos(\alpha)$ as the sides adjacent and opposite to the angle α in a right triangle on the unit circle as shown in Figure 2.1b.

If the angle α is made a linear function of time such that $\alpha = \omega_0 t + \varphi$, the output of the sine and cosine functions become a time-varying quantity, that is, a signal $x(t)$. In particular, the angle is then a function of the *angular frequency* ω_0 in radians per second (rad/s) of the sine (cosine) signal and a phase shift φ in radians (rad). Furthermore, the functions may be scaled in amplitude (i.e., have an amplitude or "height" different from 1). This leads to the following expressions for the sine and cosine signals:

$$x(t) = A\sin(\omega_0 t + \varphi) \tag{2.1}$$

and

$$x(t) = A\cos(\omega_0 t + \varphi). \tag{2.2}$$

The sine and cosine signals may also be expressed in terms of their *natural frequency* f_0 in Herz (Hz) or the *fundamental period* T_0 in seconds (s) instead. In this case, the signals are

$$x(t) = A\sin(2\pi f_0 + \varphi) = A\sin\left(\frac{2\pi}{T_0}t + \varphi\right) \tag{2.3}$$

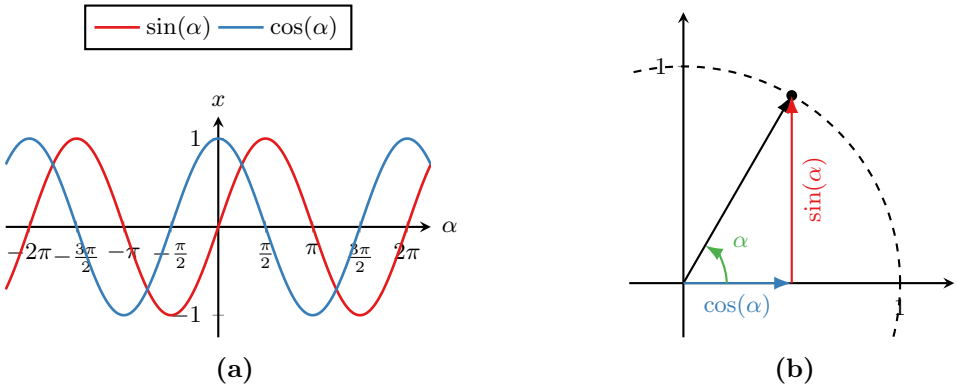

Figure 2.1. Illustration of the trigonometric functions sine and cosine for the angle α. (a) The functions as a function of the angle α and (b) the functions as the adjacent and opposite sides of a right triangle.

and

$$x(t) = A\cos(2\pi f_0 + \varphi) = A\cos\left(\frac{2\pi}{T_0}t + \varphi\right), \tag{2.4}$$

and the relationship between the different parametrizations is

$$\omega_0 = 2\pi f_0 = \frac{2\pi}{T_0}.$$

Finally, the phase shift may also be expressed in terms of a time delay Δt in s instead such that

$$\sin(\omega_0 t - \varphi) = \sin(\omega_0(t - \Delta t)),$$

or, equivalently,

$$\omega_0 \Delta t = \varphi.$$

Figure 2.2a shows an example of the sine and cosine signals with period T_0, amplitude A, and delay Δt. Note that the x-axis is now a time-axis as compared to Figure 2.1a, where the x-axis is the angle α. Figure 2.2b again shows the interpretation of the sine and cosine signals as the adjacent and opposite sides of a right triangle. However, in this case, the angle is not α but the time-varying quantity $\omega_0 t$. As the time t increases, the angle $\omega_0 t$ increases (linearly), which corresponds to the vector rotating counter clockwise along the circle of radius A. After $t = T_0$, we see that $\omega_0 t = 2\pi$, which corresponds to one full rotation.

This helps to more easily understand all the different representations encountered above: Even though they are fully equivalent, they do convey slightly different information.

- The angular frequency ω_0 describes the total angle rotated in one second,
- the natural frequency f_0 describes how many cycles (or full 2π rotations) occur per second, and

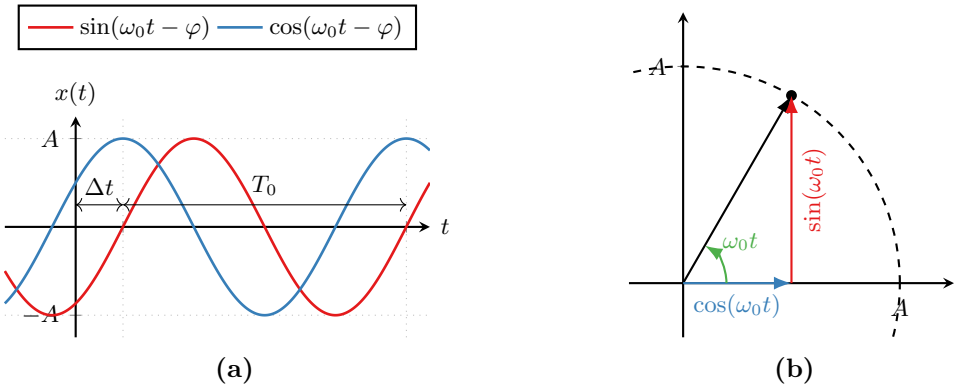

(a) (b)

Figure 2.2. Illustration of the sine and cosine signals. (a) The signals as a function of time and (b) the signals as the adjacent and opposite sides of a right triangle whose angle increases linearly with time.

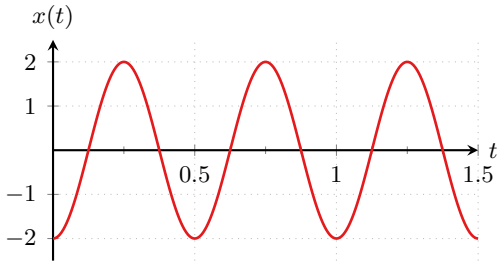

Figure 2.3. Example of a sine signal with $A = 2$, $T_0 = 0.5\,\text{s}$, and $\varphi = \frac{\pi}{2}\,\text{rad}$.

- the period T_0 describes the duration of one single cycle (or 2π rotations).

Example 2.1 illustrates how to go between the different interpretations.

Example 2.1: Representations of sine and cosine signals

Consider the sine signal shown in Figure 2.3. Based on the peaks, it can be seen that the amplitude must be $A = 2$. Furthermore, looking the first zero-crossing from negative to positive occurs at $t = 0.125\,\text{s}$ and thus, the time delay must be $\Delta t = 0.125\,\text{s}$. The second zero crossing from negative to positive (i.e., after one full cycle) occurs at $t = 0.625\,\text{s}$. Thus, the fundamental period is

$$T_0 = 0.625\,\text{s} - 0.125\,\text{s} = 0.5\,\text{s}.$$

This completely describes the signal in Figure 2.3. However, we can also determine the natural frequency f_0 and the angular frequency ω_0, which are

$$f_0 = \frac{1}{T_0} = \frac{1}{0.5\,\text{s}} = 2\,\text{Hz} \quad \text{and} \quad \omega_0 = \frac{2\pi}{T_0} = \frac{2\pi}{0.5\,\text{s}} = 4\pi\,\text{rad/s},$$

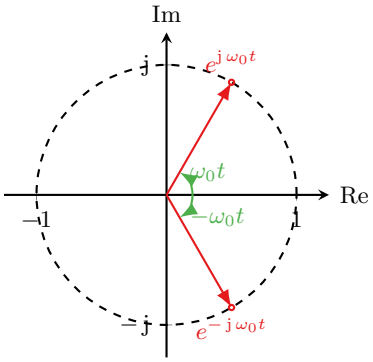

Figure 2.4. Illustration of the two complex functions $e^{j\omega_0 t}$ and $e^{-j\omega_0 t}$ in the complex plane as functions of the angles $\omega_0 t$ and $-\omega_0 t$.

respectively. Finally, the phase shift φ is

$$\varphi = \omega_0 \Delta t = 4\pi \,\text{rad/s}\, 0.125\,\text{s} = \frac{\pi}{2}\,\text{rad}.$$

Finally, there is yet one more important way of representing sines and cosines: using Euler's formulas. Recall that Euler's formulas give (see Appendix A)

$$\sin(\omega_0 t) = \frac{e^{j\omega_0 t} - e^{-j\omega_0 t}}{2j} \tag{2.5}$$

and

$$\cos(\omega_0 t) = \frac{e^{j\omega_0 t} + e^{-j\omega_0 t}}{2}. \tag{2.6}$$

Drawing $e^{j\omega_0 t}$ and $e^{-j\omega_0 t}$, a pair of complex, conjugate and time-varying numbers, for some arbitrary t, Figure 2.4 is obtained. Varying the time t will move the complex numbers along the unit circle, counter-clockwise for $e^{j\omega_0 t}$ and clockwise for $e^{-j\omega_0 t}$. Hence, we can think of these terms as *complex oscillations* and the sine and cosine functions are made up of the complex conjugate pair of these functions. This interpretation will be useful in frequency domain analysis starting in Chapter 3.

Sine and cosine signals are signals of fundamental importance and you are expected to be able to determine and interpret their different parameters without problems.

2.1.2 The Dirac Delta Function

Another very important signal is the *unit impulse function* or *Dirac delta function*[1]. As we will see later, the Dirac delta function plays another key role when working with LTI systems.

[1] Mathematically, the Dirac delta function is actually a distribution rather than a function.

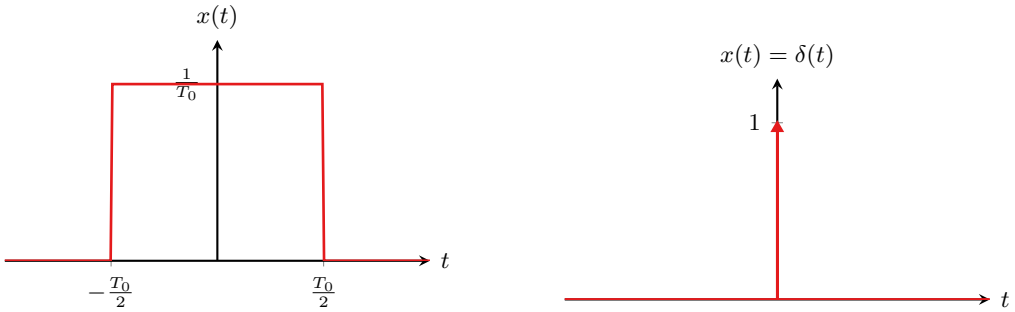

Figure 2.5. Illustration of the Dirac delta function: (a) Rectangular pulse of with T_0 and height $\frac{1}{T_0}$ with unit area, (b) Dirac delta function.

One way to obtain an expression for the Dirac delta function is to consider a rectangular pulse of width T_0 and height $1/T_0$ as illustrated in Figure 2.5a. Note that this pulse has integral $\frac{1}{T_0}T_0 = 1$, independent of the width T_0. As T_0 is decreased, the pulse becomes narrower and higher but the integral still remains 1. Then, the Dirac delta function, denoted $\delta(t)$, is obtained by taking the limit of $T_0 \to 0$, that is,

$$\delta(t) = \lim_{T_0 \to 0} \begin{cases} \frac{1}{T_0} & \text{for } |t| \leq \frac{T_0}{2}, \\ 0 & \text{for } |t| > 0. \end{cases} \tag{2.7}$$

In other words, the Dirac delta function is described by

- $\delta(t) = 0$ for $t \neq 0$, and
- $\int_{-\infty}^{\infty} \delta(t)\,\mathrm{d}t = 1$.

The Dirac delta function is drawn as an upwards pointing arrow to indicate its impulse-like nature with the height of the arrow indicating the area or *weight* of the Dirac delta function (1 by default, but not necessarily), see Figure 2.5b.

One of the most important properties of the Dirac delta function is that the integral over the product between a signal $x(t)$ and a Dirac delta function $\delta(t)$ is simply the signal's value at $t = 0$. In other words, it holds that

$$\int_{-\infty}^{\infty} x(t)\delta(t)\,\mathrm{d}t = x(0).$$

More generally, if a delta function is shifted along the x-axis by some time t_0, that is, $\delta(t - t_0)$, the integral over the product between $x(t)$ and $\delta(t - t_0)$ is the value of $x(t)$ at t_0 such that

$$\int_{-\infty}^{\infty} x(t)\delta(t - t_0)\,\mathrm{d}t = x(t_0). \tag{2.8}$$

This property is sometimes called the *sifting property* or the *sampling property* of the Dirac delta function.

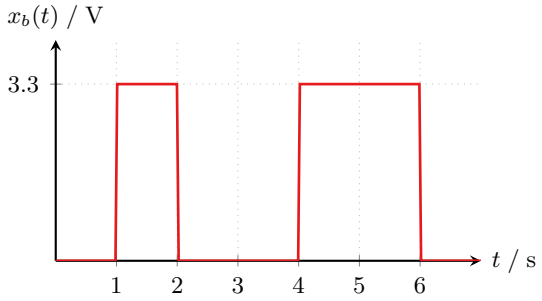

Figure 2.6. Example of the bit sequence `0 1 0 0 1 1` represented using rectangular pulses.

2.1.3 Other Elementary Signals

Sine (and cosine) signals and the Dirac delta function are very important elementary signals. However, there are also a few other signals that simplify the analysis (and synthesis) of systems considerably. This section gives a brief overview of the remaining most important signals and their properties.

Rectangular pulse. The rectangular pulse was already encountered in the derivation of the Dirac delta function above. Formally, a rectangular pulse of width T_0 is denoted $\operatorname{rect}\left(\frac{t}{T_0}\right)$ and defined as

$$\operatorname{rect}\left(\frac{t}{T_0}\right) = \begin{cases} 1 & \text{for } |t| \leq \frac{T_0}{2}, \\ 0 & \text{for } |t| > \frac{T_0}{2}. \end{cases} \tag{2.9}$$

Note that different from the rectangular pulse used above, the height (amplitude) of the pulse is 1 as illustrated in Figure 2.7a. The rectangular pulse can, for example, be used to describe a signal in digital communications (Example 2.2) or ideal filter characteristics (Chapter 5).

Example 2.2: Digital baseband signal

Consider a bit sequence, for example `0 1 0 0 1 1`, that is to be transmitted on a digital (baseband) communication channel. The simplest coding scheme simply encodes the `0`-bits as "low" (e.g., 0 V) and the `1`-bits as "high" (e.g., 3.3 V). Furthermore, each bit is to be transmitted as a pulse (or lack thereof) of length T_0 (e.g., 1 s). This leads to the signal $x(t)$ shown in Figure 2.6 which is transmitted between the sender and receiver.
This specific bit sequence can be described by using rectangular pulses by

$$x_b(t) = 3.3\operatorname{rect}\left(\frac{t-1.5}{1}\right) + 3.3\operatorname{rect}\left(\frac{t-4.5}{1}\right) + 3.3\operatorname{rect}\left(\frac{t-5.5}{1}\right) + \ldots.$$

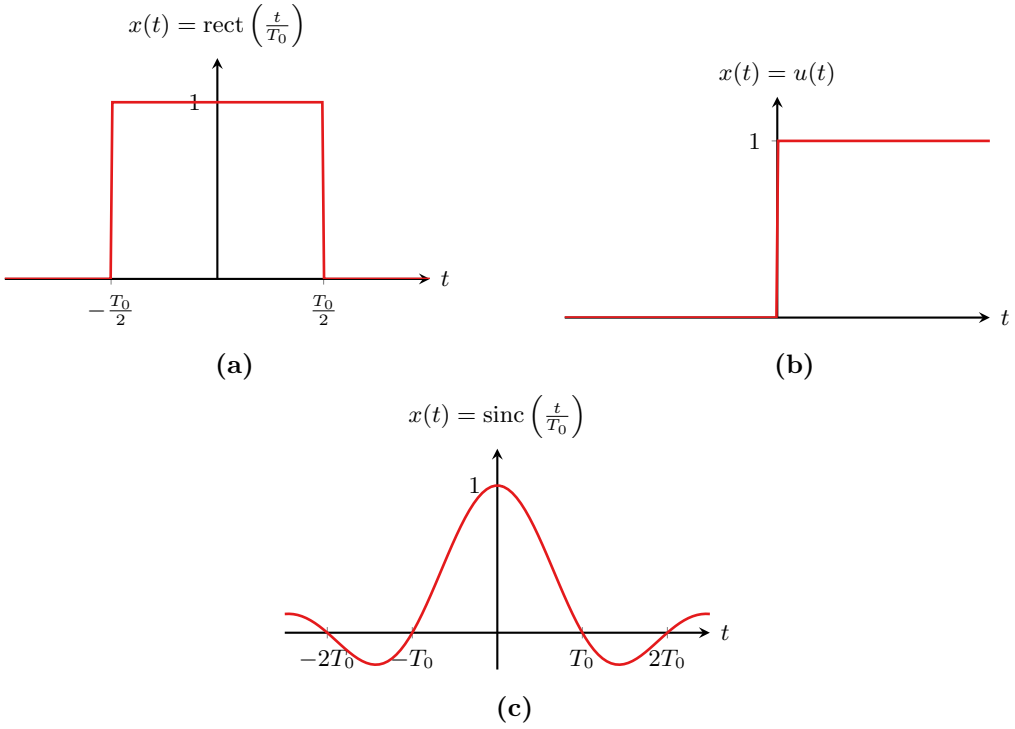

Figure 2.7. Illustrations of elementary signals. (a) rect $\left(\frac{t}{T_0}\right)$, (b) $u(t)$, (c) sinc $\left(\frac{t}{T_0}\right)$.

Unit step. The unit step or heavyside step function, denoted $u(t)$ and shown in Figure 2.7b, is a signal which is 0 for negative t and 1 for $t \geq 0$, that is,

$$u(t) = \begin{cases} 0 & \text{for } t < 0, \\ 1 & \text{for } t \geq 0. \end{cases} \tag{2.10}$$

As it can be seen, the unit step function is step-like, which can be used to describe sudden changes in the signal level. The unit step function is also used extensively in control engineering, where it is used to calculate step responses, an important property of control systems.

Sinc function. The sinc function, denoted $\text{sinc}(t)$ is defined as the ratio between a sine and the sine's argument, that is,

$$\text{sinc}\left(\frac{t}{T_0}\right) = \frac{\sin\left(\frac{\pi t}{T_0}\right)}{\frac{\pi t}{T_0}}. \tag{2.11}$$

Figure 2.7c shows an illustration of the sinc function. As it can be seen, the function exhibits zero-crossings at integer multiples of T_0. Furthermore, it exhibits a decaying oscillation that extends to infinity. The sinc function is very closely related to the rectangular function and, as it will be shown, they often appear as transform pairs.

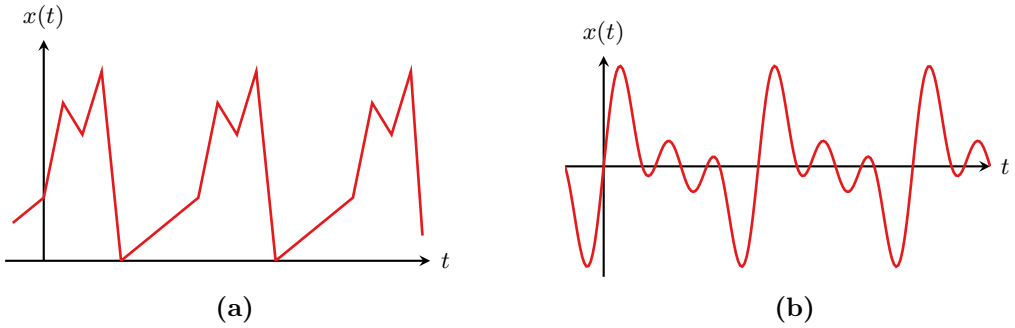

Figure 2.8. Two examples of periodic signals.

2.1.4 Periodic Signals

Signals may be *periodic* or *aperiodic*. A periodic signal repeats itself after a certain time T_0, called the signal's (fundamental) period. Hence, it is enough to know how the signal looks like for one period to know the entire signal. Formally, periodicity is defined as

$$x(t) = x(t + T_0), \tag{2.12}$$

that is, the signal at time t is equal to the signal at time t plus one (or two, three, etc.) full period(s) T_0. Consequently, if (2.12) does not hold, the signal is called *aperiodic*. The sine and cosine signals discussed in Section 2.1.1 are typical examples of periodic signals. Furthermore, Figure 2.8 shows two additional examples of periodic signals.

2.1.5 Energy and Power Signals

Signals can be divided into energy and power signals. A signal $x(t)$ is called an *energy signal* if its energy

$$E = \int_{-\infty}^{\infty} |x(t)|^2 \, \mathrm{d}t \tag{2.13}$$

is finite, that is, if $E < \infty$. If, however, a signal has infinite energy, it still may be a *power signal*. A power signal is defined as having a finite average power, that is,

$$P = \lim_{T \to \infty} \frac{1}{T} \int_{-T/2}^{T/2} |x(t)|^2 \, \mathrm{d}t. \tag{2.14}$$

In practice, all signals are energy signals since no signal can carry infinite energy. However, for the purpose of analyzing systems, it is still useful to consider power signals.

2.1.6 Orthogonal Signals

Similar to two vectors in linear algebra, two signals are said to be *orthogonal* if their inner product is zero. Recall that for two vectors x and y, the inner product $\langle x, y \rangle$ is defined as

$$\langle x, y \rangle = x^{\mathsf{T}} y = \sum_i x_i y_i.$$

For two continuous signals $x(t)$ and $y(t)$, the definition of the inner product $\langle x(t), y(t)\rangle$ is similar, but an integral takes the place of the sum. For *energy signals*, the inner product of the two signals $x(t)$ and $y(t)$ is defined as

$$\langle x(t), y(t)\rangle = \int_{-\infty}^{\infty} x(t)y^*(t)\,\mathrm{d}t \tag{2.15}$$

where * denotes the complex conjugate. Similarly, for *periodic signals*, the inner product is defined as the integral over one full period, that is,

$$\langle x(t), y(t)\rangle = \int_{-T_0/2}^{T_0/2} x(t)y^*(t)\,\mathrm{d}t. \tag{2.16}$$

Note that the period T_0 is with respect to the fundamental period of the signal $x(t)y^*(t)$.

Thus, the two signals $x(t)$ and $y(t)$ are orthogonal if

$$\langle x(t), y(t)\rangle = 0,$$

that is, if the integral (2.15) or (2.16) is zero. An example of a pair of orthogonal signals are sine (or cosine) signals of different frequencies, as shown in Example 2.3 below.

Example 2.3: Orthogonality of sine signals

Consider the two signals $x(t) = \sin(\omega_1 t)$ and $y(t) = \sin(\omega_2 t)$. The inner product of these two periodic signals is given by

$$\begin{aligned}\langle x(t), y(t)\rangle &= \int_{-T_0/2}^{T_0/2} x(t)y^*(t)\,\mathrm{d}t \\ &= \int_{-T_0/2}^{T_0/2} \sin(\omega_1 t)\sin(\omega_2 t)\,\mathrm{d}t.\end{aligned}$$

Using the trigonometric identity $\sin(\alpha)\sin(\beta) = \frac{1}{2}[\cos(\alpha-\beta) - \cos(\alpha+\beta)]$ yields

$$\langle x(t), y(t)\rangle = \frac{1}{2}\int_{-T_0/2}^{T_0/2} \cos\left((\omega_1-\omega_2)t\right)\mathrm{d}t - \frac{1}{2}\int_{-T_0/2}^{T_0/2} \cos\left((\omega_1+\omega_2)t\right)\mathrm{d}t.$$

Now, we can distinguish the following two cases: 1) $|\omega_1| \neq |\omega_2|$, and 2) $|\omega_1| = |\omega_2|$. In the first case, the integrands are cosines with frequencies $\omega_1 - \omega_2 \neq 0$ and $\omega_1 + \omega_2 \neq 0$ and the integral over a full period of a cosine is always zero. On the other hand, if $|\omega_1| = |\omega_2|$, either the first or second integrand becomes 1 (due to one of the cosines becoming $\cos(0t)$). Then, we have that

$$\frac{1}{2}\int_{-T_0/2}^{T_0/2} 1\,\mathrm{d}t = \frac{1}{2}[t]_{-T_0/2}^{T_0/2} = \frac{T_0}{2}.$$

Thus, the inner product of two sine signals is

$$\langle \sin(\omega_1 t), \sin(\omega_2 t) \rangle = \begin{cases} 0 & \text{if } |\omega_1| \neq |\omega_2|, \\ \frac{T_0}{2} & \text{if } |\omega_1| = |\omega_2|. \end{cases}$$

Hence, two sine signals are orthogonal if they have different frequencies. Finally, note that the same applies to cosine signals as well as complex oscillations.

2.1.7 Causal, Even, and Odd Signals

Causal signals are signals that are zero for negative times t, that is,

$$x(t) = 0 \quad \text{for } t < 0. \tag{2.17}$$

In practice, all signals are essentially causal as they start at some point ($t = 0$) and do not extend to negative infinity. An example of a causal signal is the unit step $u(t)$ shown in Figure 2.7b.

An *even* signal is a signal that is line symmetric (or mirror symmetric) around the x-axis, that is, if it holds that

$$x(t) = x(-t). \tag{2.18}$$

In practice, this means that the signal takes on the same values for both positive and negative t. Similarly, a signal is called *odd* if it is point symmetric about the origin, that is, if it holds that

$$x(t) = -x(-t). \tag{2.19}$$

This means that the signal takes on the negated value if the time t is negated. Note that a signal may either be even, odd, or neither of the two. Examples of even signals are cosine signals, whereas sine signals are odd signals (both assuming no phase shift). A signal that is neither even nor odd is a cosine signal with a phase shift different from multiples of $\frac{\pi}{2}$, see Figure 2.9.

2.1.8 Signal Operations

Given an arbitrary signal $x(t)$, a new, related signal $y(t)$ can be obtained by applying a set of different signal operations to it and a few of these operations have already been used implicitly in the preceding sections. Simple operations may change the signal in both the y- (amplitude) and x- (time) directions.

The former type of operations, operations that affect the y-direction, are applied to the signal $x(t)$. These simple operations are *amplitude scaling* and *offsetting*. Operations that affect the x-direction (time) of the signal are applied to the time variable t instead. These operations include *time shifting*, *time scaling*, and *time inversion*.

Amplitude scaling. Amplitude scaling increases or decreases the amplitude of the signal. The relationship between the new signal $y(t)$ and $x(t)$ is

$$y(t) = \alpha x(t), \tag{2.20}$$

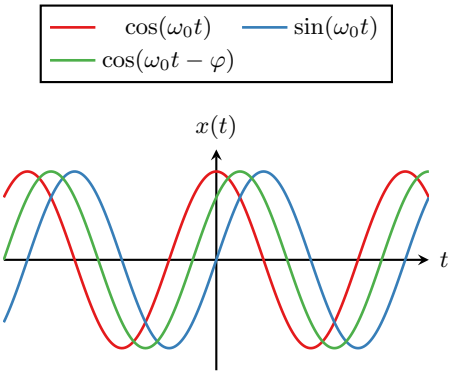

Figure 2.9. Example of even (cosine) and odd (sine) signals, together with a signal that is neither even nor odd (cosine with non-zero phase shift).

where α is the scaling constant. If $0 < |\alpha| < 1$, the signal is shrunk in y-direction whereas $|\alpha| > 1$ means that the signal is increased. If $\alpha < 0$, the signal is flipped (mirrored) along the x-axis. Figure 2.10a shows an example of amplitude scaling.

Offsetting. Offsetting moves the signal in y-direction without changing its amplitude. The new signal is given by

$$y(t) = x(t) + y_0 \tag{2.21}$$

where y_0 is the offset.

Time shifting. Time shifting moves a signal along the x-axis. A time-shifted version $y(t)$ of the signal $x(t)$ is given by

$$y(t) = x(t - \Delta t), \tag{2.22}$$

where Δt denotes the time shift. If $\Delta t > 0$, the signal is moved to the *right* along the x-axis and $y(t)$ is a delayed copy of $x(t)$. Conversely, if Δt is negative, the signal is moved to the *left* along the x-axis, see Figure 2.10b.

Time shifting was used in Example 2.2 to move the rectangular pulses from their location around the origin to the right to represent the ones in the bit stream (Figure 2.6).

Time scaling and inversion. Time scaling refers to compressing or expanding the signal $x(t)$ in the time domain such that

$$y(t) = x(\alpha t). \tag{2.23}$$

If $\alpha > 1$, the signal is compressed by the factor α, that is, it becomes narrower. On the other hand, if $0 < \alpha < 1$, the signal is expanded, making the signal wider. If $\alpha = -1$ (or generally $\alpha < 0$), the signal is mirrored about the y-axis, which is called *time inversion* or *time reversal*.

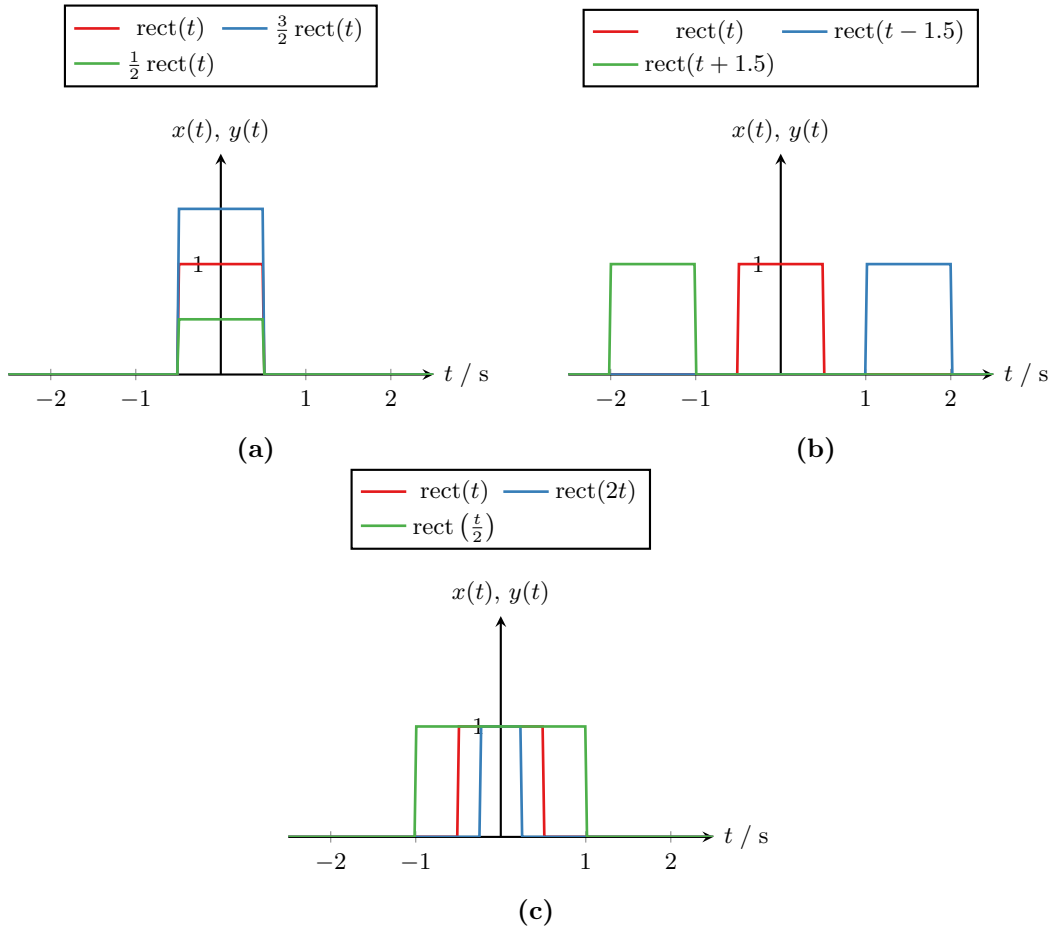

Figure 2.10. Examples of signal operations on the signal $x(t) = \text{rect}(t)$. (a) Amplitude scaling, (b) time shifting, and (c) time scaling.

Example 2.4: Signal operations

Assume that the signal $x(t)$ is $x(t) = \text{rect}(t)$. Figure 2.10 shows the results of applying the following signal operations:

a) $y(t) = \frac{3}{2}x(t) = \frac{3}{2}\,\text{rect}(t)$ and $y(t) = \frac{1}{2}x(t) = \frac{1}{2}\,\text{rect}(t)$ (amplitude scaling; Figure 2.10a),

b) $y(t) = x(t - 1.5) = \text{rect}(t - 0.25)$ and $y(t) = x(t + 1.5) = \text{rect}(t + 1.5)$ (time shifting; Figure 2.10b), and

c) $y(t) = x(2t) = \text{rect}(2t)$ and $y(t) = x(t/2) = \text{rect}\left(\frac{t}{2}\right)$ (time scaling; Fiure 2.10c).

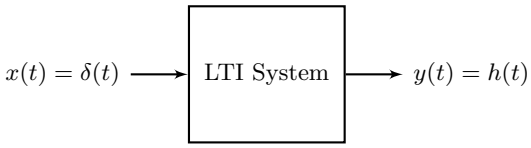

Figure 2.11. Continuous time LTI system with the Dirac delta impulse function $\delta(t)$ as the input signal and the impulse response $h(t)$ at the output.

2.2 Time Domain Analysis of Continuous Time Systems

In this section, the time domain properties of continuous time LTI systems are discussed. In particular, the concepts of the impulse response and the convolution integral are introduced, which completely describe the input-output relationship for LTI systems in the time domain. We also discuss the sine in sine out principle.

Note that continuous time LTI systems are often modeled by ordinary differential equations (ODEs). However, these are typically hard to work with in the time domain and here we start from a different perspective. We return to the ODE representation of LTI systems in Chapter 4, where we also make the connection between ODEs and the time domain interpretation presented here.

2.2.1 Impulse response

Continuous time LTI systems are completely characterized by their *impulse response* $h(t)$. As the name suggests, the impulse response is, by definition, the output $y(t)$ of the system if an impulse $\delta(t)$ is applied as the input signal, that is, if $x(t) = \delta(t)$ (Figure 2.11). This is summarized in Definition 2.1 below.

Definition 2.1: Impulse Response

The impulse response $h(t)$ of a continuous-time LTI system is the output of the system when the Dirac-delta impulse $\delta(t)$ is applied at the input, that is,

$$\delta(t) \mapsto h(t). \tag{2.24}$$

Since the system is linear and time-invariant, the impulse response satisfies

$$\alpha\delta(t - T) \mapsto \alpha h(t - T) \tag{2.25}$$

for arbitrary constants α and T.

Example 2.5: Impulse response of a simple radio channel

In free space (e.g., on an open meadow with no trees and buildings), an ideal radio channel, that is, the transmission channel between a radio transmitter and receiver (see Figure 1.2b), can be described by an attenuation and a time delay. Both of these depend on the line of sight distance s_0 (i.e., the straight path between the

transmitter and the receiver) the radio signal has to travel. The attenuation could, for example, follow an exponential attenuation $e^{-\alpha_0 s_0}$ with attenuation constant α_0 whereas the time delay depends on the time of flight and the propagation speed (speed of light):

$$t_0 = \frac{s_0}{c}.$$

Thus, the impulse response for such a channel is

$$h_0(t) = e^{-\alpha s_0}\delta(t - t_0) = e^{-\alpha s_0}\delta\left(t - \frac{s_0}{c}\right).$$

A more realistic scenario takes into account that the radio signal bounces off structures in the surroundings such as buildings, walls, vegetation, etc. This is called multipath propagation as multiple paths lead from the transmitter to the receiver. Assume that there are $m = 1, \ldots, M$ indirect paths. Each of these indirect paths attenuates the signal by a factor $e^{-\alpha_m s_m}$ and it takes the time $t_m = \frac{s_m}{c}$ for the signal along the mth path to reach the receiver. Thus, the impulse response for such a multipath scenario becomes

$$h_M(t) = \sum_{m=0}^{M} e^{-\alpha_m s_m}\delta\left(t - \frac{s_m}{c}\right).$$

Since LTI systems are completely described by their impulse response, a system satisfies some special properties if its impulse response satisfies the corresponding property.

In particular, a system is *static* (or *memoryless*) if the output of the system only depends on the input signal at the same time. Hence, memoryless LTI systems can be described by $y(t) = \alpha x(t)$. Substituting the arbitrary input signal with the impulse function, $x(t) = \delta(t)$, yields that

$$y(t) = \alpha\delta(t).$$

Thus, a continuous-time LTI system is memoryless if and only if its impulse response satisfies

$$h(t) = \alpha\delta(t) = \begin{cases} \alpha & \text{for } t = 0, \\ 0 & \text{for } t \neq 0. \end{cases}$$

Conversely, a system that is not static is called a *dynamic* system.

Furthermore, a continuous time LTI system is *causal* if the output signal at time t only depends on values of the input signal at times up to t (but not the future of t). Hence, for a system to be causal, the impulse response must not start before the impulse is observed at the input. Since the impulse response is observed in response to $\delta(t)$, which starts at at $t = 0$, the impulse response must be zero for $t < 0$ (but may be non-zero for $t > 0$ as $\delta(t)$ is in the past). In other words, the impulse response must be a *causal signal* for the system to be causal such that

$$h(t) = 0 \quad \text{for } t < 0. \tag{2.26}$$

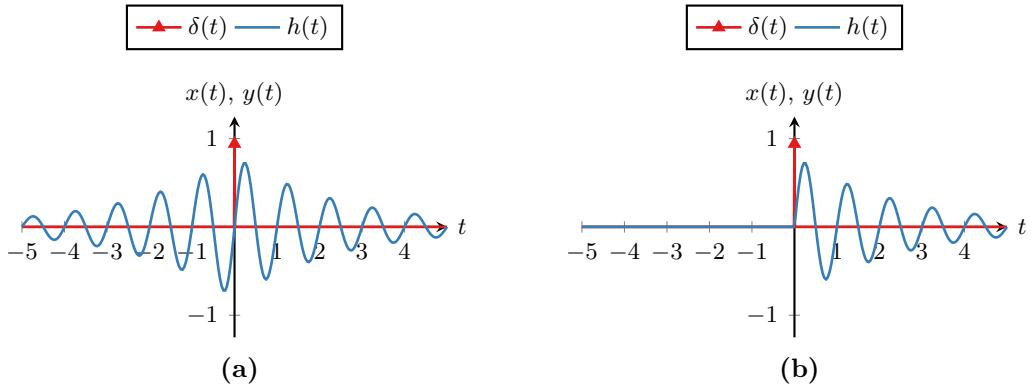

Figure 2.12. Examples of causal and non-causal systems. (a) Non-causal system with an impulse response that is non-zero for negative t (i.e., the system depends on the future and the past) and (b) causal system with an impulse response that is zero for negative t (i.e., the system only depends on the past).

Figure 2.12 shows examples for causal and non-causal systems.

Example 2.6: System properties and impulse response characteristics

Consider the systems with the following impulse responses:

a) $h(t) = \delta(t) - \delta(t-2)$: The system is dynamic (i.e., not static) as $h(t) \neq 0$ for $t = 2$. The system is causal, as it only requires past and current input signal values, which is equivalent to $h(t) = 0$ for $t < 0$.

b) $h(t) = 2\,\mathrm{rect}(t/2)$: The system is neither causal nor static since $h(t) \neq 0$ for $t < 0$.

c) $h(t) = 2e^{-4t}u(t)$: The system is dynamic as $h(t) \neq 0$ for $t > 0$ and causal, as it only requires past and current input signal values ($h(t) = 0$ for $t < 0$).

d) $h(t) = \left(1 - e^{-4t}\right) u(t)$. The system is dynamic and causal.

2.2.2 General Inputs and the Convolution Integral

In the previous section, we discussed the impulse response, which by definition is the signal observed at the output of an LTI system when the Dirac delta function is applied as the input signal. For arbitrary input signals $x(t)$, the output signal is given by the *convolution* between the input signal $x(t)$ and the impulse response $h(t)$ as shown in Definition 2.2.

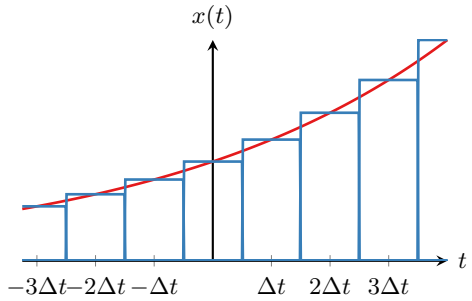

Figure 2.13. Illustration of the approximation of $x(t)$ using a sum of rectangular pulses.

Definition 2.2: Input-output relationship for continuous time systems

The output signal $y(t)$ of a continuous time LTI system is given by the convolution integral of the system's impulse response $h(t)$ and the input signal $x(t)$, that is,

$$\begin{aligned} y(t) &= \int_{-\infty}^{\infty} x(\tau)h(t-\tau)\,\mathrm{d}\tau \\ &= \int_{-\infty}^{\infty} h(\tau)x(t-\tau)\,\mathrm{d}\tau. \end{aligned} \tag{2.27}$$

Furthermore, for causal systems where $h(t) = 0$ for $t < 0$, the convolution becomes

$$y(t) = \int_{0}^{\infty} h(\tau)x(t-\tau)\,\mathrm{d}\tau. \tag{2.28}$$

The convolution integral is denoted using an asterisk, that is,

$$y(t) = x(t) * h(t), \tag{2.29}$$

which reads as "$y(t)$ is the convolution between $x(t)$ and $h(t)$".

To see why this is the case, consider an approximation of the original signal $x(t)$ using rectangular pulses of width Δt and height $x(k\Delta t)$ as illustrated in Figure 2.13. In the limit $\Delta t \to 0$, this approximation converges to the true signal $x(t)$ and formally, this can be expressed as

$$x(t) = \lim_{\Delta t \to 0} \sum_{k=-\infty}^{\infty} x(k\Delta t)\,\mathrm{rect}\left(\frac{t-k\Delta t}{\Delta t}\right).$$

Furthermore, when taking the limit $\Delta t \to 0$, the rectangular function approaches the Dirac delta function, in this case scaled by Δt to account for the non-unit area. Thus, we obtain

$$x(t) = \lim_{\Delta t \to 0} \sum_{k=-\infty}^{\infty} x(k\Delta t)\delta(t-k\Delta t)\Delta t.$$

Next, using the superposition principle ($\alpha x_1(t) + \beta x_2(t) \mapsto \alpha y_1(t) + \beta y_2(t)$) together with the definition of the impulse response above leads to the input output relationship

$$\lim_{\Delta t \to 0} \sum_{k=-\infty}^{\infty} x(k\Delta t)\delta(t - k\Delta t)\Delta t \mapsto \lim_{\Delta \to 0} \sum_{k=-\infty}^{\infty} x(k\Delta t)h(t - k\Delta t)\Delta t.$$

Taking the limit $k\Delta t \to \tau$ and $\Delta t \to \mathrm{d}\tau$ turns the sums into integrals such that

$$\int_{-\infty}^{\infty} x(\tau)\delta(t - \tau)\,\mathrm{d}\tau \mapsto \int_{-\infty}^{\infty} x(\tau)h(t - \tau)\,\mathrm{d}\tau.$$

The left hand side can further be simplified such that the input output relationship

$$x(t) \mapsto \int_{-\infty}^{\infty} x(\tau)h(t - \tau)\,\mathrm{d}\tau \tag{2.30}$$

is obtained. Finally, the right hand side is recognized to be the convolution between the input signal $x(t)$ and the system's impulse response $h(t)$ and we have that

$$x(t) \mapsto x(t) * h(t)$$

as in Definition 2.2.

Note that in order to calculate the output signal, no knowledge of the underlying physical process is necessary if the impulse response is known. Also, in order to characterize an unknown physical system, which is known to be LTI, it is sufficient to apply a unit impulse to the input of the system, and measure the output to obtain the impulse response.

The way the convolution works is somewhat difficult to see directly. Since the convolution integral is over the variable τ, it is easiest to think in terms of τ. Assuming the form

$$y(t) = \int_{-\infty}^{\infty} x(\tau)h(t - \tau)\,\mathrm{d}\tau,$$

we can see that the signal $x(\tau)$ is unchanged in the τ-domain to start with. The term of the impulse response, $h(t - \tau)$, can be thought of first mirroring the impulse response around the y-axis ($-\tau$), followed by shifting it along the τ-axis by t (note that $t > 0$ means a shift to the right and $t < 0$ a shift to the left in this case, which is due to the mirroring around the y-axis).

Then, the product of $x(\tau)$ and $h(t - \tau)$ is formed and the product is integrated over τ, which yields the value of the output at t. Repeating this process for all possible time shifts t finally yields the output signal $y(t)$. This process is illustrated in Example 2.7 and Figure 2.14.

Example 2.7: Convolution

Consider a continuous-time LTI system with impulse response $h(t) = e^{-2t}u(t)$, to which the input $x(t) = e^{-t}u(t)$ is applied. The output $y(t)$ is given by the

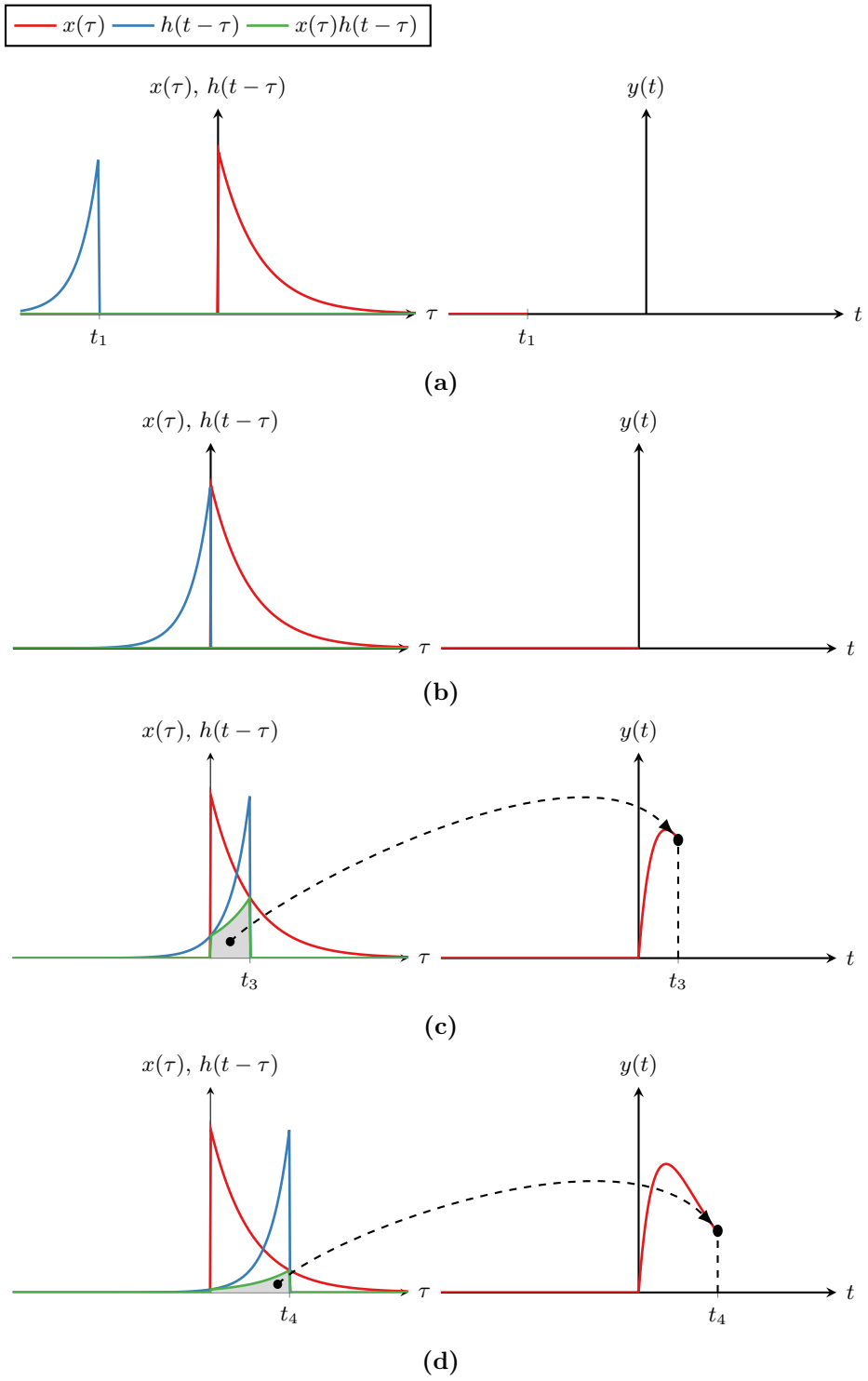

Figure 2.14. Snapshots of the convolution in Example 2.7 at different times t. (a) $t_1 = -3$, (b) $t_2 = 0$, (c) $t_3 = 1$, and (d) $t_4 = 2$.

convolution of the input signal with the impulse response, that is,

$$\begin{aligned} y(t) &= \int_{-\infty}^{\infty} e^{-\tau} u(\tau) e^{-2(t-\tau)} u(t-\tau)\,\mathrm{d}\tau \\ &= e^{-2t} \int_{-\infty}^{\infty} e^{\tau} u(\tau) u(t-\tau)\,\mathrm{d}\tau. \end{aligned}$$

Since $u(\tau) = 0$ for $\tau < 0$, this can be written as

$$y(t) = e^{-2t} \int_{0}^{\infty} e^{\tau} u(t-\tau)\,\mathrm{d}\tau.$$

Also note that $u(t-\tau) = 0$ for $\tau > t$ and $u(t-\tau) = 1$ for $\tau \leq t$. Hence, if $t < 0$ the integral is 0. For $t > 0$ it yields

$$y(t) = e^{-2t} \int_{0}^{t} e^{\tau}\,\mathrm{d}\tau = e^{-2t} \left(e^{t} - 1\right) = e^{-t} - e^{-2t}.$$

Hence, the output signal is

$$y(t) = \left(e^{-t} - e^{-2t}\right) u(t).$$

A graphical illustration of this convolution is shown in Figure 2.14 with the input signal in red, the impulse response (which is flipped around the y-axis and shifted by t) in blue and the product of the two in green.
Figure 2.14a shows the situation up to time $t = t_1 = -3$. In this case, the product between $x(\tau)$ and $h(t-\tau)$ is zero and thus, also the integral over the product is zero. This yields that the output $y(t)$ is zero. This situation continues up to time $t = t_2 = 0$, where the signals start to overlap (Figure 2.14b).
Further increasing the shift t now yields a non-zero overlap as illustrated in Figure 2.14c and Figure 2.14d for $t = t_3 = 1$ and $t = t_4 = 2$, respectively. In these cases, the product between the signal and (flipped and shifted) impulse response results in the green curve and the integral corresponds to the gray area under the green curve. Hence, the gray area under the curve corresponds to the output signal values at t_3 and t_4, that is, $y(t_3)$ and $y(t_4)$ as illustrated in the right panels of Figure 2.14d and Figure 2.14d. Increasing t further towards positive infinity finally yields the complete curve of the output signal.

The convolution integral satisfies the following elementary properties:

1. *Commutative:* The convolution of $x_1(t)$ with $x_2(t)$ is identical to the convolution of $x_2(t)$ with $x_1(t)$, that is

$$x_1(t) * x_2(t) = x_2(t) * x_1(t).$$

2. *Distributive:* The convolution is a linear operation, thus

$$x_1(t) * (x_2(t) + x_3(t)) = x_1(t) * x_2(t) + x_1(t) * x_3(t).$$

3. *Associative:* Changing the order of the convolution integrands does not change the result, that is

$$x_1(t) * (x_2(t) * x_3(t)) = (x_1(t) * x_2(t)) * x_3(t).$$

Furthermore, it also has the following additional properties.

4. *Time shifting:* If $x_1(t) * x_2(t) = z(t)$, then for any arbitrary constants T_1 and T_2, it holds that

$$x_1(t - T_1) * x_2(t - T_2) = z(t - T_1 - T_2).$$

5. *Duration:* If the "width" (time interval in which the signal is nonzero) of the signals $x_1(t)$ and $x_2(t)$ are T_1 and T_2, respectively, then the width of the convolution integral $x_1(t) * x_2(t)$ is $T_1 + T_2$.

6. *Convolution with Dirac delta function:* The convolution of a signal with a time-shifted Dirac-delta function $\delta(t - T)$ yields a time shifted version of the original signal, that is,

$$x(t) * \delta(t - T) = x(t - T).$$

7. *Time scaling:* If $z(t) = x_1(t) * x_2(t)$, then if $x_1(t)$ and $x_2(t)$ are time-scaled by an arbitrary constant α, the result is time-scaled by α and amplified by $|\alpha|$:

$$z(\alpha t) = |\alpha| x_1(\alpha t) * x_2(\alpha t).$$

Example 2.8: Received radio signal

Assume that the signal transmitted at the antenna of a transmitter in a wireless communication system is $x_{tx}(t)$ and that the channel can be modeled as in Example 2.5.
Under ideal conditions, that is, no multipath propagation and in free space, the signal received at the receiver antenna is

$$\begin{aligned} x_{rx}(t) &= x_{tx}(t) * h_0(t) \\ &= \int_{-\infty}^{\infty} e^{-\alpha_0 s_0} \delta\left(\tau - \frac{s_0}{c}\right) x_{tx}(t - \tau)\, \mathrm{d}\tau \\ &= e^{-\alpha_0 s_0} x_{tx}\left(t - \frac{s_0}{c}\right). \end{aligned}$$

Thus, in this scenario, the signal at the receiver is scaled (attenuated) by the factor $e^{-\alpha_0 s_0}$ as well as time-delayed by $\frac{s_0}{c}$.

Similarly, for the more realistic multipath propagation, the signal observed at the receiver antenna is

$$\begin{aligned} x_{rx}(t) &= x_{tx}(t) * h_M(t) \\ &= \int_{-\infty}^{\infty} \left[\sum_{m=0}^{M} e^{-\alpha_m s_m} \delta\left(\tau - \frac{s_m}{c}\right) \right] x_{tx}(t-\tau)\,\mathrm{d}\tau \\ &= \sum_{m=0}^{M} e^{-\alpha_m s_m} \int_{-\infty}^{\infty} \delta\left(\tau - \frac{s_m}{c}\right) x_{tx}(t-\tau)\,\mathrm{d}\tau \\ &= \sum_{m=0}^{M} e^{-\alpha_m s_m} x_{tx}\left(t - \frac{s_m}{c}\right). \end{aligned}$$

This shows that the received signal indeed consists of $M+1$ copies of the original signal, each of which attenuated and time-delayed according to the length of the corresponding path.

Finally, we can also derive a sufficient condition for *bounded input bounded output stability* (BIBO stability) of continuous time LTI systems. BIBO stability refers to the concept of a bounded input signal $x(t)$ giving rise to a bounded output signal $y(t)$. A bounded input signal is defined as having a finite maximum, that is,

$$|x(t)| \leq M_x$$

for some constant $M_x < \infty$ and all times t. Similarly, a abounded output signal is defined as having a finite maximum such that

$$|y(t)| \leq M_y$$

for some constant $M_y < \infty$ and all times t.

For a continuous time LTI system it must thus hold that

$$|y(t)| = \left| \int_{-\infty}^{\infty} x(\tau) h(t-\tau)\,\mathrm{d}\tau \right| \leq M_y.$$

Using the inequality $|\int f(t)\,\mathrm{d}t| \leq \int |f(t)|\,\mathrm{d}t$ yields

$$\begin{aligned} |y(t)| &= \left| \int_{-\infty}^{\infty} x(\tau) h(t-\tau)\,\mathrm{d}\tau \right| \\ &\leq \int_{-\infty}^{\infty} |x(\tau)|\,|h(t-\tau)|\,\mathrm{d}\tau \\ &\leq M_x \int_{-\infty}^{\infty} |h(\tau)|\,\mathrm{d}\tau. \end{aligned}$$

Thus, a sufficient condition for a continuous time LTI system to be BIBO stable is

$$\int_{-\infty}^{\infty} |h(t)|\,\mathrm{d}t < \infty. \tag{2.31}$$

Note, however, that this is only a sufficient condition meaning that there might be systems that do not fulfill (2.31) but are stable nevertheless.

Example 2.9: BIBO stability

Consider the systems with the following impulse responses shown in Example 2.6:

a) $h(t) = \delta(t) - \delta(t-2)$: To determine whether the system is BIBO stable, we examine the integral (2.31):

$$\int_{-\infty}^{\infty} |h(t)|\,\mathrm{d}t = \int_{-\infty}^{\infty} |\delta(t) - \delta(t-2)|\,\mathrm{d}t \leq \int_{-\infty}^{\infty} |\delta(t)|\,\mathrm{d}t + \int_{-\infty}^{\infty} |\delta(t-2)|\,\mathrm{d}t = 2,$$

which shows that the system is BIBO stable.

b) $h(t) = 2\,\mathrm{rect}(t/2)$: To determine whether the system is BIBO stable, compute the integral

$$\int_{-\infty}^{\infty} |h(t)|\,\mathrm{d}t = \int_{-1}^{1} 2\,\mathrm{d}t = 4,$$

which shows that the system is BIBO stable.

c) $h(t) = 2e^{-4t}u(t)$: The integral

$$\int_{-\infty}^{\infty} |h(t)|\,\mathrm{d}t = \int_{-\infty}^{\infty} \left|2e^{-4t}u(t)\right|\,\mathrm{d}t \leq \int_{0}^{\infty} |2e^{-4t}|\,\mathrm{d}t = 0.5$$

shows that the system is BIBO stable.

d) $h(t) = \left(1 - e^{-4t}\right)u(t)$: To determine whether the system is BIBO stable, solve the integral

$$\int_{-\infty}^{\infty} |h(t)|\,\mathrm{d}t = \int_{-\infty}^{\infty} \left|1 - e^{-4t}\right|\,\mathrm{d}t = \left[t + 0.25e^{-4t}\right]_0^{\infty} = \infty.$$

Thus, the system might not be BIBO stable. Whether the system is indeed unstable cannot be determined with the condition presented above as it is only sufficient but not necessary for stability.

2.2.3 Sine In, Sine Out Principle

We have already seen that when the Dirac delta impulse $\delta(t)$ is applied to an LTI system, the output is the impulse response $h(t)$. For arbitrary inputs $x(t)$, the output is the convolution between the input and the impulse response. In this section, we are going to

investigate another special case of an input that gives rise to a special output: sine and cosine signals.

Assume that the input to an LTI system with impulse response $h(t)$ is the sine signal $x(t) = \sin(\omega_0 t)$. Using the convolution integral (2.27) and Euler's formula for the sine (2.5), the output of the system can be written as

$$\begin{aligned} y(t) &= \int_{-\infty}^{\infty} h(\tau) \sin(\omega_0(t-\tau))\, \mathrm{d}\tau \\ &= \frac{1}{2j} \int_{-\infty}^{\infty} h(\tau)(e^{\mathrm{j}\,\omega_0(t-\tau)} - e^{-\mathrm{j}\,\omega_0(t-\tau)})\, \mathrm{d}\tau. \end{aligned}$$

This can be rewritten to

$$\begin{aligned} y(t) &= \frac{1}{2j} \left[\int_{-\infty}^{\infty} h(\tau) e^{\mathrm{j}\,\omega_0 t} e^{-\mathrm{j}\,\omega_0 \tau}\, \mathrm{d}\tau - \int_{-\infty}^{\infty} h(\tau) e^{-\mathrm{j}\,\omega_0 t} e^{\mathrm{j}\,\omega_0 \tau}\, \mathrm{d}\tau \right] \\ &= \frac{1}{2j} \left[e^{\mathrm{j}\,\omega_0 t} \int_{-\infty}^{\infty} h(\tau) e^{-\mathrm{j}\,\omega_0 \tau}\, \mathrm{d}\tau - e^{-\mathrm{j}\,\omega_0 t} \int_{-\infty}^{\infty} h(\tau) e^{\mathrm{j}\,\omega_0 \tau}\, \mathrm{d}\tau \right], \end{aligned}$$

where the last equality is due to the fact that the terms $e^{-\mathrm{j}\,\omega_0 t}$ and $e^{\mathrm{j}\,\omega_0 t}$ are independent of the integration variable τ. Next, defining the complex number

$$H(\omega_0) = \int_{-\infty}^{\infty} h(\tau) e^{-\mathrm{j}\,\omega_0 \tau}\, \mathrm{d}\tau$$

and noting that the second integral is the complex conjugate of $H(\omega_0)$, we can write

$$y(t) = \frac{1}{2j} \left[e^{\mathrm{j}\,\omega_0 t} H(\omega_0) - e^{-\mathrm{j}\,\omega_0 t} H^*(\omega_0) \right].$$

Expressing $H(\omega_0)$ in polar form (in terms of its magnitude $|H(\omega_0)|$ and phase $\angle H(\omega_0)$), we obtain

$$\begin{aligned} y(t) &= \frac{1}{2j} \left[e^{\mathrm{j}\,\omega_0 t} |H(\omega_0)| e^{\mathrm{j}\,\angle H(\omega_0)} - e^{-\mathrm{j}\,\omega_0 t} |H(\omega_0)| e^{-\mathrm{j}\,\angle H(\omega_0)} \right] \\ &= |H(\omega_0)| \frac{1}{2j} \left[e^{\mathrm{j}(\omega_0 t + \angle H(\omega_0))} - e^{-\mathrm{j}(\omega_0 t + \angle H(\omega_0))} \right]. \end{aligned}$$

Finally, this can be recognized to be another sine signal with amplitude $|H(\omega_0)|$, angular frequency ω_0, and phase shift $\angle H(\omega_0)$, that is,

$$y(t) = |H(\omega_0)| \sin(\omega_0 t + \angle H(\omega_0)). \tag{2.32}$$

Thus, the following conclusion can be drawn about continuous time LTI systems with sine signals as the input, which also holds for cosine signals.

If the input signal $x(t)$ to a continuous time LTI system is a sine or cosine signal with frequency ω_0, the system's output signal $y(t)$ is also a sine or cosine of the same frequency ω_0 but with (possibly) scaled amplitude and shifted phase. In other words, LTI systems only change the amplitude and phase of sine and cosine signals but not their frequency ω_0.

This is another fundamental property of LTI systems, which we will make use of extensively. Finally, note that it also holds that if the output of a system includes sine or cosine signals with frequencies not present at the input, the system must be nonlinear.

Chapter 3

Continuous Time Fourier Series and Transform

3.1 Continuous Time Fourier Series

It can be shown that any (real-valued) T_0-periodic signal can be written as a linear combination of infinitely many sine and cosine signals of integer multiples of the signal's *fundamental frequency* $\omega_0 = \frac{2\pi}{T_0}$. That is, any T_0-periodic continuous time signal can be expressed as

$$x(t) = a_0 + \sum_{n=1}^{\infty} \left[a_n \cos(n\omega_0 t) + b_n \sin(n\omega_0 t) \right]. \tag{3.1}$$

This is called the *trigonometric Fourier series*[1]. The trigonometric Fourier coefficients a_n and b_n are

$$a_0 = \frac{1}{T_0} \int_{(T_0)} x(t)\, \mathrm{d}t, \tag{3.2a}$$

$$a_n = \frac{2}{T_0} \int_{(T_0)} x(t) \cos(n\omega_0 t)\, \mathrm{d}t, \tag{3.2b}$$

$$b_n = \frac{2}{T_0} \int_{(T_0)} x(t) \sin(n\omega_0 t)\, \mathrm{d}t, \tag{3.2c}$$

where the integration limit (T_0) signifies that the integral is to be taken over one whole period of the signal (e.g., from $-T_0/2$ to $T_0/2$ or from 0 to T_0). Note that the coefficient a_0 is called the DC or mean coefficient since it states signals average. Example 3.1 illustrates how the trigonometric Fourier series can be calculated for the rectangular pulse train signal in Figure 3.1a.

Example 3.1: Trigonometric Fourier series of a rectangular pulse train

Consider the rectangular pulse train shown in Figure 3.1a. The trigonometric Fourier coefficients for this signal can be calculated using (3.2). For simplicity, we

[1] In honor of the French mathematician and physicist Jean-Baptiste Joseph Fourier who discovered the Fourier series.

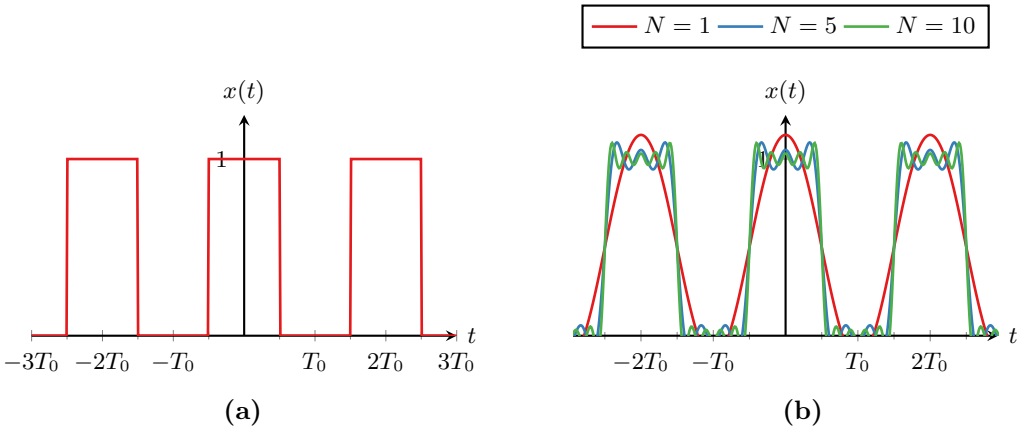

Figure 3.1. Fourier series expansion of the rectangular pulse train. (a) Rectangular pulse train, and (b) Fourier series approximation with $N = 1$, $N = 5$, and $N = 10$ terms.

choose the integration limits $t = -T_0/2$ to $t = T_0/2$. This yields

$$a_0 = \frac{1}{T_0}\int_{-T_0/2}^{T_0/2} x(t)\,\mathrm{d}t = \frac{1}{T_0}\int_{-T_0/4}^{T_0/4} 1\,\mathrm{d}t = \frac{1}{T_0}[t]_{-T_0/4}^{T_0/4} = \frac{1}{2}$$

for the DC offset,

$$\begin{aligned} a_n &= \frac{2}{T_0}\int_{-T_0/2}^{T_0/2} x(t)\cos(n\omega_0 t)\,\mathrm{d}t = \frac{2}{T_0}\int_{-T_0/4}^{T_0/4} \cos(n\omega_0 t)\,\mathrm{d}t \\ &= \frac{2}{T_0}\left[\frac{\sin(n\omega_0 t)}{n\omega_0}\right]_{-T_0/4}^{T_0/4} = \frac{2}{T_0}\left[\frac{\sin(n\omega_0 T_0/4)}{n\omega_0} - \frac{\sin(-n\omega_0 T_0/4)}{n\omega_0}\right] \\ &= \frac{2}{T_0}\left[\frac{2\sin(n\omega_0 T_0/4)}{n\omega_0}\right] = \frac{4\sin(n\omega_0 T_0/4)}{n\omega_0 T_0} = \frac{\sin(n2\pi/4)}{n2\pi/4} \\ &= \mathrm{sinc}\left(\frac{n}{2}\right) \end{aligned}$$

for the cosine coefficients, and

$$\begin{aligned} b_n &= \frac{2}{T_0}\int_{-T_0/2}^{T_0/2} x(t)\sin(n\omega_0 t)\,\mathrm{d}t = \frac{2}{T_0}\int_{-T_0/4}^{T_0/4} \sin(n\omega_0 t)\,\mathrm{d}t \\ &= \frac{2}{T_0}\left[-\frac{\cos(n\omega_0 t)}{n\omega_0}\right]_{-T_0/4}^{T_0/4} \\ &= 0 \end{aligned}$$

for the sine coefficients.

Figure 3.1b shows the result of truncating the infinite sum of the Fourier series at $N = 1$, $N = 5$, and $N = 10$. As it can be seen, the more terms we add, the closer the signal obtained through the series comes to the original signal. The latter is, however, only recovered if $N \to \infty$.

Before moving on, we have to recognize that this is a very strong (a formal derivation is given in Appendix 3.A) and important statement: Recall that in Section 2.2.3, the sine-in sine-out principle was discussed, which stated that if the input to an LTI system is a sine signal, the output of the system will also be a sine signal of the same frequency but with scaled amplitude and a possible phase shift. Thus, if periodic signals can be decomposed into the Fourier series (3.1), the output of a periodic signal must contain the same sine and cosine terms as the input signal (due to the superposition principle $\alpha x_1(t) + \beta x_2(t) \mapsto \alpha y_1(t) + \beta y_2(t)$). Thus, the system can be thought of as acting on each of the sine and cosine signals independently (linear combination) through some (complex) coefficient $H(n\omega_0) = |H(n\omega_0)|e^{\mathrm{j}\angle H(n\omega_0)}$.

Using Euler's identities for the sine and cosine signals (3.1), we can also find an alternative form for the Fourier series:

$$\begin{aligned} x(t) &= a_0 + \sum_{n=1}^{\infty} \left[a_n \frac{e^{\mathrm{j}\, n\omega_0 t} + e^{-\mathrm{j}\, n\omega_0 t}}{2} + b_n \frac{e^{\mathrm{j}\, n\omega_0 t} - e^{-\mathrm{j}\, n\omega_0 t}}{2\,\mathrm{j}} \right] \\ &= a_0 + \sum_{n=1}^{\infty} \frac{a_n - \mathrm{j}\, b_n}{2} e^{\mathrm{j}\, n\omega_0 t} + \frac{a_n + \mathrm{j}\, b_n}{2} e^{-\mathrm{j}\, n\omega_0 t}. \end{aligned}$$

Now, letting

$$c_n = \begin{cases} \frac{1}{2}(a_n + \mathrm{j}\, b_n) & n < 0, \\ a_n & n = 0, \\ \frac{1}{2}(a_n - \mathrm{j}\, b_n) & n > 0, \end{cases}$$

and rewriting the sum to go from $-\infty$ to ∞ absorbes the terms containing negative exponents into the main sum such that $e^{-\mathrm{j}\, n\omega_0 t} = e^{\mathrm{j}(-n)\omega t}$. This then yields

$$x(t) = \sum_{n=-\infty}^{\infty} c_n e^{\mathrm{j}\, n\omega_0 t}.$$

This is called the *exponential Fourier series* for continuous time signals and is given formally in Definition 3.1.

Definition 3.1: Exponential continuous time Fourier series

Any T_0-periodic continuous time signal $x(t)$ can be expressed in terms of its exponential continuous time Fourier series

$$x(t) = \sum_{n=-\infty}^{\infty} c_n e^{\mathrm{j}\, n\omega_0 t} \tag{3.3}$$

where $\omega_0 = \frac{2\pi}{T_0}$ is the *fundamental frequency* and

$$c_n = \frac{1}{T_0} \int_{(T_0)} x(t) e^{-\mathrm{j}\, n\omega_0 t}\, \mathrm{d}t \tag{3.4}$$

are the complex Fourier coefficients of the $n-1$*th harmonic frequency* $n\omega_0$.

Naturally, the coefficients of the trigonometric and exponential Fourier series are closely related (as seen in the derivation of the exponential Fourier series). In particular, the following relationships hold:

$$c_0 = a_0, \quad c_n = \frac{a_n - \mathrm{j}\, b_n}{2}, \quad c_{-n} = \frac{a_n + \mathrm{j}\, b_n}{2}, \quad \text{for } n \geq 1, \tag{3.5a}$$

and

$$a_0 = c_0, \quad a_n = 2\,\mathrm{Re}\{c_n\}, \quad b_n = -2\,\mathrm{Im}\{c_n\}, \quad \text{for } n \geq 1. \tag{3.5b}$$

Furthermore, from (3.5a) it follows that the exponential Fourier series' coefficients for n and $-n$ are a complex conjugate pair such that

$$c_n = c_{-n}^*. \tag{3.6}$$

An important property of the Fourier series is that it can split a periodic signal in its mean, even, and odd components. As discussed above, the signal's mean is reflected in the mean coefficient a_0. Furthermore, recall that the cosine is an even and the sine an odd signal. Hence, the even part of the signal is reflected in the cosine coefficients and the odd part in the sine coefficients. Thus, it also holds that:

- If $x(t)$ is an even signal, $b_n = 0$, and
- if $x(t)$ is an odd signal, $a_n = 0$.

Furthermore, from (3.5a) it can be seen that for the complex coefficients of the exponential Fourier series it must hold that

- If $x(t)$ is an even signal, c_n is purely real (because of $b_n = 0$), and
- if $x(t)$ is an odd signal, c_n is purely imaginary (because of $a_n = 0$).

This was already encountered in Example 3.1 where an even signal was considered and the sine coefficients became $b_n = 0$ and is further illustrated in Example 3.2.

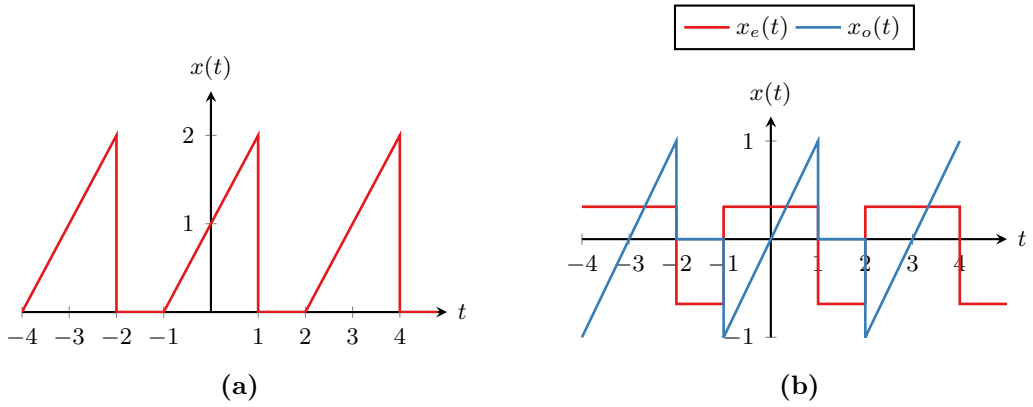

Figure 3.2. Decomposition of the sawtooth signal in its even ($x_e(t)$) and odd ($x_o(t)$) components using the Fourier series (the DC offset $a_0 = \frac{2}{3}$ is not shown): (a) Sawtooth signal and 3.2b even and odd components.

Example 3.2: Exponential Fourier series for a sawtooth signal

One period of the sawtooth signal in Figure 3.2a can be described as

$$x(t) = \begin{cases} t+1 & \text{for } -1 \le t \le 1, \\ 0 & \text{for } 1 < t < 2. \end{cases}$$

The exponential Fourier series coefficients are

$$\begin{aligned} c_n &= \frac{1}{T_0}\int_{(T_0)} x(t)e^{-\mathrm{j}\,n\omega_0 t}\,\mathrm{d}t \\ &= \frac{1}{T_0}\int_{-1}^{1}(t+1)e^{-\mathrm{j}\,n\omega_0 t}\,\mathrm{d}t \\ &= \frac{1}{T_0}\left[\int_{-1}^{1} te^{-\mathrm{j}\,n\omega_0 t}\,\mathrm{d}t + \int_{-1}^{1} e^{-\mathrm{j}\,n\omega_0 t}\,\mathrm{d}t\right]. \end{aligned}$$

The second integral above is given by

$$\begin{aligned} \int_{-1}^{1} e^{-\mathrm{j}\,n\omega_0 t}\,\mathrm{d}t &= \frac{1}{\mathrm{j}\,n\omega_0}\left[-e^{-\mathrm{j}\,n\omega_0 t}\right]_{-1}^{1} \\ &= \frac{1}{\mathrm{j}\,n\omega_0}(-e^{-\mathrm{j}\,n\omega_0} + e^{\mathrm{j}\,n\omega_0}) \\ &= \frac{2\sin(n\omega_0)}{n\omega_0}. \end{aligned}$$

Next, using integration by parts ($\int u(t)v'(t)\,\mathrm{d}t = u(t)v(t) - \int u'(t)v(t)\,\mathrm{d}t$ with $u(t) = t$ and $v'(t) = e^{-\mathrm{j}\,n\omega_0 t}$) in the first integral yields

$$\begin{aligned}
\int_{-1}^{1} te^{-\mathrm{j}\,n\omega_0 t}\,\mathrm{d}t &= -\frac{1}{\mathrm{j}\,n\omega_0}\left[te^{-\mathrm{j}\,n\omega_0 t}\right]_{-1}^{1} + \frac{1}{\mathrm{j}\,n\omega_0}\int_{-1}^{1} e^{-\mathrm{j}\,n\omega_0 t}\,\mathrm{d}t \\
&= -\frac{1}{\mathrm{j}\,n\omega_0}(e^{-\mathrm{j}\,n\omega_0} + e^{\mathrm{j}\,n\omega_0}) + \frac{1}{(\mathrm{j}\,n\omega_0)^2}\left[-e^{-\mathrm{j}\,n\omega_0 t}\right]_{-1}^{1} \\
&= \frac{2\,\mathrm{j}\cos(n\omega_0)}{n\omega_0} + \frac{1}{(\mathrm{j}\,n\omega_0)^2}(-e^{-\mathrm{j}\,n\omega_0} + e^{\mathrm{j}\,n\omega_0}) \\
&= \frac{2\,\mathrm{j}\cos(n\omega_0)}{n\omega_0} - \frac{2\,\mathrm{j}\sin(n\omega_0)}{(n\omega_0)^2}
\end{aligned}$$

Thus, the coefficients are given by

$$c_n = \frac{2}{T_0}\left[\frac{\sin(n\omega_0)}{n\omega_0} + \mathrm{j}\left(\frac{\cos(n\omega_0)}{n\omega_0} - \frac{\sin(n\omega_0)}{(n\omega_0)^2}\right)\right]$$

with $T_0 = 3$ and $\omega_0 = \frac{2\pi}{T_0} = \frac{2\pi}{3}$.
Using (3.5b), it follows that

$$\begin{aligned}
a_0 &= c_0 = \frac{2}{3}, \\
a_n &= 2\,\mathrm{Re}\{c_n\} = \frac{4\sin(n\omega_0)}{3n\omega_0}, \\
b_n &= -2\,\mathrm{Im}\{c_n\} = -\frac{4}{3}\left(\frac{\cos(n\omega_0)}{n\omega_0} - \frac{\sin(n\omega_0)}{(n\omega_0)^2}\right).
\end{aligned}$$

The sawtooth signal $x(t)$ can thus be expressed as

$$x(t) = \frac{2}{3} + \underbrace{\sum_{n=1}^{\infty} a_n \cos\left(\frac{2n\pi}{3}t\right)}_{\triangleq x_e(t)} + \underbrace{\sum_{n=1}^{\infty} b_n \sin\left(\frac{2n\pi}{3}t\right)}_{\triangleq x_o(t)}$$

where $x_e(t)$ and $x_o(t)$ denote the even and odd components of $x(t)$, which are shown in Figure 3.2b.

To see how the different harmonics of the Fourier series contribute to the overall signal, it is illustrative to plot the coefficients of Fourier series either as a function of the coefficient number n or the frequency $n\omega_0$. Since the coefficients c_n are complex numbers, this typically consists of two plots: One for the magnitude $|c_n|$ and one for the phase $\angle c_n$ as illustrated in Figure 3.3 for the signal in Example 3.2.

Finally, Example 3.3 shows another example of an important Fourier series, the one for the sine signal.

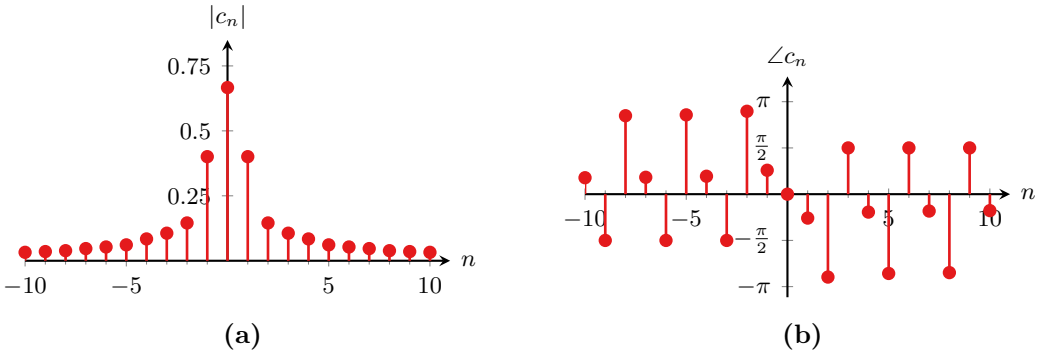

Figure 3.3. Plots of the Fourier series coefficients for the signal in Example 3.2. (a) Magnitude and (b) angle.

Example 3.3: Fourier series for the sine signal

The Fourier series coefficients for the sine

$$x(t) = \sin(\omega_0 t).$$

is given by

$$\begin{aligned} c_n &= \frac{1}{T_0}\int_0^{T_0} \sin(\omega_0 t) e^{-\mathrm{j}\, n\omega_0 t}\,\mathrm{d}t \\ &= \frac{1}{T_0}\int_0^{T_0} \frac{e^{\mathrm{j}\,\omega_0 t} - e^{-\mathrm{j}\,\omega_0 t}}{2\,\mathrm{j}} e^{-\mathrm{j}\, n\omega_0 t}\,\mathrm{d}t \\ &= \frac{1}{2\,\mathrm{j}\,T_0}\int_0^{T_0} e^{\mathrm{j}\,\omega_0 t} e^{-\mathrm{j}\, n\omega_0 t}\,\mathrm{d}t - \int_0^{T_0} e^{-\mathrm{j}\,\omega_0 t} e^{-\mathrm{j}\, n\omega_0 t}\,\mathrm{d}t \\ &= \frac{1}{2\,\mathrm{j}\,T_0}\int_0^{T_0} e^{\mathrm{j}(1-n)\omega_0 t}\,\mathrm{d}t - \int_0^{T_0} e^{-\mathrm{j}(1+n)\omega_0 t}\,\mathrm{d}t \end{aligned}$$

Since the integrands in the above are over a whole period of a complex oscillation, they are zero unless $n = 1$ (first integral) and $n = -1$ (second integral). Thus, the integrands are orthogonal (see Section 2.1.6) for all choices of n except -1 and 1. In this case, we have that

$$\begin{aligned} c_1 &= \frac{1}{2\,\mathrm{j}\,T_0}\int_0^{T_0} e^{\mathrm{j}\,0\omega_0 t}\,\mathrm{d}t - \int_0^{T_0} e^{-\mathrm{j}\,2\omega_0 t}\,\mathrm{d}t = \frac{1}{2\,\mathrm{j}\,T_0}\int_0^{T_0}\mathrm{d}t \\ &= \frac{1}{2\,\mathrm{j}} \end{aligned}$$

and

$$c_{-1} = \frac{1}{2\,\mathrm{j}\,T_0}\int_0^{T_0} e^{\mathrm{j}\,2\omega_0 t}\,\mathrm{d}t - \int_0^{T_0} e^{-\mathrm{j}\,0\omega_0 t}\,\mathrm{d}t = -\frac{1}{2\,\mathrm{j}\,T_0}\int_0^{T_0}\mathrm{d}t$$
$$= -\frac{1}{2\,\mathrm{j}}$$

Hence, the coefficients are

$$c_n = \begin{cases} \frac{1}{2\,\mathrm{j}} & \text{for } n = 1, \\ -\frac{1}{2\,\mathrm{j}} & \text{for } n = -1, \\ 0 & \text{otherwise.} \end{cases} \tag{3.7}$$

3.2 Continuous Time Fourier Transform

3.2.1 Definition

Decomposing periodic signals using the Fourier series introduced in the previous section turned out to give a lot of insight into the signals composition. Furthermore, due to the sine-in sine-out principle, the output signal of a linear system is known to contain the same components as the periodic input signal. One limitation, however, is that the Fourier series is only applicable for periodic signals. In practice, many signals are aperiodic and thus, a natural question is whether a similar tool exists for aperiodic signals.

Indeed, there is such a tool available in the form of the *continuous time Fourier transform*. An aperiodic signal can be interpreted as a periodic signal that repeats after an infinite period, that is, the signal's period T_0 approaches infinity. In this case, the fundamental frequency $\omega_0 = \frac{2\pi}{T_0}$ becomes infinitely small, meaning that when plotting the coefficients as a function of $\omega = n\omega_0$, the coefficients move closer and closer together until a continuous curve is obtained.

Formally, consider the Fourier series representation of the periodic signal $x(t)$ given by

$$x(t) = \sum_{n=-\infty}^{\infty} c_n e^{\mathrm{j}\,n\omega_0 t}$$
$$= \sum_{n=-\infty}^{\infty}\left[\frac{1}{T_0}\int_{-T_0/2}^{T_0/2} x(t)e^{-\mathrm{j}\,n\omega_0 t}\,\mathrm{d}t\right] e^{\mathrm{j}\,n\omega_0 t}.$$

Introducing the limit $T_0 \to \infty$ for aperiodic signals yields

$$\begin{aligned} x(t) &= \lim_{T_0 \to \infty} \sum_{n=-\infty}^{\infty} \left[\frac{1}{T_0} \int_{-T_0/2}^{T_0/2} x(t) e^{-\mathrm{j}\, n\omega_0 t} \,\mathrm{d}t \right] e^{\mathrm{j}\, n\omega_0 t} \\ &= \lim_{T_0 \to \infty} \sum_{n=-\infty}^{\infty} \left[\int_{-T_0/2}^{T_0/2} x(t) e^{-\mathrm{j}\, n\omega_0 t} \,\mathrm{d}t \right] e^{\mathrm{j}\, n\omega_0 t} \frac{1}{T_0} \end{aligned}$$

As outlined above, for $T_0 \to \infty$, ω_0 approaches $\mathrm{d}\omega$ and thus, $n\omega_0$ becomes a point on the ω-axis, that is, $n\omega_0 \to \omega$. Furthermore, since $\frac{1}{T_0} = \frac{\omega_0}{2\pi}$, which in turn approaches $\frac{\mathrm{d}\omega}{2\pi}$, we can take the limit and replace the outer sum by an integral, which yields

$$x(t) = \frac{1}{2\pi} \int_{-\infty}^{\infty} \left[\int_{-\infty}^{\infty} x(t) e^{-\mathrm{j}\,\omega t} \,\mathrm{d}t \right] e^{\mathrm{j}\,\omega t} \,\mathrm{d}\omega. \tag{3.8}$$

The integral term in the brackets in (3.8) is the Fourier transform summarized in Definition 3.2 below.

Definition 3.2: Continuous time Fourier transform

The continuous time Fourier transform $X(\omega)$ with angular frequency ω for the aperiodic continuous time signal $x(t)$ (analysis equation) is defined as

$$X(\omega) = \mathcal{F}\{x(t)\} = \int_{-\infty}^{\infty} x(t) e^{-\mathrm{j}\,\omega t} \,\mathrm{d}t. \tag{3.9}$$

Furthermore, the inverse continuous time Fourier transform (synthesis equation) is defined as

$$x(t) = \mathcal{F}^{-1}\{X(\omega)\} = \frac{1}{2\pi} \int_{-\infty}^{\infty} X(\omega) e^{\mathrm{j}\,\omega t} \,\mathrm{d}\omega. \tag{3.10}$$

As shown in Definition 3.2, a shorthand notation for the Fourier transform is to use the symbol $\mathcal{F}\{\cdot\}$ (and $\mathcal{F}^{-1}\{\cdot\}$ for the inverse Fourier transform). Furthermore, the continuous time signal $x(t)$ and its Fourier transform $X(\omega)$, denoted using the uppercase letter of the signals name, are called a Fourier transform pair, which is often denoted as

$$x(t) \circ\!\!-\!\!\bullet\, X(\omega). \tag{3.11}$$

Example 3.4: Fourier transform of the causal exponential function

Consider the causal exponential signal

$$x(t) = e^{-at} u(t).$$

Its Fourier transform is given by

$$\begin{aligned} X(\omega) &= \int_{-\infty}^{\infty} x(t) e^{-\mathrm{j}\,\omega t}\,\mathrm{d}t \\ &= \int_{-\infty}^{\infty} e^{-at} u(t) e^{-\mathrm{j}\,\omega t}\,\mathrm{d}t \\ &= \int_{0}^{\infty} e^{-at} e^{-\mathrm{j}\,\omega t}\,\mathrm{d}t \\ &= \int_{0}^{\infty} e^{-(a+\mathrm{j}\,\omega)t}\,\mathrm{d}t \\ &= -\frac{1}{a+\mathrm{j}\,\omega}\left[e^{-(a+\mathrm{j}\,\omega)t}\right]_0^{\infty} \\ &= \frac{1}{a+\mathrm{j}\,\omega}. \end{aligned}$$

3.2.2 Spectral Analysis

The Fourier transform $X(\omega)$ is generally a complex number, just like the exponential Fourier series' coefficients c_n. Furthermore, it is a continuous function of the frequency variable ω, hence, it is a function in the *frequency domain*. This leads to the interpretation that the signal $x(t)$ is a superposition of infinitely many complex oscillations $e^{\mathrm{j}\,\omega t}$ with amplitude $|X(\omega)|$ and phase $\angle X(\omega)$. Thus, $X(\omega)$ indicates how strong and with which phase the corresponding oscillation occurs in the signal.

Furthermore, $X(\omega)$ is called the *spectrum* of the signal $x(t)$. Similar to the coefficients c_n, the spectrum can be plotted graphically for easier interpretation. Since $X(\omega)$ is a complex number, the spectrum typically consists of two plots, a magnitude plot for $|X(\omega)|$ and a phase plot for $\angle X(\omega)$ as illustrated in Example 3.5. Note that when referring to *high* or *low* frequencies in a spectrum plot, these are defined relative to how far they are from zero. Frequencies close to zero are low frequencies and frequencies far from zero are high frequencies.

Example 3.5: Frequency domain plots

The Fourier transform pair for the causal exponential decay in Example 3.4 is

$$x(t) = e^{-at}u(t) \circ\!\!-\!\!\bullet\, X(\omega) = \frac{1}{a+\mathrm{j}\,\omega}.$$

The magnitude of the spectrum is given by

$$|X(\omega)| = \left|\frac{1}{a+\mathrm{j}\,\omega}\right| = \frac{1}{|a+\mathrm{j}\,\omega|} = \frac{1}{\sqrt{a^2+\omega^2}},$$

whereas the phase is

$$\angle X(\omega) = \angle\frac{1}{a+\mathrm{j}\,\omega} = -\angle(a+\mathrm{j}\,\omega) = -\arctan\left(\frac{\omega}{a}\right).$$

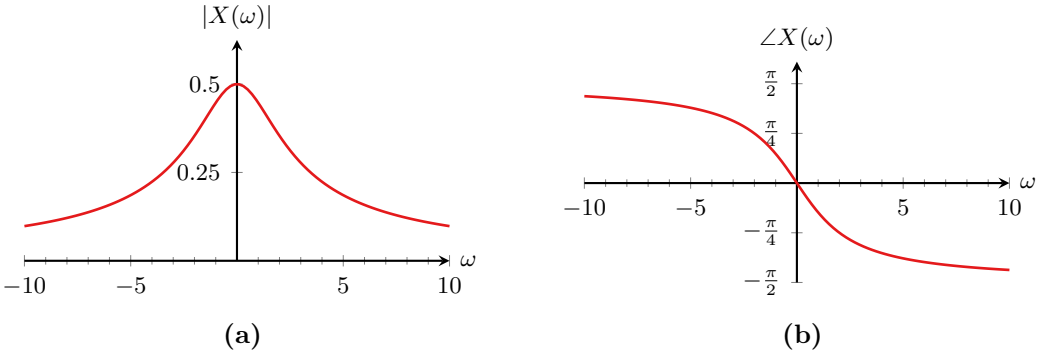

Figure 3.4. Illustration of the spectrum of the causal decaying exponential signal. (a) Magnitude and (b) phase.

Figure 3.4 shows the plots of these two functions for $a = 0.5$, that is, the magnitude and phase spectra of the causal signal. As it can be seen, the magnitude plot is even ($|X(-\omega)| = |X(\omega)|$) and the phase plot is odd ($\angle X(-\omega) = -\angle X(\omega)$). This is because the signal is real-valued, which means that each frequency component ω comes with a complex conjugate component at $-\omega$ such that they become a real-valued component together.
Furthermore, the magnitude plot shows that low frequencies have higher magnitude than higher frequencies and thus, the signal consists of more low frequencies than high frequencies. The phase plot shows that low frequencies have a low phase shift, whereas higher frequencies have a higher phase shift up to $\frac{\pi}{2}$.

Note that in many applications, the main interest is in analyzing the magnitude plot. In this case, it is mostly the contributions of the different frequencies that is of interest and thus, the phase plot is not drawn. This is often the case when trying to get qualitative insight into a signal's (or system's) behavior. However, in other applications such as control engineering, the phase plot is very important and must not be omitted.

3.2.3 Properties

The Fourier transform has some very important properties and the most important ones follow below.

Linearity. The Fourier transform is linear, that is, given the two Fourier transform pairs

$$x_1(t) \circ\!\!-\!\!\bullet\, X_1(\omega), \quad \text{and} \quad x_2(t) \circ\!\!-\!\!\bullet\, X_2(\omega),$$

their linear combination in the time domain is a linear combination in the frequency domain:

$$\alpha x_1(t) + \beta x_2(t) \circ\!\!-\!\!\bullet\, \alpha X_1(\omega) + \beta X_2(\omega). \tag{3.12}$$

Duality. The similarity between the Fourier transform and its inverse (see Definition 3.2) results in a symmetric behavior. In particular, if the time and (negated) frequency variables in a transform pair are exchanged, another transform pair is obtained. Formally, if $x(t)$ and $X(\omega)$ are a transform pair, then duality states that another transform pair is obtained according to

$$X(t) \circ\!\!-\!\!\bullet\ 2\pi x(-\omega). \tag{3.13}$$

Time and frequency scaling. The Fourier transform of a compressed signal $x(at)$ is the expanded version of the signals original Fourier transform, that is,

$$x(at) \circ\!\!-\!\!\bullet\ \frac{1}{|a|} X\left(\frac{\omega}{a}\right) \quad \text{for } a \neq 0. \tag{3.14}$$

One way to think of this relationship is as follows. Consider a signal $x(t)$ that is compressed by a factor a. Compressing the signal means that it becomes narrower in the time domain or, in other words, the signal changes more rapidly. These more rapid changes correspond to higher frequencies being present in the signal, which in turn means that the signal's spectrum must be wider to cover these higher frequencies. Since the energy of the signal is now distributed over more frequencies, the amplitude of the individual frequencies is reduced.

Time and frequency shifting. If a signal $x(t)$ is time shifted in the time domain, $x(t - \Delta t)$, the Fourier transform is phase shifted according to

$$x(t - \Delta t) \circ\!\!-\!\!\bullet\ X(\omega) e^{-\mathrm{j}\,\omega \Delta t}. \tag{3.15}$$

In other words, the magnitude of the Fourier transform $|X(\omega)|$ remains unchanged, but the phase of the time-shifted signal becomes $\angle X(\omega) - \omega \Delta t$.

Similarly, if the Fourier transform $X(\omega)$ is shifted in the frequency domain, $X(\omega - \omega_0)$, the transform pair

$$x(t) e^{\mathrm{j}\,\omega_0 t} \circ\!\!-\!\!\bullet\ X(\omega - \omega_0) \tag{3.16}$$

is obtained. This corresponds to a multiplication of the signal $x(t)$ with the complex oscillation $e^{\mathrm{j}\,\omega_0 t}$.

Convolution and multiplication. A convolution between the two signals $x_1(t)$ and $x_2(t)$ in the time domain corresponds to a multiplication in the frequency domain:

$$x_1(t) * x_2(t) \circ\!\!-\!\!\bullet\ X_1(\omega) X_2(\omega). \tag{3.17}$$

Similarly, a multiplication in the time domain yields a convolution in the frequency domain:

$$x_1(t) x_2(t) \circ\!\!-\!\!\bullet\ \frac{1}{2\pi} X_1(\omega) * X_2(\omega). \tag{3.18}$$

Note that the convolution in the frequency domain is scaled by the factor $\frac{1}{2\pi}$. This is due to the fact that we make use of the angular frequency ω rather than the natural frequency f. The convolution property is a very important property as we will see in Section 3.3 and a derivation of this property is provided in Appendix 3.B.

Differentiation and integration. When taking the derivative of a signal $x(t)$, the signal's spectrum is multiplied by the factor $\mathrm{j}\,\omega$, that is,

$$\frac{\mathrm{d}x(t)}{\mathrm{d}t} \circ\!\!-\!\!\bullet\ \mathrm{j}\,\omega X(\omega). \tag{3.19}$$

Furthermore, repeated application of (3.19) yields for higher derivatives

$$\frac{\mathrm{d}^n x(t)}{\mathrm{d}t^n} \circ\!\!-\!\!\bullet\ (\mathrm{j}\,\omega)^n X(\omega).$$

Conversely, since integration is the inverse operation of derivation, it holds that

$$\int_{-\infty}^{t} x(\tau)\,\mathrm{d}\tau \circ\!\!-\!\!\bullet\ \frac{1}{\mathrm{j}\,\omega}X(\omega) + \pi X(0)\delta(\omega). \tag{3.20}$$

Symmetries. It has already been shown that the exponential Fourier series' coefficients for real signals $x(t)$ come in complex conjugate pairs ($c_n = c_{-n}^*$). Similarly, for real signals $x(t)$, the Fourier transform is complex conjugate (Hermitian symmetry) such that

$$X^*(\omega) = X(-\omega). \tag{3.21}$$

That means that:

- $|X(\omega)|$ is even,
- $\angle X(\omega)$ is odd,
- $\mathrm{Re}\{X(\omega)\}$ is even, and
- $\mathrm{Im}\{X(\omega)\}$ is odd.

Furthermore, if $x(t)$ is real and even then $X(\omega)$ is real and even. If $x(t)$ is real and odd, $X(\omega)$ is imaginary and odd. Thus, since we know that the spectrum is symmetric for real-valued signals, it is often enough to only analyze the positive half of the ω-axis. The negative half then automatically follows.

Periodicity. For periodic signals, the spectrum is discrete and vice-versa, that is,

- If $x(t)$ is periodic, $X(\omega)$ is discrete, and
- if $x(t)$ is discrete, $X(\omega)$ is periodic.

Parseval's theorem Recall that the energy for aperiodic signals was given by

$$W = \int_{-\infty}^{\infty} |x(t)|^2\,\mathrm{d}t.$$

Parseval's theorem states that the energy in the time domain must be equal to the energy in the frequency domain. This yields

$$W = \int_{-\infty}^{\infty} |x(t)|^2\,\mathrm{d}t = \frac{1}{2\pi}\int_{-\infty}^{\infty} |X(\omega)|^2\,\mathrm{d}\omega, \tag{3.22}$$

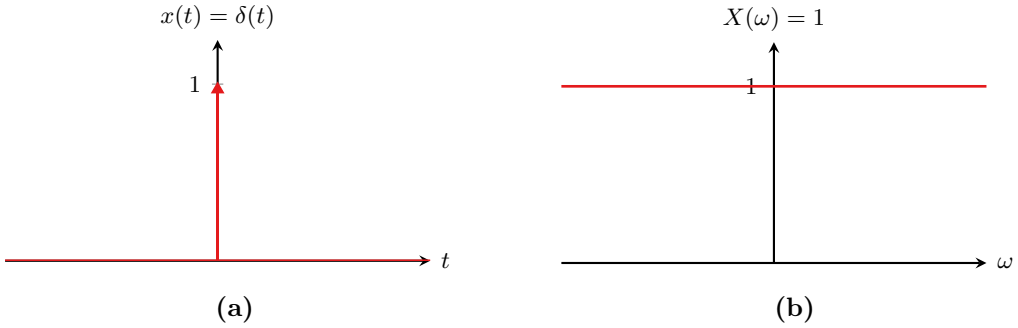

(a) **(b)**

Figure 3.5. The Dirac delta impulse and its Fourier transform. (a) Time domain and (b) frequency domain.

where the factor $\frac{1}{2\pi}$ is again due to the fact that we are working with the angular frequency ω. Note that the function $|X(\omega)|$ is called the *power spectral density* of $x(t)$.

Similarly, for periodic signals, Parseval's theorem states that the power in the time and frequency domains should be equal

$$P = \frac{1}{T_0}\int_{-T_0/2}^{T_0/2} |x(t)|\,\mathrm{d}t = \sum_{n=-\infty}^{\infty} |c_n|^2. \tag{3.23}$$

3.2.4 Fourier Transforms of Elementary Signals

The Fourier transform for a few selected signals have already been shown above. Below follow the Fourier transforms of some of the most important elementary signals.

Dirac delta function. One of the simplest in terms of its Fourier transform is the Dirac delta function $x(t) = \delta(t)$. Its Fourier transform is given by

$$X(\omega) = \int_{-\infty}^{\infty} \delta(t)e^{-j\omega t}\,\mathrm{d}t = e^{-j\omega 0} = 1$$

and thus,

$$x(t) = \delta(t) \circ\!\!-\!\!\bullet\; X(\omega) = 1. \tag{3.24}$$

The spectrum is illustrated in Figure 3.5, which shows that the Dirac delta function contains all frequencies to an equal amount (this is another indicator that this function can not be realized in practice since it would require infinite energy over an infinite range of frequencies).

Constant. The Fourier transform of a constant signal $x(t) = 1$ can be found by using the duality property (3.13) and the transformation of the Dirac delta function. Since $x(t) = 1$, the Fourier transform should be given by (duality)

$$X(\omega) = 2\pi\delta(-\omega).$$

Since $\delta(\omega) = \delta(-\omega)$, we obtain

$$x(t) = 1 \circ\!\!-\!\!\bullet\; X(\omega) = 2\pi\delta(\omega) \tag{3.25}$$

Both functions are shown in Figure 3.6.

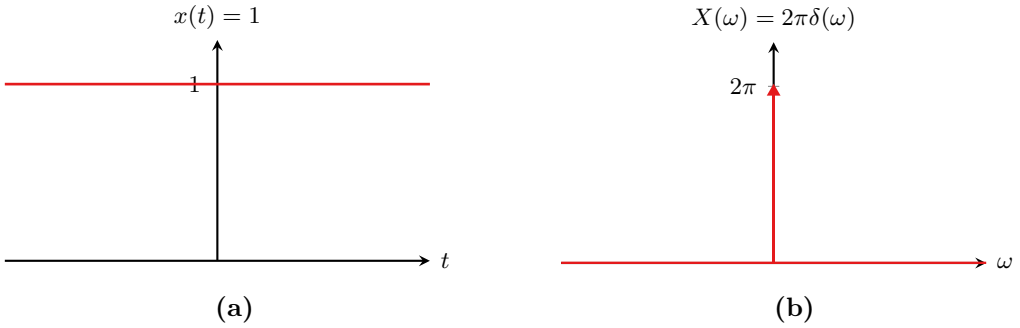

Figure 3.6. The constant function and its Fourier transform. (a) Time domain and (b) frequency domain.

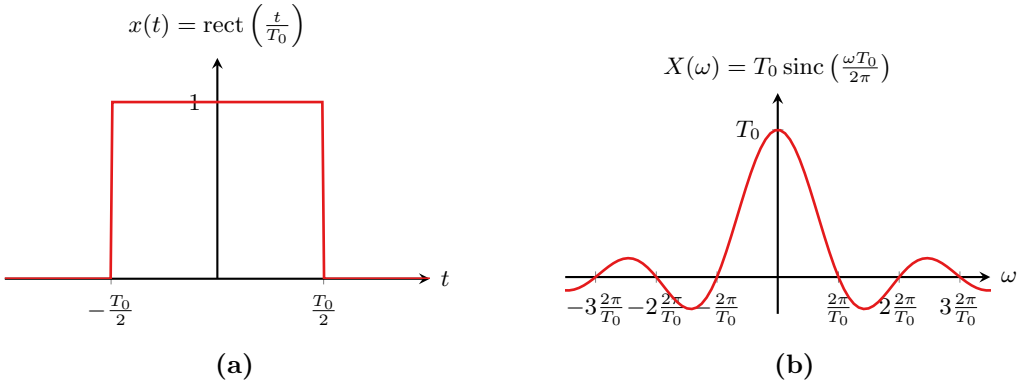

Figure 3.7. The rect function and its Fourier transform. (a) Time domain and (b) frequency domain.

Rectangular pulse. The rectangular pulse $x(t) = \text{rect}\left(\frac{t}{T_0}\right)$ has the Fourier transform

$$X(\omega) = \int_{-\infty}^{\infty} \text{rect}\left(\frac{t}{T_0}\right) e^{-\mathrm{j}\,\omega t}\,\mathrm{d}t = \int_{-T_0/2}^{T_0/2} 1 e^{-\mathrm{j}\,\omega t}\,\mathrm{d}t = \left[\frac{e^{-\mathrm{j}\,\omega t}}{-\mathrm{j}\,\omega}\right]_{-T_0/2}^{T_0/2}$$
$$= \frac{e^{-\mathrm{j}\,\frac{\omega T_0}{2}} - e^{\mathrm{j}\,\frac{\omega T_0}{2}}}{-\mathrm{j}\,\omega}$$

Using Euler's formula for the sine yields

$$X(\omega) = \frac{2\sin\left(\frac{\omega T_0}{2}\right)}{\omega} = T_0 \frac{\sin\left(\frac{\omega T_0}{2\pi}\pi\right)}{\frac{\omega T_0}{2\pi}\pi} = T_0\,\text{sinc}\left(\frac{\omega T_0}{2\pi}\right).$$

Thus, the Fourier transform of a rectangular pulse is the sinc function,

$$x(t) = \text{rect}\left(\frac{t}{T_0}\right) \circ\!\!-\!\!\bullet\; X(\omega) = T_0\,\text{sinc}\left(\frac{\omega T_0}{2\pi}\right), \tag{3.26}$$

which are both illustrated in Figure 3.7.

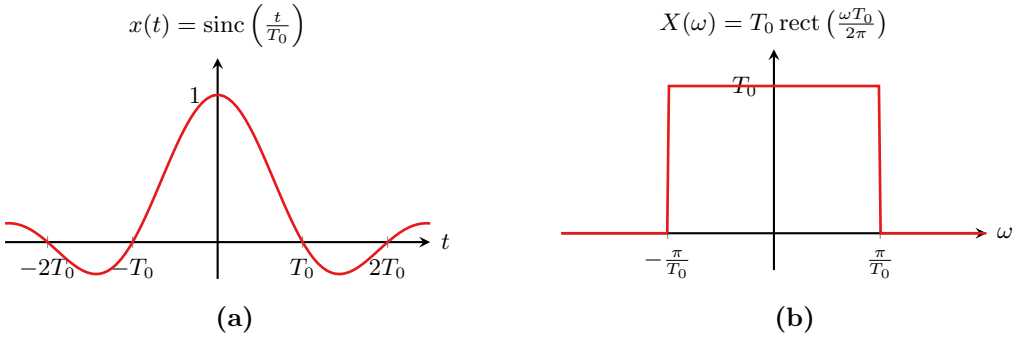

Figure 3.8. The sinc function and its Fourier transform. (a) Time domain and (b) frequency domain.

Sinc function. The Fourier transform for the sinc function $x(t) = \text{sinc}\left(\frac{t}{T_0}\right)$ can again be derived by using the duality principle and the result for the rectangular pulse above (which indicates that the Fourier transform of the sinc function must be a rectangular pulse). In particular, we have that

$$\text{sinc}\left(\frac{t}{T_0}\right) = X_{\text{rect}}\left(\frac{2\pi t}{T_0}\right)$$

where $X_{\text{rect}}(\omega) = \text{sinc}\left(\frac{\omega}{2\pi}\right)$ is the Fourier transform of the unit rectangular pulse. Thus, using the duality property together with time domain scaling yields

$$X(\omega) = 2\pi\frac{T_0}{2\pi}\,\text{rect}\left(\frac{-\omega T_0}{2\pi}\right)$$

and noting that $\text{rect}(\cdot)$ is an even function yields

$$x(t) = \text{sinc}\left(\frac{t}{T_0}\right) \circ\!\!-\!\!\bullet\; X(\omega) = T_0\,\text{rect}\left(\frac{\omega T_0}{2\pi}\right), \tag{3.27}$$

which is shown in Figure 3.8.

Note that sometimes, we are given a rectangular pulse in the frequency domain. In this case, the pulse is often specified in terms of *half* of its with (called the half-sided bandwidth ω_0, see Figure 3.9). In this case, the Fourier transform is

$$X(\omega) = \text{rect}\left(\frac{\omega}{2\omega_0}\right).$$

This leads to the alternative Fourier transform pair given by

$$x(t) = \frac{\omega_0}{\pi}\,\text{sinc}\left(\frac{\omega_0 t}{\pi}\right) \circ\!\!-\!\!\bullet\; X(\omega) = \text{rect}\left(\frac{\omega}{2\omega_0}\right). \tag{3.28}$$

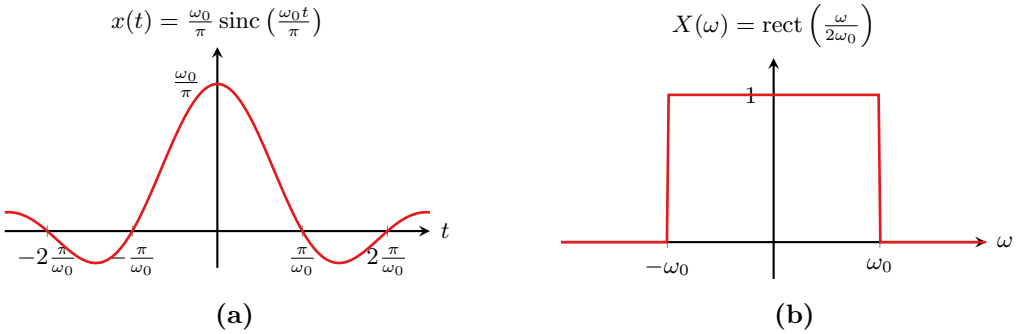

Figure 3.9. The sinc function and its Fourier transform. (a) Time domain and (b) frequency domain.

Periodic signals. The Fourier transform of T_0-periodic signals can be found from their Fourier series. Recall that

$$x(t) = \sum_{n=-\infty}^{\infty} c_n e^{\mathrm{j}\, n\omega_0 t}$$

is the Fourier series representation for a periodic signal $x(t)$. Using this in the Fourier transform yields

$$\begin{aligned} X(\omega) &= \int_{-\infty}^{\infty} \sum_{n=-\infty}^{\infty} c_n e^{\mathrm{j}\, n\omega_0 t} e^{-\mathrm{j}\,\omega t}\,\mathrm{d}t \\ &= \sum_{n=-\infty}^{\infty} c_n \int_{-\infty}^{\infty} e^{\mathrm{j}\, n\omega_0 t} e^{-\mathrm{j}\,\omega t}\,\mathrm{d}t. \end{aligned}$$

The remaining integral can be recognized as the inner product of the two complex oscillations $e^{\mathrm{j}\, n\omega_0 t}$ and $e^{\mathrm{j}\,\omega t}$ (see Section 2.1.6). Since complex oscillations are orthogonal unless their frequencies are equal, we obtain that

$$\int_{-\infty}^{\infty} e^{\mathrm{j}\, n\omega_0 t} e^{-\mathrm{j}\,\omega t}\,\mathrm{d}t = 2\pi\delta(\omega - n\omega_0)$$

and thus,

$$X(\omega) = 2\pi \sum_{n=-\infty}^{\infty} c_n \delta(\omega - n\omega_0). \tag{3.29}$$

As an example, the Fourier transforms of the sine signal is given in Example 3.6.

Example 3.6: Fourier transforms of the sine and cosine signals

It has been shown that the Fourier series representation for the sine signal is (Example 3.3)

$$\sin(\omega_0 t) = \frac{1}{2j}\left(e^{\mathrm{j}\,\omega_0 t} - e^{-\mathrm{j}\,\omega_0 t}\right),$$

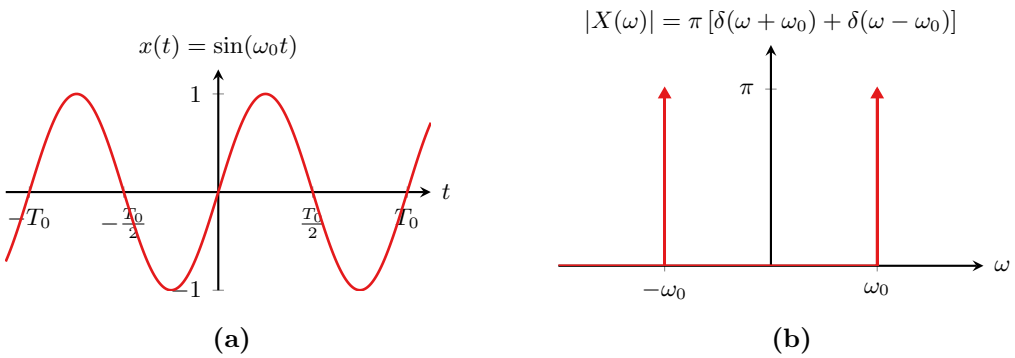

Figure 3.10. The sine function and its Fourier transform (magnitude only). (a) Time domain and (b) frequency domain.

which is equivalent to the representation using Euler's formula. The Fourier series coefficients are

$$c_n = \begin{cases} \frac{1}{2\mathrm{j}} = -\mathrm{j}\,\frac{1}{2} & \text{for } n = 1, \\ -\frac{1}{2\mathrm{j}} = \mathrm{j}\,\frac{1}{2} & \text{for } n = -1, \\ 0 & \text{otherwise,} \end{cases}$$

Thus, the Fourier transform is

$$x(t) = \sin(\omega_0 t) \;\circ\!\!-\!\!\bullet\; X(\omega) = \mathrm{j}\,\pi\,[\delta(\omega+\omega_0) - \delta(\omega-\omega_0)]\,. \tag{3.30}$$

Following the same steps, it can be shown that the Fourier transform for the cosine is

$$x(t) = \cos(\omega_0 t) \;\circ\!\!-\!\!\bullet\; X(\omega) = \pi\,[\delta(\omega+\omega_0) + \delta(\omega-\omega_0)]\,. \tag{3.31}$$

This matches with the expectation that the sine can be thought of being made up of two complex oscillations of frequency ω_0 and $-\omega_0$ (one clockwise rotating vector and one counter clockwise rotating vector, see Section 2.1.1). We also see that there is a $\frac{\pi}{2}$ (90°) phase shift between the sine and cosine, which agrees with the time domain interpretation. Figure 3.10 shows the magnitude spectrum of the sine. It can be seen that this is made up of two Dirac delta functions at the frequency ω_0, which is called a *line spectrum*.
Also note that since the sine signal is a real-valued, odd signal, it results in a purely imaginary, odd spectrum whereas the cosine, a real-valued, even signal gives a real, even spectrum.

Another example that combines the Fourier transforms of different signals as well as the Fourier transform's properties is given in Example 3.7 below.

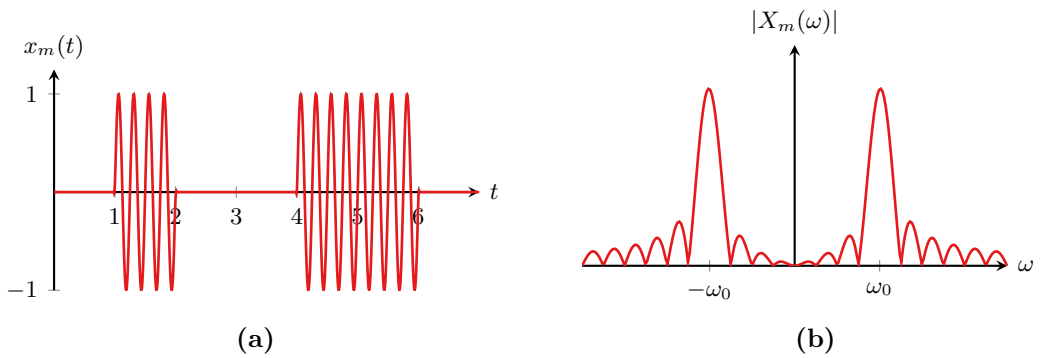

Figure 3.11. Illustration of amplitude shift keying for digital wireless communications. (a) Time domain signal and (b) signal spectrum.

Example 3.7: Spectrum of an amplitude shift keying radio signal

Amplitude shift keying (ASK) is a modulation technique used in simple digital wireless communication systems. In ASK, a sine signal with frequency ω_0 is used as a so-called *carrier* (with *carrier frequency* ω_0) and the ones and zeros are represented using different levels.
In its simplest form, ASK could be expressed as a product of the baseband signal $x_b(t)$ (Example 2.2) and the carrier signal, that is,

$$x_m(t) = x_b(t)\sin(\omega_0 t)$$

as illustrated in Figure 3.11a. Note that this has the problem that zeros are transmitted as radio silence, which can thus be mistaken for no transmission at all. In practice, zeros would be transmitted using a non-zero signal level but for simplicity, this is neglected here.
The Fourier transform of $x_m(t)$ is thus the (scaled) convolution of the Fourier transforms of the baseband signal $x_b(t)$ and the carrier signal $\sin(\omega_c t)$, that is,

$$\begin{aligned} X_m(\omega) &= \frac{1}{2\pi} X_b(\omega) * (\mathrm{j}\,\pi\,[\delta(\omega+\omega_0) - \delta(\omega-\omega_0)]) \\ &= \mathrm{j}\,\frac{1}{2}\,(X_b(\omega+\omega_0) - X_b(\omega-\omega_0))\,. \end{aligned}$$

Since the baseband signal can be expressed as a sum of rectangular signals, its Fourier transform is a sum of sincs. The resulting spectrum is illustrated in Figure 3.11b.

3.3 Frequency Domain Analysis of Continuous Time Systems

So far, only the Fourier transform, its properties, and Fourier transforms for specific signals have been considered. However, there is an important property of the Fourier

transform that has not yet been discussed. Recall that in Section 2.2, it was shown that the output of a linear system can by calculated in the time domain using the convolution between the input signal $x(t)$ and the system's impulse response $h(t)$, that is,

$$y(t) = h(t) * x(t) = \int_{-\infty}^{\infty} h(\tau)x(t-\tau)\,\mathrm{d}\tau. \tag{3.32}$$

While this is a closed-form expression, it is often cumbersome to work with and does not give much insight into the system's properties. However, taking the Fourier transform of $y(t)$ yields

$$\mathcal{F}\{y(t)\} = \mathcal{F}\{h(t) * x(t)\}.$$

Recalling that the Fourier transform turns a convolution in the time domain into a multiplication in the frequency domain then gives that

$$Y(\omega) = H(\omega)X(\omega).$$

Thus, in the frequency domain, the output is the product between the input signals spectrum $X(\omega)$ and the quantity $H(\omega)$. $H(\omega)$ is the Fourier transform of the system's impulse response and it is called the system's *frequency response*. Hence, the system's impulse response $h(t)$ and its frequency response $H(\omega)$ are a Fourier transform pair,

$$h(t) \circ\!\!-\!\!\bullet\, H(\omega). \tag{3.33}$$

This is summarized in Definition 3.3 below.

Definition 3.3: Frequency domain input-output relationship

The Fourier transform of a continuous time LTI system's output signal $Y(\omega)$ is given by the product between the input signal's Fourier transform $X(\omega)$ and the frequency response $H(\omega)$, that is,

$$Y(\omega) = H(\omega)X(\omega). \tag{3.34}$$

Furthermore, the frequency response $H(\omega)$ is the Fourier transform of the impulse response $h(t)$, that is,

$$H(\omega) = \int_{-\infty}^{\infty} h(t)e^{-\mathrm{j}\,\omega t}\,\mathrm{d}t. \tag{3.35}$$

This is an important result for several reasons. First, in most cases, a multiplication in the frequency domain is much easier to carry out than a convolution in the time domain. Thus, the system's output $y(t)$ can be calculated by first calculating the Fourier transform of the input signal and the impulse response followed by taking the inverse Fourier transform of the product of the two as illustrated in Figure 3.12.

Second, while it is difficult to understand a system's properties from the impulse response, the frequency response allows us to gain a lot of insight into the system. In particular, (3.34) essentially states that each frequency (i.e. each complex oscillation)

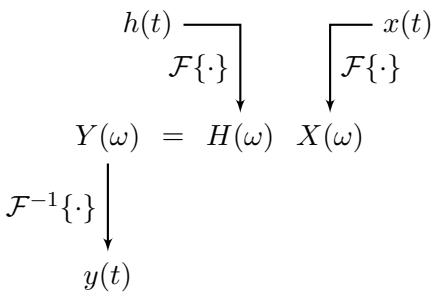

Figure 3.12. Illustration of the frequency domain input-output relationship for continuous time systems.

in $X(\omega)$ is multiplied by a complex number $H(\omega)$ to yield $Y(\omega)$. Using the polar representation $H(\omega) = |H(\omega)|e^{\mathrm{j}\angle H(\omega)}$ shows that this means that each frequency component is

- scaled by the factor $|H(\omega)|$ (*amplified* if $|H(\omega)| > 1$ and *attenuated* if $|H(\omega)| < 1$), and
- phase shifted by the angle $\angle H(\omega)$.

To further illustrate that, we can also write the product itself in terms of the polar form:

$$Y(\omega) = |X(\omega)|e^{\mathrm{j}\angle X(\omega)}|H(\omega)|e^{\mathrm{j}\angle H(\omega)} = |X(\omega)||H(\omega)|e^{\mathrm{j}(\angle X(\omega)+\angle H(\omega))}.$$

By plotting the frequency response's magnitude $|H(\omega)|$ and the angle $\angle H(\omega)$ in a way similar to a signal's spectrum, we can quickly gain insight in how the system will affect input signals of different frequencies (note that such a plot is not called a spectrum but rather a frequency response plot). Example 3.8 illustrates these aspects.

Example 3.8: Frequency domain input-output relationship

Consider the system with the impulse response

$$h(t) = 5e^{-5t}u(t).$$

The system's frequency response is given by

$$\begin{aligned} H(\omega) &= \int_{-\infty}^{\infty} 5e^{-5t}u(t)e^{-\mathrm{j}\,\omega t}\,\mathrm{d}t = 5\int_{0}^{\infty} e^{-5t}e^{-\mathrm{j}\,\omega t}\,\mathrm{d}t = 5\int_{0}^{\infty} e^{-(5+\mathrm{j}\,\omega)t}\,\mathrm{d}t \\ &= 5\left[\frac{e^{-(5+\mathrm{j}\,\omega)t}}{-(5+\mathrm{j}\,\omega)}\right]_{0}^{\infty} \\ &= \frac{5}{5+\mathrm{j}\,\omega}. \end{aligned}$$

Thus, the magnitude is given by

$$|H(\omega)| = \left|\frac{5}{5+\mathrm{j}\,\omega}\right| = \frac{5}{|5+\mathrm{j}\,\omega|} = \frac{5}{\sqrt{25+\omega^2}}$$

and the phase is

$$\angle H(\omega) = \angle\frac{5}{5+\mathrm{j}\,\omega} = -\angle(5+\mathrm{j}\,\omega) = -\arctan\left(\frac{\omega}{5}\right).$$

Next, assume that the input signal is

$$x(t) = \cos(2t) + \cos(10t)$$
$$\Updownarrow$$
$$X(\omega) = \pi\left[\delta(\omega+2) + \delta(\omega-2)\right] + \pi\left[\delta(\omega+10) + \delta(\omega-10)\right].$$

The spectrum of $X(\omega)$ (scaled to magnitude 1 instead of π) as well as the frequency response (magnitude only) of $H(\omega)$ are shown in Figure 3.13a. Multiplying the two yields that the cosine with $\omega = 2\,\mathrm{rad/s}$ is attenuated slightly, whereas the cosine with frequency $\omega = 10\,\mathrm{rad/s}$ is more than halved. In particular, we have that

$$\begin{aligned} |H(2)| = |H(-2)| = 0.93, \quad \angle H(2) = -0.38, \quad \angle H(-2) = -\angle H(2) = 0.38 \\ |H(10)| = |H(-10)| = 0.45, \quad \angle H(10) = -1.1, \quad \angle H(-10) = -\angle H(10) = 1.1. \end{aligned}$$

This yields

$$\begin{aligned} Y(\omega) &= X(\omega)H(\omega) \\ &= 0.93\pi\left[\delta(\omega+2)e^{\mathrm{j}\,0.38} + \delta(\omega-2)e^{-\mathrm{j}\,0.38}\right] \\ &\quad + 0.45\pi\left[\delta(\omega+10)e^{\mathrm{j}\,1.1} + \delta(\omega-10)e^{-\mathrm{j}\,1.1}\right] \end{aligned}$$

for the output signal's spectrum (Figure 3.13b). Finally, taking the inverse Fourier transform yields

$$y(t) = 0.93\cos(2t - 0.38) + 0.45\cos(10t - 1.1).$$

Note that the cosine signal with frequency $\omega = 10\,\mathrm{rad/s}$ is significantly reduced in amplitude and its contribution to the output signal is not very significant anymore. Hence, the system is said to *filter* out (at least) this frequency, a concept that will be discussed more thoroughly in Chapter 5.

Finally, recall that the derivation of the sine in, sine out principle in Section 2.2.3 it was shown that the output of a continuous time LTI system with input $x(t) = \sin(\omega_0 t)$ is

$$y(t) = |H(\omega_0)|\sin(\omega_0 t + \angle H(\omega_0)).$$

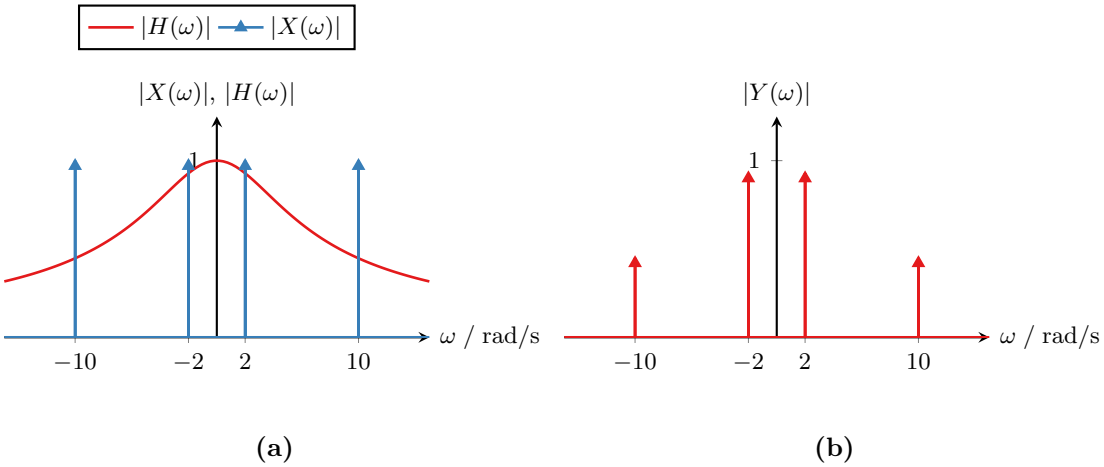

Figure 3.13. Visual illustration of the input-output relationship in the frequency domain. (a) Spectrum of the input signal $X(\omega)$ together with the system's frequency response $H(\omega)$ and (b) spectrum of the output signal $Y(\omega)$.

Indeed, the frequency domain input-output relationship has now shown that the scaling factor $|H(\omega_0)|$ and the phase shift $\angle H(\omega_0)$ actually are the values of the impulse response's Fourier transform for the frequency ω_0.

Example 3.9: Band-limitation of ASK

Consider the ASK signal in Example 3.7 and note that this spectrum is infinite, meaning that it contains all frequencies from $-\infty$ to ∞ (Figure 3.11). Hence, this signal can not be sent out by the transmitter as it would cause interference to other communication systems. Instead, the signal has to be *band-limited*, for example by removing all the frequency components outside the main peak in the spectrum.
This can be achieved by multiplying the spectrum of the modulated signal $X_m(\omega)$ by a rectangular signal in the frequency domain (see Figure 3.14) such that

$$X_t(\omega) = X_m(\omega)H(\omega).$$

In practice, this is implemented as a convolution in the time domain using a *filter*, which will be discussed in Chapter 5.

3.A Derivation of the Continuous Time Fourier Series Coefficients

The continuous time Fourier series is given by

$$x(t) = \sum_{n=-\infty}^{\infty} c_n e^{\mathrm{j}\, n\omega_0 t}.$$

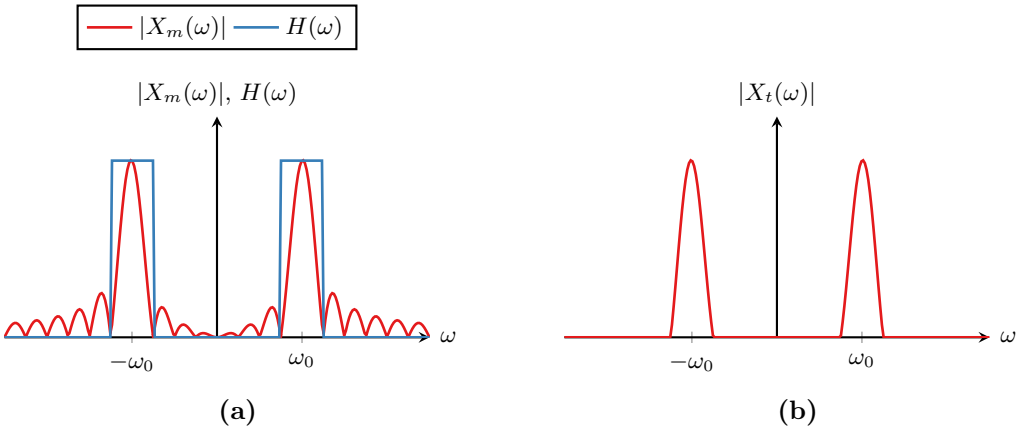

Figure 3.14. Band-limitation for an amplitude shift keying signal. (a) Original spectrum of the ASK signal together with the band-limiting window and (b) the resulting band-limited signal.

To find the expression for the coefficients, assume that we want to minimize the squared error between the Fourier series (right hand side) and the signal $x(t)$ (left hand side), that is, we want to minimize the function (least squares)

$$J(c_m) = \int_0^{T_0} \left(x(t) - \sum_{n=-\infty}^{\infty} c_n e^{\mathrm{j}\, n\omega_0 t} \right)^2 \mathrm{d}t.$$

The minimum of $J(c_m)$ with respect to c_m can be found by taking the derivative, setting it to zero and solving for the coefficient. The derivative is given by

$$\begin{aligned}
\frac{\partial J(c_m)}{\partial c_m} &= \frac{\partial}{\partial c_m} \int_0^{T_0} \left(x(t) - \sum_{n=-\infty}^{\infty} c_n e^{\mathrm{j}\, n\omega_0 t} \right)^2 \mathrm{d}t \\
&= \int_0^{T_0} \frac{\partial}{\partial c_m} \left(x(t) - \sum_{n=-\infty}^{\infty} c_n e^{\mathrm{j}\, n\omega_0 t} \right)^2 \mathrm{d}t \\
&= \int_0^{T_0} -2e^{\mathrm{j}\, m\omega_0 t} \left(x(t) - \sum_{n=-\infty}^{\infty} c_n e^{\mathrm{j}\, n\omega_0 t} \right) \mathrm{d}t
\end{aligned}$$

Rewriting the derivative yields

$$\begin{aligned}
\frac{\partial J(c_m)}{\partial c_m} &= -2 \int_0^{T_0} x(t) e^{\mathrm{j}\, m\omega_0 t}\, \mathrm{d}t + 2 \int_0^{T_0} \left[\sum_{n=-\infty}^{\infty} c_n e^{\mathrm{j}\, n\omega_0 t} \right] e^{\mathrm{j}\, m\omega_0 t}\, \mathrm{d}t \\
&= -2 \int_0^{T_0} x(t) e^{\mathrm{j}\, m\omega_0 t}\, \mathrm{d}t + 2 \sum_{n=-\infty}^{\infty} c_n \int_0^{T_0} e^{\mathrm{j}\, n\omega_0 t} e^{\mathrm{j}\, m\omega_0 t}\, \mathrm{d}t \\
&= -2 \int_0^{T_0} x(t) e^{\mathrm{j}\, m\omega_0 t}\, \mathrm{d}t + 2 \sum_{n=-\infty}^{\infty} c_n \int_0^{T_0} e^{\mathrm{j}(n+m)\omega_0 t}\, \mathrm{d}t
\end{aligned}$$

The second integral is non-zero only for $n = -m$ (orthogonality), and thus,

$$\begin{aligned}\frac{\partial J(c_m)}{\partial c_m} &= -2\int_0^{T_0} x(t)e^{\mathrm{j}\,m\omega_0 t}\,\mathrm{d}t + 2c_{-m}\int_0^{T_0} 1\,\mathrm{d}t \\ &= -2\int_0^{T_0} x(t)e^{\mathrm{j}\,m\omega_0 t}\,\mathrm{d}t + 2c_{-m}T_0.\end{aligned}$$

Setting the result to zero and solving for the coefficient yields

$$c_{-m} = \frac{1}{T_0}\int_0^{T_0} x(t)e^{\mathrm{j}\,m\omega_0 t}\,\mathrm{d}t,$$

and thus, for c_n it must hold that

$$c_m = \frac{1}{T_0}\int_0^{T_0} x(t)e^{-\mathrm{j}\,n\omega_0 t}\,\mathrm{d}t.$$

3.B Derivation of the Convolution Property

In the time domain, the convolution of two signals $x_1(t)$ and $x_2(t)$ is given by

$$x_1(t) * x_2(t) = \int_{-\infty}^{\infty} x_1(\tau)x_2(t-\tau)\,\mathrm{d}\tau.$$

Taking the Fourier transform yields

$$\begin{aligned}\mathcal{F}\{x_1(t) * x_2(t)\} &= \mathcal{F}\left\{\int_{-\infty}^{\infty} x_1(\tau)x_2(t-\tau)\,\mathrm{d}\tau\right\} \\ &= \int_{-\infty}^{\infty}\int_{-\infty}^{\infty} x_1(\tau)x_2(t-\tau)\,\mathrm{d}\tau e^{-\mathrm{j}\,\omega t}\,\mathrm{d}t.\end{aligned}$$

Switching the integration order and rearranging the terms in the integrand yields

$$\begin{aligned}\mathcal{F}\{x_1(t) * x_2(t)\} &= \int_{-\infty}^{\infty}\int_{-\infty}^{\infty} x_1(\tau)x_2(t-\tau)e^{-\mathrm{j}\,\omega t}\,\mathrm{d}t\,\mathrm{d}\tau \\ &= \int_{-\infty}^{\infty} x_1(\tau)\int_{-\infty}^{\infty} x_2(t-\tau)e^{-\mathrm{j}\,\omega t}\,\mathrm{d}t\,\mathrm{d}\tau.\end{aligned}$$

Next, using the time shift property ($x(t-\tau) \circ\!\!-\!\!\bullet\, X(\omega)e^{-\mathrm{j}\,\omega\tau}$) on the inner integral

$$\begin{aligned}\mathcal{F}\{x_1(t) * x_2(t)\} &= \int_{-\infty}^{\infty} x_1(\tau)X_2(\omega)e^{-\mathrm{j}\,\omega\tau}\,\mathrm{d}\tau \\ &= \int_{-\infty}^{\infty} x_1(\tau)e^{-\mathrm{j}\,\omega\tau}\,\mathrm{d}\tau X_2(\omega) \\ &= X_1(\omega)X_2(\omega),\end{aligned}$$

which concludes the derivation. Thus, we have that

$$x_1(t) * x_2(t) \circ\!\!-\!\!\bullet\, X_1(\omega)X_2(\omega).$$

3.C List of Continuous Time Fourier Transforms

Periodic signals

T_0-periodic with $\omega_0 = \frac{2\pi}{T_0}$,

$$x(t) = x(t+T_0) \quad \circ\!\!-\!\!\bullet \quad X(\omega) = 2\pi \sum_{n=-\infty}^{\infty} c_n \delta(\omega - n\omega_0)$$

with Fourier series coefficients

$$c_n = \frac{1}{T_0} \int_0^{T_0} x(t) e^{-\mathrm{j}\, n\omega_0 t}\, \mathrm{d}t$$

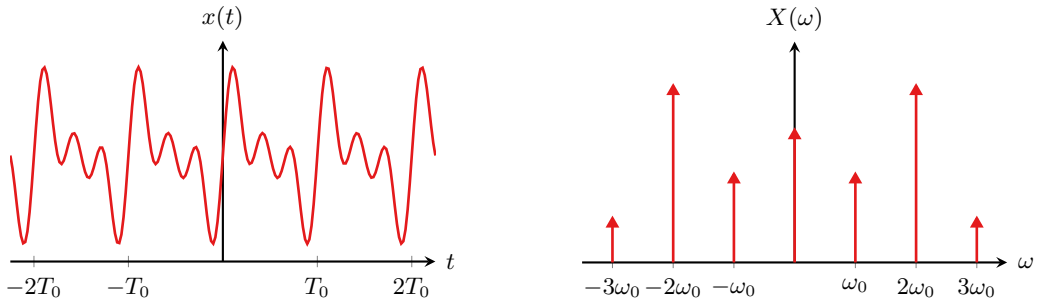

Constant

$$x(t) = 1 \quad \circ\!\!-\!\!\bullet \quad X(\omega) = 2\pi\delta(\omega)$$

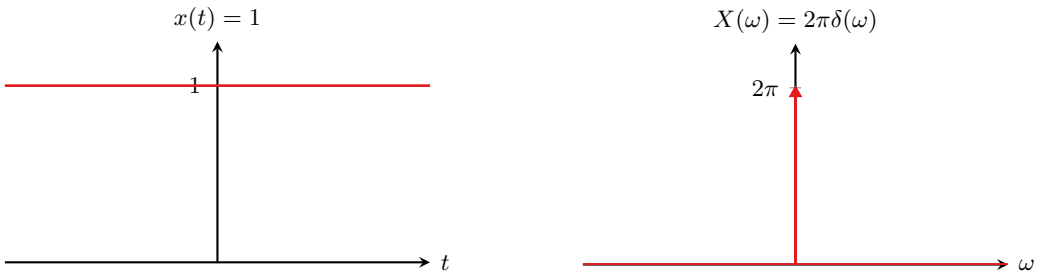

Dirac delta function

$$x(t) = \delta(t) \quad \circ\!\!-\!\!\bullet \quad X(\omega) = 1$$

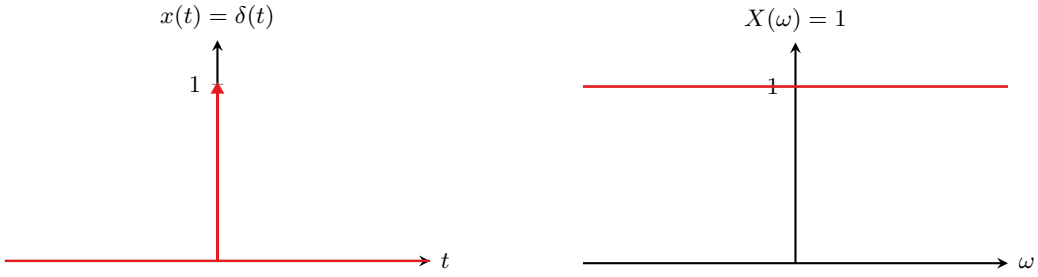

Rectangular pulse

$$x(t) = \text{rect}\left(\frac{t}{T_0}\right) \circ\!\!-\!\!\bullet\; X(\omega) = T_0\,\text{sinc}\left(\frac{\omega T_0}{2\pi}\right)$$

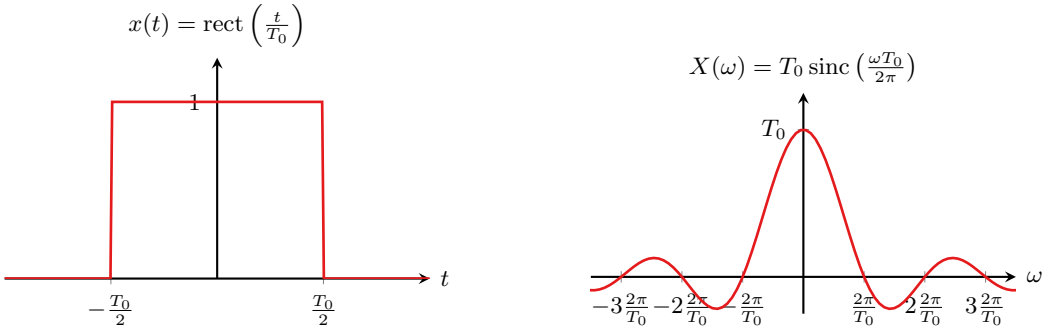

Sinc function

$$x(t) = \text{sinc}\left(\frac{t}{T_0}\right) \circ\!\!-\!\!\bullet\; X(\omega) = T_0\,\text{rect}\left(\frac{\omega T_0}{2\pi}\right)$$

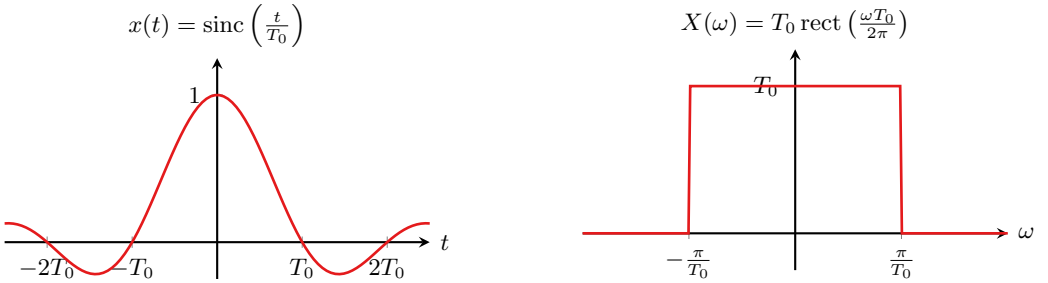

Sinc function (alternative parametrization)

$$x(t) = \frac{\omega_0}{\pi}\,\text{sinc}\left(\frac{\omega_0 t}{\pi}\right) \circ\!\!-\!\!\bullet\; X(\omega) = \text{rect}\left(\frac{\omega}{2\omega_0}\right)$$

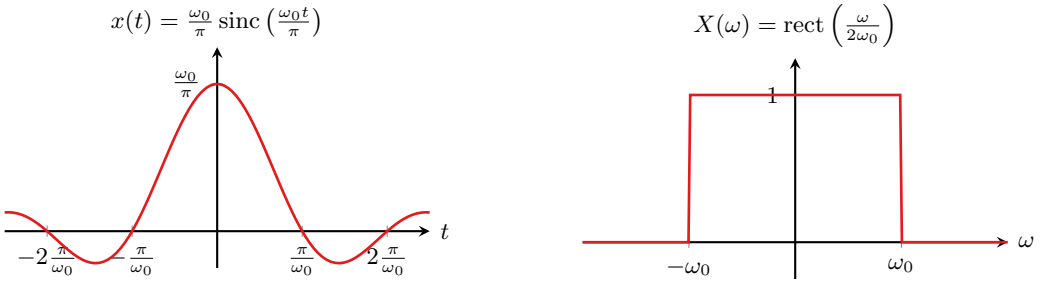

Exponential

$$x(t) = e^{-at}u(t) \circ\!\!-\!\!\bullet\; X(\omega) = \frac{1}{a + \mathrm{j}\,\omega} \quad a > 0$$

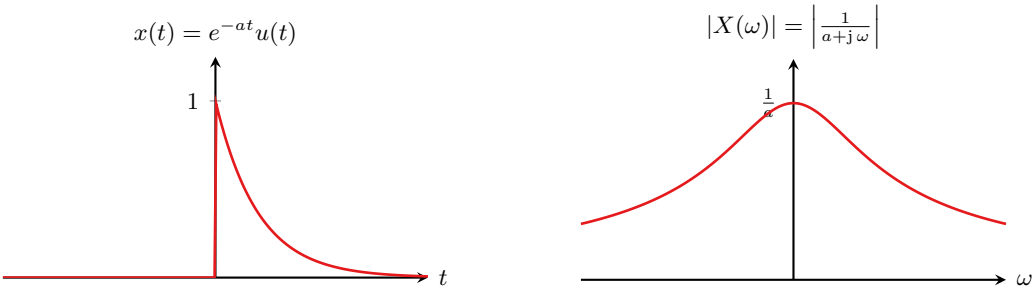

Multiple real-valued poles

$$x(t) = \frac{1}{(n-1)!}t^{n-1}e^{-at}u(t) \circ\!\!-\!\!\bullet\; X(\omega) = \frac{1}{(a + \mathrm{j}\,\omega)^n} \quad a > 0, n = 1, 2, \ldots$$

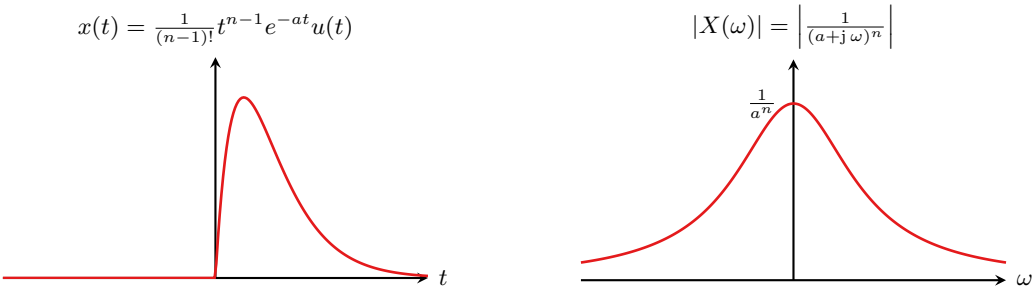

Sine

$$x(t) = \sin(\omega_0 t) \circ\!\!-\!\!\bullet\; X(\omega) = \mathrm{j}\,\pi\,[\delta(\omega + \omega_0) - \delta(\omega - \omega_0)]$$

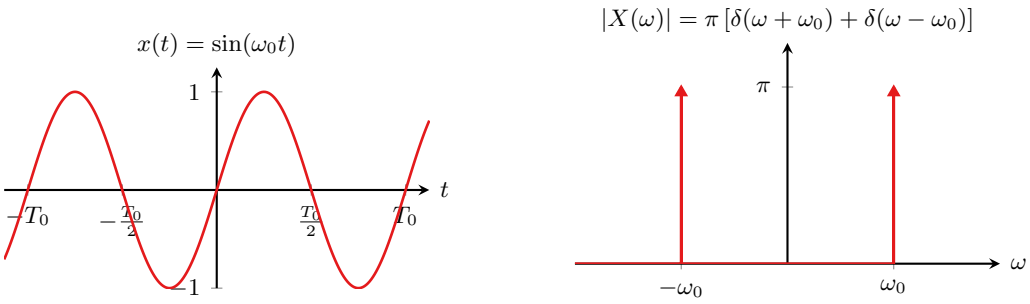

Cosine

$$x(t) = \cos(\omega_0 t) \quad \circ\!\!-\!\!\bullet \quad X(\omega) = \pi\left[\delta(\omega + \omega_0) + \delta(\omega - \omega_0)\right]$$

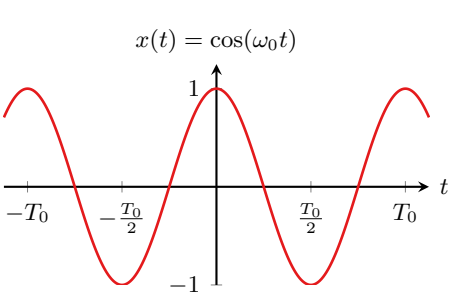

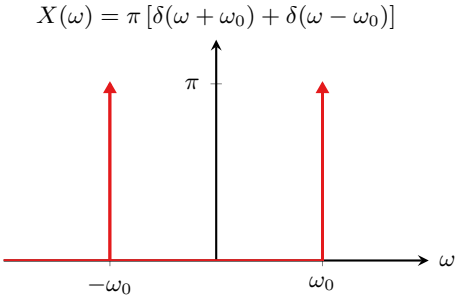

Chapter 4

Laplace Transform

4.1 Definition and Properties

4.1.1 Definition

The Laplace transform is another important tool used to analyze linear dynamic systems. It is closely related to the Fourier transform and shares many of its properties but has some distinct properties as well. Loosely speaking, it can be seen as a generalization of the Fourier transform. The Laplace transform can also be used for solving ordinary differential equations and plays an important role in control engineering.

There are multiple versions of the Laplace transform and here, we will use the *unilateral Laplace transform*. The unilateral Laplace transform is the version predominantly used in engineering and its definition is given in Defintion 4.1 below. Note that we implicitly assume the unilateral Laplace transform when referring to the Laplace transform from here on.

Definition 4.1: Unilateral Laplace transform

The unilateral Laplace transform $X(s)$ of a continuous time signal $x(t)$ is defined as

$$X(s) = \mathcal{L}\{x(t)\} = \int_0^\infty x(t)e^{-st}\,\mathrm{d}t \tag{4.1}$$

where the complex variable $s = \sigma + \mathrm{j}\,\omega$ is the Laplace variable or Laplace operator. The inverse Laplace transform is given by

$$x(t) = \mathcal{L}^{-1}\{X(s)\} = \frac{1}{2\pi\,\mathrm{j}} \int_{\sigma-\mathrm{j}\,\omega}^{\sigma+\mathrm{j}\,\omega} X(s)e^{st}\,\mathrm{d}s. \tag{4.2}$$

Similar to the Fourier transform, the Laplace transform and its inverse transform are denoted using the operators $\mathcal{L}\{\cdot\}$ and $\mathcal{L}^{-1}\{\cdot\}$, respectively. Furthermore, the time domain signal $x(t)$ and its Laplace transform $X(s)$ are again a transform pair

$$x(t) \circ\!\!-\!\!\bullet\, X(s).$$

Example 4.1: Laplace transform of elementary signals

Consider the Laplace transforms of the following signals.

a) The Dirac delta function:

$$\mathcal{L}\{\delta(t)\} = \int_0^\infty \delta(t)e^{-st}\,\mathrm{d}t = e^{-s0} = 1.$$

b) The unit step:

$$\mathcal{L}\{u(t)\} = \int_0^\infty u(t)e^{-st}\,\mathrm{d}t = \int_0^\infty e^{-st}\,\mathrm{d}t = \left[\frac{e^{-st}}{-s}\right]_0^\infty = \frac{1}{s}.$$

c) The causal exponential:

$$\mathcal{L}\{e^{at}u(t)\} = \int_0^\infty e^{at}u(t)e^{-st}\,\mathrm{d}t = \int_0^\infty e^{-(s-a)t}\,\mathrm{d}t = \left[\frac{e^{-(s-a)t}}{-(s-a)}\right]_0^\infty = \frac{1}{s-a}.$$

There are a few important points to point out about the Laplace transform (4.1). First, note that the integration limits of the transform are $t = 0$ and $t = \infty$. The fact that the integration starts at $t = 0$ stems from the fact that we are using the unilateral Laplace transform. This means that the signal $x(t)$ is assumed to be causal, that is, $x(t) = 0$ for $t < 0$. However, this is not a problem since all signals are causal in practice, meaning that they started at some point in time ($t = 0$).

Second, the Laplace operator is a complex variable $s = \sigma + \mathrm{j}\,\omega$. Hence, (4.1) can also be written as

$$\begin{aligned} X(s) &= \int_0^\infty x(t)e^{-st}\,\mathrm{d}t \\ &= \int_0^\infty x(t)e^{-\sigma t}e^{-\mathrm{j}\,\omega t}\,\mathrm{d}t, \end{aligned}$$

which can be interpreted as the Fourier transform of the causal signal $x(t)e^{-\sigma t}$. Indeed, the integral of the Fourier transform does not converge for some signals $x(t)$ and thus, the Fourier transform does not exist for these signals. However, by multiplying a non-converging $x(t)$ with $e^{-\sigma t}$, it can be ensured that the integral converges (for an appropriate choice of σ). Hence, the Laplace transform can be used in cases where the Fourier transform fails.

Third, the integration limits of the inverse Laplace transform (4.2) indicate that the integral is to be taken along a straight line parallel to the $\mathrm{j}\,\omega$-axis in the complex s-plane, which intersects the x-axis at σ. However, in practice, the inverse transform is never calculated using (4.2). Instead, transform tables containing well-known transform pairs are used and a transform table for the elementary signals is shown in Table 4.1. If an expression is not available in the form known from a transform table, partial fraction

Table 4.1. Table of unilateral Laplace transform pairs for causal signals $x(t)$ ($x(t) = 0$ for $t < 0$).

Time domain $x(t)$	Laplace transform $X(s)$	ROC
Dirac delta function		
$x(t) = \delta(t)$	$X(s) = 1$	All s
Unit step		
$x(t) = u(t)$	$X(s) = \frac{1}{s}$	$\mathrm{Re}\{s\} > 0$
Exponential		
$x(t) = e^{-at}u(t)$	$X(s) = \frac{1}{a+s}$	$\mathrm{Re}\{s\} > -a$
Ramp		
$x(t) = tu(t)$	$X(s) = \frac{1}{s^2}$	$\mathrm{Re}\{s\} > 0$
Higher order ramp		
$x(t) = t^n u(t)$	$X(s) = \frac{n!}{s^{n+1}}$	$\mathrm{Re}\{s\} > 0$
Cosine		
$x(t) = \cos(\omega_0 t)u(t)$	$X(s) = \frac{s}{\omega_0^2 + s^2}$	$\mathrm{Re}\{s\} > 0$
Sine		
$x(t) = \sin(\omega_0 t)u(t)$	$X(s) = \frac{\omega_0}{\omega_0^2 + s^2}$	$\mathrm{Re}\{s\} > 0$
Decaying cosine		
$x(t) = e^{-at}\cos(\omega_0 t)u(t)$	$X(s) = \frac{a+s}{(a+s)^2 + \omega_0^2}$	$\mathrm{Re}\{s\} > -a$
Decaying sine		
$x(t) = e^{-at}\sin(\omega_0 t)u(t)$	$X(s) = \frac{\omega_0}{(a+s)^2 + \omega_0^2}$	$\mathrm{Re}\{s\} > -a$

expansion is used to break down the expression into elementary terms (see Appendix A). This will be discussed in more detail in Section 4.2.

Fourth, for each transform pair, there is a region of convergence (ROC). The region of convergence defines the region in the s-plane for which the transform integral in (4.1) converges, that is, that the integral over $x(t)e^{-st}$ is finite and a transform exists (Example 4.2).

Example 4.2: Region of convergence for the Laplace transform

a) The Laplace transform for the Dirac delta function converges for all s:

$$\mathcal{L}\{\delta(t)\} = e^{-s0} = 1,$$

which is 1 independent of the value of s.

b) The Laplace transform for the unit step is

$$\mathcal{L}\{u(t)\} = \int_0^\infty e^{-st}\,\mathrm{d}t = \int_0^\infty e^{-\sigma t}e^{-\mathrm{j}\,\omega t}\,\mathrm{d}t.$$

If $\sigma \leq 0$, the integral is unbounded and diverges. Hence, the integral converges if and only if $\sigma > 0$ and thus, the region of convergence for the unit step is $\mathrm{Re}\{s\} > 0$.

c) The Laplace transform for the causal exponential (with real a) is

$$\mathcal{L}\{e^{-at}u(t)\} = \int_0^\infty e^{-at}e^{-st}\,\mathrm{d}t = \int_0^\infty e^{-(a+\sigma)t}e^{-\mathrm{j}\,\omega t}\,\mathrm{d}t.$$

For the integral to converge, $e^{-(a+\sigma)t}$ must decay to zero as t goes to infinity. This is the case if $a + \sigma > 0$ or $\sigma > -a$. Thus, the region of convergence for the causal exponential is $\mathrm{Re}\{s\} > -a$.

4.1.2 Properties

Many of the properties of the Laplace transform are the same or similar to the properties of the Fourier transform, but there are a few very important properties not shared with the Fourier transform. An overview of the most often used properties follows below.

Linearity. As the Fourier transform, the Laplace transform is a linear transformation too. That is, a linear combination of two signals $x_1(t)$ and $x_2(t)$ in the time domain leads to a linear combination of their Laplace transforms:

$$\alpha x_1(t) + \beta x_2(t) \circ\!\!-\!\!\bullet\ \alpha X_1(s) + \beta X_2(s). \tag{4.3}$$

Time and frequency scaling. A scaling in the time domain leads to the inverse scaling in the Laplace domain, that is,

$$x(at) \circ\!\!-\!\!\bullet\ \frac{1}{a}X\left(\frac{s}{a}\right) \quad \text{for } a > 0. \tag{4.4}$$

Note that the scaling factor must be positive ($a > 0$) since the signal must remain causal even after scaling.

Time and frequency shifting. A shift in the time domain by Δt leads to multiplication with the factor $e^{-s\Delta t}$ in the Laplace domain and vice-versa:

$$x(t-\Delta t) \circ\!\!-\!\!\bullet\ X(s)e^{-s\Delta t} \tag{4.5}$$

and

$$x(t)e^{at} \circ\!\!-\!\!\bullet\ X(s-a). \tag{4.6}$$

Note that Δt must not make $x(t)$ non-causal.

Convolution and multiplication. As for the Fourier transform, a convolution in the time domain turns into a multiplication in the Laplace domain,

$$x_1(t) * x_2(t) \circ\!\!-\!\!\bullet\ X_1(s)X_2(s). \tag{4.7}$$

Similarly, a multiplication in the time domain yields a scaled convolution in the Laplace domain,

$$x_1(t)x_2(t) \circ\!\!-\!\!\bullet\ \frac{1}{2\pi\,\mathrm{j}} X_1(s) * X_2(s). \tag{4.8}$$

Differentiation and integration. One of the most important (and arguably most often used) properties is related to differentiation and integration. In particular, the derivative of a signal $x(t)$ leads to a transform that is scaled by the Laplace operator s *plus the initial conditions*. Formally, the property states that

$$\frac{\mathrm{d}x(t)}{\mathrm{d}t} \circ\!\!-\!\!\bullet\ sX(s) - x(0) \tag{4.9}$$

where $x(0)$ denotes the initial condition. Repeated application of (4.9) yields

$$\frac{\mathrm{d}^n x(t)}{\mathrm{d}t^n} \circ\!\!-\!\!\bullet\ s^n X(s) - s^{n-1}x(0) - s^{n-2}x^{(1)}(0) - \cdots - x^{(n-1)}(0) \tag{4.10}$$

where $x^{(n-1)}(0)$ is the initial condition for the $n-1$th derivative. As we will see in Section 4.2, this is an extremely important and useful property, which can be used to solve differential equations (and more).

Similarly, for integration it holds that

$$\int_0^t x(\tau)\,\mathrm{d}\tau \circ\!\!-\!\!\bullet\ \frac{X(s)}{s}. \tag{4.11}$$

Initial and final value theorems. Finally, the initial value theorem states that the initial value of a signal in the time domain, that is, the value of $x(t)$ as t approaches zero ($t \to 0$) can be calculated in the Laplace domain according to

$$\lim_{t\to 0} x(t) = \lim_{s\to\infty} sX(s), \tag{4.12}$$

given that the initial value exists.

Similarly, the final value theorem is concerned with the signals value as t approaches infinity ($t \to \infty$) and states that

$$\lim_{t\to\infty} x(t) = \lim_{s\to 0} sX(s), \tag{4.13}$$

given that the final value exists.

The initial an final value theorems are again very important in control engineering, where they are used to calculate the long-term behavior of control systems.

4.2 Transfer Function

4.2.1 Differential Equations and Transfer Functions

In Section 2.2, we have seen that linear systems can be completely characterized by their impulse response $h(t)$. However, another way of characterizing linear systems is by using linear ordinary differential equations (ODEs). This is often used in so-called *first principles modeling*, where a system is modeled using, for example, physical or kinematic relationships as illustrated in Example 4.3.

Example 4.3: ODE of a spring-damper system

Consider the spring-damper system in Figure 4.1. From Newton's second law of motion, we know that

$$m\frac{\mathrm{d}^2 y(t)}{\mathrm{d}t^2} = -F_d - F_s + x(t),$$

where F_d is the force in the damper and F_s the force in the spring, which both act in the opposite direction of motion, and $x(t)$ is an external force applied to the system. Assuming linear damping which is proportional to the velocity of the motion, F_d is given by

$$F_d = \eta\frac{\mathrm{d}y(t)}{\mathrm{d}t}$$

with damping constant η. Furthermore, for the spring, Hooke's law states that

$$F_s = ky(t),$$

where k is the spring constant.
Thus, the differential equation describing the system becomes

$$m\frac{\mathrm{d}^2 y(t)}{\mathrm{d}t^2} = -\eta\frac{\mathrm{d}y(t)}{\mathrm{d}t} - ky(t) + x(t)$$

or

$$m\frac{\mathrm{d}^2 y(t)}{\mathrm{d}t^2} + \eta\frac{\mathrm{d}y(t)}{\mathrm{d}t} + ky(t) = x(t).$$

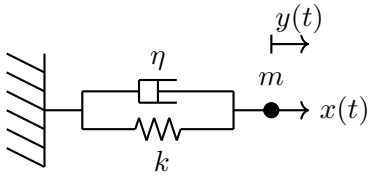

Figure 4.1. A textbook spring-damper system.

In general, the input-output relationship of a continuous time linear dynamic system can be described by the linear ODE

$$a_N \frac{\mathrm{d}^N y(t)}{\mathrm{d}t^N} + a_{N-1} \frac{\mathrm{d}^{N-1} y(t)}{\mathrm{d}t^{N-1}} + \cdots + a_0 y(t) = b_M \frac{\mathrm{d}^M x(t)}{\mathrm{d}t^M} + b_{M-1} \frac{\mathrm{d}^{M-1} x(t)}{\mathrm{d}t^{M-1}} + \cdots + b_0 x(t),$$

or more compactly,

$$\sum_{n=0}^{N} a_n \frac{\mathrm{d}^n y(t)}{\mathrm{d}t^n} = \sum_{m=0}^{M} b_m \frac{\mathrm{d}^m x(t)}{\mathrm{d}t^m}. \tag{4.14}$$

Here, a_n and b_m are constants and the system is called to be of order $\max(N, M)$ (i.e. N if $N > M$ or M if $N < M$).

Assuming zero initial conditions, that is,

$$\frac{\mathrm{d}^{N-1} y(0)}{\mathrm{d}t^{N-1}} = \frac{\mathrm{d}^{N-2} y(0)}{\mathrm{d}t^{N-2}} = \cdots = y(0) = 0,$$

and taking the Laplace transform of (4.14) by using the transform's linearity and differentiation properties yields

$$s^N a_n Y(s) + s^{N-1} a_{N-1} Y(s) + \cdots + a_0 Y(s) = s^M b_M X(s) + s^{M-1} b_{M-1} X(s) + \cdots + b_0 X(s). \tag{4.15}$$

This is already a very important result: The Laplace transform has turned the Nth order ODE in (4.14) into the *algebraic equation* (4.15). While it is rather complicated to work with ODEs directly, handling algebraic equations in the Laplace domain is straight forward.

We can now proceed and simplify (4.15) further by breaking out $Y(s)$ on the left hand side and $X(s)$ on the right hand side

$$Y(s) \left(s^N a_n + s^{N-1} a_{N-1} + \cdots + a_0 \right) = \left(s^M b_M + s^{M-1} b_{M-1} + \cdots + b_0 \right) X(s).$$

Finally, dividing by the factor on the left hand side yields an expression for the output signal $Y(s)$ in the Laplace domain given by

$$Y(s) = \underbrace{\frac{s^M b_M + s^{M-1} b_{M-1} + \cdots + b_0}{s^N a_n + s^{N-1} a_{N-1} + \cdots + a_0}}_{\triangleq H(s)} X(s). \tag{4.16}$$

The fraction to the left of $X(s)$ in (4.16) is called the system's *transfer function* $H(s)$ that *transfers* the input $X(s)$ to the ouptut $Y(s)$.

The transfer function can also be seen to be the ratio between $Y(s)$ and $X(s)$ by dividing by $X(s)$ in (4.16):

$$\frac{Y(s)}{X(s)} = \frac{s^M b_M + s^{M-1} b_{M-1} + \cdots + b_0}{s^N a_n + s^{N-1} a_{N-1} + \cdots + a_0}$$

The transfer function is another important property of linear systems and its formal definition follows in Definition 4.2.

Definition 4.2: Transfer function of continuous time LTI systems

The transfer function $H(s)$ for a linear, continuous time system described by the ODE

$$\sum_{n=0}^{N} a_n \frac{\mathrm{d}^n y(t)}{\mathrm{d}t^n} = \sum_{m=0}^{M} b_m \frac{\mathrm{d}^m x(t)}{\mathrm{d}t^m}.$$

is the ratio between the output $Y(s)$ and the input $X(s)$ given by

$$H(s) = \frac{Y(s)}{X(s)} = \frac{s^M b_M + s^{M-1} b_{M-1} + \cdots + b_0}{s^N a_n + s^{N-1} a_{N-1} + \cdots + a_0}. \tag{4.17}$$

The transfer function consists of two polynomials, the numerator polynomial

$$B(s) = s^M b_M + s^{M-1} b_{M-1} + \cdots + b_0$$

and the denominator polynomial

$$A(s) = s^N a_n + s^{N-1} a_{N-1} Y(s) + \cdots + a_0.$$

Furthermore, the output $Y(s)$ of the system is the product between the input $X(s)$ and the transfer function $H(s)$:

$$Y(s) = H(s)X(s). \tag{4.18}$$

Calculation of the transfer function for the spring-damper system in Example 4.3 is shown in Example 4.4

Example 4.4: Transfer function of the spring-damper system

Consider the spring-damper system in Example 4.3 described by the linear ODE

$$m\frac{\mathrm{d}^2 y(t)}{\mathrm{d}t^2} + \eta\frac{\mathrm{d}y(t)}{\mathrm{d}t} + ky(t) = x(t).$$

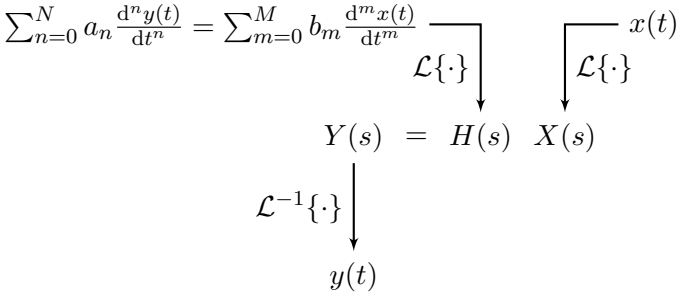

Figure 4.2. Illustration of the process for solving ODEs using the Laplace transform: Transforming the ODE yields the transfer function $H(s)$. The output in the Laplace domain $Y(s)$ is the product between the transfer function and the input's Laplace transform $X(s)$. Finally, the output is obtained by taking the inverse Laplace transform of $Y(s)$.

Assuming zero initial conditions (i.e., $y(0) = 0$ and $\frac{\mathrm{d}y(0)}{\mathrm{d}t} = 0$) and taking the Laplace transform of the differential equation yields

$$s^2 m Y(s) + s\eta Y(s) + kY(s) = X(s).$$

Next, $Y(s)$ is broken out on the left hand side such that

$$Y(s)(s^2 m + s\eta + k) = X(s).$$

Dividing by the term $s^2 m + s\eta + k$ as well as $X(s)$ then yields

$$\frac{Y(s)}{X(s)} = \frac{1}{s^2 m + s\eta + k}$$

and thus, the transfer function for the spring-damper system is

$$H(s) = \frac{1}{s^2 m + s\eta + k}.$$

Having solved the algebraic equation in the Laplace domain, the output of a system can now be calculated for any arbitrary input signal $x(t)$. This is achieved by first calculating the Laplace transform of $x(t)$ to obtain $X(s)$ followed by taking the inverse Laplace transform of the product between the transfer function $H(s)$ and the input $X(s)$ as illustrated in Figure 4.2 and shown in Example 4.5. Note that for higher order systems, the inverse transform may not be readily available from a Laplace transform table. In this case, partial fraction expansion (see Appendix A.7) can be used to break up $Y(s)$ into a linear combination of more elementary transform terms, which can then be transformed back easily.

Example 4.5: Solution to differential equation

Assume that the input to the spring-damper system in Example 4.3 is a unit step, that is,

$$x(t) = u(t) \quad \circ\!\!-\!\!\bullet \quad X(s) = \frac{1}{s}.$$

Furthermore, for simplicity, assume that $\eta = 0$, that is, no damping. This yields the simplified transfer function

$$H(s) = \frac{1}{s^2 m + k} = \frac{\frac{1}{m}}{s^2 + \frac{k}{m}}.$$

The output of the system in the Laplace domain is the product between the transfer function $H(s)$ and the input $X(s)$,

$$Y(s) = H(s)X(s) = \frac{\frac{1}{m}}{s^2 + \frac{k}{m}} \frac{1}{s} = \frac{\frac{1}{m}}{s(s^2 + \frac{k}{m})}.$$

A quick look at Table 4.1 shows that there is no transform pair that corresponds to the expression above. Thus, to find the inverse transform, we have to use partial fraction expansion. First, we rewrite the output as a sum of first and second order terms according to

$$Y(s) = \frac{c_1}{s} + \frac{d_1 s + e_1}{s^2 + \frac{k}{m}}.$$

Expanding the fraction yields

$$\begin{aligned} Y(s) &= \frac{c_1(s^2 + \frac{k}{m}) + s(d_1 s + e_1)}{s(s^2 + \frac{k}{m})} \\ &= \frac{c_1 s^2 + c_1 \frac{k}{m} + d_1 s^2 + e_1 s}{s^2 + \frac{k}{m}} \\ &= \frac{s^2(c_1 + d_1) + e_1 s + c_1 \frac{k}{m}}{s^2 + \frac{k}{m}} \end{aligned}$$

Comparing the numerator of the original output above and the expanded partial fraction expansion shows that the following equations must hold for the coefficients to match:

$$\begin{aligned} c_1 + d_1 &= 0, \\ e_1 &= 0, \\ c_1 \frac{k}{m} &= \frac{1}{m}, \end{aligned}$$

from which it follows that $c_1 = \frac{1}{k}$ and $d_1 = -c_1 = -\frac{1}{k}$.

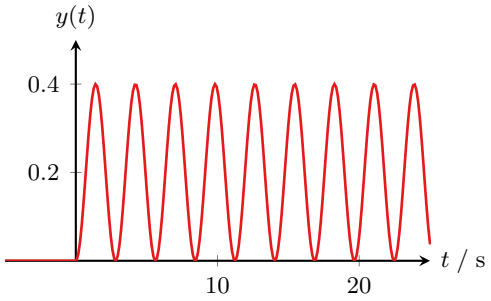

Figure 4.3. Output signal for the spring-damper system in Example 4.5.

Thus, the partial fraction expansion of $Y(s)$ is

$$Y(s) = \frac{\frac{1}{k}}{s} - \frac{\frac{1}{k}s}{s^2 + \frac{k}{m}} = \frac{1}{k}\left(\frac{1}{s} - \frac{s}{s^2 + \frac{k}{m}}\right).$$

Taking the inverse Laplace transform using Table 4.1 then yields

$$y(t) = \frac{1}{k}\left[u(t) - \cos\left(\sqrt{\frac{k}{m}}t\right)u(t)\right] = \frac{1}{k}\left[1 - \cos\left(\sqrt{\frac{k}{m}}t\right)\right]u(t).$$

The resulting output signal for $k = 5$ and $m = 1$ is shown in Figure 4.3, where it can be seen that this is an undamped oscillation that is shifted in the y-direction.

4.2.2 Transfer Function and Impulse Response

Recall again that the output of an LTI system is given by the convolution between the input $x(t)$ and the systems impulse response $h(t)$, that is,

$$y(t) = h(t) * x(t).$$

Taking the Laplace transform yields

$$Y(s) = H(s)X(s),$$

where we have made use of the Laplace transform's convolution property. Hence, it must hold that the impulse response $h(t)$ and the transfer function $H(s)$ are a Laplace transform pair (Definition 4.3).

Definition 4.3: Relationship between the impulse response and transfer function

An LTI system's impulse response $h(t)$ and its transfer function $H(s)$ are a Laplace transform pair, that is,

$$h(t) \circ\!\!-\!\!\bullet\ H(s), \tag{4.19}$$

where

$$H(s) = \int_0^\infty h(t)e^{-st}\,\mathrm{d}t.$$

This can also be seen by recalling the definition of the impulse response: The impulse response is observed when the Dirac delta function $\delta(t)$ is applied at the system's input, $x(t) = \delta(t)$. Taking the Laplace transform then yields $X(s) = 1$ (see Table 4.1) and using the input-output relationship (4.18) yields

$$\begin{array}{c} y(t) = h(t) * \delta(t) \\ \updownarrow \\ Y(s) = H(s)X(s) = H(s). \end{array}$$

Example 4.6: Impulse response of the spring-damper system

The impulse response of the spring-damper system is given by the inverse Laplace transform of the transfer function $H(s)$, that is, the inverse Laplace transform of

$$H(s) = \frac{1}{s^2 m + s\eta + k} = \frac{1/m}{s^2 + s\frac{\eta}{m} + \frac{k}{m}}$$

Comparing $H(s)$ to the Laplace transforms in Table 4.1, we can see that the expression for the decaying sine is the most similar one:

$$\frac{\omega_0}{(a+s)^2 + \omega_0^2} = \frac{\omega_0}{s^2 + 2sa + a^2 + \omega_0^2}.$$

Comparing the denominators of the two expressions, we can see that they become equal if

$$2a = \frac{\eta}{m} \Rightarrow a = \frac{\eta}{2m}$$

and

$$a^2 + \omega_0^2 = \frac{k}{m} \Rightarrow \omega_0 = \sqrt{\frac{k}{m} - a^2} = \sqrt{\frac{k}{m} - \frac{\eta}{2m}}$$

Thus, $H(s)$ can be rewritten as

$$H(s) = \frac{1}{m\omega_0}\frac{\omega_0}{(s+a)^2 + \omega_0}$$

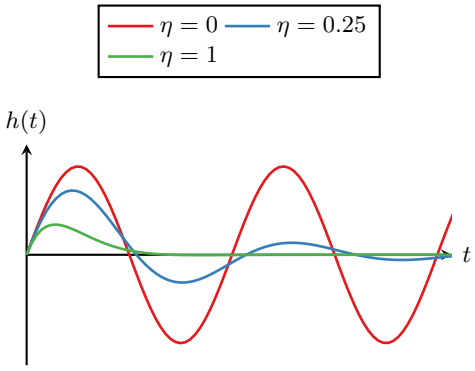

Figure 4.4. Impulse response of the spring-damper system for different values of the damping constant η.

with a and ω_0 as defined above. Thus, the inverse Laplace transform and thus the impulse response is a decaying sine

$$h(t) = \frac{1}{m\omega_0} e^{-at} \sin(\omega_0 t) u(t).$$

Figure 4.4 shows the impulse response for $k = m = 1$ and varying η. The figure shows that

- For $\eta = 0$ (i.e., no damping at all), the impulse response is a pure sine.
- For $\eta = 0.5$ (i.e., some damping), the impulse response is sine with exponentially decaying amplitude, which eventually decays to zero.
- For $\eta = 1$, there is only one small bump, after which the impulse response returns to zero.

These observations match well with our intuition: A spring-damper system that is damped little will continue to oscillate for a long time, even if we push it only briefly. On the other hand, a high damping will cause the system to come to rest quickly.

4.2.3 Transfer Function and Frequency Response

In Section 3.3, it was shown that the Fourier transform of the impulse response is an LTI system's frequency response, while Definition 4.3 states that the impulse response's Laplace transform is the transfer function. Hence, there must be a close connection between the transfer function and the frequency response. Indeed, we have already seen that there is a close relationship between the Fourier and Laplace transforms. In particular, recall that the definitions of the Fourier and Laplace transforms are

$$X(\omega) = \int_{-\infty}^{\infty} x(t) e^{-\mathrm{j}\,\omega t}\,\mathrm{d}t$$

and

$$X(s) = \int_0^\infty x(t)e^{-st}\,\mathrm{d}t,$$

respectively. Furthermore, the Laplace operator is $s = \sigma + \mathrm{j}\,\omega$. Hence, if $x(t)$ is causal (which all practical signals are) and if we set $\sigma = 0$, the Fourier and Laplace transforms are equivalent. In other words, if the Laplace transform $X(s)$ is evaluated along the imaginary axis, $s = \mathrm{j}\,\omega$, the Fourier transform of the *causal* signal $x(t)$ is obtained. This is denoted as

$$X(\mathrm{j}\,\omega) = X(s)|_{s=\mathrm{j}\,\omega},$$

where the imaginary unit variable j is included in the argument to emphasize that $X(\mathrm{j}\,\omega)$ is $X(s)$ evaluated in $s = \mathrm{j}\,\omega$. Also note that for this relationship to hold, the imaginary axis of the s-plane must be inside the region of convergence of $X(s)$.

Finally, it can be concluded that the relationship between the transfer function $H(s)$ and the frequency response $H(\mathrm{j}\,\omega)$ must be as summarized in Definition 4.4 below.

Definition 4.4: Relationship between the transfer function and frequency response

The relationship between the transfer function $H(s)$ and the frequency response $H(\mathrm{j}\,\omega)$ of a continuous time LTI system is given by

$$H(\mathrm{j}\,\omega) = H(s)|_{s=\mathrm{j}\,\omega}, \tag{4.20}$$

that is, the transfer function is evaluated along the imaginary axis in the s-plane.

We have now developed a quite comprehensive set of tools based on the Fourier and Laplace transforms already: We can go from a system description given by a linear ODE to the transfer function and calculate both the frequency response as well as the impulse response, all using the Laplace transform. However, there are more system properties that can be analyzed using the Laplace transform as shown next.

4.2.4 Poles and Zeros, and Stability

The transfer function derived from an ODE model takes on the form of a ratio of a numerator polynomial $B(s)$ of order M and a denominator polynomial (sometimes called the characteristic polynomial) $A(s)$ of order N,

$$H(s) = \frac{B(s)}{A(s)} = \frac{s^M b_M + s^{M-1} b_{M-1} + \cdots + b_0}{s^N a_n + s^{N-1} a_{N-1} + \cdots + a_0}.$$

As such, they can be rewritten in terms of the polynomials' (possibly complex-valued) roots, which are the solutions to the equations

$$B(s) = 0 \quad \text{and} \quad A(s) = 0.$$

In other words, the roots are the points in the s-plane where the polynomials become zero: If z_i is a root of the numerator polynomial $B(s)$, it must hold that

$$B(z_i) = 0,$$

and if p_j is a root of the denominator polynomial $A(s)$, it must hold that

$$A(p_j) = 0.$$

The M roots $z_1, z_2, \ldots, z_M$ of the numerator polynomial $B(s)$ are called the transfer function's *zeros*. This is because the whole transfer function becomes zero whenever s is equal to one of $z_1, z_2, \ldots, z_M$. Similarly, the N roots $p_1, p_2, \ldots, p_N$ are called the transfer function's *poles*: Whenever s approaches a pole, the denominator of the transfer function approaches zero, which means that $H(s)$ approaches infinity (like a tent pole holds up the tent's fabric).

Using the transfer function's poles and zeros, the numerator and denominator polynomials can be rewritten according to

$$B(s) = s^M b_M + s^{M-1} b_{M-1} + \cdots + b_0 = b_M (s - z_1)(s - z_2) \ldots (s - z_M)$$

and

$$A(s) = s^N a_N + s^{N-1} a_{N-1} + \cdots + a_0 = a_N (s - p_1)(s - p_2) \ldots (s - p_N),$$

which leads to the pole-zero form of the transfer function (Definition 4.5).

Definition 4.5: Pole-zero form of the transfer function

The pole-zero form of the transfer function $H(s)$ is given by

$$H(s) = K \frac{(s - z_1)(s - z_2) \ldots (s - z_M)}{(s - p_1)(s - p_2) \ldots (s - p_N)}, \tag{4.21}$$

where $K = \frac{b_M}{a_N}$, the zeros $z_1, z_2, \ldots, z_M$ are the roots of the numerator polynomial, that is, the solutions to

$$B(s) = s^M b_M + s^{M-1} b_{M-1} + \cdots + b_0 = 0$$

and the poles $p_1, p_2, \ldots, p_N$ are the roots of the denominator polynomial, that is, the solutions to

$$A(s) = s^N a_n + s^{N-1} a_{N-1} + \cdots + a_0 = 0.$$

If the system has complex poles, they always come in complex conjugate pairs, meaning that if $p_i = \sigma_i + \mathrm{j}\,\omega_i$ is a complex pole, there is another pole p_j for which it holds that $p_j = p_i^* = \sigma_i - \mathrm{j}\,\omega_i$ (the same is true for a system's zeros)[1]. Hence, gathering

[1]Strictly speaking, this only holds for systems with real-valued impulse response, which is the vast majority of all linear systems, though.

complex conjugate pole pairs and expanding the product between the two, we obtain a second order term of the form

$$(s-p_i)(s-p_i^*) = s^2 - 2s\sigma_i + \sigma_i^2 + \omega_i^2 = s^2 + 2\zeta_i\omega_{n,i}s + \omega_{n,i}^2, \tag{4.22}$$

where

$$\omega_{n,i} = \sqrt{\sigma_i^2 + \omega_i^2}, \tag{4.23a}$$

$$\zeta_i = -\frac{\sigma_i}{\omega_{n,i}}, \tag{4.23b}$$

and similar for a complex conjugate zero pair.

The locations of the poles and zeros can be visualized using a *pole-zero map*. A pole zero-map is a figure of the complex s-plane where each pole is marked with a cross ($\times$) and each zero is marked with a circle ($\circ$). This is illustrated in Example 4.7 and Figure 4.5.

Example 4.7: Poles and zeros

Consider the following systems

a) The system with the transfer function

$$H(s) = \frac{2s+4}{s^2+4s+3}.$$

To find the zeros, we set the numerator polynomial to zero, that is,

$$\begin{aligned} 2s+4 &= 0 \\ 2s &= -4s = -2, \end{aligned}$$

which shows that the system has a zero in $z_1 = -2$. Furthermore, the poles of the systems are found by finding the roots of the denominator polynomial:

$$\begin{aligned} s^2+4s+3 &= 0 \\ (s+1)(s+3) &= 0, \end{aligned}$$

which shows that the poles are $p_1 = -1$ and $p_2 = -3$. Finally, the constant K is given by $K = \frac{b_M}{a_N} = 2$. The pole-zero map for this system is shown in Figure 4.5a.

b) The system with transfer function

$$H(s) = \frac{1}{s^2-2s+2}$$

has no zeros since M = 0. Furthermore, the poles are found from

$$s^2 - 2s + 2 = 0.$$

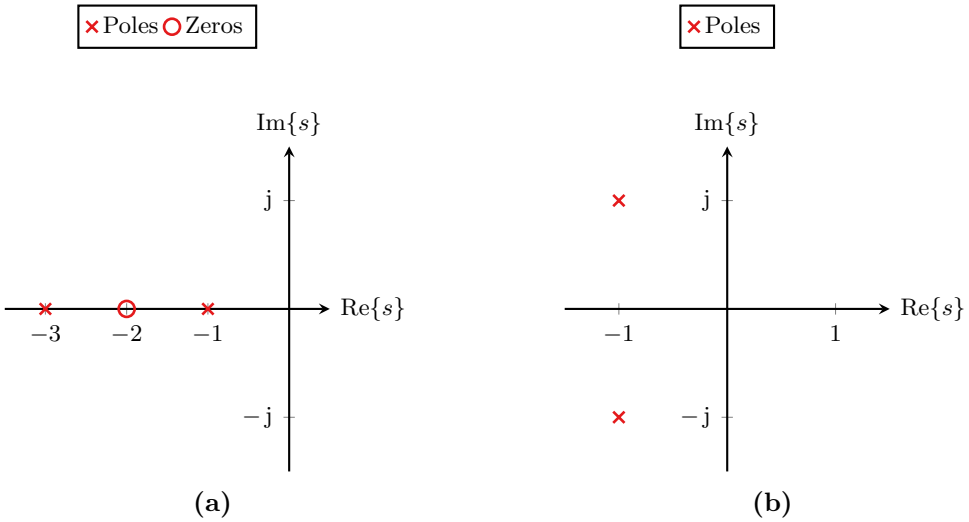

Figure 4.5. Pole-zero maps for the transfer functions in Example 4.7.

Using the quadratic formula yields that

$$\begin{aligned} p_{1,2} &= -\frac{2}{2} \pm \frac{\sqrt{2^2 - 4 \cdot 2}}{2} \\ &= -1 \pm \frac{\sqrt{4-8}}{2} \\ &= -1 \pm \frac{\sqrt{-4}}{2} \\ &= -1 \pm \mathrm{j}\,1. \end{aligned}$$

Hence, the system has one complex conjugate pole pair in $p_1 = 1 + \mathrm{j}$ and $p_2 = 1 - \mathrm{j}$ as illustrated in Figure 4.5b. In this case, the constant K is $K = 1$.

A system's poles (and to a lesser extent its zeros) are an extremely important property of a system. Assuming all poles are unique (i.e., no poles fulfill $p_i = p_j$ for any $i \neq j$) and using partial fraction expansion (see Appendix A.7), the transfer function can be rewritten as a sum of first order terms

$$H(s) = \frac{c_1}{s - p_1} + \frac{c_2}{s - p_2} + \cdots + \frac{c_N}{s - p_N}. \tag{4.24}$$

Here, $c_1, c_2, \ldots, c_N$ are the (possibly complex-valued) constants from the partial fraction expansion. Taking the inverse Laplace transform of (4.24) to obtain the impulse response $h(t)$ then yields

$$h(t) = c_1 e^{p_1 t} + c_2 e^{p_2 t} + \cdots + c_N e^{p_N t}.$$

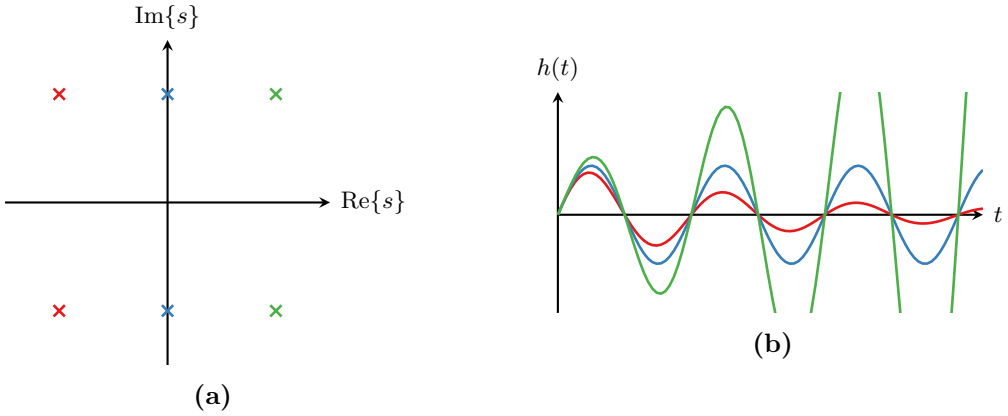

Figure 4.6. Pole locations and their effect on the impulse response. (a) Pole-zero map and (b) impulse responses.

This can be rewritten by recalling that the ith pole is a complex number of the form $p_i = \sigma_i + \mathrm{j}\,\omega_i$, which yields

$$h(t) = c_1 e^{\sigma_1 t} e^{\mathrm{j}\,\omega_1 t} + c_2 e^{\sigma_2 t} e^{\mathrm{j}\,\omega_2 t} + \cdots + c_N e^{\sigma_N t} e^{\mathrm{j}\,\omega_N t} \quad \text{for } t \geq 0. \tag{4.25}$$

Now it can be seen that each pole p_i contributes with a constant c_i, an exponential function $e^{\sigma_i t}$, and a complex oscillation $e^{\mathrm{j}\,\omega_i t}$ to the impulse response. (Note that since complex poles always come in complex conjugate pairs, there will always be two complex oscillations that actually add up to sine and cosine signals through Euler's formulas.) While c_i and $e^{\mathrm{j}\,\omega_i t}$ are constant in amplitude, the exponential term $e^{\sigma_i t}$ is crucial in whether the impulse response decays to zero, stays constant, or grows to infinity:

- If $\sigma_i < 0$ ($\mathrm{Re}\{p_i\} < 0$), the term $e^{\sigma_i t}$ is a decaying exponential and the impulse response decays to zero as $t \to \infty$,
- if $\sigma_i = 0$ ($\mathrm{Re}\{p_i\} = 0$), the term $e^{\sigma_i t} = 1$ is constant and the impulse response retains a constant amplitude forever, and
- if $\sigma_i > 0$ ($\mathrm{Re}\{p_i\} > 0$), the term $e^{\sigma_i t}$ grows exponentially and the impulse response grows to infinity as $t \to \infty$.

Hence, the following condition must hold for an LTI system to be stable.

A continuous time LTI system is stable if and only if the real part of all of its poles $p_1, p_2, \ldots, p_N$ is negative, that is, it must hold that

$$\mathrm{Re}\{p_i\} < 0 \tag{4.26}$$

for all $i = 1, \ldots, N$.

Different pole locations and their effect on the impulse response are illustrated in Figure 4.6.

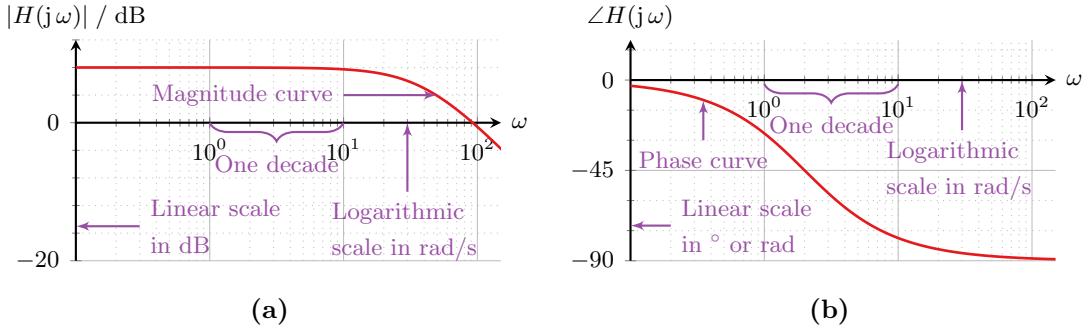

(a) **(b)**

Figure 4.7. Anatomy of a bode plot: (a) Bode magnitude plot and (b) phase plot.

Finally, recall that the frequency response of a system was given by evaluating the transfer function in $s = \mathrm{j}\omega$, that is, along the imaginary axis in the s-plane. Thus, a pole close to the imaginary axis will cause an oscillation at the frequency which gives the shortest distance to the pole. This is called a resonance peak in the frequency response and the closer the pole is to the imaginary axis, the higher the peak. Similarly, a zero close to the imaginary axis causes a dip in the frequency response, that is, the frequency closest to the zero is attenuated. If the zero is on the imaginary axis, the frequency is cancelled completely.

4.3 Bode Plots

4.3.1 Introduction

Frequency domain analysis of LTI systems is important and useful to understand a system's behavior for different inputs. Furthermore, we have already encountered one way of plotting a signal's spectrum and system's frequency response. However, in practice, these ways of plotting the frequency domain functions are not the most useful ones for gaining quick and sufficiently accurate insight. For more rigorous analysis, *Bode plots* are the tool of choice. Bode plots can relatively easily be constructed by hand, which was paramount before the computer era for analyzing complex dynamic systems. Nowadays, Bode plots are mostly sketched using computers. However, good understanding of how Bode plots are drawn helps to gain quick insight in a system's behavior without even drawing the plots themselves. Furthermore, Bode plots play a very important role in control engineering.

Bode plots are a standardized way of plotting a system's frequency response function and a Bode plot actually consists of two plots: A *Bode magnitude plot* (or simply *magnitude plot*) and a *Bode phase plot* (or simply a *phase plot*). The anatomy of a Bode plot is shown in Figure 4.7. Bode plots make use of logarithmic x-axes with equal spacing between $\ldots, 10^{-1}, 10^{0}, 10^{1}, \ldots$ to give insight in how a system behaves at the order of magnitude of ω. Here, one interval between 10^{n} and 10^{n+1} x-axis is called a *decade*.

Furthermore, the magnitude plot shows the magnitude of the frequency response, that is, $|H(\mathrm{j}\omega)|$ (the magnitude curve). This is actually often shown in decibels (dB),

that is, in the form of

$$|H(\mathrm{j}\,\omega)|_{\mathrm{dB}} = 20\log_{10}(|H(\mathrm{j}\,\omega)|)$$

where the subscript dB indicates the magnitude is in dB. (Recall that conversion to dB and back is given by

$$a_{\mathrm{dB}} = 10\log_{10}(a) \quad \Leftrightarrow \quad a = 10^{\frac{a_{\mathrm{dB}}}{20}} \tag{4.27}$$

where a denotes the plain number and a_{dB} the number in dB.) Representing the magnitude curve in dB has some important advantages as we will see shortly. Note that the magnitude plot is not always in decibels but sometimes shows $|H(\mathrm{j}\,\omega)|$ but on a logarithmic y-scale instead (which has a similar effect as taking representing it in dB).

The phase plot simply shows the phase of the frequency response, that is, $\angle H(\mathrm{j}\,\omega)$. The y-axis uses linear scaling and may either be in radians or degrees.

4.3.2 Bode Form of the Transfer Function

To sketch Bode plots, we start from the pole-zero form (4.21) of the transfer function

$$H(s) = K\frac{(s-z_1)\dots(s-z_M)}{s^l(s-p_1)\dots(s-p_{N-l})},$$

where we have assumed that there are l poles in the origin (the term s^{-l}). This form is then rewritten to the so-called *Bode form* of the transfer function. First, if there are any complex poles or zeros, the complex conjugate pairs are combined to obtain second order terms as in (4.22)–(4.23) such that

$$H(s) = K\frac{(s-z_1)\dots(s^2-2\zeta_j\omega_{n,j}s+\omega_{n,j}^2)\dots}{s^l(s-p_1)\dots(s^2-2\zeta_i\omega_{n,i}s+\omega_{n,i}^2)\dots}.$$

Next, the poles, zeros, and $\omega_{n,i}^2$ are broken out to obtain terms of the form $\frac{s}{p_i}+1$ and $\left(\frac{s}{\omega_{n,i}}\right)^2+2\frac{\zeta_i}{\omega_{n,i}}+1$, that is,

$$\begin{aligned} H(s) &= K\frac{\prod_i(-z_i)}{\prod_j(-p_j)}\frac{\left(\frac{s}{z_1}+1\right)\dots\left(\left(\frac{s}{\omega_{n,i}}\right)^2+2s\frac{\zeta_i}{\omega_{n,i}}+1\right)\dots}{s^l\left(\frac{s}{p_1}+1\right)\dots\left(\left(\frac{s}{\omega_{n,j}}\right)^2+2s\frac{\zeta_j}{\omega_{n,j}}+1\right)\dots} \\ &= K_0\frac{\left(\frac{s}{z_1}+1\right)\dots\left(\left(\frac{s}{\omega_{n,i}}\right)^2+2s\frac{\zeta_i}{\omega_{n,i}}+1\right)\dots}{s^l\left(\frac{s}{p_1}+1\right)\dots\left(\left(\frac{s}{\omega_{n,j}}\right)^2+2s\frac{\zeta_j}{\omega_{n,j}}+1\right)\dots} \end{aligned}$$

with

$$K_0 = K\frac{\prod_i(-z_i)}{\prod_j(-p_j)}.$$

Furthermore, the frequency response function then becomes

$$\begin{aligned} H(\mathrm{j}\,\omega) &= H(s)|_{s=\mathrm{j}\,\omega} \\ &= K_0 \frac{\left(\frac{\mathrm{j}\,\omega}{z_1}+1\right)\ldots\left(\left(\frac{\mathrm{j}\,\omega}{\omega_{n,i}}\right)^2+2\,\mathrm{j}\,\omega\frac{\zeta_i}{\omega_{n,i}}+1\right)\ldots}{(\mathrm{j}\,\omega)^l\left(\frac{\mathrm{j}\,\omega}{p_1}+1\right)\ldots\left(\left(\frac{\mathrm{j}\,\omega}{\omega_{n,j}}\right)^2+2\,\mathrm{j}\,\omega\frac{\zeta_j}{\omega_{n,j}}+1\right)\ldots}. \end{aligned} \tag{4.28}$$

Example 4.8: Bode form of the transfer function

Consider the transfer function

$$H(s) = 20\frac{s+5}{s(s+50)}$$

with zeros in $z_1 = -5$ and poles in $p_1 = 0$ and $p_2 = -50$.
By breaking out the zero in the numerator and the pole p_2 in the denominator, the Bode form is obtained:

$$H(s) = 20\frac{5\left(\frac{s}{5}+1\right)}{50s\left(\frac{s}{50}+1\right)} = 2\frac{\left(\frac{s}{5}+1\right)}{s\left(\frac{s}{50}+1\right)}.$$

From (4.28), it can be seen that the frequency response function on Bode form consists of a product of four elementary terms:

1. A constant K_0,
2. a first order term of the $(\mathrm{j}\,\omega)^{-l}$ (poles ($l > 0$), the more common case, or zeros ($l < 0$) at the origin),
3. a first order term of the form $\left(\frac{\mathrm{j}\,\omega}{\alpha}+1\right)^{\pm 1}$ where the exponent is $+1$ if the term appears in the numerator (α is a zero) and -1 if it appears in the denominator (α is a pole), and
4. a second order term of the form $\left[\left(\frac{\mathrm{j}\,\omega}{\omega_n}\right)^2+2\,\mathrm{j}\,\omega\frac{\zeta}{\omega_n}+1\right]^{\pm 1}$ where the exponent is $+1$ if the term appears in the numerator and -1 if it appears in the denominator.

Hence, the frequency response function can be written in terms of these elementary terms as

$$H(\mathrm{j}\,\omega) = K_0(\mathrm{j}\,\omega)^{-l}\left(\frac{\mathrm{j}\,\omega}{\alpha_1}+1\right)^{\pm 1}\ldots\left[\left(\frac{\mathrm{j}\,\omega}{\omega_{n,i}}\right)^2+2\,\mathrm{j}\,\omega\frac{\zeta_i}{\omega_{n,i}}+1\right]^{\pm 1}\ldots$$

where the dots indicate that there are more terms of the same form.

The next step is to calculate the magnitude and phase functions. The magnitude function is given by

$$|H(\mathrm{j}\,\omega)| = K_0\left|(\mathrm{j}\,\omega)^{-l}\right|\left|\frac{\mathrm{j}\,\omega}{\alpha_1}+1\right|^{\pm 1}\ldots\left|\left(\frac{\mathrm{j}\,\omega}{\omega_{n,i}}\right)^2+2\,\mathrm{j}\,\omega\frac{\zeta_i}{\omega_{n,i}}+1\right|^{\pm 1}\ldots.$$

In other words, the magnitude function is a product of the magnitudes of the individual terms. Second, recalling that the magnitude curve is plotted in dB in a Bode plot, we obtain

$$\begin{aligned}|H(\mathrm{j}\,\omega)|_{\mathrm{dB}} &= 20\log_{10}\left(K_0\left|(\mathrm{j}\,\omega)^{-l}\right|\left|\frac{\mathrm{j}\,\omega}{\alpha_1}+1\right|^{\pm 1}\ldots\left|\left(\frac{\mathrm{j}\,\omega}{\omega_{n,i}}\right)^2+2\,\mathrm{j}\,\omega\frac{\zeta_i}{\omega_{n,i}}+1\right|^{\pm 1}\ldots\right)\\ &= 20\log_{10}(K_0)-l\log_{10}(\omega)\pm 20\log_{10}\left(\left|\frac{\mathrm{j}\,\omega}{\alpha_1}+1\right|\right)\pm\ldots\\ &\quad\pm 20\log_{10}\left(\left|\left(\frac{\mathrm{j}\,\omega}{\omega_{n,i}}\right)^2+2\,\mathrm{j}\,\omega\frac{\zeta_i}{\omega_{n,i}}+1\right|\right)\pm\ldots\end{aligned}$$

for the magnitude function. Note that the logarithm has turned the product into a sum. This means that instead of sketching a complicated magnitude curved based on a product of different terms, we can sketch curves for the individual elementary terms and sum them together to obtain the complete curve.

Similarly, we can derive the phase curve, given by

$$\begin{aligned}\angle H(\mathrm{j}\,\omega) &= \angle\left(K_0(\mathrm{j}\,\omega)^{-l}\left(\frac{\mathrm{j}\,\omega}{\alpha_1}+1\right)^{\pm 1}\ldots\left[\left(\frac{\mathrm{j}\,\omega}{\omega_{n,i}}\right)^2+2\,\mathrm{j}\,\omega\frac{\zeta_i}{\omega_{n,i}}+1\right]^{\pm 1}\ldots\right)\\ &= \angle K_0+\angle(\mathrm{j}\,\omega)^{-l}\pm\angle\left(\frac{\mathrm{j}\,\omega}{\alpha_1}+1\right)\pm\cdots\pm\angle\left[\left(\frac{\mathrm{j}\,\omega}{\omega_{n,i}}\right)^2+2\,\mathrm{j}\,\omega\frac{\zeta_i}{\omega_{n,i}}+1\right]\pm\ldots\\ &= \angle K_0+\angle(\mathrm{j}\,\omega)^{-l}\pm\angle\left(\frac{\mathrm{j}\,\omega}{\alpha_1}+1\right)\pm\cdots\pm\angle\left[\left(\frac{\mathrm{j}\,\omega}{\omega_{n,i}}\right)^2+2\,\mathrm{j}\,\omega\frac{\zeta_i}{\omega_{n,i}}+1\right]\pm\ldots\end{aligned}$$

Again, the originally complex phase function has turned into a sum of phase functions of first and second order terms. Example 4.9 shows how to derive the magnitude and phase functions.

Example 4.9: Magnitude and phase functions

The frequency response for the system in Example 4.8 is

$$H(\mathrm{j}\,\omega)=H(s)|_{s=\mathrm{j}\,\omega}=2\frac{\frac{s}{5}+1}{s\left(\frac{s}{50}+1\right)}\bigg|_{s=\mathrm{j}\,\omega}=2\frac{\frac{\mathrm{j}\,\omega}{5}+1}{\mathrm{j}\,\omega\left(\frac{\mathrm{j}\,\omega}{50}+1\right)}.$$

Thus, the magnitude function is

$$|H(\mathrm{j}\,\omega)|=\left|2\frac{\frac{\mathrm{j}\,\omega}{5}+1}{\mathrm{j}\,\omega\left(\frac{\mathrm{j}\,\omega}{50}+1\right)}\right|=2\frac{\left|\frac{\mathrm{j}\,\omega}{5}+1\right|}{|\mathrm{j}\,\omega|\left|\frac{\mathrm{j}\,\omega}{50}+1\right|}$$

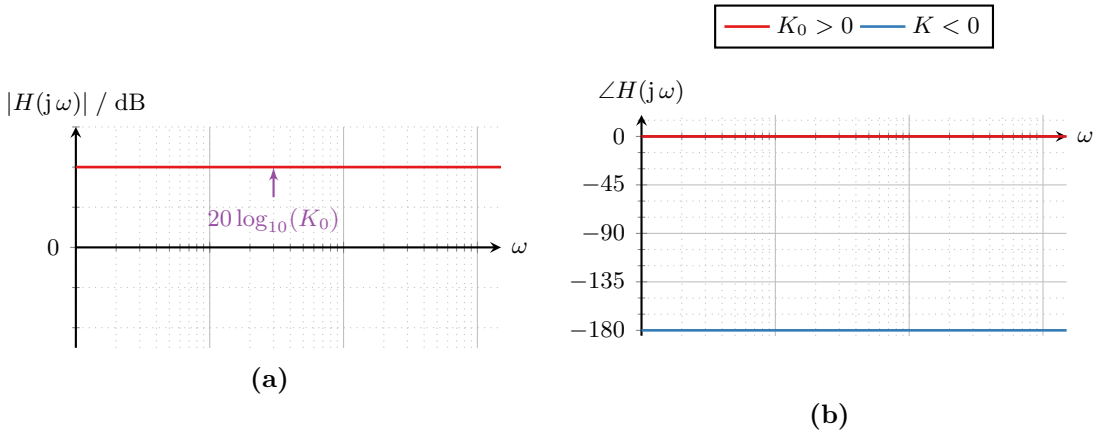

Figure 4.8. Bode plot for a constant: (a) Magnitude and (b) phase.

and the phase function

$$\angle H(\mathrm{j}\,\omega) = \angle 2\frac{\frac{\mathrm{j}\,\omega}{5}+1}{\mathrm{j}\,\omega\left(\frac{\mathrm{j}\,\omega}{50}+1\right)} = \angle\left(\frac{\mathrm{j}\,\omega}{5}+1\right) - \angle\,\mathrm{j}\,\omega - \angle\left(\frac{\mathrm{j}\,\omega}{50}+1\right).$$

4.3.3 Sketching Bode Plots

As mentioned above, the somewhat mechanical manipulations have turned an arbitrary transfer function into two functions that are simple sums of simple terms. Hence, if we know how to interpret and sketch these individual terms, we can interpret and sketch transfer functions of arbitrary complexity by simply decomposing it into sums as above. Hence, we discuss each of these terms individually next.

Constant: The gain K_0 appears as a constant function independent of the frequency ω in the Bode plot. The magnitude function in dB is simply

$$|K_0|_{\mathrm{dB}} = 20\log_{10}(|K_0|).$$

An example of a constant is shown in Figure 4.8. Furthermore, the phase is either 0 if $K_0 > 0$ and $-\pi$ if $K_0 < 0$.

Note that when writing the transfer function on Bode form, the constant K_0 also has another significance. In particular, it is equal to the DC gain of the system, since letting $\omega \to 0$ in (4.28) yields $H(\mathrm{j}\,0) = K_0$.

Poles at the origin: Poles in the origin yield the term $(\mathrm{j}\,\omega)^{-l}$ in the frequency response. This has magnitude

$$|(\mathrm{j}\,\omega)^{-l}| = (\omega)^{-l}$$

or

$$20\log_{10}(|(\omega)^{-l}|) = -20l\log_{10}(\omega).$$

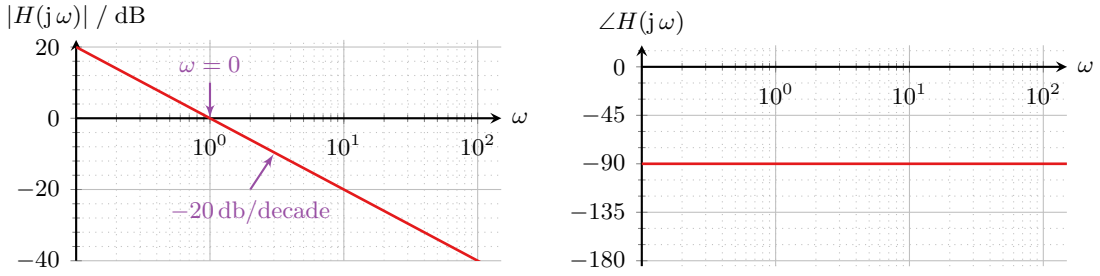

(a) **(b)**

Figure 4.9. Bode plot for a pole at the origin: (a) Magnitude and (b) phase.

Hence, the magnitude function for such a term is a linear function (since the Bode plot is a log-log plot) that intersects the x-axis in $\omega = 1$. Furthermore, the slope of the function is $-20l$ db/decade as illustrated in Figure 4.9a for $l = 1$.

The phase of one or multiple poles at the origin is

$$\angle(\mathrm{j}\,\omega)^{-l} = -l\frac{\pi}{2},$$

that is, a negative phase of l times minus 90°. This is illustrated for $l = 1$ in Figure 4.9b.

First order term: A first order term has the form $\left(\frac{\mathrm{j}\,\omega}{\alpha} + 1\right)^{\pm 1}$. For the magnitude, we have that

$$\left|\frac{\mathrm{j}\,\omega}{\alpha} + 1\right|^{\pm 1} = \left(\sqrt{\left(\frac{\omega}{\alpha}\right)^2 + 1}\right)^{\pm 1},$$

or

$$20\log_{10}\left(\left|\frac{\mathrm{j}\,\omega}{\alpha} + 1\right|^{\pm 1}\right) = \pm 20\log_{10}\left(\sqrt{\left(\frac{\omega}{\alpha}\right)^2 + 1}\right) \tag{4.29}$$

in dB. We can now inspect the behavior of the term (4.29) for different frequencies:

- If $\omega \ll \alpha$, we have $\frac{\omega}{\alpha} \ll 1$ and thus, $\pm 20\log_{10}\left(\sqrt{\left(\frac{\omega}{\alpha}\right)^2 + 1}\right) \approx \pm 20\log_{10}(1) = 0\,\mathrm{dB}$.
- If $\omega \approx \alpha$, we have $\frac{\omega}{\alpha} \approx 1$ and thus, $\pm 20\log_{10}\left(\sqrt{\left(\frac{\omega}{\alpha}\right)^2 + 1}\right) \approx \pm 20\log_{10}(\sqrt{2}) = \pm 3\,\mathrm{dB}$.
- If $\omega \gg \alpha$, we have $\frac{\omega}{\alpha} \gg 1$ and thus, $\pm 20\log_{10}\left(\sqrt{\left(\frac{\omega}{\alpha}\right)^2 + 1}\right) \approx \pm 20\log_{10}\left(\frac{\omega}{\alpha}\right)$.

Thus, the magnitude curve for a first order term in the denominator (i.e., negative sign) is zero up to approximately the point where $\omega \approx \alpha$, from where it starts to decrease at a rate of $-20\,\mathrm{db/decade}$ as illustrated in Figure 4.10a. For a first order term in the numerator, the behvior is the same but the curve increases at a rate of $20\,\mathrm{db/decade}$ after $\omega \approx \alpha$.

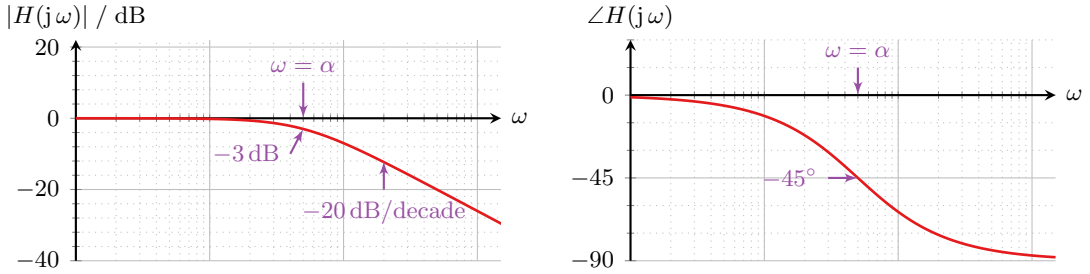

(a) **(b)**

Figure 4.10. Bode plot for a first order term in the denominator: (a) Magnitude and (b) phase.

For the phase function of the first order term we have that

$$\pm\angle\left(\frac{\mathrm{j}\,\omega}{\alpha}+1\right)=\pm\arctan\left(\frac{\omega}{\alpha}\right).$$

Again inspecting the behavior at different frequencies gives:

- If $\omega \ll \alpha$, we have that $\pm\angle\left(\frac{\mathrm{j}\,\omega}{\alpha}+1\right)\approx\pm\arctan(0)=0$.
- If $\omega \approx \alpha$, we have that $\pm\angle\left(\frac{\mathrm{j}\,\omega}{\alpha}+1\right)\approx\pm\arctan(1)=\pm\frac{\pi}{4}$.
- If $\omega \gg \alpha$, we have that $\pm\angle\left(\frac{\mathrm{j}\,\omega}{\alpha}+1\right)\approx\pm\frac{\pi}{2}$.

Thus, a first order term adds no phase shift for frequencies below the pole (or zero) and a phase shift of $-\frac{\pi}{2}$ for high frequencies for a pole or $\frac{\pi}{2}$ for a zero. The transition between these asymptotes is smooth with the curve crossing $\pm\frac{\pi}{4}$ at $\omega=\alpha$. The resulting phase curve is illustrated in Figure 4.10b for a pole. For a zero, the sign is changed and the curve goes from zero to $\frac{\pi}{2}$.

Second order term: The second order term can be rewritten as

$$\left(\left(\frac{\mathrm{j}\,\omega}{\omega_{n,i}}\right)^2+2\,\mathrm{j}\,\omega\frac{\zeta_i}{\omega_{n,i}}+1\right)^{\pm1}=\left(1-\frac{\omega^2}{\omega_{n,i}^2}+\mathrm{j}\,\frac{2\omega\zeta_i}{\omega_{n,i}}\right)^{\pm1}.$$

This yields the magnitude function

$$\left|1-\frac{\omega^2}{\omega_n^2}+\mathrm{j}\,\frac{2\omega\zeta}{\omega_n}\right|^{\pm1}=\left(\sqrt{\left(1-\frac{\omega^2}{\omega_n^2}\right)^2+\frac{4\omega^2\zeta^2}{\omega_n^2}}\right)^{\pm1},$$

or

$$20\log_{10}\left(\left|1-\frac{\omega^2}{\omega_n^2}+\mathrm{j}\,\frac{2\omega\zeta}{\omega_n}\right|^{\pm1}\right)=\pm20\log_{10}\left(\sqrt{\left(1-\frac{\omega^2}{\omega_n^2}\right)^2+\frac{4\omega^2\zeta^2}{\omega_n^2}}\right)$$

in dB. To see how this term behaves as a function of the frequency ω, we again inspect the asymptotic behavior:

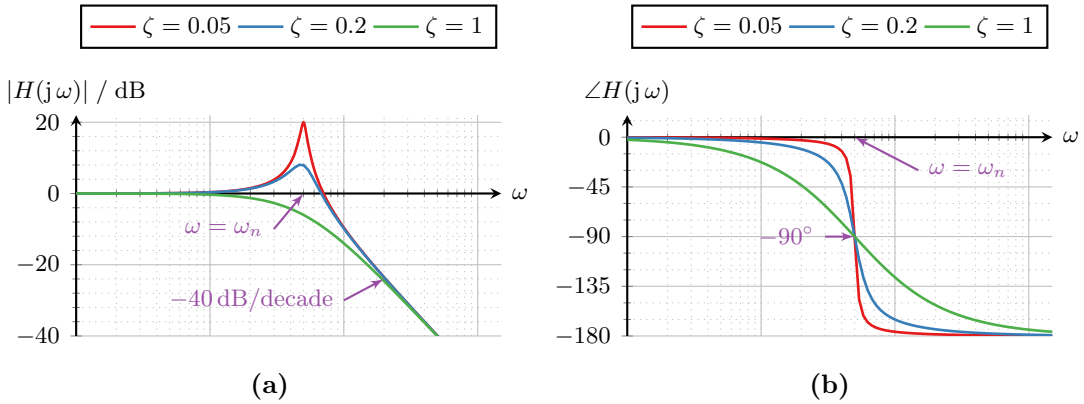

Figure 4.11. Bode plot for second order terms in the denominator: (a) Magnitude and (b) phase.

- If $\omega \to 0$, we have

$$\pm 20 \log_{10} \left(\sqrt{\left(1 - \frac{\omega^2}{\omega_n^2}\right)^2 + \frac{4\omega^2\zeta^2}{\omega_n^2}} \right) \to \pm 20 \log_{10}(1) = 0 \,\text{dB}.$$

- If $\omega \to \infty$, the term containing ω^4 dominates. Thus, we have

$$\pm 20 \log_{10} \left(\sqrt{\left(1 - \frac{\omega^2}{\omega_n^2}\right)^2 + \frac{4\omega^2\zeta^2}{\omega_n^2}} \right) \to \pm 20 \log_{10} \left(\frac{\omega^2}{\omega_n^2} \right) = \pm 40 \log_{10} \left(\frac{\omega}{\omega_n} \right)$$

Hence, the magnitude of the second order system is zero for low frequencies and follows a $\pm 40\,\text{dB/decade}$ increase or decrease for high frequencies. The behavior between these regimes around $\omega \approx \omega_n$ is determined by the *damping ratio* ζ:

- If ζ is small, the first term dominates and the argument to the logarithm becomes a small number. The logarithm of a small number is a large negative number and thus, the term causes a peak (if in the denominator) or a dip (if in the numerator).
- Increasing ζ up to 1 reduces the effect of the peak (or dip) and for $\zeta \geq 0.7$, the peak (or dip) starts to vanish entirely.

An example of the magnitude function of a second order term in the denominator for three different values of ζ is shown in Figure 4.11a.

The phase function for the second order term is given by

$$\pm \angle \left(1 - \frac{\omega^2}{\omega_n^2} + \mathrm{j}\,\frac{2\omega\zeta}{\omega_n}\right) = \begin{cases} \pm \arctan\left(\frac{\frac{2\omega\zeta}{\omega_n}}{1-\frac{\omega^2}{\omega_n^2}}\right) & \omega \leq \omega_n, \\ \pm\pi \pm \arctan\left(\frac{\frac{2\omega\zeta}{\omega_n}}{1-\frac{\omega^2}{\omega_n^2}}\right) & \omega > \omega_n. \end{cases}$$

For the phase function, it holds thus that

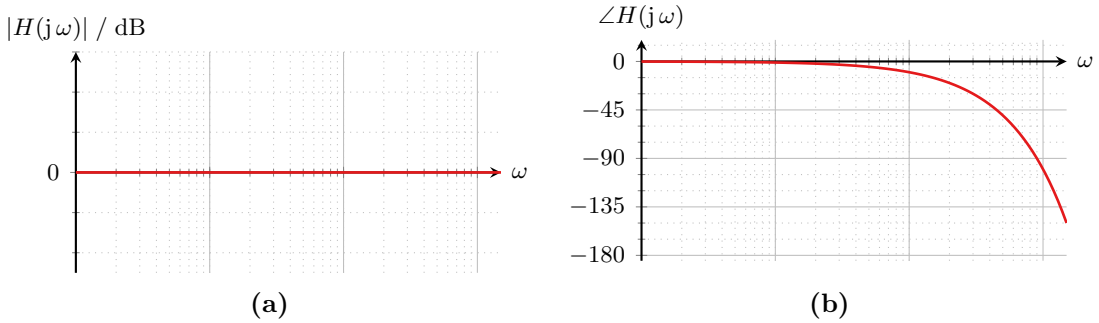

Figure 4.12. Bode plot of the phase shift: (a) Magnitude and (b) phase.

- for $\omega \to 0$,

$$\pm\angle\left(1-\frac{\omega^2}{\omega_n^2}+\mathrm{j}\,\frac{2\omega\zeta}{\omega_n}\right)=\pm\arctan\left(\frac{\frac{2\omega\zeta}{\omega_n}}{1-\frac{\omega^2}{\omega_n^2}}\right)\to 0,$$

- for $\omega=\omega_n$,

$$\pm\angle\left(1-\frac{\omega^2}{\omega_n^2}+\mathrm{j}\,\frac{2\omega\zeta}{\omega_n}\right)=\pm\arctan\left(\frac{\frac{2\omega\zeta}{\omega_n}}{1-\frac{\omega^2}{\omega_n^2}}\right)=\pm\frac{\pi}{2},$$

- for $\omega \to \infty$,

$$\pm\angle\left(1-\frac{\omega^2}{\omega_n^2}+\mathrm{j}\,\frac{2\omega\zeta}{\omega_n}\right)=\pm\pi\pm\arctan\left(\frac{\frac{2\omega\zeta}{\omega_n}}{1-\frac{\omega^2}{\omega_n^2}}\right)\to\pm\pi.$$

Thus, the phase function starts at 0 and transitions to $-\pi$ ($-180°$) for a second order term in the denominator and for a second order term in the numerator, it starts at 0, passes through $-\frac{\pi}{2}$ ($-90°$) at $\omega=\omega_n$, and goes to π ($180°$). The sharpness of the transition is again controlled by the damping ratio ζ. If ζ is small, the transition is steep, whereas ζ close to 1 gives a slow transition. The phase function of a second order term in the denominator for varying values of ζ is shown in Figure 4.11b.

Phase shift: Finally, there is one additional term that has not been discussed yet, the phase shift $e^{-\mathrm{j}\,\omega T}$. The phase shift is a complex number on the unit circle, which has magnitude 1 and thus, this term does not add to the magnitude function. The phase, however, is

$$\angle e^{-\mathrm{j}\,\omega T}=-\omega T.$$

Hence, the phase is a linear function of the frequency ω, where the slope is T. However, since the Bode plot uses a logarithmic x-axis, the phase shift shows up like a nonlinear function as shown in Figure 4.12.

Now that we have derived how the different terms affect the Bode plot, we actually do not have to derive the magnitude and phase functions explicitly anymore but can simply use the drawing rules above to sketch a rough Bode plot. This is illustrated in Example 4.10 below.

Example 4.10: Sketching a Bode plot

Consider the system in Examples 4.8–4.9. The transfer function on Bode form was given by

$$H(s) = 2\frac{\frac{s}{5}+1}{s\left(\frac{s}{50}+1\right)}.$$

Thus, it consists of a constant, a first order term in the nominator, and a pole at the origin and a first order term in the denominator.
Using the sketching rules derived above, we can now sketch the Bode diagram without even deriving the magnitude and phase functions. The individual terms contribute as follows:

- The constant 2 gives a constant magnitude at $20\log_{10}(2) = 6\,\text{dB}$ and zero phase shift.
- The first order term $\frac{s}{5}+1$ in the numerator is zero in the interval $0\,\text{rad/s} \leq \omega \leq 5\,\text{rad/s}$ and increases with $20\,\text{dB/decade}$ after $\omega = 5\,\text{rad/s}$.

  The phase is zero up to approximately $\omega \approx 0.5\,\text{rad/s}$, from where it increases linearly to $90°$ at $\omega \approx 50\,\text{rad/s}$.
- The pole at the origin gives a linear $-20\,\text{dB/decade}$ decrease that passes through $\omega = 1$. The phase is constant at $-90°$.
- The first order term $\frac{s}{50}+1$ in the denominator is zero in the interval $0\,\text{rad/s} \leq \omega \leq 50\,\text{rad/s}$ and decreases at a rate of $-20\,\text{dB/decade}$.

  The phase is zero up to approximately $\omega \approx 5\,\text{rad/s}$. Between $5\,\text{rad/s}$ and $500\,\text{rad/s}$, it decreases linearly to $-90°$, where it remains constant as ω increases.

These components are sketched using dashed lines in Figure 4.13. The complete curves are then found by summing the individual parts, which results in the solid lines.

Finally, Example 4.11 shows how to create Bode plots using Python and SciPy.

Example 4.11: Bode plots in Python and SciPy

In this example, the Bode plot for the system discussed in Examples 4.8–4.10 is re-created using Python and SciPy.
First, the necessary libraries, in this case SciPy for calculating the Bode plot and Matplotlib for plotting, have to be imported:

```
from scipy import signal
import matplotlib as plt
```

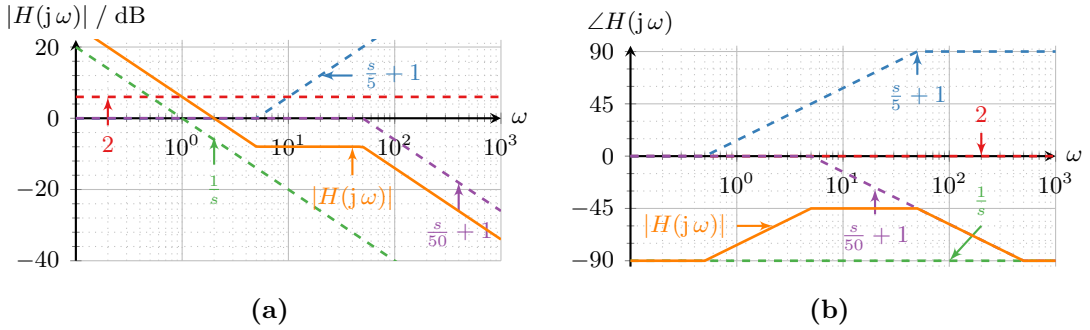

(a) (b)

Figure 4.13. Sketched Bode plot for Example 4.10: (a) Magnitude and (b) phase.

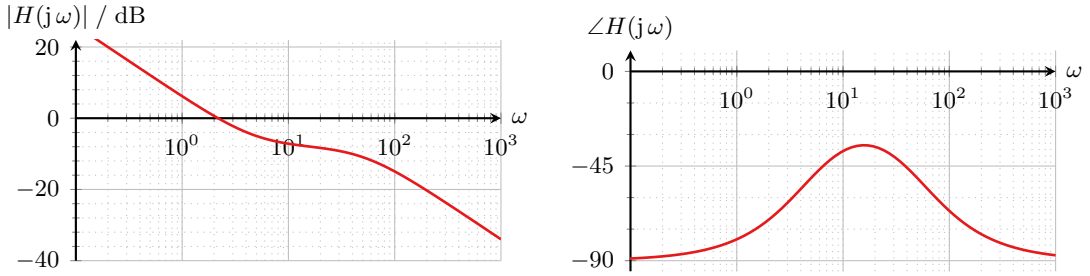

(a) (b)

Figure 4.14. Bode plot generated using Python and SciPy for Example 4.11: (a) Magnitude and (b) phase.

Next, an LTI system object has to be created. This can be achieved in several ways, for example by using the coefficients of the numerator and denominator polynomials using the function `scipy.signal.TransferFunction` or by using the zero-pole form with the help of `scipy.signal.ZerosPolesGain`. In this case, we choose the latter option as we already have the pole-zero form available from Example 4.8.

$$H(s) = 20\frac{s+5}{s(s+50)}.$$

This is done by

```
H = signal.ZerosPolesGain([-5], [0, -50], 20)
```

Next, the magnitude and phase curves are calculated using `scipy.signal.bode` as follows:

```
w, mag, phase = signal.bode(H)
```

This returns a vector `w` containing a grid of frequencies ω, a vector of magnitudes `mag` at the frequencies in `w` in dB, and a vector of phase angles `phase` at the frequencies in `w` in °.

Plotting the result gives the Bode plot in Figure 4.14. Naturally, this is more accurate than the sketch in Figure 4.13. In particular, the transitions around the different breakpoints are smoother, something that was neglected in the sketch. Nevertheless, comparing Figure 4.13 and Figure 4.14, it can be seen that the sketch is a good approximation of the actual Bode plot.

Chapter 5

Filtering Theory and Continuous Time Filters

5.1 Filtering Theory and Ideal Filters

5.1.1 Background

It has been shown that LTI systems affect the frequency content of signals applied to them. Certain frequencies may be amplified while other frequencies may be suppressed and the system is said to have a *filtering* behavior for certain frequencies. This kind of property is desirable in many applications and the aim of *filter design* is to design different LTI systems that exhibit a specific, application-defined filtering behavior. Such a system is called a *filter*. Two examples where filters are used in practice are:

1. Radio communication where the filter is used to tune in to the desired communication channel and remove all communication from the signal outside the desired channel (Example 5.1), and
2. professional audio where the filter is used to reduce noise, ground loops, crosstalk, etc., or

Filters are specified and designed in the frequency domain since their aim is to remove certain frequency components from the signal. However, their implementation is in the time domain, either as analog electronics (continuous time filters) or in a digital computer (digital filters, see Chapter 10).

Example 5.1: Radio communication signal at the receiver

Consider the radio communication signal discussed in Example 3.9 with the spectrum shown in Figure 5.1a. At the receiver, the aim is to recover the original baseband signal $x_b(t)$ (and eventually, the digital bitstream). However, since there are many more radio signals than the desired one in the air, the spectrum observed at the receiver's antenna $Y_r(\omega)$ looks more like the one shown in Figure 5.1b.
Hence, before the receiver can try to recover the baseband signal $x_b(t)$, it needs to remove all the noise outside the frequency range where the signal was transmitted. This can be achieved by a properly designed linear filter.

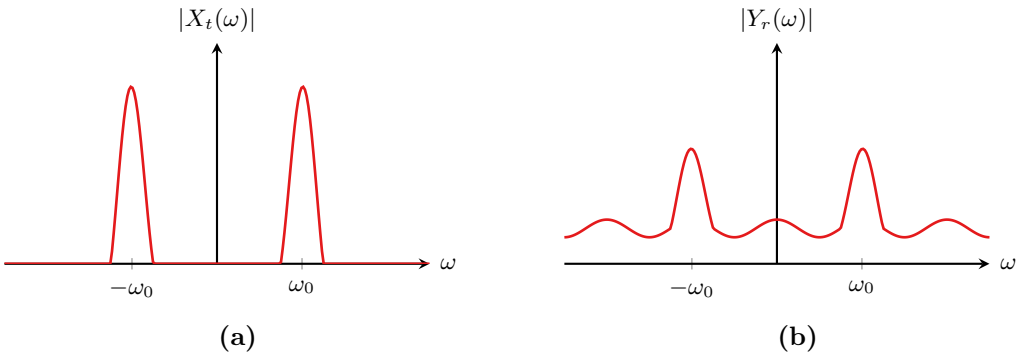

Figure 5.1. Illustration of a radio communication signal's spectrum at the transmitter and receiver. (a) Clean spectrum at the transmitter and (b) corrupted spectrum at the receiver.

5.1.2 Ideal Filters and Filter Types

An ideal filter consists of a *passband* and a *stopband*. The passband is a frequency range where all frequencies pass unaltered by the filter, that is, without being amplified or delayed (i.e., zero phase shift). The frequency response for the passband is thus $H(\omega) = 1$ for frequencies ω inside the passband. Conversely, the stopband is the frequency range in which the signal is attenuated completely (i.e., these frequencies are completely stopped from passing through the system). Hence, the ideal frequency response in the stopband is $H(\omega) = 0$ for frequencies ω inside the stopband. Between the pass- and stopband, there is an infinitely sharp transition at the *cutoff frequency* ω_c. Hence, the ideal filter frequency response is in general

$$H(\omega) = \begin{cases} 1 & \text{for } \omega \text{ in the passband,} \\ 0 & \text{for } \omega \text{ in the stopband.} \end{cases}$$

There are four elementary filter types:

1. Lowpass (LP) filters,
2. highpass (HP) filters,
3. bandpass (BP) filters, and
4. bandstop (BS) filters.

The naming of the filters is based on which frequencies they let pass (or stop from passing). Note that it is more instructive to look at the positive half of the frequency response function (i.e., the one-sided frequency response function for $\omega \geq 0$) to gain intuition for the different terms. However, since we are almost always working with real-valued signals, the frequency responses are actually symmetric about the y-axis.

Lowpass filter. A lowpass filter is a filter that lets low frequencies pass through and blocks high frequencies. Here, low frequencies refers to frequencies being close to zero, below the cutoff frequency ω_c as illustrated in the one-sided frequency response in Figure 5.2a.

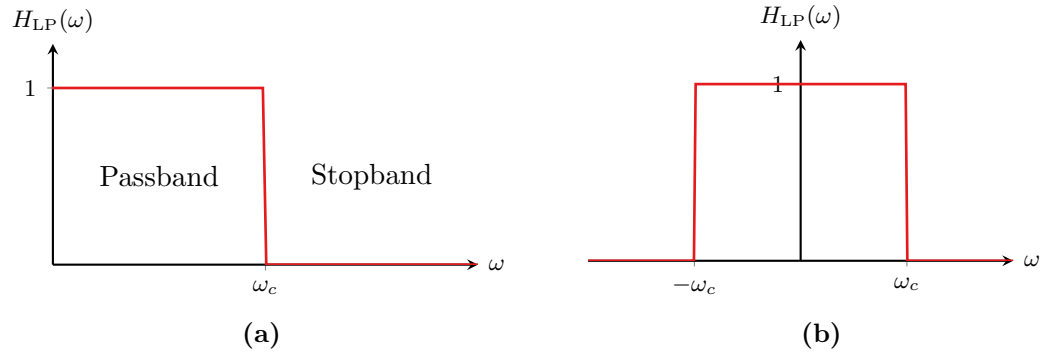

Figure 5.2. Illustration of the ideal lowpass filter's frequency response: (a) One-sided frequency response that shows that low frequencies close to zero are unaffected while high frequencies above the cutoff frequency ω_c are blocked and (b) full frequency response function.

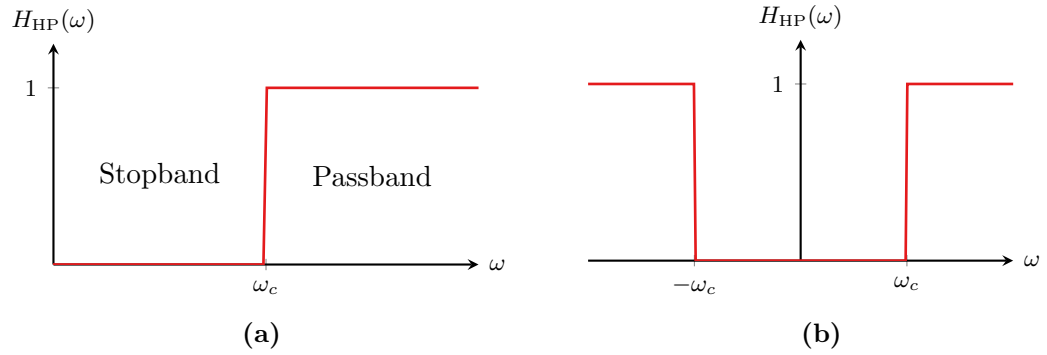

Figure 5.3. Illustration of the ideal highpass filter's frequency response: (a) One-sided frequency response that shows that high frequencies far from zero are unaffected while low frequencies below the cutoff frequency ω_c are blocked and (b) full frequency response function.

To obtain the expression for the lowpass filter's ideal frequency response function, we have to turn to the full frequency response in Figure 5.2b. As we can see, the lowpass filter lets frequencies in the range $-\omega_c < \omega < \omega_c$ pass and blocks all other frequencies. This can be expressed by using a rectangular pulse in the frequency domain as follows

$$H_{\mathrm{LP}}(\omega) = \mathrm{rect}\left(\frac{\omega}{2\omega_c}\right). \tag{5.1}$$

Highpass filter. A highpass filter is the inverse of a lowpass filter, which lets high frequencies, that is, frequencies far from zero and above some cutoff frequency ω_c pass and stops low frequencies from passing. This is illustrated in the one-sided frequency response in Figure 5.3a.

The expression for the frequency response can again be found from the full frequency response illustrated in Figure b. This is given by

$$H_{\mathrm{HP}}(\omega) = 1 - \mathrm{rect}\left(\frac{\omega}{2\omega_c}\right). \tag{5.2}$$

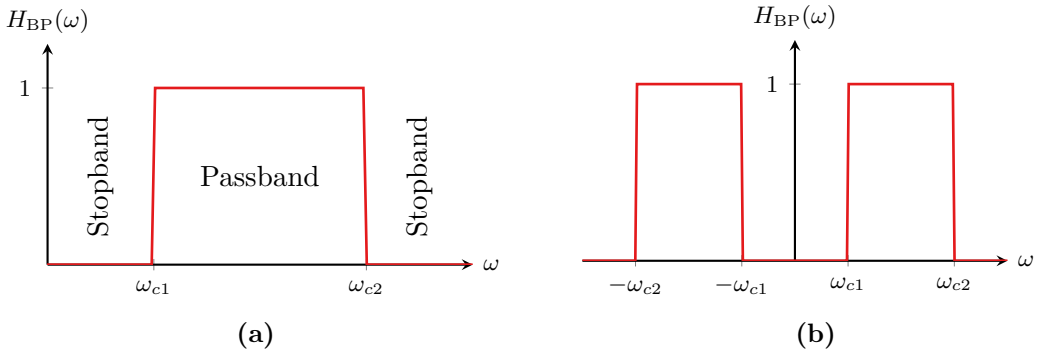

Figure 5.4. Illustration of the ideal bandpass filter's frequency response: (a) One-sided frequency response that shows that frequencies in the band between $\omega_{c1} < \omega < \omega_{c2}$ pass and frequencies outside that band are blocked and (b) full frequency response function.

In other words, all frequencies that fulfill $|\omega| > \omega_c$ pass the highpass filter while frequencies $|\omega| < \omega_c$ are blocked.

Bandpass filter. The one-sided frequency response function for the ideal bandpass filter is shown in Figure 5.4a. In a bandpass filter, only frequencies within a certain frequency band $\omega_{c1} < \omega < \omega_{c2}$ pass the filter whereas frequencies outside that band are blocked.

The bandpass filter can be seen as a combination of a lowpass filter with cutoff frequency ω_{c2} and a highpass filter with cutoff frequency ω_{c1} (with $\omega_{c1} < \omega_{c2}$). The expression for the frequency response is (Figure 5.4b)

$$H_{\mathrm{BP}}(\omega) = \mathrm{rect}\left(\frac{\omega}{2\omega_{c2}}\right) - \mathrm{rect}\left(\frac{\omega}{2\omega_{c1}}\right). \tag{5.3}$$

Bandstop filter. Finally, the bandstop filter is the inverse of the bandpass filter, meaning that frequencies within a specific frequency band $\omega_{c1} < \omega < \omega_{c2}$ are removed from the signal. Frequencies outside that band pass the filter unaltered, see Figure 5.5a.

The ideal frequency response function is again found from Figure 5.5b and is given by

$$H_{\mathrm{BS}}(\omega) = 1 - \mathrm{rect}\left(\frac{\omega}{2\omega_{c2}}\right) + \mathrm{rect}\left(\frac{\omega}{2\omega_{c1}}\right). \tag{5.4}$$

Note that a *notch filter* is a special case of a bandstop filter where the stopband is very narrow. Notch filters are useful for removing single frequencies from a signal, for example the 50 Hz power line distortion induced by ground loops or poorly shielded cables.

Example 5.2: Filter selection

The receiver of the radio communication system in Example 5.1 needs to isolate the frequency range carrying the actual communication signal. Hence, the receiver should contain a bandpass filter with lower cutoff frequency $\omega_{c1} = \omega_0 - \omega_b$ and

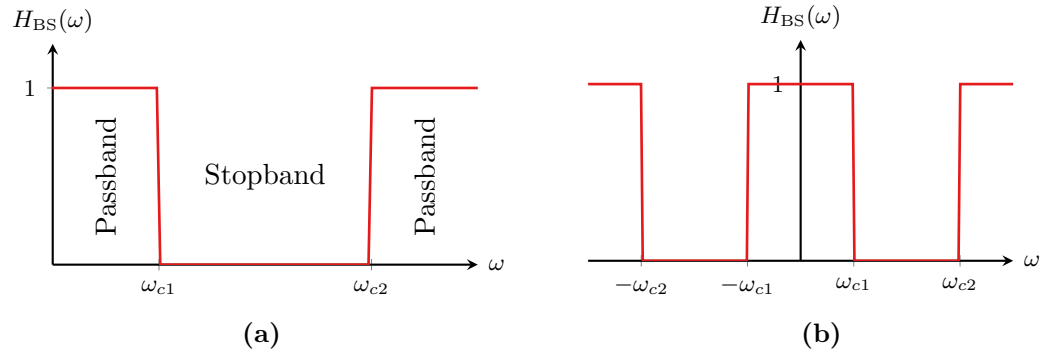

Figure 5.5. Illustration of the ideal bandstop filter's frequency response: (a) One-sided frequency response that shows that frequencies in the band between $\omega_{c1} < \omega < \omega_{c2}$ are blocked and frequencies outside that band pass and (b) full frequency response function.

upper cutoff frequency $\omega_0 + \omega_b$ (where ω_0 is the carrier frequency and ω_b is the baseband signal's one-sided bandwidth).

Arbitrary filters can be constructed by cascading these four elementary filters (strictly speaking, the bandstop and bandpass filters are already constructed using low- and highpass filters). However, once a signal component is removed, that component can not be brought back. Finally, note that these filters are called *ideal* for a reason: All the ideal frequency responses are made up of rectangular pulses with infinitely sharp edges. The corresponding impulse responses thus consist of infinitely long, non-causal sinc functions, which can of course not be implemented in practice. Hence, we can only use the ideal frequency responses as blueprints and try to approximate them as well as possible in practice.

5.2 Filter Approximations

5.2.1 Practical Filter Approximation

As discussed above, the ideal filters in Section 5.1 can not be implemented in practice. Instead, approximations that make certain compromises have to be used. The main challenges that prevent us from using ideal filters are:

- Non-causal impulse response,
- infinitely sharp transition between the pass- and stopbands, and
- perfect stopband attenuation.

Filter approximations are instead realized as Nth order causal LTI systems with rational transfer functions of the form

$$\begin{aligned} H(s) &= \frac{b_N s^N + b_{N-1} s^{N-1} + \cdots + b_1 s + b_0}{a_N s^N + a_{N-1} s^{N-1} + \cdots + a_1 s + a_0} \\ &= K \frac{(s - z_1)(s - z_2) \ldots (s - z_N)}{(s - p_1)(s - p_2) \ldots (s - p_N)}. \end{aligned}$$

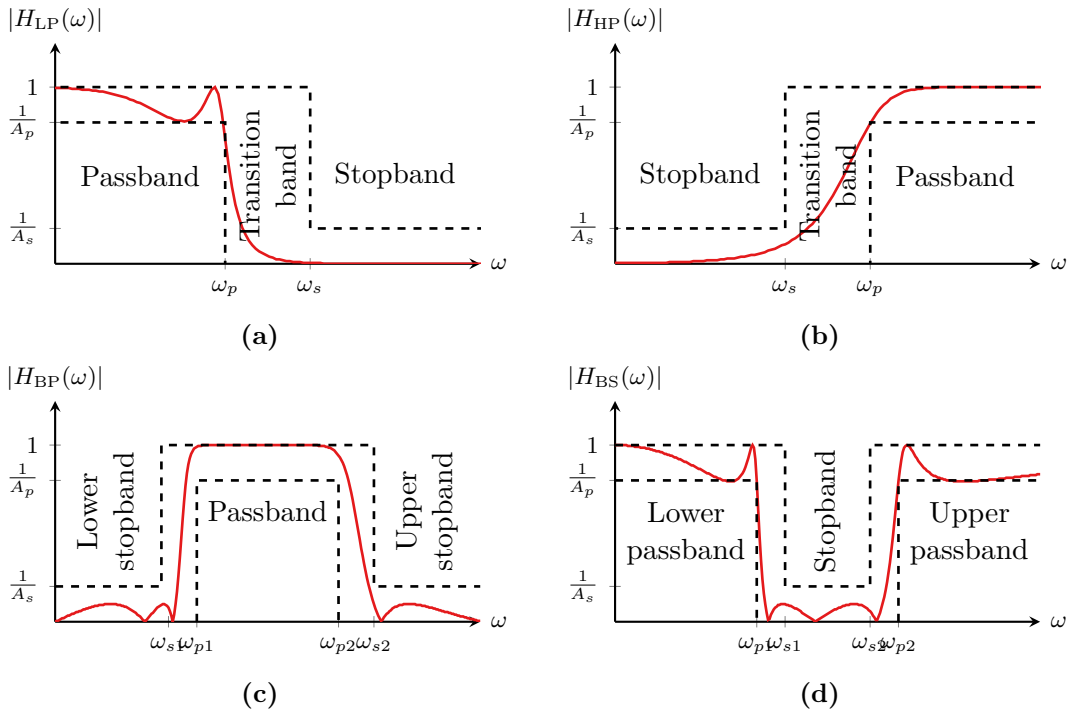

Figure 5.6. Illustration of real filter frequency responses with passband ripple and stopband ripple and a transition band. (a) Lowpass, (b) higpass, (c) bandpass, and (d) bandstop.

As such, the ideal filter characteristics can not be achieved and we have to make certain trade-offs. In particular, filters are designed based on brick wall requirements: Instead of achieving the exact frequency response of an ideal filter, we allow for some deviation around the ideal frequency response. Hence, we require that the real filter's frequency response is within a certain band around the ideal frequency response instead as illustrated in Figure 5.6. Instead of only specifying the pass- and stopband, we thus also have to specify how far we allow the real filter to deviate from the ideal filter. This is achieved through the following parameters:

- The *passband ripple* A_p, the maximum amount of attenuation allowed in the passband, that is, how much the gain $|H(\omega)|$ is allowed to drop below 1 (0 dB) in the passband (typically specified in dB, for example 1 dB),
- the *passband edge frequency* ω_p (or lower passband edge frequency ω_{p1} and upper passband edge frequency ω_{p2}), the frequency that marks the end of the requirement on the passband ripple and also marks the start of the transition band,
- the *stopband attenuation* A_s, the minimum attenuation in the stopband (typically specified in dB, for example 40 dB), and

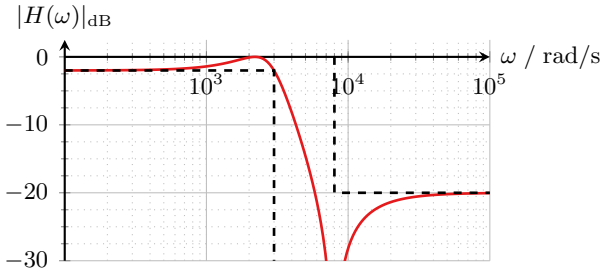

Figure 5.7. Magnitude of the frequency response for the lowpass filter in Example 5.3.

- the *stopband edge frequency* ω_s (or lower stopband edge frequency ω_{s1} and upper stopband edge frequency ω_{s2}), the frequency that marks the start of the requirement on the stopband attenuation and also marks the end of the transition band.

In addition to the pass- and stopbands, real filters thus also have a *transition band*, where the frequency response transitions from the passband to the stopband. Furthermore, the filter is also characterized by the cutoff frequency, which often follows implicitly from the filter requirements, defined as follows.

Definition 5.1: Filter cutoff frequency

The cutoff frequency is defined as the frequency ω_c where the filter gain has decreased to

$$|H(\omega_c)| = \frac{1}{\sqrt{2}} \approx 0.707, \tag{5.5}$$

or, equivalently,

$$|H(\omega_c)|_{\text{dB}} = -3\,\text{dB}. \tag{5.6}$$

At the cutoff frequency ω_c, the amplitude and power of the signal are reduced by a factor $\sqrt{2}$ (amplitude) and 2 (power), respectively.

Finally, the *roll off rate* indicates how quickly the real filter transitions between the pass- and stopband. It is defined as

$$R = \frac{\mathrm{d}}{\mathrm{d}\omega} \log_{10}\left(|H(\omega)|^2\right)\Big|_{\omega=\omega_c} = 2\,\frac{\mathrm{d}}{\mathrm{d}\omega} \log_{10}\left(|H(\omega)|\right)\Big|_{\omega=\omega_c}, \tag{5.7}$$

that is, the slope of the filter's gain function evaluated in the cutoff frequency ω_c. A low roll off rate indicates that the filter transitions slowly from the passband to the stopband (wide transition band) and vice-versa.

Example 5.3 illustrates the properties and requirements of a real filter.

Example 5.3: Filter example

Figure 5.7 shows an example of a real lowpass filter designed with the following requirements:

- Passband ripple $A_p = 2\,\text{dB}$,
- passband edge frequency $\omega_p = 3000\,\text{rad/s}$,
- stopband attenuation $A_s = 20\,\text{dB}$, and
- stopband edge frequency $\omega_s = 8000\,\text{rad/s}$.

Furthermore, the cutoff frequency (where $|H(\omega)|_{\text{dB}} = -3\,\text{dB}$) is approximately $\omega_c \approx 3200\,\text{rad/s}$.

To design the filter, the user has to determine the filter order N as well as the filter coefficients $a_1, a_2, \ldots, a_N$ and $b_1, b_2, \ldots, b_N$ (or, alternatively, the poles and zeros $p_1, p_2, \ldots, p_N$ and $z_1, z_2, \ldots, z_N$) to obtain a frequency response that fulfills the requirements. In practice, this is achieved by first choosing a particular approximation type, which defines the structure of the polynomials and pole and zero locations, followed by determining which filter order is required for the particular filter type. Furthermore, filters are typically designed by starting from a low-pass filter, which is then later transformed into the desired filter type (highpass, bandpass, etc.). Hence, the different approximations will be discussed in terms of the lowpass filter in the following sections.

5.2.2 Approximation Types

There are several filter approximation types. The three of the most commonly used filter approximations discussed here are:

- Butterworth filters,
- Chebyshev type I and type II filters, and
- Elliptic filters (also called Cauer filters).

Each filter type and its most important properties are briefly discussed below. A guide on how to design filters based on these approximations is provided in the next section.

Butterworth filters. Butterworth filters are characterized by a smooth frequency response (i.e., no ripples) in the pass- and stopbands. However, they have a low roll off rate that increases linearly with the filter order N and thus, the transition band is wide for high order filters. As a consequence, to achieve a high stopband attenuation, a high filter order is required. This, in turn, may push Butterworth filters towards instability.

The magnitude of the frequency response for an Nth order Butterworth filter is

$$|H(\omega)| = \frac{1}{\sqrt{1 + \left(\frac{\omega}{\omega_c}\right)^{2N}}}, \tag{5.8}$$

where ω_c is the cutoff frequency. Figure 5.8a shows the magnitude of the frequency response for Butterworth filters of order $N = 1$ through $N = 4$ with $\omega_c = 1\,\text{rad/s}$.

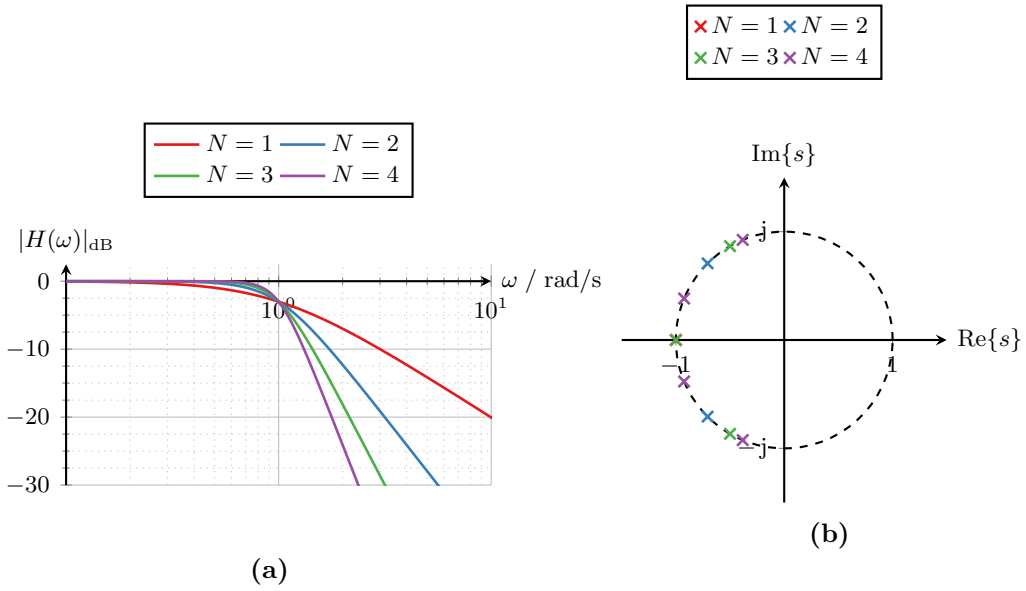

Figure 5.8. Butterworth lowpass filters of orders $N = 1$ to $N = 4$ with $\omega_c = 1\,\text{rad/s}$: (a) Magnitude of the frequency response, and (b) poles.

Note that by letting $\omega = \omega_c$ in (5.8), it can be seen that ω_c indeed is the cutoff frequency:

$$|H(\omega_c)| = \frac{1}{\sqrt{1 + \left(\frac{\omega_c}{\omega_c}\right)^{2N}}} = \frac{1}{\sqrt{1 + 1^{2N}}} = \frac{1}{\sqrt{2}}.$$

The roll off rate of a Butterworth filter is given by

$$R = 2\,\frac{\mathrm{d}}{\mathrm{d}\omega}\log_{10}\left(|H(\omega)|\right)\Big|_{\omega=\omega_c} = -N.$$

Hence, the roll off rate increases linearly with the order of the filter. Furthermore, the gain for Butterworth filters decreases to zero at the rate $-N20\,\text{dB/decade}$ in the stopband as ω increases.

The N poles $p_1, p_2, \ldots, p_N$ of the transfer function $H(s)$ are evenly distributed on a half circle of radius ω_c around the origin in the left half of the s-plane (stable poles), as far from the imaginary axis as possible (Figure 5.8b). This gives the pole locations

$$p_n = \omega_c e^{\mathrm{j}\,\pi\left(\frac{n-1/2}{N}+\frac{1}{2}\right)}. \tag{5.9}$$

Increasing the filter order moves the pole pair closest to the imaginary axis closer and closer to the imaginary axis (Figure 5.8b). This means that this pole pair approaches the border to instability, which can cause problems when implementing the filter in practice (e.g., component tolerances may cause the poles to actually end up in the unstable area). Finally, the Butterworth filter does not have any zeros.

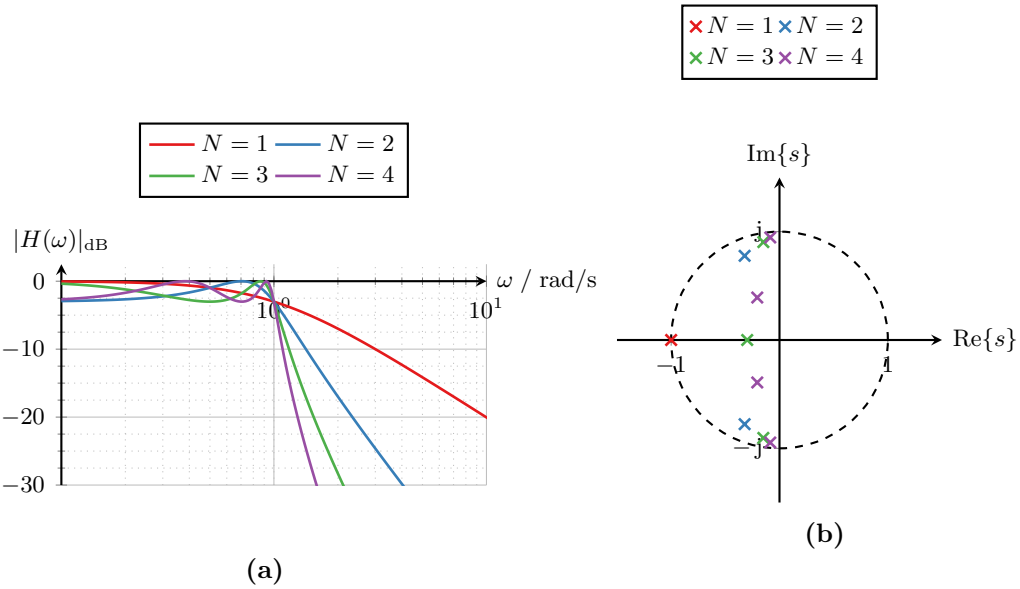

Figure 5.9. Chebyshev type I lowpass filters of orders $N = 1$ to $N = 4$ with $\omega_p = 1\,\text{rad/s}$ and $\epsilon = 1$: (a) Magnitude of the frequency response, and (b) poles.

Chebyshev type I filters. Chebyshev filters, named after the Russian mathematician Pafnuty Lvovich Chebyshev, are based on the Chebyshev polynomials. Type I Chebyshev filters are characterized by ripples in the passband, a steep transition band, and no ripples as well as $-N20\,\text{dBb/decade}$ decay in the stopband.

An Nth order Chebyshev filter is based on the Chebyshev polynomial of the first kind $T_N(\omega)$ given by

$$T_N(\omega) = \begin{cases} \cos\left(N \arccos(\omega)\right) & \text{for } |\omega| \leq 1, \\ \cosh\left(N \operatorname{arccosh}(\omega)\right) & \text{for } |\omega| > 1. \end{cases}$$

In particular, the magnitude of the frequency response is

$$|H(\omega)| = \frac{1}{\sqrt{1 + \epsilon^2 T_N^2\left(\frac{\omega}{\omega_p}\right)}},$$

where ϵ is called the *ripple control factor* and ω_p is the passband edge frequency. The ripple control factor ϵ controls how much ripple there is in the passband. A large ϵ leads to a lot of ripples, whereas a small ϵ leads to little ripple. Figure 5.9a shows the magnitude of the frequency response for $N = 1$ to $N = 4$ for $\omega_p = 1\,\text{rad/s}$ and $\epsilon = 1$. Note that the gain approaches $|H(\omega)| \to \frac{1}{\sqrt{1+\epsilon^2}}$ as $\omega \to 0$ for even filter orders.

The roll off rate for Chebyshev Type I filters is given by

$$R = 2\,\frac{\mathrm{d}}{\mathrm{d}\omega} \log_{10}\left(|H(\omega)|\right)\Big|_{\omega=\omega_c} = -2N^2 \frac{\epsilon^2}{\epsilon^2 + 1}.$$

First, note that the roll off rate is a quadratic function of the filter order N. Hence, the transition from the passband to the stopband is much faster than for Butterworth filter (i.e., Chebyshev Type I filters have a narrower transition band). This means that for the same filter specifications (edge frequencies, ripple and attenuation), the Chebyshev type I filter has the lower order. Second, the ripple control factor also affects the roll of. If ϵ is large (large ripples), the roll off is more or less exactly quadratic in N. On the other hand, if ϵ is small (low ripples), the roll off rate is reduced. Hence, there is a trade-off between the roll off rate and the ripples that needs to be taken into account when designing the filter.

The poles of the Nth order Chebyshev type I filter are located on the right half (stable poles) of an ellipse around the origin in the s-plane. Specifically, the locations of the poles are given by

$$p_n = \mathrm{j}\,\omega_p \cosh\left(\mu + \mathrm{j}\,\pi\frac{n-1/2}{N}\right) \tag{5.10}$$

with

$$\mu = \frac{1}{N}\operatorname{arcsinh}\left(\frac{1}{\epsilon}\right)$$

and illustrated in Figure 5.9b. As for the Butterworth filter, Chebyshev type I filters do not have any zeros.

Chebyshev Type II filters. Chebyshev type II filters are also based on the same Chebyshev polynomials as Chebyshev Type I filters. However, they are used in a different way, which yields a filter that has no ripples in the passband, high roll off rate (narrow transition band), but ripples in the stopband instead.

The magnitude of the frequency response for Chebyshev type II filters is given by

$$|H(\omega)| = \frac{1}{\sqrt{1+\left[\epsilon^2 T_N^2\left(\frac{\omega_s}{\omega}\right)\right]^{-1}}} = \sqrt{\frac{\epsilon^2 T_N^2\left(\frac{\omega_s}{\omega}\right)}{1+\epsilon^2 T_N^2\left(\frac{\omega_s}{\omega}\right)}}, \tag{5.11}$$

where ω_s is the stopband edge frequency. Again, the ripple control factor ϵ affects how much ripple there is. In this case, however, this applies to the stopband rather than the passband (where the Chebyshev type I filter had a monotonic decrease). Figure 5.10a shows the gain function for $N = 1$ to $N = 4$ with $\omega_s = 1\,\mathrm{rad/s}$ and $\epsilon = 0.1$.

The poles of the Chebyshev type II filter are given by

$$p_n = -\,\mathrm{j}\,\frac{\omega_s}{\cosh\left(\mu + \mathrm{j}\,\pi\frac{n-1/2}{N}\right)} \tag{5.12}$$

with

$$\mu = \frac{1}{N}\operatorname{arcsinh}(\epsilon).$$

In contrast to the Butterworth and Chebyshev type I filters, the Chebyshev type II filters has zeros. These are located in

$$z_n = \mathrm{j}\,\frac{\omega_s}{\cos\left(\pi\frac{n-1/2}{N}\right)}, \tag{5.13}$$

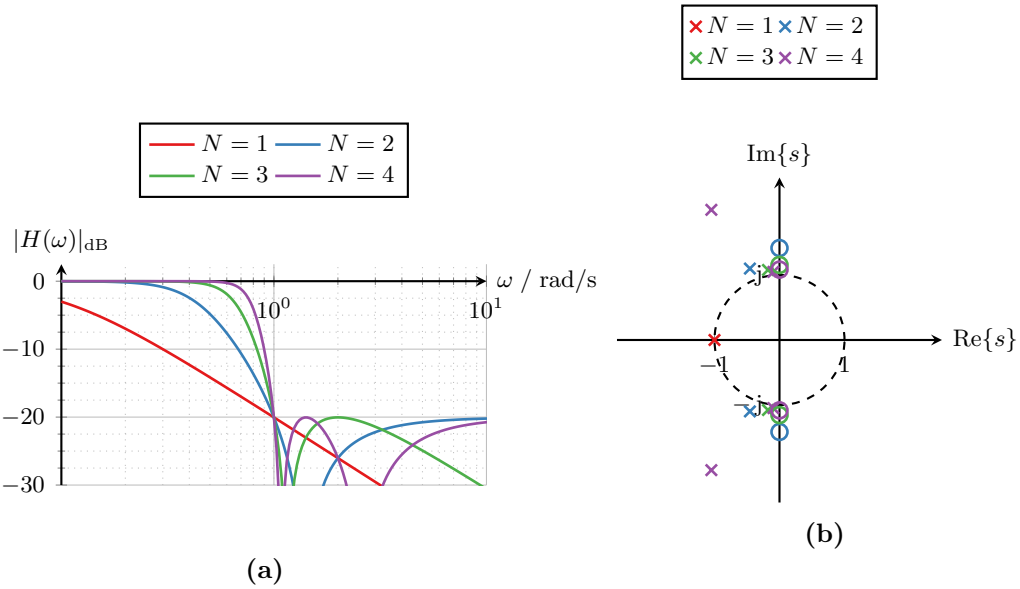

Figure 5.10. Chebyshev type II lowpass filters of orders $N = 1$ to $N = 4$ with $\omega_s = 1\,\text{rad/s}$ and $\epsilon = 0.1$: (a) Magnitude of the frequency response, and (b) poles and zeros (note that one pole at $p = -3.4$ for $N = 3$ is not shown for better readability).

where only the finite zeros are considered. The Poles and zeros for different orders are shown in Figure b.

Elliptic filters. Comparing Butterworth and Chebyshev filters, one can see that allowing some ripples in the frequency response improves the filter's roll off and reduces the transition band. The Chebyshev filters had ripples either in the pass- or stopband. Elliptic filters on the other hand combine this and have ripples in both the pass- and the stopband. This allows for even narrower transition bands or smaller orders for any given set of specifications.

Unfortunately, elliptic filters do not have closed form expressions for the frequency response, roll off, or poles and zeros. However, they can be calculated numerically using filter design toolboxes. Figure 5.11 shows the magnitude of the frequency response for elliptic filters of order $N = 1$ to $N = 4$. Note that as the Chebyshev type II filter, the attenuation does not decrease monotonically as $\omega \to \infty$.

5.2.3 Filter Design

The typical filter design process consists of the following steps:

1. Determining the filter requirements (passband ripple, pass- and stopband edge frequencies, stopband attenuation),
2. filter type selection,
3. calculation of the filter order and coefficients,
4. fine tuning, and
5. implementation in hardware.

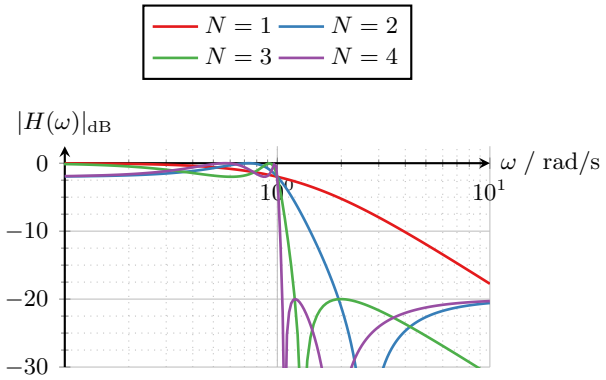

Figure 5.11. Magnitude of the frequency response for elliptic filters for orders $N = 1$ to $N = 4$ with $\omega_p = 1\,\text{rad/s}$, passband ripple $A_p = 2\,\text{dB}$, and stopband attenuation $A_s = 20\,\text{dB}$.

These steps are often done iteratively, until a filter is obtained that fulfills the desired requirements (recall that the last step involves selecting electronic components that are only available for specific values, which affects the resulting filter's properties).

Filter design can be done by hand or using computers and the latter is of course the predominant and more flexible way nowadays. When doing filter design by hand, the filter requirements need to be turned into the actual filter parameters (filter order, transfer function coefficients, poles and zeros, etc.). The required relationships are shown in Table 5.1 and an example of filter design by hand is provided in Example 5.4.

Example 5.4: Filter design by hand

Consider the task of designing a lowpass filter with the following requirements:

- Passband ripple: 2 dB,
- passband edge frequency: $\omega_p = 2\pi 1000\,\text{rad/s} \approx 6283\,\text{rad/s}$ (i.e., $f_p = 1000\,\text{Hz}$),
- stopband attenuation: 40 dB,
- stopband edge frequency: $\omega_s = 2\pi 3000\,\text{rad/s} \approx 18\,850\,\text{rad/s}$ (i.e., $f_s = 3000\,\text{Hz}$).

First, the passband ripple and stopband attenuation are converted from dB to gains:

$$A_p = 10^{\frac{2}{20}} = 1.26 \quad \text{and} \quad A_s = 10^{\frac{40}{20}} = 100.$$

Next, we have to decide what type of filter to implement. For illustration, we choose both a Butterworth and Chebyshev type I filter, starting with the Butterworth filter.

Butterworth filter. The order required for the Butterworth filter is given by

$$N \geq \frac{\log\left(\sqrt{\frac{A_s^2-1}{A_p^2-1}}\right)}{\log\left(\frac{\omega_s}{\omega_p}\right)} = \frac{\log\left(\sqrt{\frac{100^2-1}{1.26^2-1}}\right)}{\log\left(\frac{2\pi 3000}{2\pi 1000}\right)} = 4.44,$$

which means that we have to choose a 5th order Butterword filter. Furthermore, we have to choose the cutoff frequency. This is either chosen such that the passband requirements are met exactly, that is,

$$\omega_c = \frac{\omega_p}{(A_p^2-1)^{\frac{1}{2N}}} = \frac{2\pi 1000}{(1.26^2-1)^{\frac{1}{10}}} = 2\pi 1055\,\text{rad/s} \approx 6629\,\text{rad/s}.$$

The second alternative is to choose the cutoff frequency such that the stopband requirement is met exactly, in which case,

$$\omega_c = \frac{\omega_s}{(A_s^2-1)^{\frac{1}{2N}}} = \frac{2\pi 3000}{(100^2-1)^{\frac{1}{10}}} = 2\pi 1194\,\text{rad/s} \approx 7504\,\text{rad/s}.$$

The resulting frequency responses are shown in Figure 5.12a. The next steps would be to determine the filter's poles and zeros, filter coefficients, and eventually the electronic component values.

Chebyshev filter. For the Chebyshev type I filter, the order is

$$N \geq \frac{\operatorname{arccosh}\left(\sqrt{\frac{A_s^2-1}{A_p^2-1}}\right)}{\operatorname{arccosh}\left(\frac{\omega_s}{\omega_p}\right)} = \frac{\operatorname{arccosh}\left(\sqrt{\frac{100^2-1}{1.26^2-1}}\right)}{\operatorname{arccosh}\left(\frac{2\pi 3000}{2\pi 1000}\right)} = 3.16.$$

Hence, we have to choose a 4th order Chebyshev type I filter. The ripple control factor that ensures that the gain does not drop below $-2\,\text{dB}$ in the passband is

$$\epsilon = \sqrt{A_p^2 - 1} = \sqrt{1.26^2 - 1} = 0.76.$$

The resulting frequency response is shown in Figure 5.12b. Again, the next step would be to determine the filter coefficients and implement (and verify) the filter using analog electronics.

When designing filters using computers, specific filter design tools or appropriate toolboxes for scientific computation language are used. In Python, the corresponding functions are implemented in the package `SciPy.signal`. The second half of Table 5.1 shows the corresponding functions while Example 5.5 illustrates how filter design can be done using Python (minus the actual implementation and choice of components, which is beyond the scope of this course).

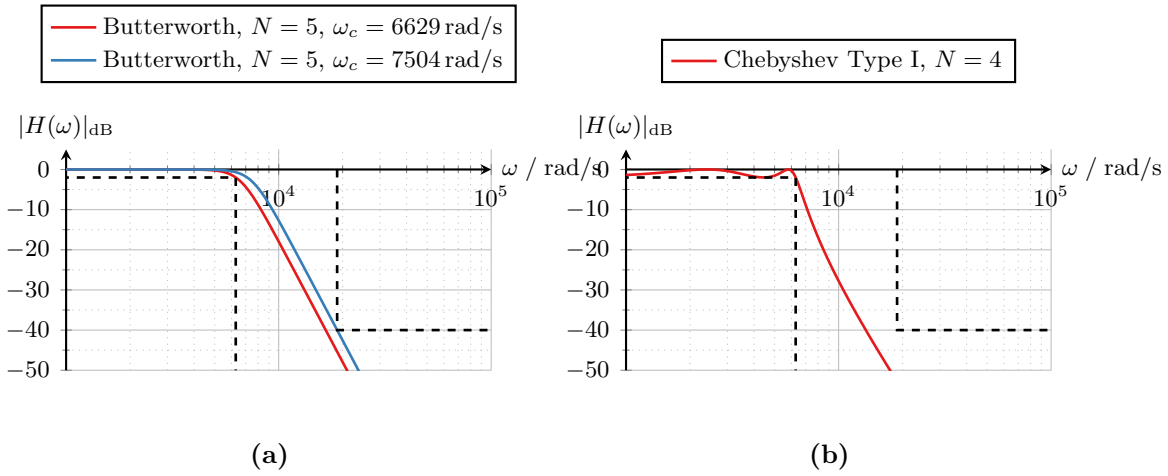

Figure 5.12. Magnitudes of the frequency responses for the filters in Example 5.4. (a) Butterworth filter and (b) Chebyshev type I filter.

Example 5.5: Filter design using Python

In this example, the procedure for designing the same filters as in Example 5.4 using `SciPy` is shown.
The first step is to include the necessary libraries, which are NumPy (`numpy`) and the signal processing functionality from SciPy (`scipy.signal`):

```
import numpy as np
from scipy import signal
```

Next, the filter requirements are defined:

```
# Pass- and stopband edge frequencies
wp = 2*np.pi*1000
ws = 2*np.pi*3000

# Passband ripple and stopband attenuation in dB
Ap = 2
As = 40
```

Note that SciPy's functions expect the passband ripple and stopband attenuation to be in dB. Thus, we do not convert these from dB to gains in this case.
The Butterworth filter is designed using the functions `buttord()` and `butter()`, followed by calculating the frequency response:

```
# Determine the filter order
Nb, wc = signal.buttord(wp, ws, Ap, As, analog=True)

# Calculate the filter coefficients
bb, ab = signal.butter(Nb, wc, analog=True)
```

```
# Calculate the frequency response
wb, Hb = signal.freqs(bb, ab)
```

Note, the argument `analog=True` tells the functions that we want to design a continuous time filter rather than a digital filter. The cutoff frequency `wc` returned by the `buttord` function is the cutoff frequency that gives a tight fit of the stopband requirements. Furthermore, the function `butter()` returns the filter polynomial coefficients b (numerator) and a (denominator). However, the function can also be used to calculate the poles, zeros, and gain factor K.
The Chebyshev filter is designed in the same way as the Butterworth filter but using the functions `cheb1ord()` and `cheby1()` instead:

```
# Determine the filter order
Nc, wn = signal.cheb1ord(wp, ws, Ap, As, analog=True)

# Calculate the filter coefficients
bc, ac = signal.cheby1(Nc, Ap, wn, analog=True)

# Calculate the frequency response
wc, Hc = signal.freqs(bc, ac)
```

Note that in this case, the normalization frequency `wn` is equivalent to the passband edge frequency ω_p. Plotting the frequency responses calculated using `freqs()` again leads to Figure 5.12.

Table 5.1. Filter design formulas and Python functions.

Parameter	Butterworth	Chebyshev Type I	Chebyshev Type II
Design by hand			
Order N	$N \geq \frac{\log\left(\sqrt{\frac{A_s^2-1}{A_p^2-1}}\right)}{\log\left(\frac{\omega_s}{\omega_p}\right)}$	$N \geq \frac{\operatorname{arccosh}\left(\sqrt{\frac{A_s^2-1}{A_p^2-1}}\right)}{\operatorname{arccosh}\left(\frac{\omega_s}{\omega_p}\right)}$	
Normalization frequency	• Passband reqs.: $\omega_c = \frac{\omega_p}{(A_p^2-1)^{\frac{1}{2N}}}$ • Stopband reqs.: $\omega_c = \frac{\omega_s}{(A_s^2-1)^{\frac{1}{2N}}}$	ω_p	ω_s
Ripple control factor ϵ	n/a	$\epsilon = \sqrt{A_p^2 - 1}$	$\epsilon = \frac{1}{\sqrt{A_s^2-1}}$
Gain factor K	$K = 1$	$K = \frac{\prod_{n=1}^{N}(-p_n)}{\sqrt{1+\epsilon^2 \cos^2\left(N\frac{\pi}{2}\right)}}$	$K = \frac{\prod_{n=1}^{N}(-p_n)}{\prod_{n=1}^{N}(-z_n)}$
Poles p_n and zeros z_n	Eq. (5.9)	Eq. (5.10)	Eqs. (5.12)–(5.13)
Design using Python (`SciPy.signal`)			
Order N	`buttord()`	`cheb1ord()`	`cheb2ord()`
Coefficients or poles and zeros	`butter()`	`cheby1()`	`cheby2()`

Chapter 6

Sampling and Reconstruction

6.1 Background

Sampling and reconstruction are the bridges between continuous and discrete time and analog and digital signal processing as illustrated in Figure 6.1. *Sampling* is the process of turning a continuous time signal $x(t)$ into a discrete time signal $x[k]$. The typical way of sampling is by periodically, every T_s seconds, read a new value at the ADC. Mathematically, sampling can be described as

$$x[k] \triangleq x(kT_s). \tag{6.1}$$

This means that the sampled signal $x[k]$ is defined as the signal $x(t)$ at time instants kT_s, where k is an integer number equal to the discrete time variable as illustrated in Figure 6.2. *Reconstruction* on the other hand turns a discrete time signal $y[k]$ into a continuous time signal $y(t)$. This is achieved by sending out the discrete time signal values $y[k]$ through a DAC.

6.2 Sampling

6.2.1 Nyquist–Shannon Sampling Theorem

The elementary question when sampling is then how to choose the sampling time T_s or, equivalently, the sampling frequency $f_s = \frac{1}{T_s}$ or $\omega_s = \frac{2\pi}{T_s}$. The elementary requirement is that there is no loss of information when sampling the signal $x(t)$. This means that in an ideal case, if we would set

$$y[k] = x[k],$$

that is, the output equal to the input, reconstruction should exactly yield the original signal $x(t)$. In other words, the sampling time (or sampling frequency) should be

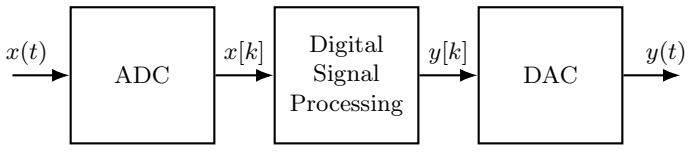

Figure 6.1. Digital signal processing of analog signals.

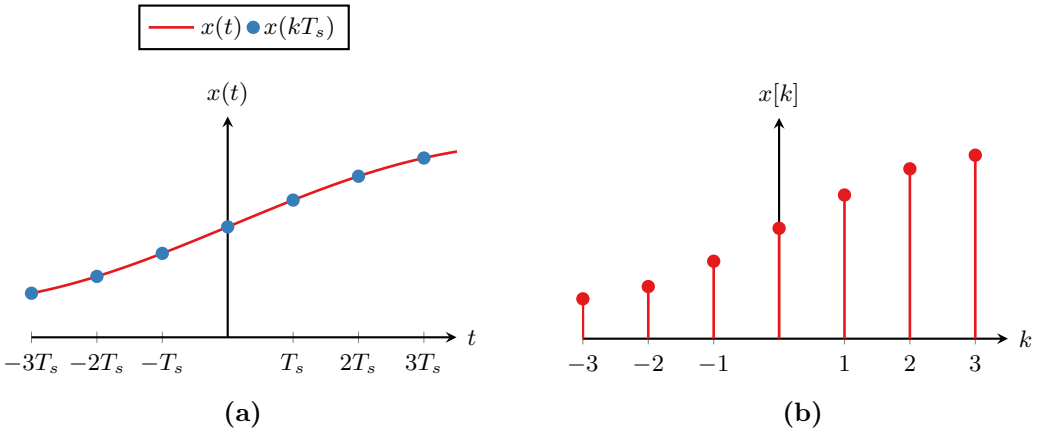

Figure 6.2. Illustration of the sampling process: (a) The continuous time signal $x(t)$ is sampled every T_s seconds, which yields the sampled signal $x(kT_s)$. (b) The resulting discrete time signal $x[k]$ only contains the samples at $x(kT_s)$, without the information between the samples.

chosen such that a signal $x(t)$ can be exactly reconstructed from its samples $x[k]$. The Nyquist–Shannon sampling theorem in Definition 6.1 states this necessary condition.

Definition 6.1: Nyquist–Shannon Sampling Theorem

A band-limited continuous time signal $x(t)$ with one-sided bandwidth $\omega_b = 2\pi f_b$ can exactly be reconstructed from its samples $x[k] \triangleq x(kT_s)$ if the sampling frequency $\omega_s = \frac{2\pi}{T_s}$ satisfies

$$\omega_s > 2\omega_b, \tag{6.2}$$

or, equivalently,

$$f_s > 2f_b \quad \text{or} \quad T_s < \frac{1}{2f_b}.$$

Furthermore, the Nyquist frequency f_N is defined as the maximum allowed one-sided bandwidth for any given sampling frequency

$$\omega_N = \frac{\omega_s}{2}. \tag{6.3}$$

To see why this is the case, we have to reconsider the sampling process. In particular, the sampling relationship in (6.1): The sampled signal $x[k]$ can be seen as the product of the continuous time signal $x(t)$ and a so-called *impulse train* $s(t)$ consisting of T_s-periodic Dirac delta functions

$$s(t) = \sum_{k=-\infty}^{\infty} \delta(t - kT_s). \tag{6.4}$$

The product of $x(t)$ and $s(t)$ can be seen as another continuous time signal $x_s(t)$:

$$x_s(t) = x(t)s(t) = x(t) \sum_{k=-\infty}^{\infty} \delta(t - kT_s) = \sum_{k=-\infty}^{\infty} x(kT_s), \tag{6.5}$$

where the last equality is due to the Dirac delta function's sampling property (see Section 2.1.2). This process is illustrated in the left column of Figure 6.3.

Recalling that every operation in the time domain has a corresponding operation in the frequency domain, we can investigate what effect sampling has in the frequency domain. First, assume that the spectrum of the signal $x(t)$ is $X(\omega)$ as illustrated qualitatively in Figure 6.3b. Note that it is assumed that $X(\omega)$ is zero for $|\omega| > \omega_b$.

The Fourier transform of the impulse train is again an impulse train in the frequency domain where the pulses are spaced by ω_s (Figure 6.3d), that is,

$$S(\omega) = \mathcal{F}\{s(t)\} = \frac{2\pi}{T_s} \sum_{m=-\infty}^{\infty} \delta(\omega - m\omega_s)$$

Furthermore, a product in the time domain yields a (scaled) convolution in the frequency domain (Section 3.2.3). Thus, we have that

$$\begin{aligned} X_s(\omega) &= \frac{1}{2\pi} X(\omega) * S(\omega) \\ &= \frac{1}{2\pi} X(\omega) * \frac{2\pi}{T_s} \sum_{m=-\infty}^{\infty} \delta(\omega - m\omega_s) \\ &= \frac{1}{T_s} \sum_{m=-\infty}^{\infty} X(\omega) * \delta(\omega - m\omega_s) \\ &= \frac{1}{T_s} \sum_{m=-\infty}^{\infty} X(\omega - m\omega_s). \end{aligned}$$

Hence, the spectrum of the sampled signal $X_s(\omega)$ consists of infinitely many, equally spaced copies of $X(\omega)$ centered at $m\omega_s$ for $m = -\infty, \ldots, -1, 0, 1, \ldots, \infty$ as illustrated in Figure 6.3f.

In order to reconstruct the signal $x(t)$ from its samples $x[k]$ (or, equivalently, $x_s(t)$), we must not change the signal in any way. This means that the spectrum of the signal must be preserved and from Figure 6.3f, it can be seen that the original spectrum in Figure 6.3b can be extracted by lowpass filtering $x_s(t)$ for the given scenario. However, if ω_s is chosen smaller, such that the copies of $X(\omega)$ start to overlap with the original spectrum located around zero, the spectrum is altered and $X(\omega)$ can not be extracted anymore. Hence, to avoid overlap, the locations of the copies must be at least $2\omega_b$ apart, which yields the Nyquist–Shannon sampling theorem in Definition 6.1. Example 6.1 shows how to choose the sampling frequency based on a given spectrum and what can happen if the sampling frequency is chosen poorly.

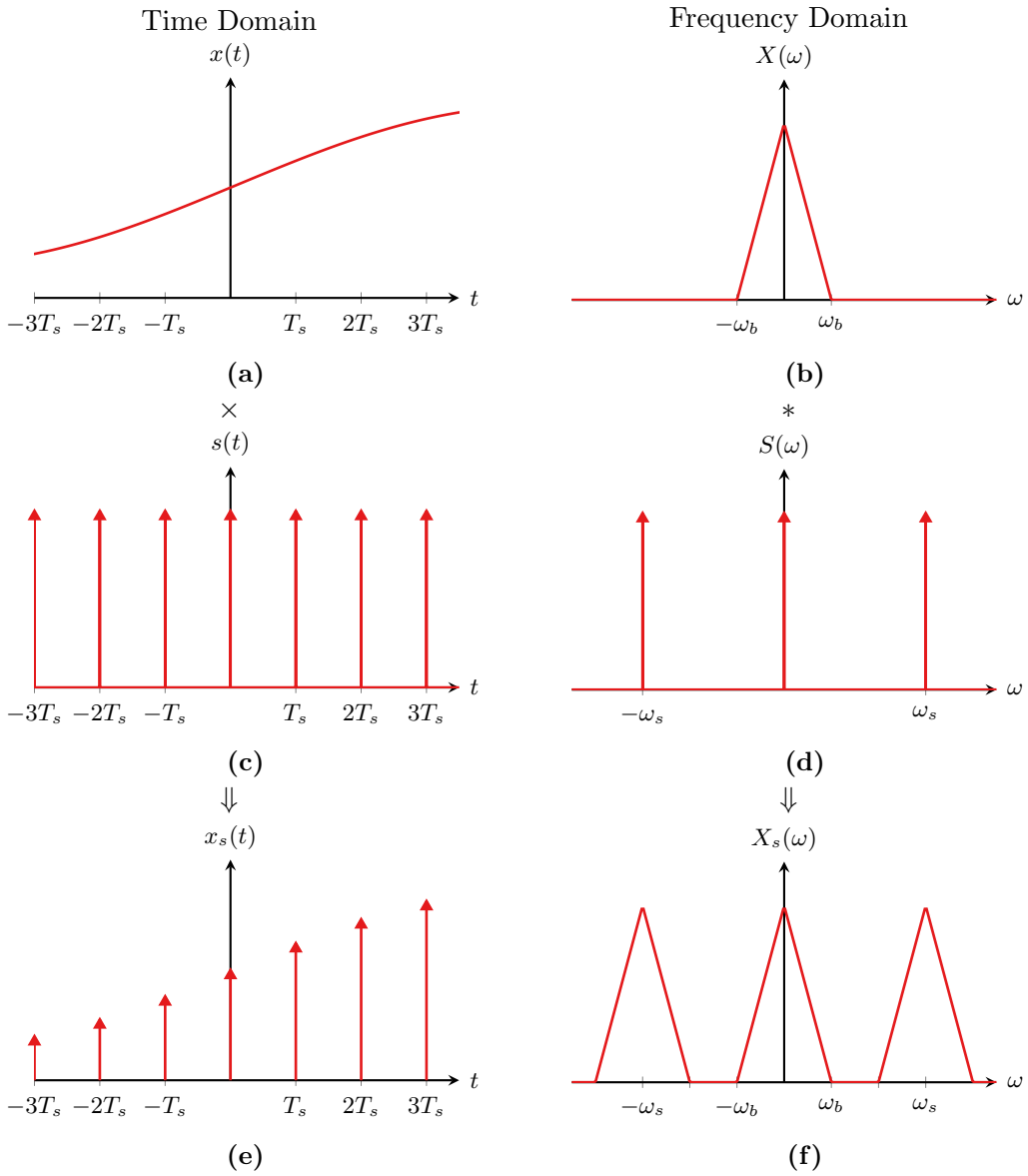

Figure 6.3. Ideal impulse train sampling in the time domain (left column) and frequency domain (right column).

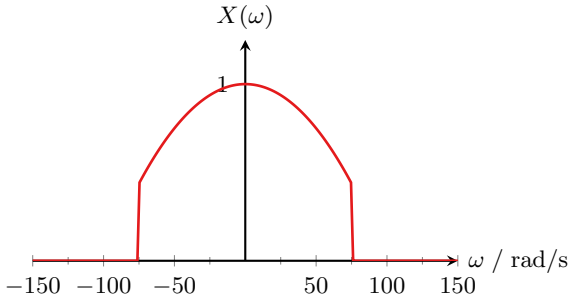

Figure 6.4. Spectrum of the input signal in Example 6.1.

Example 6.1: Choice of the sampling frequency

Consider the choice of the sampling frequency for the following two examples.

a) Consider the signal with the spectrum shown in Figure 6.4. Assuming that the spectrum is zero outside the shown range, it can be seen that the signal is bandlimited to $|\omega| < 75\,\text{rad/s}$. Thus, the minimal sampling frequency is

$$\omega_s > 2 \cdot 75\,\text{rad/s} = 150\,\text{rad/s}.$$

Note that we are using the *one sided bandwidth* here, that is, half the width of the spectrum.

b) Consider sampling of the cosine signal

$$x(t) = \cos(2\pi t)$$

with a sampling frequency of $\omega_s = \frac{2\pi}{0.66}$ rad/s. Clearly, the Nyquist–Shannon sampling theorem is violated as the cosine's frequency is $\omega_0 = 2\pi\,\text{rad/s}$.

The spectrum with this choice of sampling frequency is shown in Figure 6.5a. This shows that sampling with the too-low sampling frequency has introduced a new frequency component at $\omega = \omega_s - \omega_0 = \pi\,\text{rad/s}$. When reconstructing the signal, the signal would thus appear to be a cosine of $\omega = \pi\,\text{rad/s}$ as illustrated in Figure 6.5b. Note that both cosines do pass through the same sampling points. In fact, there are infinitely many possible cosines that pass through these points but without further knowledge of the signal, we would have to assume that the cosine with the lowest frequency is the correct one, which is wrong in this case.

In practice, the sampling frequency ω_s is always chosen such that there is a small safety margin between the maximum frequency ω_b and the Nyquist frequency ω_N, which is called *oversampling*.

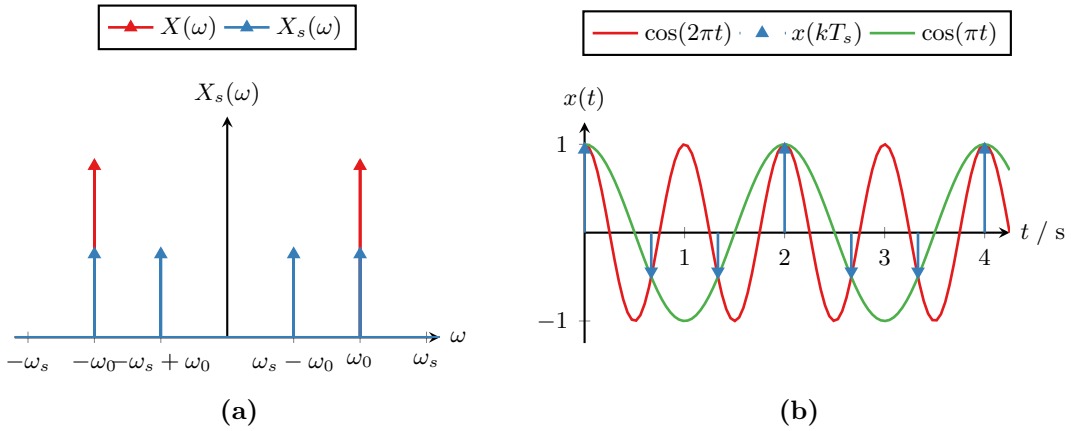

Figure 6.5. Sampling of a cosine with a too low sampling frequency. (a) The spectra of the cosine and an excerpt of the sampled signal's spectrum close to zero. (b) time domain illustration of the two cosines with lowest frequencies and the coinciding samples.

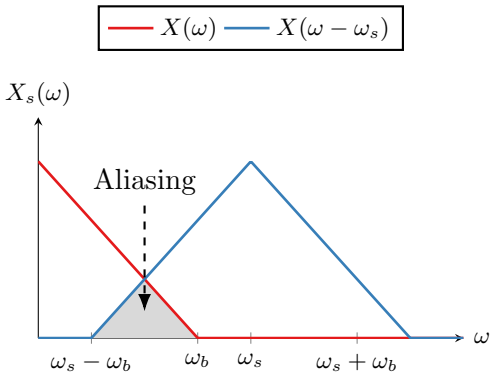

Figure 6.6. Illustration of the aliasing effect: The sampling frequency ω_s is chosen too low such that $\omega_s - \omega_b < \omega_b$, which causes an overlap of the original signal's spectrum $X(\omega)$ (red) and its copy $X(\omega - \omega_s)$ at ω_s (copies at $2\omega_s$, $3\omega_s$, etc. omitted for readability).

6.2.2 Aliasing and Anti-Aliasing

As discussed above, if the sampling frequency is chosen too low, the repeated copies of the original signal start to overlap with the copy centered around zero (and each other). This phenomenon is called *aliasing* and is illustrated in Figure 6.6. Aliasing modifies the spectrum in a way that it is impossible to recover the original signal's spectrum $X(\omega)$ and must thus be avoided.

So far, it has been assumed that the spectrum of the signal that is sampled is clean in the sense that it is zero above ω_b. In practice, however, the spectrum is never zero; at the very least, there will be noise entering the system. This in turn will cause aliasing and thus corrupt the sampled signal $x[k]$. To avoid this from happening, an (analog) anti-aliasing lowpass filter has to be placed right before the sampler as illustrated in Figure 6.7a.

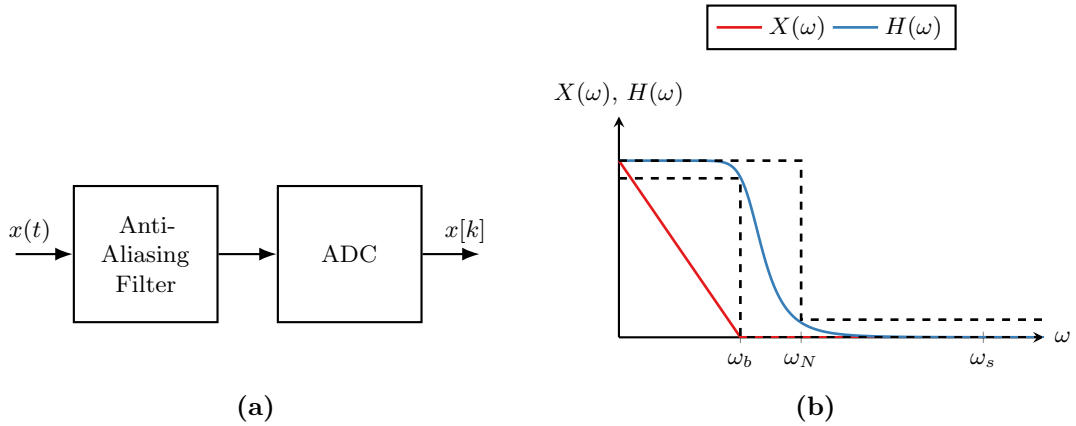

Figure 6.7. Illustration of an anti-aliasing filter design preceding the ADC. (a) Blockdiagram and (b) frequency response design.

Ideally, the anti-aliasing filter would block everything above the maximum signal frequency ω_b. However, we saw in Chapter 5 that infinitely sharp filters are not possible to implement in practice. Hence, a real-world anti-aliasing filter instead places the passband edge frequency at the signal bandwidth ω_b and the stopband edge frequency at the Nyquist frequency ω_N. Thus, the margin between the theoretically minimal sampling frequency and the actually used one is used as the transition band (Figure 6.7b). This implies that the larger the oversampling, the wider the transition band, and thus, the lower the requirements for the anti-aliasing filter. Furthermore, since real filters never completely filter out everything in the stopband, there will always be a small amount of aliasing leaking through.

Example 6.2: Anti-aliasing filter

The human ear can hear frequencies up to about $f_b \approx 20\,000\,\text{Hz}$ (a value that decreases with age and exposure to harmful sound). Digital audio (e.g., compact discs) is typically sampled at $f_s = 44\,100\,\text{Hz}$, which gives a Nyquist frequency of $f_N = 22\,050\,\text{Hz}$.
Hence, digital recording equipment may employ anti-aliasing filters with a transition band between 20 000 Hz and 22 050 Hz.

6.3 Reconstruction

The derivation of the Nyquist–Shannon sampling theorem showed that reconstruction can be achieved by recovering the signal's original spectrum $X(\omega)$ from the sampled spectrum $X_s(\omega)$. Recalling that $X_s(\omega)$ consists of $X(\omega)$ and infinitely many, frequency-shifted copies $X(\omega - m\omega_s)$, reconstruction can be achieved by filtering the signal $x_s(t)$ using an ideal lowpass filter with cutoff frequency $\omega_c = \omega_N$ as illustrated in Figure 6.8.

Unfortunately, a real DAC can not generate infinitely short Dirac delta impulses. Furthermore, the ideal reconstruction filter has an infinitely sharp transition and is

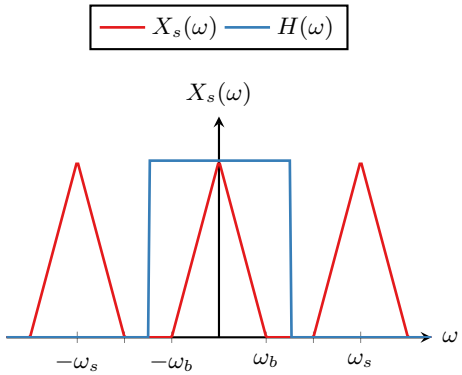

Figure 6.8. Ideal reconstruction using an ideal lowpass filter.

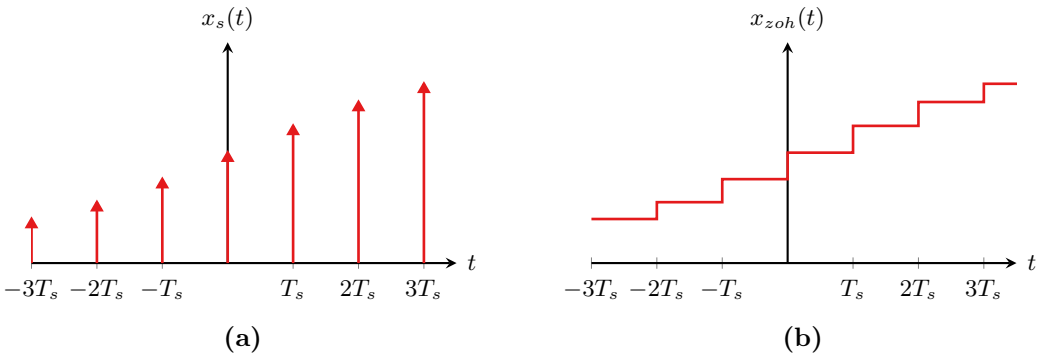

Figure 6.9. Reconstruction using zero-order hold: (a) The sampled signal $x_s(t)$ and (b) its ZOH version $x_{zoh}(t)$.

non-causal. Instead, real DACs use *zero-order hold* (ZOH) followed by a smoothing filter for reconstruction. In ZOH reconstruction, the DAC simply keeps the output constant during the complete sampling period rather than generating an impulse, as illustrated in Figure 6.9b.

The ZOH signal $x_{zoh}(t)$ can be described by a convolution of the impulse signal $x_s(t)$ and a rectangular pulse, that is,

$$x_{zoh}(t) = x_s(t) * \text{rect}\left(\frac{t - T_s/2}{T_s}\right).$$

In the frequency domain, this thus yields a product of the sampled signal's spectrum $X_s(\omega)$ and a sinc function given by

$$X_{zoh}(\omega) = X_s(\omega) T_s \,\text{sinc}\left(\frac{\omega T_s}{2\pi}\right) e^{-\mathrm{j}\,\omega\frac{T_s}{2}} = T_s X_s(\omega) \,\text{sinc}\left(\frac{\omega}{\omega_s}\right) e^{-\mathrm{j}\,\omega\frac{T_s}{2}}.$$

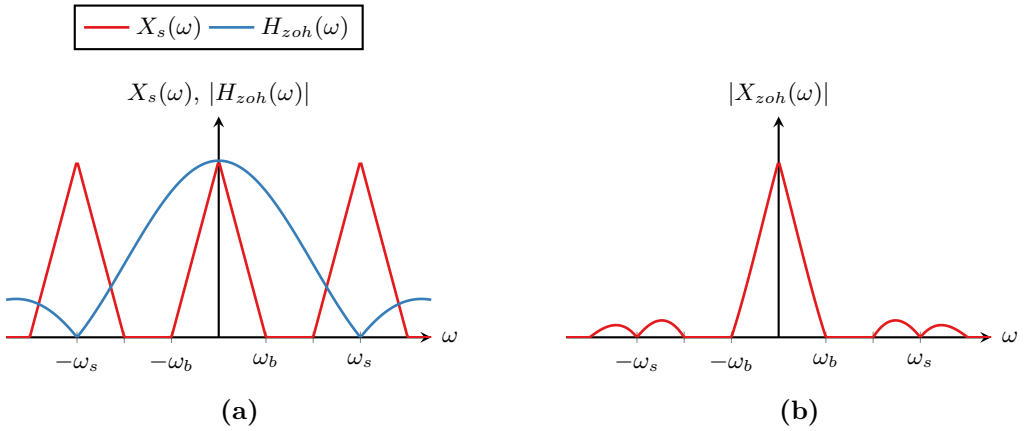

Figure 6.10. Effect of zero-order hold reconstruction in the frequency domain. (a) Sampled signal $X_s(\omega)$ together with the frequency response of the ZOH filter and (b) output after the ZOH $X_{zoh}(\omega)$.

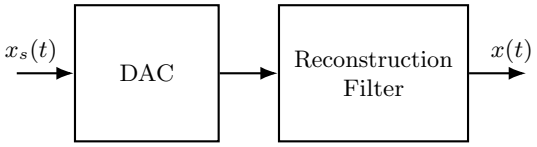

Figure 6.11. Zero-order-hold reconstruction with reconstruction filter.

Thus, as illustrated in the frequency domain in Figure 6.10, ZOH also acts as a lowpass filter with frequency response

$$H_{zoh}(\omega) = T_s \,\mathrm{sinc}\left(\frac{\omega}{\omega_s}\right) e^{-\mathrm{j}\,\omega\frac{T_s}{2}}$$

that attenuates the frequency-shifted copies of $X(\omega)$. To get rid of the remaining higher frequency components, which manifest as the sharp step transitions in the ZOH signal $x_{zoh}(t)$, an additional lowpass smoothing filter is used. This yields the complete reconstruction chain illustrated in Figure 6.11.

6.4 Quantization

Sampling as discussed above simply converts a continuous time signal into a discrete time signal. Each sample represents the amplitude of the continuous time signal at the particular sampling instant. However, the amplitude is still a continuous variable that can take on infinitely many values. Since digital computers can not represent an infinite number of values, each sample value has to be mapped to a finite number of values, a step called *quantization*. Quantization is performed at the A/D converter and a sampled and quantized signal is called a digital signal.

Quantization is characterized by the number of *quantization levels* L that can be represented. For example, an 8 bit A/D converter has $L = 2^8 = 256$ different quantization

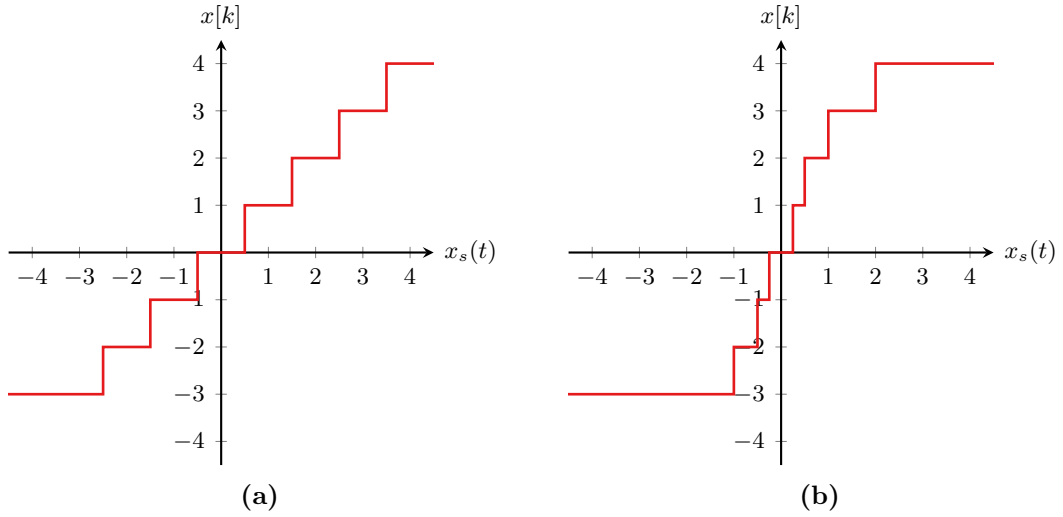

Figure 6.12. Example input-output relationship of two 3 bit quantizers (with $L = 2^3 = 8$ quantization levels): (a) uniform quantizer and (b) non-uniform quantizer.

Table 6.1. Raw data rates for digital audio used in commercial applications.

Application	Bandwidth Hz	Sampling rate / 1/s	Quantization levels L	Raw data bytes/s
Telephone	200–3400	8000	2^8	8000
Compact disc (stereo)	20–20 000	44 100	2^{16}	176 400
Digital audio tape	20–20 000	48 000	2^{16}	192 000
High resolution audio	20–20 000	192 000	2^{24}	3 072 000

levels. The most common way of quantization is *uniform quantization* where the input levels are mapped uniformly onto the different quantization levels, see Figure 6.12a.

In many applications, the distribution of the amplitude of the input is skewed towards low values. Using a uniform quantizer would lead to many samples having the same quantization level and hence loosing a lot of information. Thus, using a non-uniform quantizer with fine quantization at frequently occurring amplitude ranges and coarse quantization at amplitude ranges that occur more seldom, gives a better quantization result. A non-uniform quantizer is illustrated in Figure 6.12b.

Note that in all forms of quantization, there is a saturation level due to the limited number of quantization levels. This means that all values above (and below) some threshold are all mapped to the same quantization level. It is thus important to make sure that the input signal to the A/D converter is properly scaled such that its dynamic range does not exceed the saturation thresholds.

A few examples of the bandwidth, sampling frequency, quantization levels, and data rates for common commercial applications are shown in Table 6.1.

Chapter 7

Discrete Time Signals and Systems

In this chapter, the elementary discrete time signals and their properties, together with the time domain input-output relationship for discrete time LTI systems are discussed. Many of the signals and properties are very similar to their continuous time counterparts. However, there are some important differences highlighted below.

7.1 Discrete Time Signals

7.1.1 Elementary Discrete Time Signals

As discussed in Chapter 1, a discrete time signal $x[k]$ is a signal that only has signal values at discrete time instants k where k is an integer. In other words, $x[k]$ is only defined for $\ldots, x[-2], x[-1], x[0], x[1], x[2], \ldots$ but not for, for example $x[-2.5]$ or $x[0.5]$. Furthermore, the values of $x[k]$ are typically called the signals *samples*. Below follows a summary of some of the most important analytic discrete time signals.

Sine and cosine signals. The discrete time sine and cosine signals with amplitude A, discrete frequency $\Omega_0 = 2\pi f_0 = \frac{2\pi}{K_0}$, and phase φ are defined as

$$x[k] = A\sin(\Omega_0 k + \varphi) \tag{7.1}$$

and

$$x[k] = A\cos(\Omega_0 k + \varphi), \tag{7.2}$$

respectively. Note that for a pure discrete time sine or cosine, the period K_0 must be a natural number and an example of a discrete time sine is given in Figure 7.1

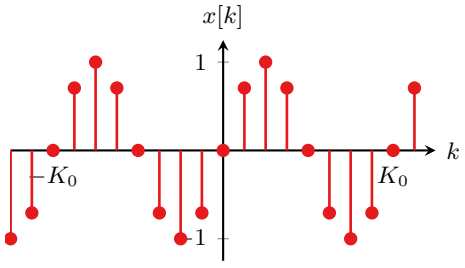

Figure 7.1. Illustration of a discrete time sine.

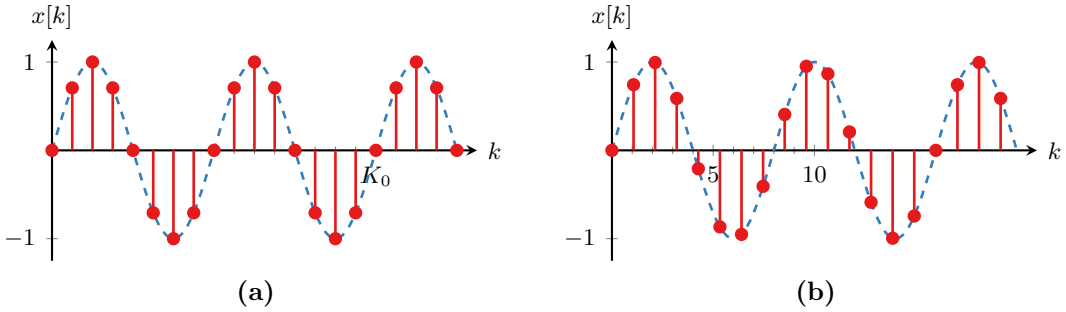

Figure 7.2. Continuous time sines sampled with (a) natural and (b) rational ratio $\frac{T_0}{T_s}$.

Furthermore, sampling continuous time sine and cosine signals (Section 2.1.1) gives rise to the sampled discrete time sines and cosines given by

$$x[k] = A\sin(\omega_0 T_s k + \varphi) \quad \text{and} \quad x[k] = A\cos(\omega_0 T_s k + \varphi). \tag{7.3}$$

Recall that $\omega_0 T_s = \frac{2\pi}{T_0} T_s$, whereas for the discrete time sine and cosine we have that $\Omega_0 = \frac{2\pi}{K_0}$ with K_0 a natural number. Thus, sampled sines and cosines as in (7.3) are only equivalent to discrete time sines and cosines as in (7.1)–(7.2) if the ratio $\frac{T_0}{T_s}$ is a natural number (Figure 7.2a).

If the ratio $\frac{T_0}{T_s}$ is rational instead, the sampled sine or cosine is still periodic, but not a discrete time sine or cosine as in (7.1)–(7.2). The periodicity is over multiple continuous time periods instead as illustrated in Figure 7.2b.

Unit impulse. The discrete time unit impulse function, also called the *Kronecker* delta function is defined as

$$\delta[k] = \begin{cases} 1 & \text{for } k = 0, \\ 0 & \text{for } k \neq 0, \end{cases} \tag{7.4}$$

and is illustrated in Figure 7.3a. Note that in contrast to the Dirac delta function $\delta(t)$, the discrete time unit impulse $\delta[k]$ is a function and not defined over the limit. Furthermore, its value at $k = 0$ is exactly 1.

Rectangular pulse. In discrete time, the rectangular pulse is denoted as

$$\operatorname{rect}\left[\frac{k}{2N+1}\right] = \begin{cases} 1 & \text{for } |k| \neq N, \\ 0 & \text{for } |k| > N. \end{cases} \tag{7.5}$$

As illustrated in Figure 7.3b, the discrete time rectangular pulse has value one from $k = -N$ to $k = N$, also including the sample at $k = 0$. Thus, different from the continuous time case, the width of the pulse is $2N + 1$.

Unit step. The discrete time unit step $u[k]$ is defined in the same way as the continuous time unit step:

$$u[k] = \begin{cases} 0 & \text{for } k < 0, \\ 1 & \text{for } k \geq 0, \end{cases} \tag{7.6}$$

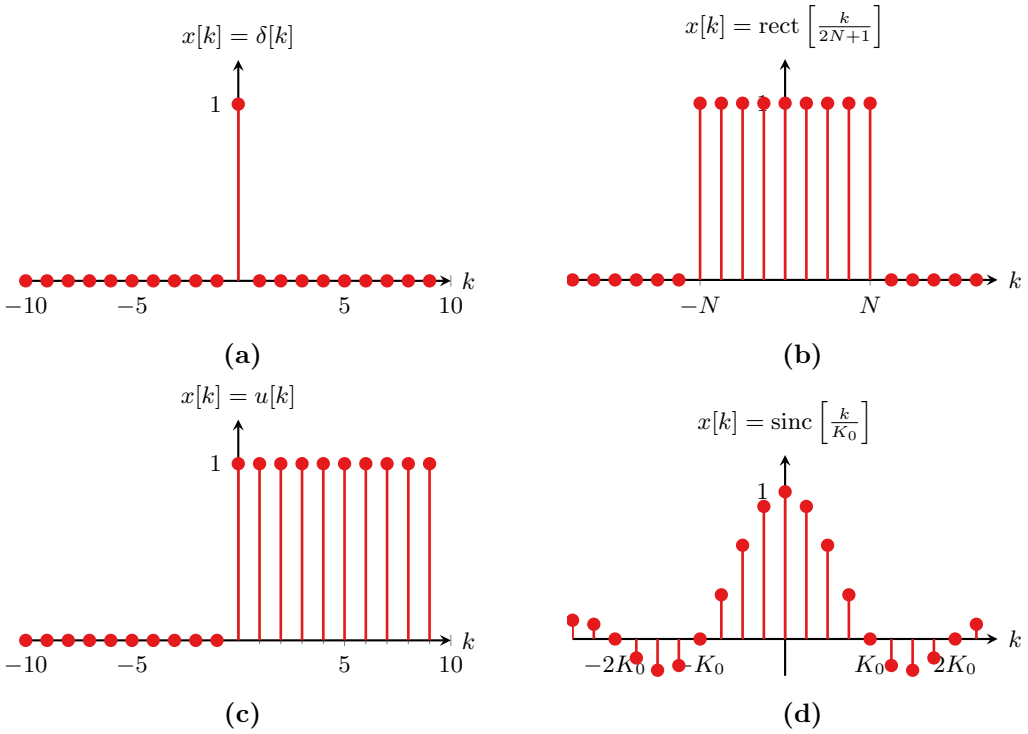

Figure 7.3. Illustration of elementary discrete time signals: (a) unit impulse function (Kronecker delta function), (b) rectangular pulse, (c) unit step, and (d) sinc.

and is illustrated in Figure 7.3c.

Sinc. The discrete time sinc function is defined as

$$\text{sinc}\left[\frac{k}{K_0}\right] = \frac{\sin\left(\pi\frac{k}{K_0}\right)}{\pi\frac{k}{K_0}}. \tag{7.7}$$

Figure 7.3d shows the sinc function. Note that the zero crossings are located at integer multiples of K_0. Furthermore, if K_0 is not an integer, no sample will coincide with the zero crossing.

7.1.2 Discrete Time Signal Properties

Periodic signals. A periodic discrete time signal fulfills the condition that

$$x[k] = x[k + K_0], \tag{7.8}$$

where K_0 is the smallest natural number (a non-negative integer) that fulfills the above condition. K_0 is called the fundamental period and the fundamental frequency Ω_0 of a periodic discrete time signals is

$$\Omega_0 = \frac{2\pi}{K_0}.$$

A signal that does not fulfil the above condition is called an aperiodic (discrete time) signal. Note that a continuous time sine signal that is sampled using a sampling time T_s is not necessarily a periodic discrete time signal as illustrated in Example 7.1.

Example 7.1: Periodicity of discrete time signals

a) Consider the discrete time sine

$$x[k] = \sin\left(\frac{2\pi}{8}k\right)$$

with $K_0 = 8$ shown in Figure 7.1. This signal is periodic, since

$$x[k+K_0] = \sin\left(\frac{2\pi}{8}(k+8)\right) = \sin\left(\frac{2\pi}{8}k + 2\pi\right) = \sin\left(\frac{2\pi}{8}k\right).$$

b) The sampled sine

$$x[k] = x(kT_s) = \sin\left(\frac{2\pi}{T_0}kT_s\right)$$

is periodic if it holds that

$$x[k] = x[k+K_0] = \sin\left(\frac{2\pi T_s}{T_0}(k+K_0)\right) = \sin\left(\frac{2\pi T_s}{T_0}k + 2\pi n\right)$$

for natural numbers K_0 and n, where the last equality follows from the 2π-periodicity of the sine. Thus, if

$$\frac{2\pi T_s K_0}{T_0} = 2\pi n,$$

or equivalently,

$$\frac{T_s}{T_0}K_0 = n,$$

the sampled sine is periodic (over n continuous time periods). This is illustrated in Figure 7.2b for $T_0 = 8\,\text{s}$, $T_s = \frac{16}{15}\,\text{s}$, and $K_0 = 15$, which yields that the signal is periodic over 2 continuous time periods.

Causal signals. A causal discrete time signal is zero for negative time values $k < 0$, that is, a causal signal $x[k]$ fulfills

$$x[k] = 0 \quad \text{for } k < 0. \tag{7.9}$$

Again, in practice, all signals are causal as they have some starting point, which can be considered $k = 0$.

Energy and power signals. For discrete time signals, the energy is defined as

$$E = \sum_{k=-\infty}^{\infty} |x[k]|^2 . \tag{7.10}$$

Furthermore, the average power for aperiodic signals is defined as

$$P = \lim_{K\to\infty} \frac{1}{K+1} \sum_{k=-K/2}^{K/2} |x[k]|^2 . \tag{7.11}$$

For periodic signals this becomes

$$P = \frac{1}{K_0} \sum_{k=0}^{K_0-1} |x[k]|^2 . \tag{7.12}$$

Again, a discrete time signal is called an *energy signal* if the total energy E is non-zero and finite, that is, $0 < E < \infty$. Similarly, a discrete time *power signal* has non-zero, finite power P. Note that a signal can be a power signal, an energy signal, or neither, but never both a power signal and an energy signal.

7.2 Time Domain Analysis of Discrete Time Systems

7.2.1 Impulse Response

In the same way as continuous time LTI systems can completely be described by their impulse response $h(t)$, discrete time LTI systems can be described by their discrete time impulse response $h[k]$ when the input $x[k] = \delta[k]$ is applied to the system (Definition 7.1).

Definition 7.1: Discrete Time Impulse Response

The impulse response $h[k]$ of a discrete time LTI system is the output of the system when the Kroenecker delta impulse function $\delta[k]$ is applied at the input

$$\delta[k] \mapsto h[k]. \tag{7.13}$$

Furthermore, the impulse response satisfies

$$\alpha\delta[k-k_0] \mapsto \alpha h[k-k_0] \tag{7.14}$$

for arbitrary α and integer k_0.

A discrete time system is called causal if its impulse response only depends on the current (k) and past ($k-1$, $k-2$, ...) and no future samples ($k+1$, $k+2$, etc.). Thus, for a discrete time LTI system to be causal it must hold that

$$h[k] = 0 \quad \text{for } k < 0. \tag{7.15}$$

A non-causal and causal impulse responses are shown in Figure 7.4. Note that in practice, all systems are of course causal as it is possible for a system to anticipate the future.

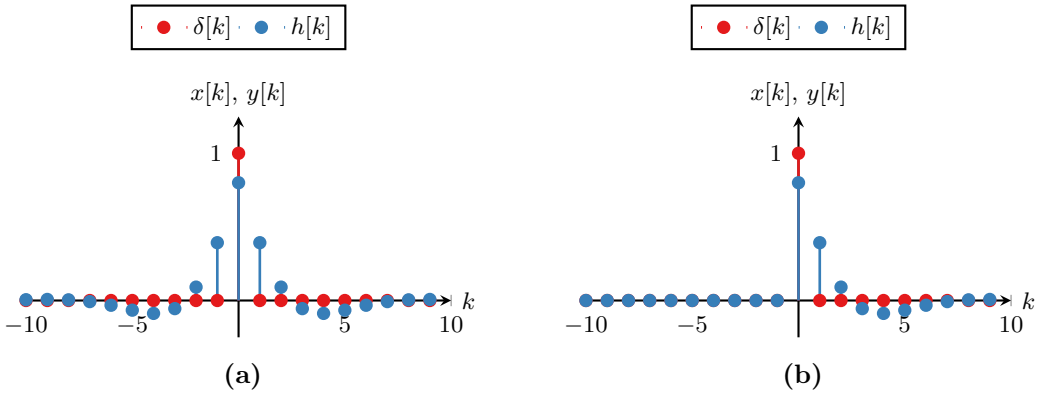

Figure 7.4. Examples of discrete time impulse responses. (a) Non-causal, and (b) causal.

7.2.2 Convolution Sum

By definition, an impulse $\delta[k]$ at the input of a discrete time LTI system leads to the impulse response $h[k]$ at the output of a system. Furthermore, note that any discrete time signal $x[k]$ can be written as a weighted sum of time-shifted impulses with weights $x[m]$, that is, as

$$x[k] = \sum_{m=-\infty}^{\infty} x[m]\delta[k-m].$$

Hence, when applying the signal $x[k]$ to a discrete time LTI system, each term in the sum must give rise to a scaled, and time-shifted copy of the impulse response $x[m]h[k-m]$, see (7.13). Thus, the output is

$$y[k] = \sum_{m=-\infty}^{\infty} x[m]h[k-m],$$

which is the convolution sum. This is the discrete time equivalent of the general input-output relationship for continuous time systems and is summarized in Definition 7.2. Furthermore, some important properties of the convolution sum are given in Table 7.1.

Definition 7.2: Input-output relationship for discrete time systems

The output signal $y[k]$ of a discrete time LTI system is given by the discrete convolution of the system's impulse response $h[k]$ and the input signal $x[k]$,

$$y[k] = \sum_{m=-\infty}^{\infty} x[m]h[k-m] \tag{7.16a}$$

$$= \sum_{m=-\infty}^{\infty} h[k]x[k-m]. \tag{7.16b}$$

Table 7.1. Properties of the discrete time convolution sum.

Property	
Commutation	$x_1[k] * x_2[k] = x_2[k] * x_1[k]$
Distribution	$x_1[k] * (x_2[k] + x_3[k]) = x_1[k] * x_2[k] + x_1[k] * x_3[k]$
Association	$x_1[k] * (x_2[k] * x_3[k]) = x_1[k] * x_2[k] * x_3[k]$
Time shifting	$x_1[k - k_1] * x_2[k - k_2] = y[k - k_1 - k_2]$
Duration	$x_1[k] = 0$ for $k \geq K_1$, $x_2[k] = 0$ for $k \geq K_2 \Rightarrow$ $x_1[k] * x_2[k] = 0$ for $k \geq K_1 + K_2$
Convolution with impulse function	$x[k] * \delta[k - K] = x[k - K]$
Convolution with step function	$x[k] * u[k] = \sum_{m=-\infty}^{k} x[m]$

For causal systems with $h[k] =$ for $k < 0$, the convolution reduces to

$$y[k] = \sum_{m=0}^{\infty} h[m]x[m - k]. \tag{7.17}$$

The discrete time convolution is denoted using an asterisk, that is,

$$y[k] = x[k] * h[k]. \tag{7.18}$$

Finally, a discrete time LTI system is BIBO stable if any arbitrary bounded input signal produces a bounded output signal. Assume that the input signal is bounded according to

$$|x[k]| \leq M_x < \infty$$

for all times k. Then, the system is BIBO stable if the output signal is bounded according to

$$|y[k]| \leq M_y < \infty$$

for all k. Hence, for the system to be stable it must hold that

$$\begin{aligned} |y[k]| &= \left| \sum_{m=-\infty}^{\infty} x[m]h[k-m] \right| \\ &\leq \sum_{m=-\infty}^{\infty} |x[m]|\,|h[k-m]| \\ &\leq M_x \sum_{m=-\infty}^{\infty} |h[m]|\,. \end{aligned}$$

A sufficient condition on the impulse response for discrete time BIBO stability is thus

$$\sum_{k=-\infty}^{\infty} |h[k]| < \infty. \tag{7.19}$$

Chapter 8

Discrete Time Fourier Analysis

8.1 Discrete Time Fourier Series and Transform

8.1.1 Definition and Properties

Similar to the continuous time case, periodic discrete time signals can be expressed in terms of their discrete time Fourier series as given in Definition 8.1.

Definition 8.1: Discrete time Fourier series

The discrete time Fourier series of a K_0-periodic discrete time signal $x[k]$ with fundamental frequency $\Omega_0 = \frac{2\pi}{K_0}$ is

$$x[k] = \sum_{n=0}^{K_0-1} c_n e^{\mathrm{j}\, n\Omega_0 k} \tag{8.1}$$

where the coefficients c_n are given by

$$c_n = \frac{1}{K_0} \sum_{k=0}^{K_0-1} x[k] e^{-\mathrm{j}\, n\Omega_0 k}. \tag{8.2}$$

Similarly, the discrete time Fourier transform (DTFT) is the equivalent of the Fourier transform for discrete time systems. To find the expression for the DTFT, consider the Fourier transform of a sampled signal

$$x_s(t) = \sum_{k=-\infty}^{\infty} x(t)\delta(t - kT_s)$$

given by

$$\begin{aligned} X(\omega) &= \int_{-\infty}^{\infty} x_s(t) e^{-\mathrm{j}\,\omega t}\,\mathrm{d}t \\ &= \int_{-\infty}^{\infty} \sum_{k=-\infty}^{\infty} x(t)\delta(t - kT_s) e^{-\mathrm{j}\,\omega t}\,\mathrm{d}t. \end{aligned}$$

Switching the order of the sum and the integral and using the integration property of the Dirac delta function yields

$$\begin{aligned} X(\omega) &= \sum_{k=-\infty}^{\infty} \int_{-\infty}^{\infty} x(t)\delta(t - kT_s)e^{-\mathrm{j}\,\omega t}\,\mathrm{d}t \\ &= \sum_{k=-\infty}^{\infty} x(kT_s)e^{-\mathrm{j}\,\omega kT_s}. \end{aligned}$$

Note now that the first term in the sum is $x[k] \triangleq x(kT_s)$. Furthermore, the quantity $\Omega \triangleq \omega T_s$ can be seen as a frequency normalized with respect to the sampling freqeuency. That is, we define the *normalized frequency* Ω as

$$\Omega = \omega T_s = 2\pi \frac{f}{f_s}. \tag{8.3}$$

This yields the expression

$$X(\Omega) = \sum_{k=-\infty}^{\infty} x[k]e^{-\mathrm{j}\,\Omega k},$$

which is the expression for the DTFT. Note that the dependency is now on the normalized (or discrete) frequency variable Ω, which is indicated on the left hand side the equation. The formal definition of the DTFT and its inverse transform are given in Defintion 8.2.

Definition 8.2: Discrete time Fourier transform

The discrete time Fourier transform $X(\Omega)$ with discrete frequency Ω for the discrete time signal $x[k]$ (analysis equation) is defined as

$$X(\Omega) = \sum_{k=-\infty}^{\infty} x[k]e^{-\mathrm{j}\,\Omega k}. \tag{8.4}$$

The inverse discrete time Fourier transform (synthesis equation) is defined as

$$x[k] = \frac{1}{2\pi} \int_{0}^{2\pi} X(\Omega)e^{\mathrm{j}\,\Omega k}\,\mathrm{d}\Omega. \tag{8.5}$$

Note that the discrete time Fourier transform can of course be applied to any discrete time signal $x[k]$, not only sampled signals. Furthermore, the discrete time signal $x[k]$ and its discrete time Fourier transform $X(\Omega)$ are again a transform pair

$$x[k] \circ\!\!-\!\!\bullet\, X(\Omega).$$

One important property of the discrete time Fourier transform is that it is 2π-periodic. This means that the relationship

$$X(\Omega) = X(\Omega + 2\pi) \tag{8.6}$$

Table 8.1. Properties of the discrete time Fourier transform.

Property	Time Domain	Frequency Domain
Periodicity	-	$X(\Omega) = X(\Omega + 2\pi)$
Symmetry	Real-valued	$X(-\Omega) = X^*(\Omega)$
Linearity	$\alpha x_1[k] + \beta x_2[k]$	$\alpha X_1(\Omega) + \beta X_2(\Omega)$
Time shifting (k_0: integer)	$x[k - k_0]$	$e^{-\mathrm{j}\,\Omega k_0} X(\Omega)$
Time differencing	$x[k] - x[k-1]$	$\left(1 - e^{-\mathrm{j}\,\Omega}\right) X(\Omega)$
Frequency domain differentiation	$-\mathrm{j}\,k x[k]$	$\dfrac{\mathrm{d}X(\Omega)}{\mathrm{d}\Omega}$
Time summation	$\displaystyle\sum_{n=-\infty}^{k} x[n]$	$\dfrac{X(\Omega)}{1 - e^{-\mathrm{j}\,\Omega}} + \pi X(0) \displaystyle\sum_{m=-\infty}^{\infty} \delta(\Omega - 2\pi m)$
Convolution	$x_1[k] * x_2[k]$	$X_1(\Omega) X_2(\Omega)$
Multiplication†	$x_1[k] x_2[k]$	$\dfrac{1}{2\pi} X_1(\Omega) * X_2(\Omega)$
Parseval's theorem	$E = \displaystyle\sum_{k=-\infty}^{\infty} \lvert x[k] \rvert^2$	$E = \dfrac{1}{2\pi} \displaystyle\int_0^{2\pi} \lvert X(\Omega) \rvert^2 \,\mathrm{d}\Omega$

†The convolution is on the interval $0 \ldots 2\pi$.

must hold. To see why this is the case, note that in the discrete time Fourier transform, the signal $x[k]$ is multiplied by the factor $e^{-\mathrm{j}\,\Omega k}$, see (8.4). Since $e^{-\mathrm{j}\,\Omega k}$ is a complex number on the unit circle, it must hold that

$$e^{-\mathrm{j}\,\Omega k} = e^{-\mathrm{j}(\Omega + 2\pi)k}$$

and thus

$$x[k] e^{-\mathrm{j}\,\Omega k} = x[k] e^{-\mathrm{j}(\Omega + 2\pi)k}.$$

The 2π-periodicity of the discrete time Fourier transform is also consistent with the continuous time Fourier transform of a sampled signal, which is ω_s-periodic. Recall that for sampled signals, we have that $\Omega = \omega T_s$. Thus, it follows that for sampled signals, it

must hold that

$$\frac{1}{T_s}(\Omega + 2\pi) = \frac{1}{T_s}(\omega T_s + 2\pi) = \omega + \omega_s. \tag{8.7}$$

Many of the other properties of discrete time Fourier transform are the same or equivalent to the corresponding properties of the continuous time Fourier transform. These are listed in Table 8.1. Note that two important exceptions are the time and frequency scaling properties, which do not apply to the discrete time Fourier transform. The discrete time Fourier transforms for the elementary signals are shown in Section 8.A.

Example 8.1: DTFT of the rectangular pulse

Consider the discrete time rectangular pulse

$$x[k] = \text{rect}\left[\frac{k}{2N+1}\right].$$

Its DTFT is given by

$$X(\Omega) = \sum_{k=-\infty}^{\infty} x[k]e^{-\mathrm{j}\,\Omega k} = \sum_{k=-N}^{N} 1e^{-\mathrm{j}\,\Omega k} = e^{j\Omega N}\sum_{k=0}^{2N} e^{-\mathrm{j}\,\Omega k}.$$

The sum in the last term above can be identified as a geometric series of the form

$$\sum_{m=0}^{M-1} rq^m = r\frac{1-q^M}{1-q}$$

with

$$r = 1,\ q = e^{-\mathrm{j}\,\Omega},\ \text{and}\ M = 2N+1.$$

Thus, the sum can be simplified as

$$X(\Omega) = e^{\mathrm{j}\,\Omega N}\frac{1-e^{-\mathrm{j}(2N+1)\Omega}}{1-e^{-\mathrm{j}\,\Omega}}.$$

Next, breaking out $e^{-\mathrm{j}\,\frac{(2N+1)\Omega}{2}}$ in the numerator and $e^{-\mathrm{j}\,\frac{\Omega}{2}}$ in the denominator yields

$$X(\Omega) = e^{\mathrm{j}\,\Omega N}\frac{e^{-\mathrm{j}\,\frac{(2N+1)\Omega}{2}}}{e^{-\mathrm{j}\,\frac{\Omega}{2}}}\frac{e^{-\mathrm{j}\,\frac{(2N+1)\Omega}{2}} - e^{-\mathrm{j}\,\frac{(2N+1)\Omega}{2}}}{e^{\mathrm{j}\,\frac{\Omega}{2}} - e^{-\mathrm{j}\,\frac{\Omega}{2}}},$$

where it can be seen that the first terms cancel out and the second term is a ratio of two sine functions. This finally yields

$$X(\Omega) = \frac{\sin\left(\frac{(2N+1)\Omega}{2}\right)}{\sin\left(\frac{\Omega}{2}\right)}$$

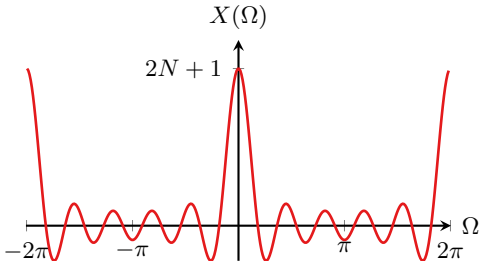

Figure 8.1. DTFT of the discrete time rectangular pulse with $N = 5$.

for the DTFT of the rectangular pulse. Note that in contrast to the continuous time case, this is not the sinc function, but a very closely related function as illustrated in Figure 8.1 for $N = 5$. In particular, this is sometimes called the *aliased sinc* function due to unavoidable aliasing: Recall that sampling turns a continuous time spectrum into a periodic spectrum. Furthermore, since the sinc function extends to infinity, the "arms" of the different sincs overlap, which causes aliasing.

8.1.2 Frequency Domain Analysis of Discrete Time Systems

As we have seen, similar to continuous time LTI systems, the output $y[k]$ of a discrete time LTI system is the convolution between the input signal $x[k]$ and the system's impulse response $h[k]$ in the time domain, that is,

$$y[k] = h[k] * x[k].$$

Taking the discrete time Fourier transform and using the convolution property (Table 8.1) yields

$$Y(\Omega) = H(\Omega)X(\Omega).$$

Again, the output of a discrete time system in the frequency domain is the product of the input signal's spectrum and the Fourier transform of the impulse response $h[k]$. This is again called the *frequency response* and it holds that the impulse response $h[k]$ and the frequency response $H(\Omega)$ are a discrete time Fourier transform pair, that is,

$$h[k] \circ\!\!-\!\!\bullet\ H(\Omega).$$

Definition 8.3: Frequency domain input-output relationship (discrete time)

The Fourier transform of a discrete time LTI system's output signal $Y(\Omega)$ is the product between the input signals discrete time Fourier transform $X(\Omega)$ and the

frequency response $H(\Omega)$

$$Y(\Omega) = H(\Omega)X(\Omega). \tag{8.8}$$

The discrete time system's frequency response is the discrete time Fourier transform of the impulse response, that is,

$$H(\Omega) = \sum_{k=-\infty}^{\infty} h[k]e^{-\mathrm{j}\,\Omega k}. \tag{8.9}$$

Again, calculating the output in the frequency domain is much simpler (a product) than in the time domain (a convolution). Since the frequency response in general is a complex function, $H(\Omega) = |H(\Omega)|e^{\mathrm{j}\angle H(\Omega)}$, it can again be seen that spectrum of the output of an LTI system is scaled by the magnitude of the transfer function $|H(\Omega)|$ and phase shifted by its phase $\angle H(\Omega)$,

$$Y(\Omega) = H(\Omega)X(\Omega) = |H(\Omega)|e^{\mathrm{j}\angle\Omega}|X(\Omega)|e^{\mathrm{j}\angle X(\Omega)} = |H(\Omega)||X(\Omega)|e^{\mathrm{j}(\angle X(\Omega)+\angle H(\Omega))}.$$

The frequency response can be plotted in the same way as for continuous time systems. Note, however, that since $H(\Omega)$ and $X(\Omega)$ (and hence $Y(\Omega)$) are 2π-periodic, it is enough to only plot the interval $0 \leq \Omega < 2\pi$. An example follows in Example 8.2.

Example 8.2: Discrete time frequency response

Consider the discrete time system with impulse response

$$h[k] = 0.5 \cdot 0.5^k u[k].$$

The system's frequency response is (see Section 8.A)

$$H(\Omega) = \frac{0.5}{1 - 0.5e^{-\mathrm{j}\,\Omega}}.$$

Applying the input $x[k] = \cos(\frac{2\pi}{8}k)$ with DTFT

$$X(\Omega) = \pi \sum_{m=-\infty}^{\infty} \left[\delta\left(\Omega + \frac{2\pi}{8} - 2\pi m\right) + \delta\left(\Omega - \frac{2\pi}{8} - 2\pi m\right)\right]$$

yields the output

$$\begin{aligned} Y(\Omega) &= H(\Omega)X(\Omega) \\ &= \frac{0.5}{1 - 0.5e^{-\mathrm{j}\,\Omega}}\pi \sum_{m=-\infty}^{\infty} \left[\delta\left(\Omega + \frac{2\pi}{8} - 2\pi m\right) + \delta\left(\Omega - \frac{2\pi}{8} - 2\pi m\right)\right]. \end{aligned}$$

This is again a scaled and phase-shifted discrete time cosine and the spectra and time domain signals are shown in Figure 8.2.

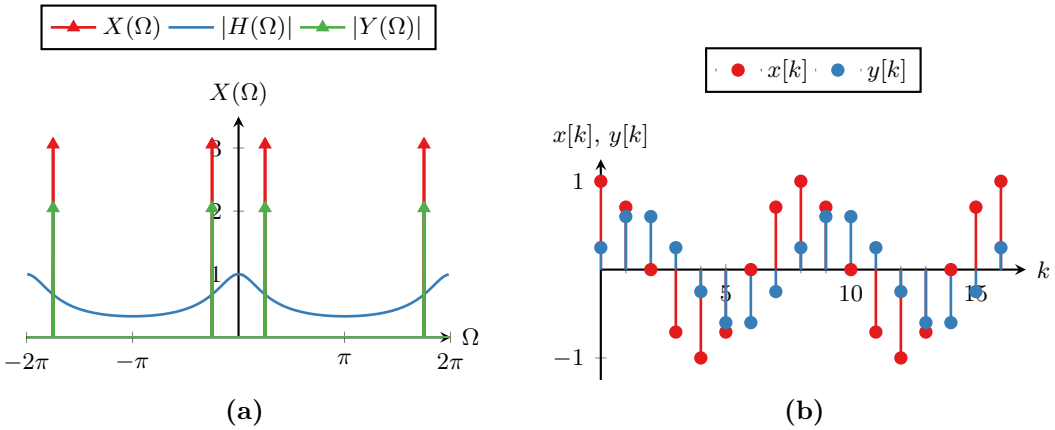

Figure 8.2. Illustration of the input-output relationship for the discrete time system in Example 8.2. (a) Frequency domain and (b) time domain.

8.2 Discrete Fourier Transform

8.2.1 Definition

Many problems involve analyzing a signal's spectrum based on a finite set of samples of the signal. In particular, assume that we are given a set of K samples $x[0], x[1], \ldots, x[K-1]$ of a signal and we would like to calculate its Fourier transform using a digital computer. However, the discrete time Fourier transform introduced in Section 8.1 requires knowledge of the full signal, not only a finite set of samples. A solution would be to simply use the discrete time Fourier transform and assume that the signal is zero for the unknown samples. This gives

$$\begin{aligned} X(\Omega) &= \sum_{k=-\infty}^{\infty} x[k] e^{-\mathrm{j}\,\Omega k} \\ &= \sum_{k=0}^{K-1} x[k] e^{-\mathrm{j}\,\Omega k}. \end{aligned}$$

However, this is still a continuous function in Ω, which can not be represented in a digital computer. Instead, we can also sample the frequency variable Ω. Knowing that $X(\Omega)$ is 2π-periodic, it is enough to divide the interval 0 to 2π into L equispaced *frequency bins* $0, \frac{2\pi}{L}, 2\frac{2\pi}{L}, \ldots, L-1\frac{2\pi}{L}$. This yields

$$X\left(l\frac{2\pi}{L}\right) = \sum_{k=0}^{K-1} x[k] e^{-\mathrm{j}\,kl\frac{2\pi}{L}}.$$

for the lth frequency bin. It can be shown that only the choice $L = K$ yields a full set of linearly independent frequency bins, which leads to the discrete Fourier transform (DFT) in Definition 8.4, with its most important properties summarized in Table 8.2.

Table 8.2. Properties of the DFT.

Property	Time Domain	Frequency Domain
Periodicity	-	$X[l] = X[l+K]$
Symmetry	Real-valued	$X[l] = X^*[K-l]$
Linearity	$\alpha x_1[k] + \beta x_2[k]$	$\alpha X_1[l] + \beta X_2[l]$
Parseval's Theorem	$E = \sum_{k=0}^{K-1} \lvert x[k]\rvert^2$	$E = \frac{1}{K}\sum_{l=0}^{K-1} \lvert X[l]\rvert^2$

Definition 8.4: Discrete Fourier transform

The discrete Fourier transform (DFT) of a finite set of K samples $x[0], x[1], \ldots, x[K-1]$ of the discrete time signal $x[k]$ is

$$X[l] = \sum_{k=0}^{K-1} x[k] e^{-\mathrm{j}\, lk\frac{2\pi}{K}}. \tag{8.10}$$

Similarly, the inverse DFT is given by

$$x[k] = \frac{1}{K}\sum_{l=0}^{K-1} X[l] e^{\mathrm{j}\, lk\frac{2\pi}{K}}. \tag{8.11}$$

Another important property of the DFT is that it can be written as a matrix product. First, note that the sum in (8.10) can be rewritten as a vector multiplication as

$$X[l] = \begin{bmatrix} 1 & e^{-\mathrm{j}\, l\frac{2\pi}{K}} & e^{-\mathrm{j}\, 2l\frac{2\pi}{K}} & \ldots & e^{-\mathrm{j}(K-1)l\frac{2\pi}{K}} \end{bmatrix} \begin{bmatrix} x[0] \\ x[1] \\ x[2] \\ \vdots \\ x[K-1] \end{bmatrix}.$$

Next, stacking all the DFT values in a column vector $\boldsymbol{X} \triangleq \begin{bmatrix} X[0] & X[1] & \ldots & X[K-1] \end{bmatrix}^{\mathsf{T}}$ yields

$$\begin{bmatrix} X[0] \\ X[1] \\ \vdots \\ X[K-1] \end{bmatrix} = \begin{bmatrix} 1 & 1 & \ldots & 1 \\ 1 & e^{-\mathrm{j}\,\frac{2\pi}{K}} & \ldots & e^{-\mathrm{j}(K-1)\frac{2\pi}{K}} \\ \vdots & & \ddots & \vdots \\ 1 & e^{-\mathrm{j}(K-1)\frac{2\pi}{K}} & \ldots & e^{-\mathrm{j}(K-1)(K-1)\frac{2\pi}{K}} \end{bmatrix} \begin{bmatrix} x[0] \\ x[1] \\ \vdots \\ x[K-1] \end{bmatrix}, \tag{8.12}$$

or, more compactly,

$$\boldsymbol{X} = \boldsymbol{W}\boldsymbol{x} \tag{8.13}$$

where $\boldsymbol{x} = \begin{bmatrix} x[0] & x[1] & \dots & x[K-1] \end{bmatrix}^\mathsf{T}$ and $\boldsymbol{W}$ is the $K \times K$ DFT matrix. Furthermore, the inverse DFT is given by

$$\boldsymbol{x} = \frac{1}{K}\boldsymbol{W}^{-1}\boldsymbol{X} = \frac{1}{K}\boldsymbol{W}^{*}\boldsymbol{X}. \tag{8.14}$$

Note that a different choice of the number of frequency bins L would lead to a different number of rows in $\boldsymbol{W}$ (the matrix would become an $L \times K$ matrix). This in turn leads to a non-square matrix $\boldsymbol{W}$, which either has more rows than columns or vice versa. From linear algebra it thus follows that if $L \neq K$, $\boldsymbol{W}$ is not full rank and thus either has linearly dependent columns or rows. Thus, the choice $L = K$ is ideal in terms extracting all information of $x[k]$. Finally, it can also be shown that $\boldsymbol{W}$ has orthogonal rows if $L = K$.

8.2.2 Graphical Interpretation of the DFT

Often, the aim is to analyze and process a sampled continuous time signal using the DFT. Hence, it is important to know how the DFT is related to the continuous time Fourier transform and how the DFT can be used to approximate the latter. Calculating the DFT of a sampled continuous time signal consists of the following three steps:

1. Time domain sampling,
2. time limiting,
3. frequency domain sampling.

All of these steps affect the resulting the outcome of the DFT and how it is related to the spectrum of the original, continuous time signal $x(t)$. Here, we discuss the effect of these steps in the time and frequency domain graphically, based on the signal and its spectrum shown in Figure 8.3a–b.

Time domain sampling. Sampling has already been discussed in detail in Chapter 6. Recall that in the time domain, sampling can be expressed as the product of the signal $x(t)$ and the impulse train sampling signal $s(t)$ (Figure 8.3c). In the frequency domain, this corresponds to a convolution of $X(\omega)$ and $S(\omega)$, where the latter is a pulse train with periodicity ω_s. Hence, the resulting spectrum for the sampled signal $x_s(t)$ is a ω_s-periodic spectrum with frequency-shifted copies of $X(\omega)$ as illustrated in Figure 8.3d.

Time limiting. Time limiting can be understood as multiplying the sampled signal $x_s(t)$ with a (time shifted) rectangular pulse $w(t)$ of width KT_s such that the sampled and windowed signal $x_{sw}(t) = x_s(t)w(t)$ as illustrated in Figure 8.3e. The Fourier transform is thus a convolution between the sampled signal's Fourier transform $X_s(\omega)$ and $W(\omega)$ (a sinc function), which yields the spectrum $X_{sw}(\omega)$ shown in Figure 8.3f.

Frequency domain sampling. The last step is sampling the frequency domain with a sampling interval $\frac{\omega_s}{L}$. This can be expressed as a multiplication of the (time domain) sampled and windowed signal $x_{sw}(t)$ with an impulse train in the frequency domain

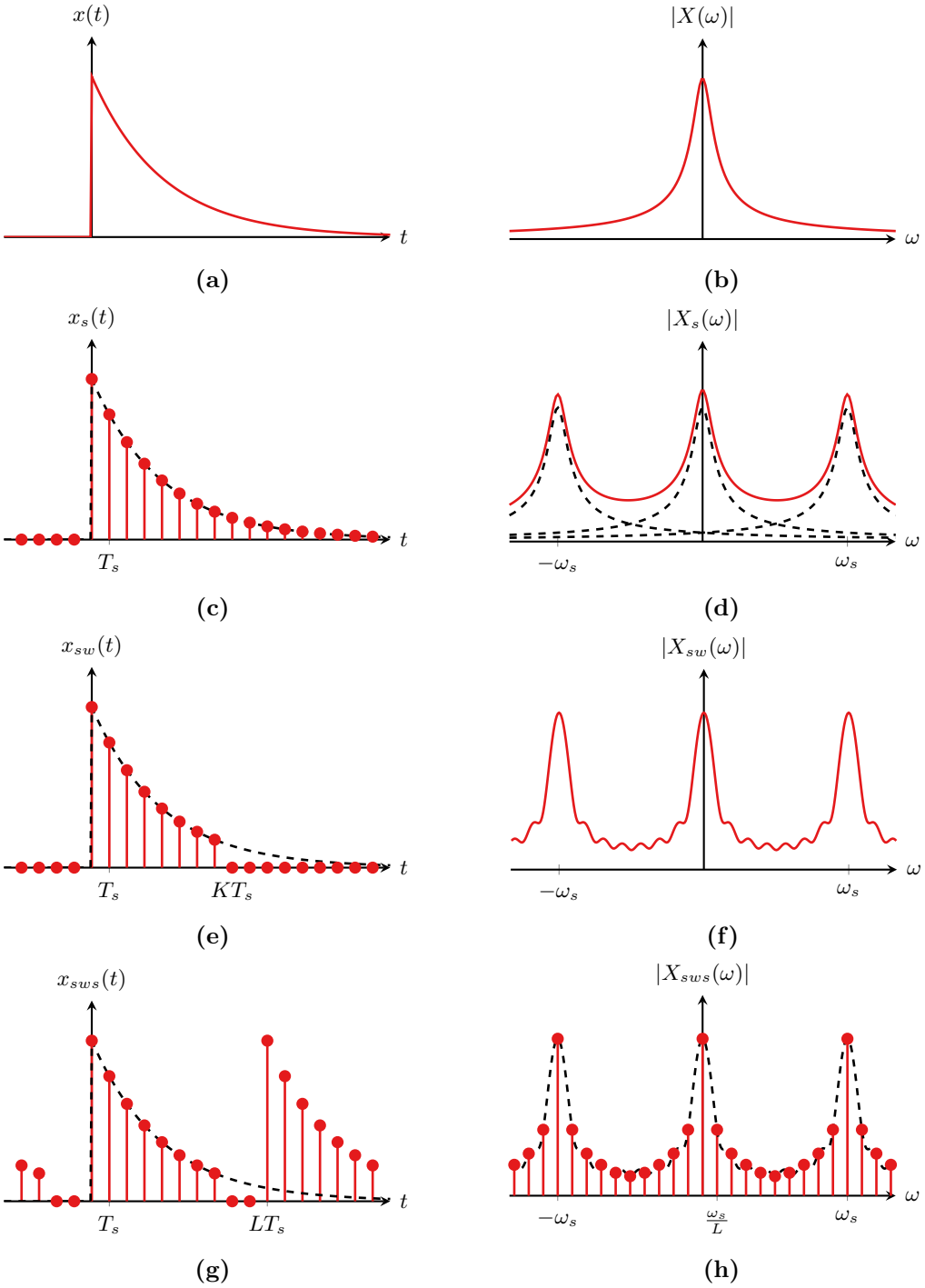

Figure 8.3. Graphical interpretation of the DFT: (a)–(b) Original continuous time signal and its spectrum, (c)–(d) sampled signal and its Fourier transform, (e)–(f) sampled and windowed signal and its spectrum, and (g)–(h) sampled, windowed, and frequency domain sampled signal and its spectrum.

(Figure 8.3h). This in turn corresponds to a convolution with another impulse train with period LT_s in the time domain. Thus, the result is an LT_s-periodic signal $x_{sws}(t)$ in the time domain as illustrated in Figure 8.3g.

8.2.3 Relationship to the Continuous and Discrete Time Fourier Transforms

As mentioned above, we are often interested in analyzing a finite set of samples of a (discrete time or sampled continuous time) signal in the frequency domain. Thus, it is important to know how the DFT relates to the continuous time and discrete time Fourier transforms.

First, recall that the DFT is given by (Defintion 8.4)

$$X[l] = \sum_{k=0}^{K-1} x[k] e^{-\mathrm{j}\, lk\frac{2\pi}{L}}.$$

The discrete time Fourier transform on the other hand is given by (Definition 8.2)

$$X(\Omega) = \sum_{k=-\infty}^{\infty} x[k] e^{-\mathrm{j}\,\Omega k}.$$

Thus, if and only if the signal $x[k]$ is limited to the interval $0, \ldots, K-1$, that is, $x[k] = 0$ for $k < 0$ and $k \geq K$, the DFT at the lth frequency bin is equivalent to the discrete time Fourier transform at the frequency

$$\Omega_l = l\frac{2\pi}{L}.$$

In other words, we have that

$$X(\Omega)|_{\Omega = l\frac{2\pi}{L}} = X[l]. \tag{8.15}$$

However, if the signal is non-zero outside the interval $0, \ldots, K-1$, the DFT is only an approximation of the discrete time Fourier transform.

For sampled continuous time signals, the relationship to the continuous time Fourier transform is as follows. First, note that from frequency domain sampling, it follows that the relationship between the lth frequency bin to the natural and angular frequencies are

$$f_l = l\frac{f_s}{L} \quad \text{and} \quad \omega_l = l\frac{\omega_s}{L},$$

respectively. Furthermore, it can be shown that the lth complex Fourier coefficient of a periodic signal is related to the DFT at the lth frequency bin according to

$$c_l \approx \frac{1}{K} X[l]. \tag{8.16}$$

Note that this only holds if the length of the window is exactly an positive integer multiple of the signal's period T_0, that is, $KT_s = MT_0$ for any natural number M.

Finally, for aperiodic signals, the continuous time Fourier transform can be approximated as

$$X(\omega)|_{\omega=l\frac{\omega_s}{L}} \approx T_s X[l] \tag{8.17}$$

if the continuous time signal is limited to the interval $0, \ldots, (K-1)T_s$, that is, $x(t) = 0$ for $t < 0$ and $T \geq KT_s$.

8.2.4 Zero-Padding, Graphical Resolution, and Spectral Resolution

As discussed in Section 8.2.1, the ideal choice of the number of frequency bins L in terms of extracting the maximum information is equal to the number of samples K, that is, $L = K$. However, nothing prevents us from choosing a different (larger) number of frequency bins to improve the *graphical* resolution of the DFT. As an example, consider the signal

$$x(t) = \cos(4\pi t)$$

which is sampled with $\omega_s = 40\pi$ and for which we have $K = 16$ samples. Figure 8.4a shows the DFT of these samples for $L = K = 16$, for which we get frequency bins at

$$0\,\text{rad/s}, \frac{5\pi}{2}\,\text{rad/s}, \ldots, \frac{75\pi}{2}\,\text{rad/s}.$$

The figure shows that none of the frequency bins coincides with the true frequency of the cosine, and thus, determining the correct frequency is not possible. Figure 8.4b shows the DFT for the same signal with $K = 16$ and $L = 20$. In this case, the frequency bins are

$$0\,\text{rad/s}, 2\pi\,\text{rad/s}, \ldots, 38\pi\,\text{rad/s}.$$

It can be seen that the improved graphical resolution with a bin at the true frequency gives a more accurate representation of the underlying signal. Thus, choosing $L > K$ helps to reveal the real location of the peak in this case. By further increasing L, that is, sampling the spectrum even more densely, the black, dashed curve would eventually be retrieved.

Calculating the DFT for $L > K$ is called *zero-padding* the DFT, because of the way the DFT is calculated in this case. In particular, if $L > K$, we can add $L - K$ zeros to the original set of samples $x[0], x[1], \ldots, x[K-1]$ such that the new, zero-padded signal $\tilde{x}[k]$ becomes

$$\tilde{x}[k] = \begin{cases} x[k] & 0 \leq k < K, \\ 0 & K \leq k < L. \end{cases}$$

The DFT for this new signal is then

$$\tilde{X}[l] = \sum_{k=0}^{L} \tilde{x}[k] e^{-\mathrm{j}\, lk\frac{2\pi}{L}}.$$

Note that the sum on the right hand side is, of course, equivalent to the DFT with $L = K$ since adding zeros to a sum does not change the sum. However, adding zeros is in fact

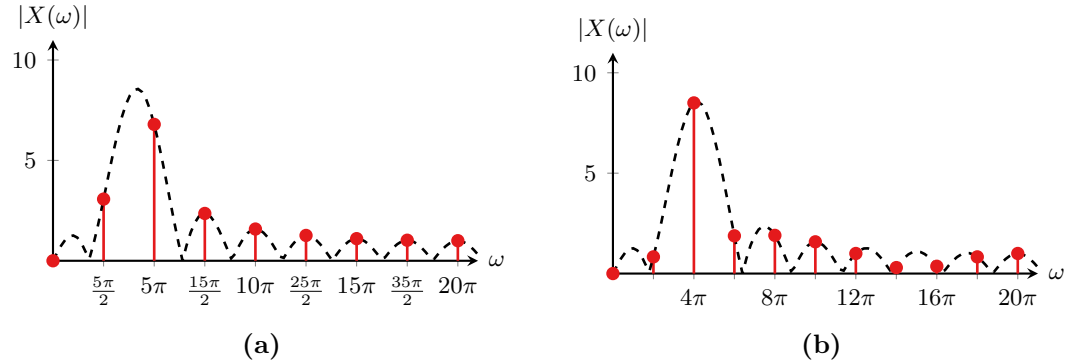

Figure 8.4. Illustration of the DFT of a cosine without and with zero padding (only the first half of the DFT is shown due to the Hermitian symmetry). (a) No zero-padding and (b) with zero-padding.

beneficial from a computational aspect when calculating the DFT using the fast Fourier transform (FFT) described in Section 8.2.6 below.

As shown above, zero-padding improves the *graphical resolution*, that is, the appearance of the spectrum plot. However, it does not improve the *spectral resolution*, that is, the resolution which determines how accurate the calculated Fourier transform is. This can only be improved by either increasing the sampling frequency or the number of samples K.

8.2.5 Windowing

The previous section showed that time limitation has an important effect on the spectrum calculated using the DFT. More generally, time limitation can be seen as a *windowing* operation where we simply consider a window of the original signal such that

$$x_w[k] = x[k]w[k],$$

where the windowing function $w[k]$ is zero for $k < 0$ and $k \geq K$. In the previous section, the windowing function was a rectangular window of the form

$$w_r[k] = \text{rect}\left[\frac{k - \frac{K-1}{2}}{K}\right].$$

In the frequency domain, this resulted in the convolution with an aliased sinc function, that has one large peak around zero and infinitely many peaks of decaying amplitude as the frequency increases. The large peak around zero is called the window's *mainlobe*, whereas the remaining peaks are called the window's *sidelobes* (Figure 8.5).

The convolution of the signal $x[k]$ with the window $w[k]$ thus causes two effects, *smearing* and *leakage*. Smearing is the effect of the mainlobe smearing out the spectral contents onto other frequencies. Leakage is the effect the sidelobes adding new spectral contents that were not present in the beginning (Figure 8.4).

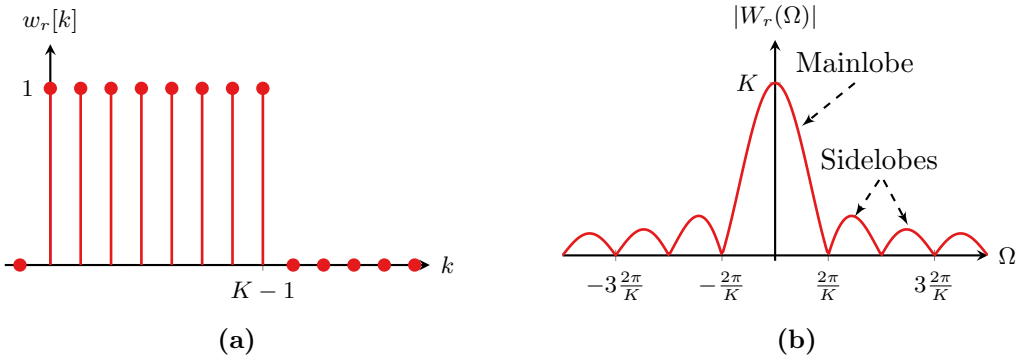

Figure 8.5. Rectangular window and its Fourier transform.

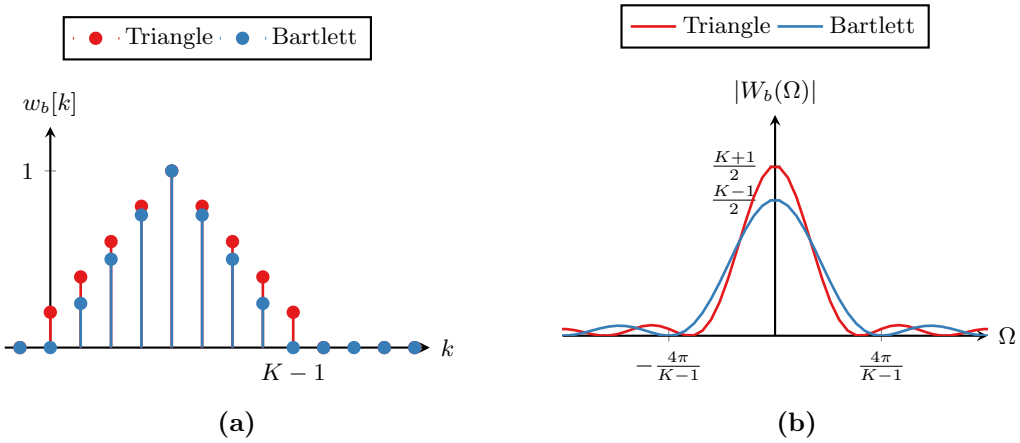

Figure 8.6. Bartlett window and its Fourier transform.

However, by choosing a different window $w[k]$, the lobes and thus smearing and leakage can be affected. Indeed, there are many different windowing functions available and few common ones are:

- Rectangular window: The rectangular window, also called a boxcar window, shown in Figure 8.5, is the standard window, that is, the window that is implicitly applied when no windowing is performed. The rectangular window has the most narrow mainlobe but the strongest sidelobes.

- Bartlett and triangle windows: The Bartlett and triangle windows are both triangular windows in the time domain. However, there is a small and subtle difference between the two: The Bartlett window has zeros at the first and last sample (i.e., $w_b[0] = w_b[K-1] = 0$), whereas these samples are non-zero for the triangle window. Both windows can be derived as a convolution of a rectangular window with itself and thus, the frequency domain function is a squared aliased sinc (see Figure 8.6). The Bartlett window has a wider mainlobe but smaller sidelobes compared to the rectangular window.

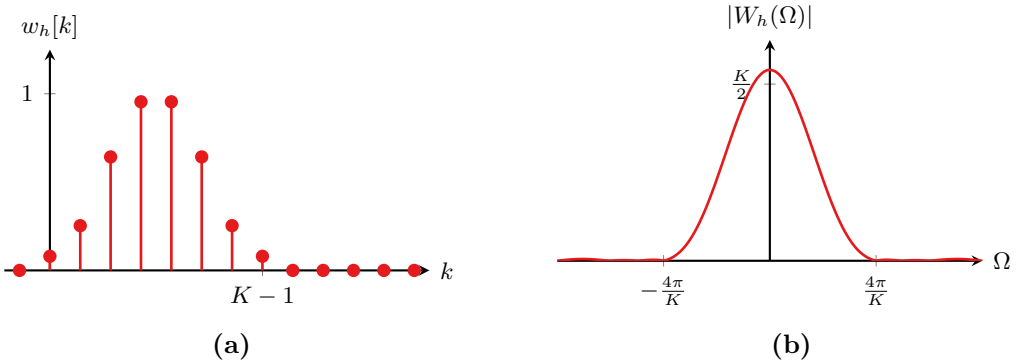

Figure 8.7. Hamming window and its Fourier transform.

- Hamming window: The Hamming window (Figure 8.7) is similar in shape to the Bartlett window but with smoother transitions rather than sharp corners. This leads to even smaller sidelobes, whereas the mainlobe has the same width as the Bartlett window's mainlobe.

8.2.6 Fast Fourier Transform

The fast Fourier transform (FFT) is an efficient way of implementing the DFT for the cases when the number of samples K is a power of two, that is, $K = 2^M$ for any natural number M. Recall that the DFT could be calculated using a matrix product in (8.12). Implementing the DFT in this way would require $\mathcal{O}(K^2)$ arithmetic operations. Using the FFT, the same can be implemented using $\mathcal{O}(K \log_2(K))$ operations instead.

Several algorithmic implementations of the FFT exist but their underlying principles are similar. The general idea is based on the fact that product $x[k]e^{-\mathrm{j}\,lk\frac{2\pi}{K}}$ can be factorized into a chain of products and then reuse earlier results. In particular, we can define the *twiddle factor*

$$W_K = e^{-\mathrm{j}\,\frac{2\pi}{K}}$$

and rewrite the DFT as

$$\begin{aligned} X[l] &= \sum_{k=0}^{K-1} x[k] W_K^{lk} \\ &= \sum_{k=0}^{\frac{K}{2}-1} x[2k] W_K^{lk} + \sum_{k=0}^{\frac{K}{2}-1} x[2k+1] W_K^{(2k+1)l} \\ &= \sum_{k=0}^{\frac{K}{2}-1} x[2k] W_K^{lk} + W_K^l \sum_{k=0}^{\frac{K}{2}-1} x[2k+1] W_K^{2kl}. \end{aligned}$$

Here, the first sum is a sum over the samples at even k ($x[0]$, $x[2]$, ...) and the second sum is over the odd samples ($x[1]$, $x[3]$, ...). Defining two new signals $x_1[k]$ and $x_2[k]$ as

$$x_1[k] = x[2k] \quad \text{and} \quad x_2[k] = x[2k+1],$$

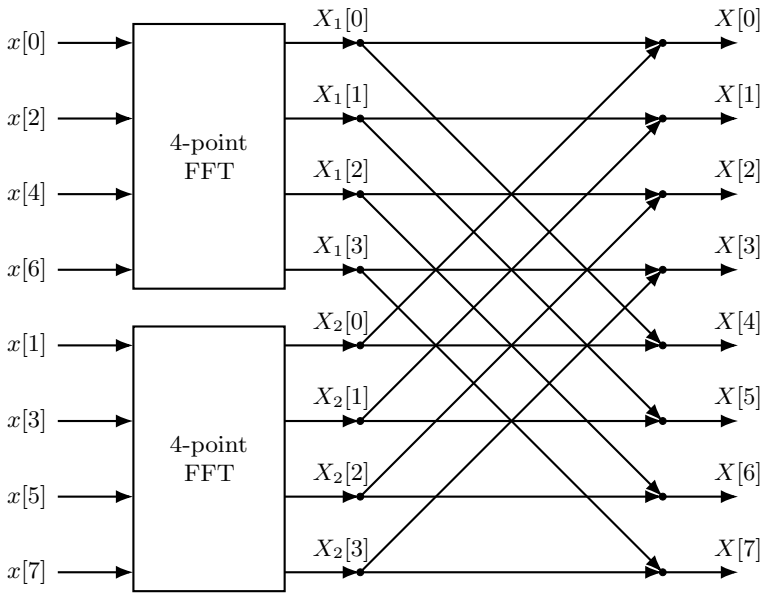

Figure 8.8. Illustration of the 8-point FFT that consists of two 4-point FFTs.

this can further be rewritten as

$$\begin{aligned} X[l] &= \sum_{k=0}^{\frac{K}{2}-1} x_1[k] W_K^{lk} + W_K^l \sum_{k=0}^{\frac{K}{2}-1} x_2[k] W_{K/2}^{kl} \\ &= X_1[l] + W_K^l X_2[l]. \end{aligned}$$

Here, $X_1[l]$ and $X_2[l]$ are two $\frac{K}{2}$-point DFTs and thus, the K-point DFT can be calculated based on a (weighted) sum of two $\frac{K}{2}$-point DFTs as illustrated in Figure 8.8. This splitting can be applied repeatedly, down to $\frac{K}{2}$ 2-point DFTs, which eventually yields the FFT algorithm.

As mentioned initially, a requirement for being able to calculate the DFT using the FFT is that $K = 2^M$. If this is not the case, the FFT can still be used by first zero-padding the signal $x[k]$ as outlined above such that the zero-padded signal's length is a power of two. This may be beneficial to reduce the computational cost.

8.A List of Discrete Time Fourier Transform Pairs

Periodic signals

K_0-periodic with $\Omega_0 = \frac{2\pi}{K_0}$,

$$x[k] = x[k + K_0] \quad \circ\!\!-\!\!\bullet \quad X(\Omega) = 2\pi \sum_{n=-\infty}^{\infty} c_n \delta(\Omega - n\Omega_0)$$

with discrete time Fourier series coefficients

$$c_n = \frac{1}{K_0} \sum_{k=0}^{K_0-1} x[k] e^{-\mathrm{j}\, n\Omega_0 k}$$

Constant

$$x[k] = 1 \quad \circ\!\!-\!\!\bullet \quad X(\Omega) = 2\pi \sum_{m=-\infty}^{\infty} \delta(\Omega - 2\pi m)$$

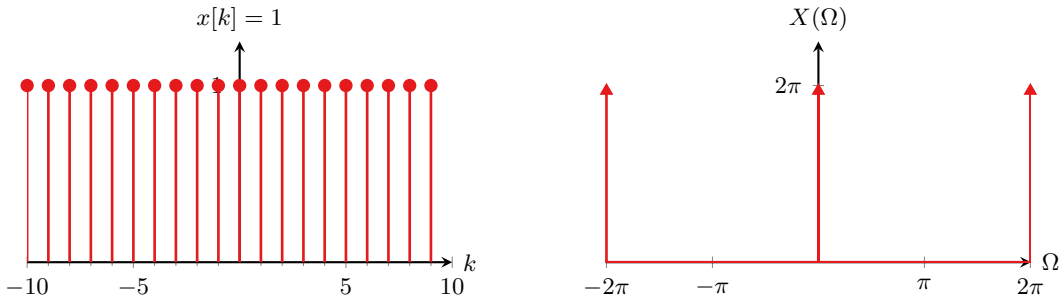

Unit impulse

$$x[k] = \delta[k] \quad \circ\!\!-\!\!\bullet \quad X(\Omega) = 1$$

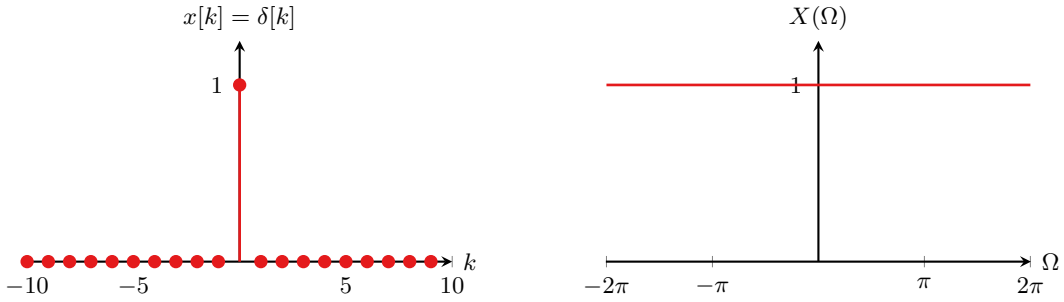

Unit step

$$x[k] = u[k] \quad \circ\!\!-\!\!\bullet \quad X(\Omega) = \pi \sum_{m=-\infty}^{\infty} \delta(\Omega - 2\pi m) + \frac{1}{1 - e^{-\mathrm{j}\,\Omega}}$$

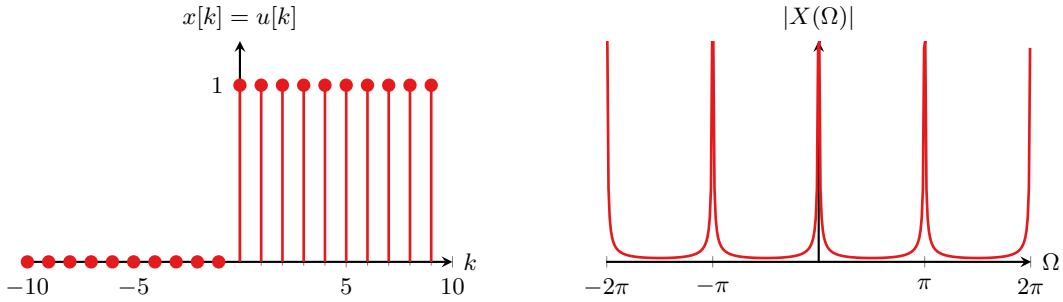

Rectangular pulse

$$x[k] = \mathrm{rect}\left[\frac{k}{2N+1}\right] \quad \circ\!\!-\!\!\bullet \quad X(\Omega) = \frac{\sin\left(\frac{(2N+1)\Omega}{2}\right)}{\sin\left(\frac{\Omega}{2}\right)}$$

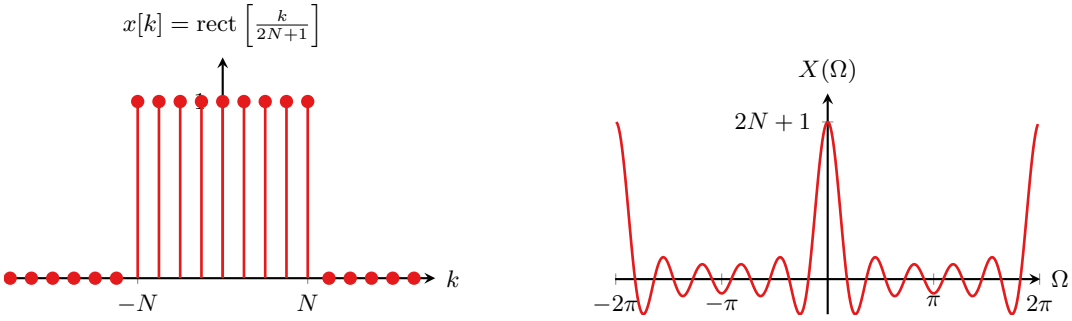

Sinc function

$$x[k] = \mathrm{sinc}\left[\frac{k}{K_0}\right] \quad \circ\!\!-\!\!\bullet \quad X(\Omega) = K_0 \sum_{m} \mathrm{rect}\left(\frac{\Omega - 2\pi m}{\frac{2\pi}{K_0}}\right)$$

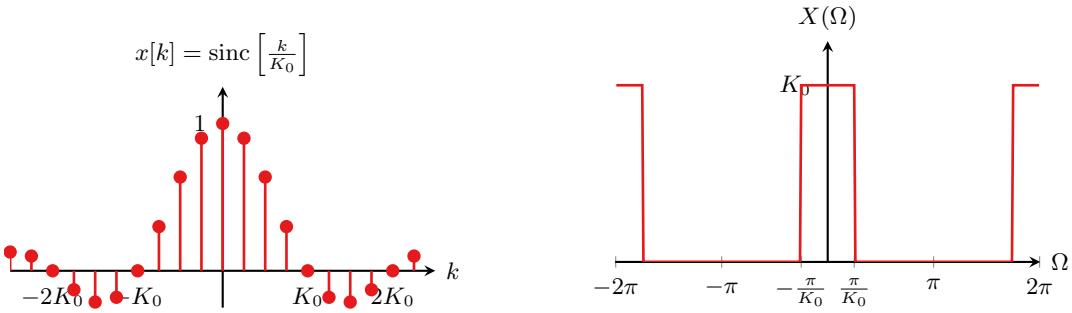

Sinc function (alternative parametrization)

$$x[k] = \frac{\Omega_0}{\pi} \operatorname{sinc}\left[\frac{\Omega_0 k}{\pi}\right] \circ\!\!-\!\!\bullet\; X(\Omega) = \sum_m \operatorname{rect}\left(\frac{\Omega - 2\pi m}{2\Omega_0}\right)$$

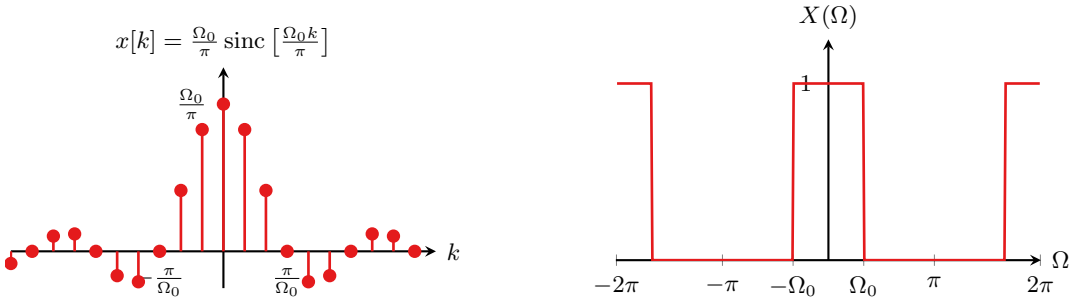

Exponential

$$x[k] = a^k u[n] \circ\!\!-\!\!\bullet\; X(\Omega) = \frac{1}{1 - ae^{-\mathrm{j}\,\Omega}} \quad |a| < 1$$

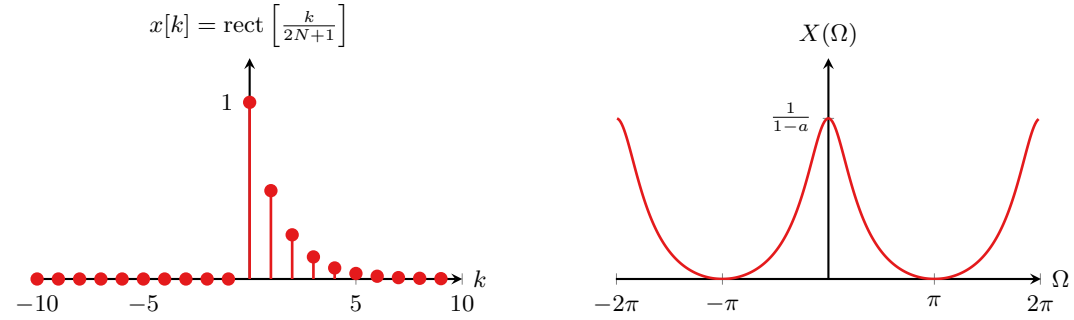

Sine

$$x[k] = \sin(\Omega_0 k) \circ\!\!-\!\!\bullet\; X(\Omega) = \mathrm{j}\,\pi \sum_m \left[\delta(\Omega + \Omega_0 - 2\pi m) - \delta(\Omega - \Omega_0 - 2\pi m)\right]$$

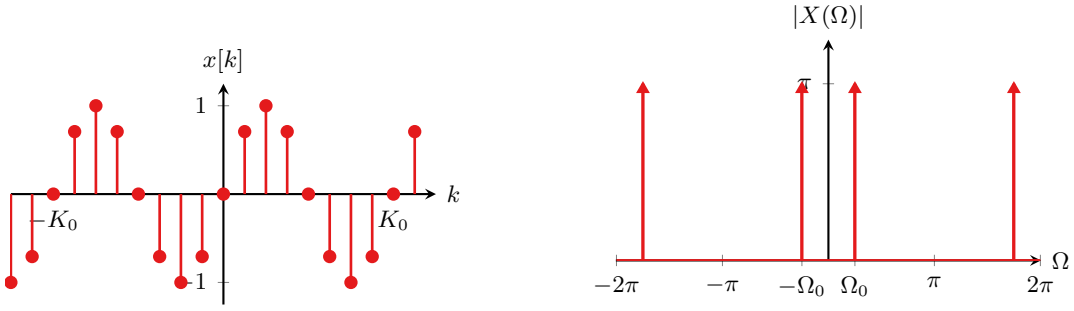

Cosine

$$x[k] = \cos(\Omega_0 k) \quad \circ\!\!-\!\!\bullet \quad X(\Omega) = \pi \sum_{m=-\infty}^{\infty} [\delta(\Omega + \Omega_0 - 2\pi m) + \delta(\Omega - \Omega_0 - 2\pi m)]$$

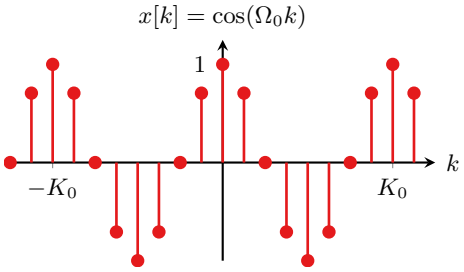

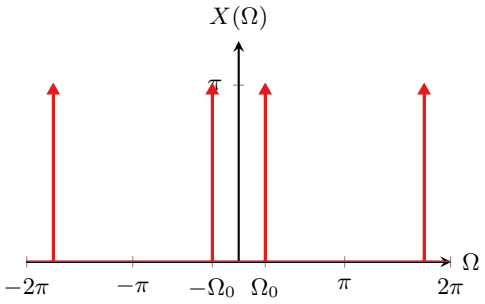

Chapter 9

z-Transform

9.1 Definition and Properties

9.1.1 Definition

The z-transform is to discrete time systems what the Laplace transform is to continuous time systems. Recall that the discrete time Fourier transform for a causal signal $x[k]$ ($x[k] = 0$ for $k < 0$) is given by

$$X(\Omega) = \sum_{k=0}^{\infty} x[k] e^{-\mathrm{j}\,\Omega k}.$$

Unfortunately, the sum above does not always converge. However, convergence can be ensured by scaling the signal $x[k]$ with an exponentially decaying function r^{-k}. This yields

$$X(\Omega) = \sum_{k=0}^{\infty} x[k] r^{-k} e^{-\mathrm{j}\,\Omega k}.$$

Letting $z = re^{\mathrm{j}\,\Omega}$, this can be rewritten as

$$X(z) = \sum_{k=0}^{\infty} x[k] z^{-k},$$

which is the unilateral z-transform (Definition 9.1).

Definition 9.1: Unilateral z-transform

The unilateral z-transform for causal discrete time signals $x[k]$ is given by

$$X(z) = \sum_{k=0}^{\infty} x[k] z^{-k}. \tag{9.1}$$

The inverse z-transform is given by a closed counter-clockwise contour integral inside the z-transform's region of convergence given by

$$x[k] = \frac{1}{2\pi\,\mathrm{j}} \oint X(z) z^{k-1}\,\mathrm{d}z. \tag{9.2}$$

Note that there also exists a bilateral z-transform for non-causal signals. However, since all signals are causal in practice, this is not discussed further here and the unilateral z-transform is meant whenever the term z-transform is used. Furthermore, for each z-transform $X(z)$, there is also a associated ROC (region of convergence) which indicates for which choices of z the transform (9.1), that is, the sum over $x[k]z^{-k}$, converges.

The discrete time signal $x[k]$ and its z-transform $X(z)$ are again a transform pair,

$$x[k] \circ\!\!-\!\!\bullet\ X(z).$$

Three examples of the z-transform and their ROCs are given in Example 9.1. Furthermore, Table 9.1 shows the z-transforms for elementary discrete time signals.

Example 9.1: z-transform of elementary signals

Consider the z-transforms of the following elementary signals:

a) The unit impulse $\delta[k]$:

$$X(z) = \sum_{k=0}^{\infty} \delta[k]z^{-k} = \delta[0]z^{-0} = 1.$$

Since the sum converges for all choices of z ($z^0 = 1$, always), the ROC is the entire complex z-plane.

b) The unit step $u[k]$:

$$X(z) = \sum_{k=0}^{\infty} u[k]z^{-k} = \sum_{k=0}^{\infty} z^{-k}.$$

This is a geometric series (see Appendix A.5) with

$$r = 1,\ q = z^{-1},\ \text{and}\ M = \infty,$$

which yields

$$X(z) = \frac{1}{1 - z^{-1}}.$$

Note that if $|z| < 1$ the terms z^{-k} in the sum increase as k increases. Thus, the sum diverges rather than converges. Conversely, the sum converges if $|z| > 1$ and thus, the ROC for z-transform of the unit step $u[k]$ is $|z| > 1$.

c) The exponential sequence $a^k u[k]$:

$$X(s) = \sum_{k=0}^{\infty} a^k u[k]z^{-k} = \sum_{k=0}^{\infty} (az^{-1})^k.$$

This is again a geometric series with

$$r = 1,\ q = az^{-1},\ \text{and}\ M = \infty,$$

Table 9.1. Table of unilateral z-transform pairs for causal signals $x[k]$ ($x[k] = 0$ for $k < 0$).

Time domain $x[k]$	z-Transform $X(z)$	ROC
Unit impulse		
$x[k] = \delta[k]$	$X(z) = 1$	all z
Unit step		
$x[k] = u[k]$	$X(z) = \dfrac{1}{1 - z^{-1}}$	$\lvert z\rvert > 1$
Exponential		
$x[k] = a^k u[k]$	$X(z) = \dfrac{1}{1 - az^{-1}}$	$\lvert z\rvert > \lvert a\rvert$
Ramp		
$x[k] = ku[k]$	$x(z) = \dfrac{z^{-1}}{(1 - z^{-1})^2}$	$\lvert z\rvert > 1$
Cosine		
$x[k] = \cos(\Omega_0 k)u[k]$	$X(z) = \dfrac{1 - z^{-1}\cos(\Omega_0)}{1 - 2z^{-1}\cos(\Omega_0) + z^{-2}}$	$\lvert z\rvert > 1$
Sine		
$x[k] = \sin(\Omega_0 k)u[k]$	$X(z) = \dfrac{z^{-1}\sin(\Omega_0)}{1 - 2z^{-1}\cos(\Omega_0) + z^{-2}}$	$\lvert z\rvert > 1$
Decaying cosine		
$x[k] = a^k \cos(\Omega_0 k)u[k]$	$X(z) = \dfrac{1 - az^{-1}\cos(\Omega_0)}{1 - 2az^{-1}\cos(\Omega_0) + a^2 z^{-2}}$	$\lvert z\rvert > \lvert a\rvert$
Decaying sine		
$x[k] = a^k \sin(\Omega_0 k)u[k]$	$X(z) = \dfrac{az^{-1}\sin(\Omega_0)}{1 - 2az^{-1}\cos(\Omega_0) + a^2 z^{-2}}$	$\lvert z\rvert > \lvert a\rvert$

which becomes

$$X(z) = \frac{1}{1 - az^{-1}}.$$

Note that for the sum to converge, the term az^{-1} must converge to zero as $k \to \infty$. Hence, we have that $|az^{-1}| < 1$, which yields that the ROC is $|z| > |a|$.

9.1.2 Properties

Table 9.2 shows the properties of the z-transform. Additionally, a few very important and frequently used properties are discussed below.

Table 9.2. Properties of the z-transform.

Property	Time Domain	z-Domain
Linearity	$\alpha x_1[k] + \beta x_2[k]$	$\alpha X_1(z) + \beta X_2(z)$
Time shifting	$x[k-m]$	$z^{-m}X(z)$
Convolution	$x_1[k] * x_2[k]$	$X_1(z)X_2(z)$
Scaling	$a^k x[k]$	$X\left(\frac{z}{a}\right)$
Time difference	$x[k] - x[k-1]$	$(1-z^{-1})X(z)$
Accumulation	$\sum_{m=0}^{k} x[m]$	$\frac{1}{1-z^{-1}}X(z)$
Initial value theorem	-	$x[0] = \lim_{z\to\infty} X(z)$
Final value theorem	-	$\lim_{k\to\infty} x[k] = \lim_{z\to 1}(z-1)X(z)$

Linearity. The z-transform is a linear transformation and thus, the z-transform of a linear combination of two signals $x_1[k]$ and $x_2[k]$ is the linear combination of the corresponding z-transforms $X_1(z)$ and X_2(z). That is,

$$\alpha x_1[k] + \beta x_2[k] \circ\!\!-\!\!\bullet\ \alpha X_1(z) + \beta X_2(z), \tag{9.3}$$

for arbitrary constants α and β and where $X_1(z)$ and $X_2(z)$ are the z-transforms of $x_1[k]$ and $x_2[k]$, respectively.

Time shifting. One of the most important properties of the z-transform is the time shift property. The z-transform of a time-shifted signal $x[k-m]$ is the original signal's z-transform $X(z)$ multiplied by z^{-m}, that is,

$$x[k-m] \circ\!\!-\!\!\bullet\ z^{-m}X(z), \tag{9.4}$$

where m is an integer. Hence, z^{-1} corresponds to a time shift backwards equal to a single sampling period.

Convolution and multiplication. A convolution of the two signals $x_1[k]$ and $x_2[k]$ in the time domain corresponds to a multiplication of their z-transforms $X_1(z)$ and $X_2(z)$ in the z-domain:

$$x_1[k] * x_2[k] \circ\!\!-\!\!\bullet\ X_1(z)X_2(z). \tag{9.5}$$

9.2 Transfer Function

9.2.1 Difference Equations and Transfer Functions

The input-output relationship for discrete time systems can be written in terms of *difference equations*. Linear difference equations are the discrete time equivalent to linear ODEs and relate the current output of the system $y[k]$ to the current and previous inputs $x[k], x[k-1], x[k-2], \ldots$ and previous outputs $y[k-1], y[k-2], \ldots$. The generic form of a difference equation is

$$y[k] + a_1 y[k-1] + \cdots + a_N y[k-N] = b_0 x[k] + b_1 x[k-1] + \cdots + b_M x[k-M] \quad (9.6)$$

where a_n and b_m are the difference equations constant coefficients. The higher number of M and N determines the system order. By rewriting (9.6), we obtain

$$y[k] = -\sum_{n=1}^{N} a_n y[k-n] + \sum_{m=0}^{M} b_m x[k-m],$$

which more clearly illustrates that the current output of the system $y[k]$ consists of a recursive term that depends on past output values (the first sum) and a non-recursive term that depends on the current and past input values (the second sum). If all coefficients a_n are zero, the recursive term becomes zero and the system is called a *non-recursive* system. Otherwise, the system is recursive.

Note that sometimes, difference equations are given in a form that looks N steps into the future such that $y[k+N]$ is the newest sample, that is,

$$y[k+N] + a_1 y[k+N-1] + \cdots + a_N y[k] = b_0 x[k+N] + b_1 x[k+N-1] + \ldots b_M x[k+N-M].$$

It is often instructive to shift the whole difference equation by N steps into the past such that the current output $y[k]$ is the newest sample as in (9.6) and only depends on current and past inputs and outputs as described above. This time shift does not affect the system but only accounts to a change in perspective.

Example 9.2: Shifting of difference equations

Consider the difference equation

$$y[k+2] + y[k+1] + 0.25y[k] = 0.5x[k+2].$$

The newest output sample here is at time index $k+2$. Hence, shifting the whole difference equation by $N = 2$ steps to the right yields

$$y[k] + y[k-1] + 0.25y[k-2] = 0.5x[k],$$

or

$$y[k] = -y[k-1] - 0.25y[k-2] + 0.5x[k].$$

Applying the z-transform to the difference equation (9.6) yields

$$Y(z) + a_1 z^{-1} Y(z) + \cdots + z^{-N} Y(z) = b_0 X(z) + b_1 z^{-1} X(z) + \cdots + b_M z^{-M} X(z), \quad (9.7)$$

where the linearity and time shifting properties of the z-transform were used. From (9.7), it can be seen that the difference equation has been transformed into an algebraic equation in $X(z)$ and $Y(z)$, in the same way as the Laplace transform turned an ODE into an algebraic equation. Hence, (9.7) can be solved for the output in the z-domain $Y(z)$ by first breaking out $Y(x)$ on the left hand side and $X(z)$ on the right hand side of the equation,

$$Y(z)(1 + a_1 z^{-1} + \cdots + a_N z^{-N}) = (b_0 + b_1 z^{-1} + \cdots + b_M z^{-M}) X(z).$$

Dividing by the factor following $Y(z)$ on the left hand side then yields

$$Y(z) = \underbrace{\frac{b_0 + b_1 z^{-1} + \cdots + b_M z^{-M}}{1 + a_1 z^{-1} + \cdots + a_N z^{-N}}}_{\triangleq H(z)} X(z). \quad (9.8)$$

The factor $H(z)$ in front of $X(z)$ on the right hand side in (9.8) is the discrete time system's *transfer function*, that is, the input-output relationship of the discrete time LTI system in the z-domain as summarized in Definition 9.2 and illustrated in Example 9.3.

Definition 9.2: Transfer function of discrete time LTI systems

The transfer function $H(z)$ for a discrete time, linear, time-invariant system described by the difference equation

$$y[k] + a_1 y[k-1] + \cdots + a_N y[k-N] = b_0 x[k] + b_1 x[k-1] + \cdots + b_M y[k-M]$$

is the ratio between the output $Y(z)$ and the input $X(z)$ given by

$$H(z) = \frac{Y(z)}{X(z)} = \frac{b_0 + b_1 z^{-1} + \cdots + b_M z^{-M}}{1 + a_1 z^{-1} + \cdots + a_N z^{-N}}. \quad (9.9)$$

The transfer function consists of a numerator polynomial

$$B(z) = b_0 + b_1 z^{-1} + \cdots + b_M z^{-M}$$

and a denominator polynomial

$$A(z) = 1 + a_1 z^{-1} + \cdots + a_N z^{-N}.$$

The output $Y(z)$ is the product between the transfer function $H(z)$ and the input $X(z)$, that is,

$$Y(z) = H(z) X(z). \quad (9.10)$$

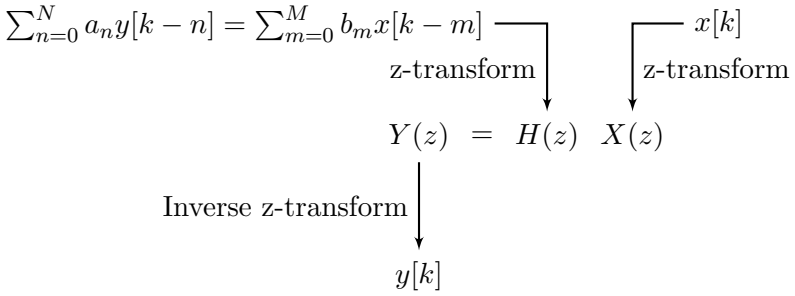

Figure 9.1. Illustration of the difference equation solving process using the z-transform.

Example 9.3: Transfer function

Consider the discrete time LTI system described by the difference equation (Example 9.2)

$$y[k] + y[k-1] + 0.25y[k-2] = 0.5x[k].$$

Taking the z-transform yields

$$Y(z) + z^{-1}Y(z) + 0.25z^{-2}Y(z) = 0.5X(z).$$

Breaking out $Y(z)$ on the left hand side yields

$$Y(z)(1 + z^{-1} + 0.25z^{-2}) = 0.5X(z).$$

Finally, rearranging the resulting algebraic equation in the z-domain yields the transfer function

$$H(z) = \frac{Y(z)}{X(z)} = \frac{0.5}{1 + z^{-1} + 0.25z^{-2}}.$$

Finally, to solve the difference equation (9.6), the approach follows the same steps as for solving ODEs using the Laplace transform. First, we calculate the system's transfer function $H(z)$ as well as the z-transform of the input signal $X(z)$. Then, the output in the z-domain $Y(z)$ is given by the product of the two, see (9.10). The last step is then to take the inverse z-transform using a transform table such as Table 9.1. Note that the last step might again involve partial fraction expansion (Figure 9.1).

9.2.2 Transfer Function and Impulse Response

Recall that in the time domain, the output of a discrete time LTI system is given by the convolution sum between the input $x[k]$ and the system's impulse response $h[k]$

$$y[k] = h[k] * x[k]. \tag{9.11}$$

Applying the z-transform to the input-output equation (9.11) using the convolution property (9.5) yields that

$$Y(z) = H(z)X(z),$$

where $H(z)$ is the z-transform of the impulse response $h[k]$. This is equivalent to the input-output relationship in the z-domain (9.10) (Definition 9.2). Hence, it follows that the impulse response $h[k]$ and the transfer function $H(z)$ must be a z-transform pair as shown in Definition 9.3.

Definition 9.3: Relationship between the discrete time impulse response and transfer function

The impulse response of a discrete time LTI system $h[k]$ and its transfer function $H(z)$ are a transform pair

$$h[k] \circ\!\!-\!\!\bullet\ H(z), \tag{9.12}$$

where

$$H(z) = \sum_{k=0}^{\infty} h[k] z^{-k}.$$

9.2.3 Transfer Function and Frequency Response

Recall that for causal signals, the discrete time Fourier transform is given by

$$X(\Omega) = \sum_{k=0}^{\infty} x[k] e^{-\mathrm{j}\,\Omega k},$$

whereas the z-transform is given by

$$X(z) = \sum_{k=0}^{\infty} x[k] z^{-k},$$

where $z = r^{\mathrm{j}\,\Omega}$. Thus, choosing $r = 1$ yields that $z = e^{\mathrm{j}\,\Omega}$ and the discrete time Fourier transform and the z-transform become the same. In other words, the discrete time Fourier transform of $x[k]$ is equal to the z-transform of $x[k]$ evaluated in $z = e^{\mathrm{j}\,\Omega}$, that is,

$$X(e^{\mathrm{j}\,\Omega}) = X(z)|_{z=e^{\mathrm{j}\,\Omega}}. \tag{9.13}$$

Note that the argument of the discrete time Fourier transform is written as $e^{\mathrm{j}\,\Omega}$ rather than simply Ω to emphasize the substitution.

It can be seen that $z = e^{\mathrm{j}\,\Omega}$ is a complex number with magnitude 1 and angle Ω. This corresponds to a point on the unit circle in the complex z-plane where Ω is the counter-clockwise angle from the real axis. Hence, the discrete time Fourier transform of $x[k]$ is obtained by evaluating the z-transform along the unit circle. Since a full rotation around the unit circle returns to the same point, the result is 2π-periodic. This is again in line with the requirement of the discrete time Fourier transform being 2π-periodic.

Applying the relationship (9.13) to the transfer function $H(z)$ thus yields the system's frequency response $H(e^{\mathrm{j}\,\Omega})$ (Definition 9.4).

Definition 9.4: Relationship between the discrete time transfer function and frequency response

The relationship between a discrete time LTI system's transfer function $H(z)$ and its frequency response $H(e^{\mathrm{j}\,\Omega})$ is given by the evaluation of $H(z)$ along the unit circle $z = e^{\mathrm{j}\,\Omega}$, that is,

$$H(e^{\mathrm{j}\,\Omega}) = H(s)|_{z=e^{\mathrm{j}\,\Omega}}. \tag{9.14}$$

9.2.4 Poles and Zeros, and Stability

The transfer function for discrete time LTI system is a ratio of an Mth order numerator polynomial $B(z)$ and a Nth order denominator polynomial $A(z)$,

$$H(z) = \frac{B(z)}{A(z)} = \frac{b_0 + b_1 z^{-1} + \cdots + b_M z^{-M}}{1 + a_1 z^{-1} + \ldots a_N z^{-N}}.$$

The system's poles and zeros are defined in the same way as for continuous time systems. The zeros z_i are the values of z for which the transfer function $H(z)$ becomes zero, that is,

$$H(z_i) = 0.$$

For this to be the case, the numerator polynomial has to become zero at $z = z_i$

$$B(z_i) = 0.$$

In other words, the zeros are the roots of the numerator polynomial $B(z)$.

Similarly, for the poles p_j, it holds that the transfer function approaches infinity,

$$\lim_{z \to p_j} |H(z)| \to \infty.$$

This means that a pole corresponds to a root of the denominator polynomial $A(z)$ such that

$$A(p_j) = 0.$$

Using the transfer function's poles and zeros, the polynomials can be rewritten as

$$\begin{aligned} B(z) &= b_0 z^{-M}(z^M + b_1/b_0 z^{M-1} + \cdots + b_M/b_0) \\ &= b_0 z^{-M}(z - z_1)(z - z_2)\ldots(z - z_M) \end{aligned}$$

and

$$\begin{aligned} A(z) &= z^{-N}(z^N + a_1 z^{N-1} + \ldots a_N) \\ &= z^{-N}(z - p_1)(z - p_2)\ldots(z - p_N) \end{aligned}$$

Thus, the pole-zero form of the transfer function $H(z)$ is as given in Definition 9.5.

Definition 9.5: Pole-zero form of the discrete time transfer function

The pole-zero form of the discrete time transfer function

$$H(z) = \frac{B(z)}{A(z)} = \frac{b_0 + b_1 z^{-1} + \cdots + b_M z^{-M}}{1 + a_1 z^{-1} + \ldots a_N z^{-N}}.$$

is given by

$$H(z) = b_0 z^{N-M} \frac{(z - z_1)(z - z_2)\ldots(z - z_M)}{(z - p_1)(z - p_2)\ldots(z - p_N)}. \tag{9.15}$$

The M roots (for $i = 1, \ldots, M$) of the numerator polynomial $B(z)$ are called the system's zeros. Similarly, the N roots p_j (for $j = 1, \ldots, N$) of the denominator polynomial $A(z)$ are called the system's poles. Additionally, if $M > N$ there are $M - N$ poles in the origin and if $M < N$ there are $N - M$ zeros in the origin.

Note that the poles (zeros) in the origin are caused by the factor z^{N-M} in the front of the fraction in 9.15. Furthermore, systems with real coefficients a_i and b_i have either purely real poles and zeros or their poles and zeros come in complex conjugate pairs. For example, if $p_i = r_i e^{\mathrm{j}\,\Omega_i}$ and $p_j = p_i^* = r_i e^{-\mathrm{j}\,\Omega_i}$, then grouping the pair yields

$$\begin{aligned}(z - r_i e^{\mathrm{j}\,\Omega_i})(z - r e^{-\mathrm{j}\,\Omega_i}) &= z^2 - r_i z(e^{\mathrm{j}\,\Omega_i} + e^{-\mathrm{j}\,\Omega_i}) + r_i^2 e^{\mathrm{j}\,\Omega_i} e^{-\mathrm{j}\,\Omega_i} \\ &= z^2 - 2r_i \cos(\Omega_i) + r_i^2. \end{aligned} \tag{9.16}$$

The locations of the poles and zeros can again be visualized using a pole-zero map, a plot of the complex z-plane. Here, a pole is marked as a cross ($\times$) whereas a zero is marked using a circle ($\circ$) as illustrated in Example 9.4 and Figure 9.2.

Example 9.4: Poles and zeros

Consider the following transfer functions:

a) The system considered in Examples (9.2)–(9.3) with

$$H(z) = \frac{0.5}{1 + z^{-1} + 0.25 z^{-2}}.$$

Rewriting the transfer function to pole-zero form by breaking out 0.5 in the numerator and z^{-2} in the denominator yields

$$H(z) = 0.5 z^2 \frac{1}{z^2 + z + 0.25}.$$

We can see that there are two zeros at $z_1 = z_2 = 0$. Furthermore, the roots of the denominator are found by factorizing the denominator polynomial

$$\begin{aligned} z^2 + z + 0.25 &= 0 \\ (z + 0.5)^2 &= 0. \end{aligned}$$

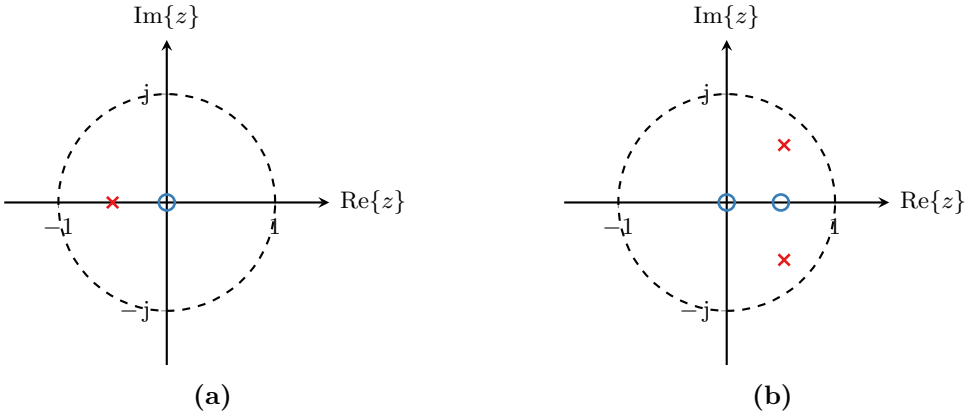

Figure 9.2. Pole-zero maps for the transfer functions in Example 9.4.

This shows that there are two poles in $p_1 = p_2 = -0.5$. This yields the pole-zero map in Figure 9.2a.

b) The system with transfer function

$$H(z) = \frac{2 - 0.5z^{-1}}{1 - 1.06z^{-1} + 0.56z^{-2}}.$$

Rewriting $H(z)$ yields

$$H(z) = 2z\frac{z - 0.5}{z^2 - 1.06z + 0.56z},$$

which shows that the system has one zero in $z_1 = 0$ and one in $z_2 = 0.5$. The poles can be found by using the quadratic formula on the denominator polynomial:

$$\begin{aligned} p_{1,2} &= \frac{-(-1.06) \pm \sqrt{(-1.06)^2 - 4 \cdot 0.56}}{2} \\ &= 0.53 \pm 0.5\sqrt{-1.1164} \\ &= 0.53 \pm \mathrm{j}\, 0.53 \\ &= 0.75e^{\pm \mathrm{j}\frac{\pi}{4}}. \end{aligned}$$

Hence, the poles are in $p_1 = 0.53 + \mathrm{j}\, 0.53$ and $p_2 = p_1^* = 0.53 - \mathrm{j}\, 0.53$. The pole-zero map for this transfer function is shown in Figure 9.2b.

Analog to the poles of a continuous time system, the poles of a discrete time transfer function $H(z)$ can be used to determine the system's stability. Note that we can write

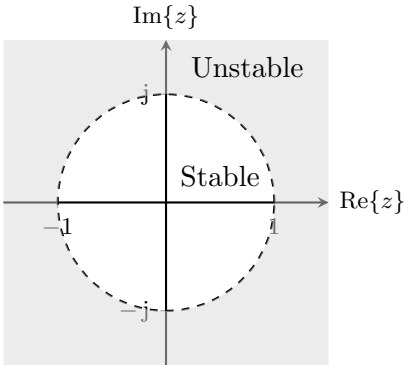

Figure 9.3. Illustration of the stable and unstable regions of the poles in the complex z-plane.

the transfer function as

$$\begin{aligned} H(z) &= \frac{b_0 + b_1 z^{-1} + \cdots + b_M z^{-M}}{1 + a_1 z^{-1} + \ldots a_N z^{-N}} \\ &= z^N \frac{b_0 + b_1 z^{-1} + \cdots + b_M z^{-M}}{(z - p_1)(z - p_2) \ldots (z^2 - 2r_i \cos(\Omega_i) + r_i^2) \ldots (z^2 - 2r_j \cos(\Omega_j) + r_j^2) \ldots} \\ &= \frac{b_0 + b_1 z^{-1} + \cdots + b_M z^{-M}}{(1 - p_1 z^{-1}) \ldots (1 - 2r_i z^{-1} \cos(\Omega_i) + r_i^2 z^{-2}) \ldots} \end{aligned}$$

where the factor z^N has been multiplied into the poles and second order terms in the denominator. Assuming that $N > M$ and using partial fraction expansion (Section A.7), this can be rewritten to

$$H(z) = \frac{c_1}{1 - p_1 z^{-1}} + \cdots + \frac{d_1 + e_1 z^{-1}}{1 - 2r_i z^{-1} \cos(\Omega_i) + r_i^2 z^{-2}} + \ldots. \tag{9.17}$$

Taking the inverse z-transform (Table 9.1) yields an impulse response of the form

$$h[k] = p_1^k u[k] + p_2^k u[k] + \cdots + r_i^k \cos(\Omega_i k) u[k] + \cdots + r_j^k \cos(\Omega_i k) u[k] + \ldots. \tag{9.18}$$

Thus, each pole p_n contributes to the impulse response either through an exponential term p_n^k (real poles) or an exponentially scaled sine or cosine, where the basis is the magnitude of the pole $|p_n| = r_n$. Thus, if and only if the magnitude of the nth pole $|p_n| = r_n$ is smaller than one ($|p_n| < 1$), the exponential terms r_n^k decay to zero as $k \to \infty$. Thus, the following condition must hold for a discrete time LTI system to be stable.

A discrete time LTI system is stable if and only if the magnitude of all of its poles $p_1, p_2, \ldots, p_N$ is smaller than one. That is, it must hold that

$$|p_n| < 1 \tag{9.19}$$

for all $n = 1, \ldots, N$. In other words, the poles of a discrete time LTI system *must lie inside the unit circle* for the system to be stable (Figure 9.3).

Chapter 10

Digital Filters

10.1 Introduction

10.1.1 Background

Analog (continuous time) filters as discussed in Chapter 5 have the important drawbacks that the filter implementation using analog electronics is not flexible and limiting. In particular, once a filter design has been chosen, we have only limited options to make changes to the filter. Furthermore, we are limited by component choices and higher order filters are cumbersome (and expensive) to implement. *Digital filters*, that is, filters that are implemented in software in, for example, a digital computer or a digital signal processor, provide solutions to these drawbacks. Digital filters can be replaced by software updates (e.g., through over-the-air updates) or by a change in parameters through a user interface and they do (most of the time) not require changes in the hardware architecture. Naturally, this comes at the expense of maintaining a signal processing software stack, possible software bugs, and vulnerabilities to cyber attacks.

A basic architecture of a digital filter is shown in Figure 10.1. In its simplest form, a digital filter is simply applied to a sampled signal and the output of the filter is directly reconstructed. This could, for example, be the case in a digital audio mixer/equalizer system in a concert hall. Another application, however, could be a video conferencing system where the audio (and video) is recorded, filtered to remove noise, cross-talk, echoes, etc., and streamed to other participants. In this case, the audio is reconstructed at the other participant's end, which may be geographically far from where it was sampled.

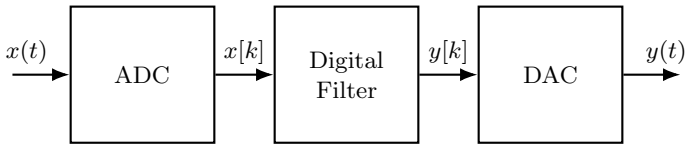

Figure 10.1. Illustration of the basic digital filtering architecture: A continuous time signal is sampled using an ADC and the resulting discrete time signal $x[k]$ is passed through a digital filter. The resulting output signal $y[k]$ is reconstructed using an DAC to obtain the filtered continuous time signal $y(t)$.

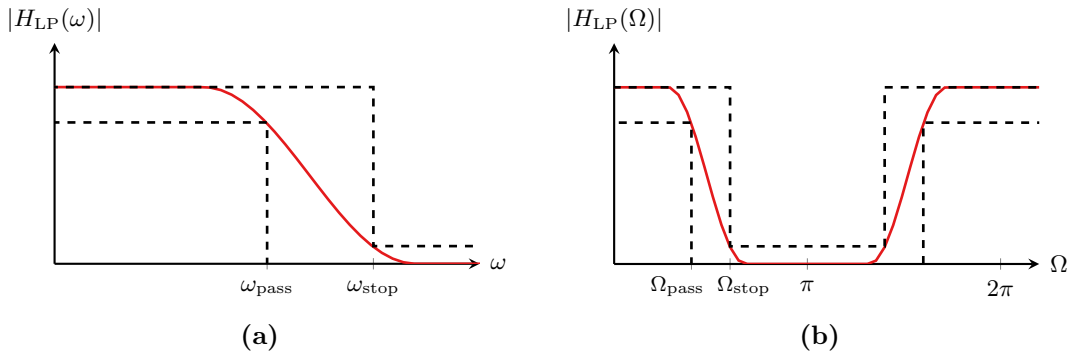

Figure 10.2. Illustration of the conversion of filter frequency requirements from continuous to discrete time for a lowpass filter. (a) Continuous time requirements and (b) discrete time requirements where the pass- and stopband edge frequencies are normalized with respect to the sampling time T_s, $\Omega_{\mathrm{pass}} = \omega_{\mathrm{pass}} T_s$ and $\Omega_{\mathrm{stop}} = \omega_{\mathrm{stop}} T_s$. Also note that the discrete time frequency response is 2π-periodic (see Chapter 8).

10.1.2 Continuous Time Requirements and Digital Filters

As for analog filters, the requirements for digital filters are typically specified in the frequency domain in general, and in the continuous time domain in particular[1]. Hence, the frequency domain requirements have to be translated from the continuous time into the discrete time. Recall that for sampled continuous time signals, the relationship between the discrete time frequency Ω (normalized frequency) and the continuous time frequency ω was

$$\Omega = \omega T_s = 2\pi \frac{f}{f_s}.$$

Hence, if we are given specifications for the cutoff frequency ω_c, the passband edge frequency ω_{pass}, or the stopband edge frequency ω_{stop}, these need to be converted to normalized frequencies according to

$$\Omega_c = \omega_c T_s, \ \Omega_{\mathrm{pass}} = \omega_{\mathrm{pass}} T_s, \ \text{and} \ \Omega_{\mathrm{stop}} = \omega_{\mathrm{stop}} T_s.$$

Also note that the corresponding discrete time frequency response $H(\Omega)$ must be 2π-periodic such that $H(\Omega + 2\pi) = H(\Omega)$. These relationships are illustrated in Figure 10.2.

10.1.3 Digital Filters and LTI Systems

Digital filters are implemented as discrete time LTI systems. Thus, an Nth order digital filter can be described by rational transfer functions of the form

$$H(z) = \frac{b_0 + b_1 z^{-1} + \cdots + b_N z^{-N}}{1 + a_1 z^{-1} + \cdots + a_N z^{-N}}.$$

[1]This is the case for digital filters that act on sampled continuous time signals. Naturally, digital filters can also act on purely discrete time signals that have no relationship to continuous time signals, something that is not discussed explicitly here.

The task of filter design is then again to determine the coefficients $b_0, b_1, \ldots, b_N$ and $a_0, a_1, \ldots, a_N$ of the numerator and denominator polynomials

$$B(z) = b_0 + b_1 z^{-1} + \cdots + b_N z^{-N}$$

and

$$A(z) = a_0 + a_1 z^{-1} + \cdots + a_N z^{-N},$$

respectively (or equivalently the poles $p_1, p_2, \ldots, p_N$, zeros $z_1, z_2, \ldots, z_N$, and gain K). This is done based on the (translated) frequency domain specifications, but the actual implementation is done in the time domain as a difference equation as follows.

Recall that the output of a discrete time system in the z-domain is given by

$$Y(z) = H(z)X(s) = \frac{b_0 + b_1 z^{-1} + \cdots + b_N z^{-N}}{1 + a_1 z^{-1} + \cdots + a_N z^{-N}} X(z).$$

Instead of deriving the impulse response $h[k]$ and then implementing the filter as a convolution, digital filters are implemented as difference equations corresponding to the system's transfer function. The difference equation is found by applying the reverse sequence of steps taken when deriving the transfer function based on a difference equation: First, by multiplying with the denominator of the transfer function and expanding both sides yields

$$Y(z) + a_1 z^{-1} Y(z) + \cdots + a_N z^{-N} Y(z) = b_0 X(z) + b_1 z^{-1} X(z) + \cdots + b_N z^{-N} X(z).$$

Then, taking the inverse z-transform (using the time-shift property) and solving for the current output $y[k]$ in terms of the past outputs $y[k-1], y[k-2], \ldots, y[k-N]$ and current and past inputs $x[k], x[k-1], \ldots, x[k-N]$ yields

$$\begin{aligned} y[k] &= -a_1 y[k-1] - \cdots - a_N y[k-N] + b_0 x[k] + b_1 x[k-1] + \cdots + b_N x[k-N] \\ &= -\sum_{n=1}^{N} a_n y[k-n] + \sum_{n=0}^{N} b_n x[k-n]. \end{aligned}$$

This gives rise to two elementary types of digital filters: Non-recursive filters that do not depend on the past outputs $y[k-1], y[k-2], \ldots, y[k-N]$ at all, for which all $a_n = 0$ (for $n > 0$). These filters are called *finite impulse response* (FIR) filters. The second type of filters are recursive filters, that is, filters that depend on past values of the output $y[k]$. These filters are called *infinite impulse response* (IIR) filters. Both filter types are discussed next.

10.2 Finite Impulse Response Filters

10.2.1 Definition and Properties

FIR filters solely depend on the current and past inputs $x[k], x[k-1], \ldots, x[k-N]$, but not on past outputs $y[k-n]$. Thus, their difference equation is given by

$$y[k] = \sum_{n=0}^{M} b_n x[k-n] = b_0 x[k] + b_1 x[k-1] + \cdots + b_N x[k-N].$$

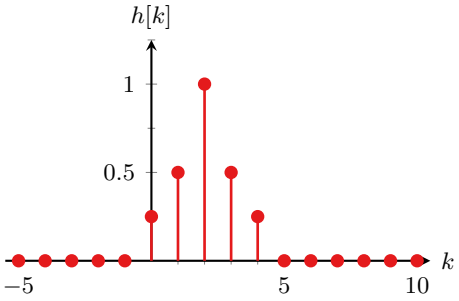

Figure 10.3. Impulse response of the FIR filter in Example 10.1

This in turn yields the transfer function

$$H(z) = b_0 + b_1 z^{-1} + \cdots + b_N z^{-N}. \tag{10.1}$$

Taking the inverse z-transform of (10.1) using the transform pair $\delta[k] \circ\!\!-\!\!\bullet\ 1$ together with the time shift property yields the FIR filters impulse response

$$h[k] = b_0\delta[k] + b_1\delta[k-1] + \cdots + b_N\delta[k-N]. \tag{10.2}$$

Eq. (10.2) shows that the FIR filter's impulse response consists of exactly $N+1$ components. Hence, since the impulse response becomes zero for $k > N$, the impulse response is *finite*, which gives rise to the name *finite impulse response* filter. The coefficients b_n are called the *filter taps* and thus, an Nth order filter has $N+1$ filter taps. This is illustrated in Example 10.1 and Figure 10.3.

Example 10.1: FIR filter

Consider the 4th order FIR filter with impulse response

$$h[k] = 0.25\delta[k] + 0.5\delta[k-1] + \delta[k-2] + 0.5\delta[k-3] + 0.25\delta[k-4].$$

The filter's taps are $b_0 = 0.25$, $b_1 = 0.5$, $b_2 = 1$, $b_3 = 0.5$, and $b_4 = 0.25$, and the impulse response is illustrated in Figure 10.3.

By breaking out z^{-N} in (10.1), the transfer function can be rewritten as

$$H(z) = z^{-N}(b_0 z^N + b_1 z^{N-1} + \cdots + b_N) = \frac{b_0 z^N + b_1 z^{N-1} + \cdots + b_N}{z^N}.$$

This shows that FIR filters have all their poles at the origin, which leads to the following conclusion.

FIR filters are always stable since all their poles are located inside the unit circle, at the origin.

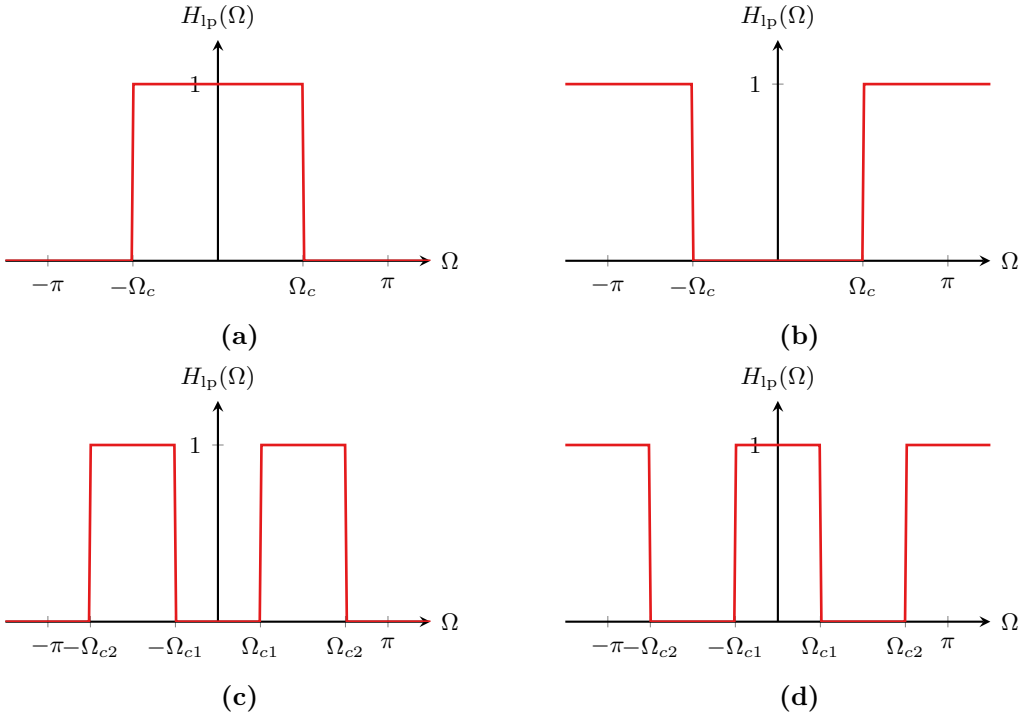

Figure 10.4. Frequency responses for the ideal discrete time filters for the interval $-\pi \leq \Omega \leq \pi$. (a) Lowpass, (b) highpass, (c) bandpass, and (d) bandstop.

10.2.2 FIR Filter Design

There are several approaches for designing FIR filters. Here, we discuss the *windowing* and the *Parks–McClellan* (or *optimal*) methods. The former is illustrative and can easily be done by hand, whereas the latter can be considered a de-facto standard for FIR filter design.

Windowing

The windowing filter design approach is based on a causal approximation of the ideal filter impulse response. Figure 10.4 shows the ideal discrete time filter frequency responses for the interval $-\pi \leq \Omega < \pi$. Here, it is important to recall that the discrete time frequency response must be 2π-periodic and thus, it is enough to only consider a single 2π interval (see Chapter 8). The interval $-\pi$ to π is particularly instructive as the frequency responses then readily map to the continuous time filter frequency responses. Furthermore, also note that for sampled signals, the point $\Omega = \pi$ corresponds to $\omega_N T_s$, that is, the Nyquist frequency.

The expressions for the frequency responses for the interval $-\pi \leq \Omega < \pi$ are given in Table 10.1, together with the ideal impulse responses that are obtained by applying the inverse discrete time Fourier transform (see Chapter 8). However, the impulse responses are non-causal and can not be implemented in practice. Nevertheless, since they all decay

Table 10.1. Ideal discrete time filter frequency responses and their impulse responses.

Ideal Frequency Response ($\pi \leq \Omega < \pi$)	Ideal Impulse Response
Lowpass	
$H(\Omega) = \text{rect}\left(\frac{\Omega}{2\Omega_c}\right)$	$h[k] = \frac{\Omega_c}{\pi}\,\text{sinc}\left[\frac{\Omega_c k}{\pi}\right]$
Highpass	
$H(\Omega) = 1 - \text{rect}\left(\frac{\Omega}{2\Omega_c}\right)$	$h[k] = \delta[k] - \frac{\Omega_c}{\pi}\,\text{sinc}\left[\frac{\Omega_c k}{\pi}\right]$
Bandpass	
$H(\Omega) = \text{rect}\left(\frac{\Omega}{2\Omega_{c2}}\right) - \text{rect}\left(\frac{\Omega}{2\Omega_{c1}}\right)$	$h[k] = \frac{\Omega_{c2}}{\pi}\,\text{sinc}\left[\frac{\Omega_{c2} k}{\pi}\right] - \frac{\Omega_{c1}}{\pi}\,\text{sinc}\left[\frac{\Omega_{c1} k}{\pi}\right]$
Bandstop	
$H(\Omega) = 1 - \text{rect}\left(\frac{\Omega}{2\Omega_{c2}}\right) + \text{rect}\left(\frac{\Omega}{2\Omega_{c1}}\right)$	$h[k] = \delta[k] - \frac{\Omega_{c2}}{\pi}\,\text{sinc}\left[\frac{\Omega_{c2} k}{\pi}\right] + \frac{\Omega_{c1}}{\pi}\,\text{sinc}\left[\frac{\Omega_{c1} k}{\pi}\right]$

to zero as $k \to -\infty$ and $k \to \infty$, they can be truncated (time-limited) at some lower limit $k = -\frac{N}{2}$ and upper limit $k = \frac{N}{2}$. This yields a finite impulse response of length $N+1$. Furthermore, time-shifting the truncated ideal impulse response by $\frac{N}{2}$ to the right makes the impulse response causal. This is illustrated in Figure 10.5 (left column) and Example 10.2.

Example 10.2: FIR filter design using the windowing method

Assume that an FIR filter with cutoff frequency $\Omega_c = \frac{\pi}{4}$ is to be designed using the windowing method. The filter's ideal impulse response is given by (Table 10.1)

$$h[k] = \frac{1}{4}\,\text{sinc}\left[\frac{k}{4}\right],$$

which is illustrated in Figure 10.5a. This impulse response is non-causal and infinite. However, time-limiting the impulse response to $N+1 = 25$ samples using the samples from $k = -12$ to $k = 12$ makes it finite (Figure 10.5c). This can be expressed as a multiplication of the sinc with a rectangular window of width 25, that is,

$$h[k] = \frac{1}{4}\,\text{sinc}\left[\frac{k}{4}\right]\text{rect}\left[\frac{k}{25}\right].$$

Finally, the impulse response is made causal by time-shifting it $\frac{M}{2} = 12$ samples to the right such that

$$h[k] = \frac{1}{4}\,\text{sinc}\left[\frac{k-12}{4}\right]\text{rect}\left[\frac{k-12}{25}\right],$$

which yields the final impulse response shown in Figure 10.5e.

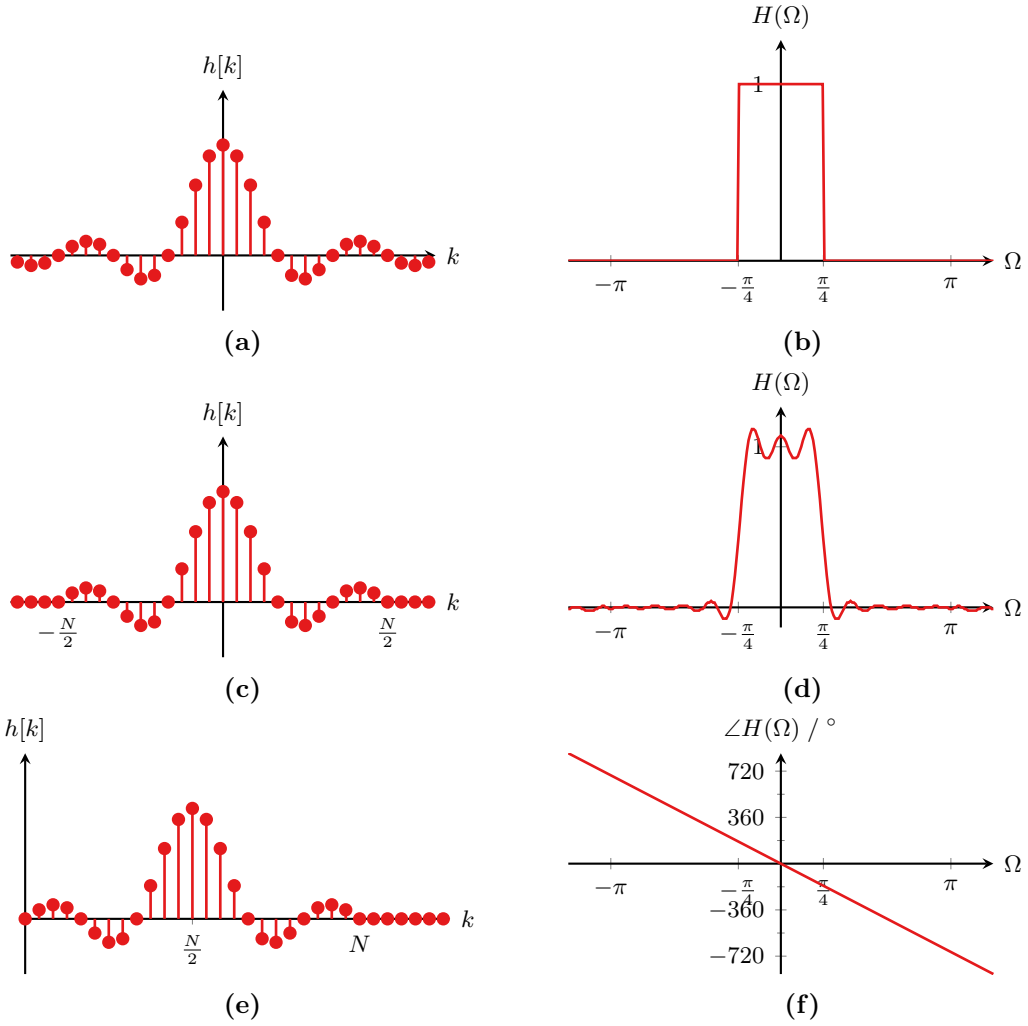

Figure 10.5. Illustration of the windowing FIR filter design steps. (a)–(b) ideal impulse and frequency responses, (c)–(d) truncated (time-limited) impulse and frequency responses, and (e)–(f) time-shifted impulse response and phase of the frequency response. Note that the phase of the ideal and truncated frequency responses are zero and that the magnitude of the time-shifted frequency response is the same as the magnitude of the truncated frequency response.

Naturally, truncation and time-shifting affect the frequency response that is actually implemented by the filter. Truncation can be seen as a windowing (hence, the name of the method) similar to windowing in the DFT (Chapter 8). This corresponds to a multiplication with a rectangular signal of width $N+1$. In the frequency domain, we thus have the convolution between the ideal frequency response and an aliased sinc. Furthermore, time shifting by $\frac{N}{2}$ samples to the right does not affect the magnitude of the frequency response but adds a phase shift, that is,

$$h\left[k-\frac{N}{2}\right] \circ\!\!-\!\!\bullet\; H(\Omega)e^{-\mathrm{j}\,\Omega\frac{N}{2}}.$$

The effects of these operations on the ideal frequency response for the filter in Example 10.2 are shown in Figure 10.5 (right column).

More generally, the final, windowed and time shifted frequency response can be expressed as

$$H(\Omega) = \frac{1}{2\pi} \left[H_{\text{ideal}}(\Omega) * W(\Omega) \right] e^{-\mathrm{j}\,\Omega \frac{N}{2}}. \tag{10.3}$$

As for the DFT, different windows $W(\Omega)$ may be used (see Section 8.2): Windows such as the Bartlett or Hamming windows will cause less ripples in the final frequency response $H(\Omega)$ due to their lower sidelobes (compared to the rectangular window). However, due to the wider mainlobe, the transition band is increased instead. Thus, the choice of window becomes a trade-off between ripples and transition band and the right choice depends entirely on the application.

Parks–McClellan

The Parks–McClellan method (also known under several other names such as the optimal method) for designing FIR filters is an iterative algorithm that aims at exploiting the full tolerances of the filter requirements. In other words, it maximizes the ripples in both the pass- and stopbands and exploits the full transition band in order to minimize the resulting FIR filter order.

The actual description of the algorithm is quite extensive and outside of the scope of these notes. A full description can, for example, be found in Mandal and Asif (2007). However, the basic idea is as follows. Given the filter order N, the algorithm iteratively optimizes the frequency response by minimizing the maximum (weighted) error of the frequency response with respect to the ideal frequency response, that is, it solves the optimization problem

$$\epsilon_{\max} = \min \left[\max \left| W(\Omega)(H_{\text{ideal}}(\Omega) - H(\Omega)) \right| \right]$$

where $W(\Omega)$ is a weighting function. This is achieved by using a polynomial approximation of the frequency response and finding the frequencies that give the same maximum ripples $\epsilon_{\max}$ using a so-called Remez–Exchange algorithm. In the final step, the filter taps are determined from the optimized frequency response.

Figure 10.6 shows the frequency response for two $N = 47$ order FIR lowpass filters, one designed using windowing (with a rectangular window) and one using the Parks–McClellan method. The figure shows that the two filters achieve a similar transition band, but the filter designed using the Parks–McClellan method achieves a lower stopband attenuation. This could be improved for the filter designed using the windowing method by using a different window, at the expense of a wider transition band (assuming that the order is kept constant). The code for designing these two filters in Python is shown in Example 10.3.

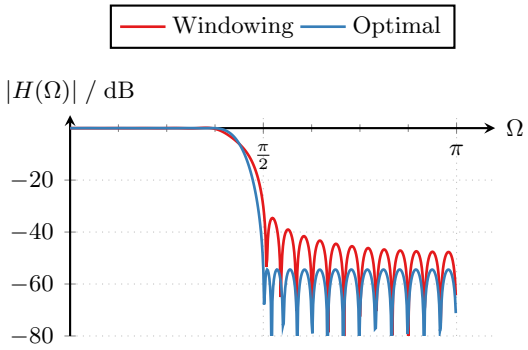

Figure 10.6. Comparison of the frequency response of two FIR filters of order $N = 47$ designed using the windowing and Parks–McCleallan method.

Example 10.3: FIR filter design using Python

The following Python code is used to design the two FIR filters with frequency responses shown in Figure 10.6. As usual, the first step is to include the necessary libraries, NumPy and the signal processing toolbox from SciPy.

```
import numpy as np
from scipy import signal
```

Next, the filter specifications are defined. Note that the FIR filter design tools require a set of frequency bands together with their gains. Unfortunately, the design functions interfaces are not consistent in this respect: The windowing function needs specifications at the corner frequencies, whereas the Parks–McClellan method requires the gains inside the whole band. This leads to:

```
# Define filter order
N = 47

# Define the ideal frequency response, normalized with respect
# to the Nyquist frequency
Ws = np.array([0, 0.375, 0.5, 1])
Aswin = np.array([1, 1, 0, 0])
Asopt = np.array([1, 0])
```

The last three lines are the specification of the frequency response: The filter should have a passband with gain 1 between the frequencies $0 \leq \Omega \leq 0.375\pi$, a transition band between $0.375\pi < \Omega < 0.5\pi$, and a stopband in the range $0.5\pi \leq \Omega < \pi$ with gain 0.
Then, the filter coefficients can be calculated using the functions `signal.firwin2()` for the windowing method and `signal.remez()` for the Parks–McClellan method.

```
bwin = signal.firwin2(N+1, Ws, Aswin, window='boxcar')
bopt = signal.remez(N+1, Ws/2, Asopt)
```

Note that `signal.remez()` suffers from another interface inconsistency: Instead of expecting the frequency specification being normalized with respect to the Nyquist frequency, they should be normalized with respect to the sampling frequency instead. Thus, the frequencies are scaled by two, that is, `Ws/2`.

10.3 Infinite Impulse Response Filters

10.3.1 Definition and Properties

An Nth order IIR filter has the general form of transfer functions given by

$$H(z) = \frac{b_0 + b_1 z^{-1} + \cdots + b_N z^{-N}}{1 + a_1 z^{-1} + \cdots + b_N z^{-N}},$$

which leads to the output equation

$$y[k] = -\sum_{n=1}^{N} a_n y[k-n] + \sum_{n=0}^{N} b_n x[k-n]. \tag{10.4}$$

Applying the unit impulse $x[k] = \delta[k]$ as the input in (10.4) shows that the impulse remains in the system forever as the current output depends on N previous outputs and the current input. Hence, the impulse response is *infinite*, such that

$$h[k] = \sum_{i=0}^{\infty} h[i]\delta[k-i],$$

which gives rise to the name *infinite impulse response* filter.

The poles of IIR filters do not necessarily lie inside the unit circle. Thus, in contrast to FIR filters, IIR filters may not be stable. However, for properly designed IIR filters, the poles are inside the unit circle and the filter is thus stable. In this case, it can also be shown that despite the impulse response being infinite, it converges to zero as k increases, that is,

$$\lim_{k\to\infty} h[k] \to 0$$

for stable IIR filters.

10.3.2 IIR Filter Design Using the Bilinear Transform

IIR filter design methods can be divided into two types:

1. *Indirect methods* that are based on converting continuous time filters to discrete time, and
2. *direct methods* that directly design digital IIR filters in the discrete time domain.

In this section, we introduce the bilinear transform, an indirect method and one of the most common IIR filter design techniques. For other methods, please refer to, for example, Mandal and Asif (2007).

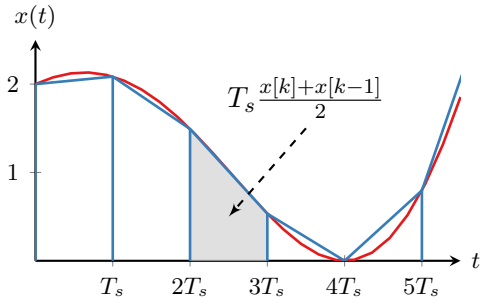

Figure 10.7. Illustration of the trapezoidal approximation of the integral of the signal $x(t)$. The integral is approximated using finite trapezoids of width T_s, left height $x[k-1] \triangleq x((k-1)T_s)$, and right height $x[k] \triangleq x(kT_s)$. The resulting contribution to the total integral of each trapezoid is $T_s \frac{x[k]+x[k-1]}{2}$.

The bilinear transform filter design method is based on using the bilinear transform (also called Tustin's method) to convert a continuous time analog filter (Chapter 5) to discrete time.

The bilinear transform is based on a trapezoidal approximation of integration. Consider the integral $i(t)$ of a function $x(t)$ up to some time t given by

$$i(t) = \int_0^t x(\tau)\,\mathrm{d}\tau. \tag{10.5}$$

This integral can be approximated using trapezoidal integration as illustrated in Figure 10.7, which is given by

$$i[k] = \sum_{n=1}^{N} T_s \frac{x[n] + x[n-1]}{2} = i[k-1] + T_s \frac{x[k] + x[k-1]}{2}, \tag{10.6}$$

where T_s is the distance between sampling points of the function $x(t)$.

Then, taking the Laplace transform of (10.5) and the z-transform of (10.6) yields

$$I(s) = \frac{X(s)}{s}$$

and

$$I(z) = z^{-1}I(z) + \frac{T_s}{2}(1 + z^{-1})X(z) \;\Rightarrow\; I(z) = \frac{2}{T_s}\frac{1 + z^{-1}}{1 - z^{-1}}X(z),$$

respectively. Thus, we can conclude that the trapezoidal approximation approximates the integral operator $\frac{1}{s}$ by $\frac{T_s}{2}\frac{1+z^{-1}}{1-z^{-1}}$, that is,

$$\frac{1}{s} \approx \frac{T_s}{2}\frac{1 + z^{-1}}{1 - z^{-1}} = \frac{T_s}{2}\frac{z + 1}{z - 1}.$$

Thus, given a continuous time filter transfer function $H(s)$, a discrete time approximation of the filter $H(z)$ can be obtained by the substitution

$$s = \frac{2}{T_s}\frac{1-z^{-1}}{1+z^{-1}} = \frac{2}{T_s}\frac{z-1}{z+1} \tag{10.7}$$

such that

$$H(z) = H(s)|_{s=\frac{2}{T_s}\frac{z-1}{z+1}}. \tag{10.8}$$

Note that it can be shown that the bilinear transform maps the left half plane of the s-plane into the interior of the unit circle in the z-plane, where the imaginary axis of the s-plane is mapped onto the unit circle.

The steps to design the discrete time filter are then:

1. Filter requirement specification (passband and stopband edge frequencies, passband ripple, stopband attenuation);
2. Design of the analog filter transfer function $H(s)$ (see Chapter 5);
3. Approximation of the analog filter transfer function using the bilinear transform.

This is illustrated in Example 10.4 below.

Example 10.4: IIR filter design using the bilinear transform

Consider the design of an IIR Butterworth lowpass filter with the following requirements:

- Passband edge frequency: $\omega_{\text{pass}} = 1000\,\text{rad/s}$,
- passband ripple: 3 dB,
- stopband edge frequency: $\omega_{\text{stop}} = 10\,000\,\text{rad/s}$,
- stopband attenuation: 20 dB, and
- sampling time $T_s = 0.1\,\text{ms}$.

The order of the filter is given by (see Chapter 5)

$$N \geq \frac{\log\left(\sqrt{\frac{A_s^2-1}{A_p^2-1}}\right)}{\log\left(\frac{\omega_{\text{stop}}}{\omega_{\text{pass}}}\right)} = 0.998$$

and the cutoff frequency is

$$\omega_c = \frac{\omega_{\text{pass}}}{(A_p^2-1)^{\frac{1}{2N}}} = 1000\,\text{rad/s}.$$

This yields a first order filter with continuous time filter transfer function

$$H(s) = \frac{1}{\frac{s}{1000}+1} = \frac{1000}{s+1000}.$$

The digital filter transfer function is then found by using the bilinear transform according to

$$H(z) = H(s)|_{s=\frac{2}{T_s}\frac{z-1}{z+1}} = \frac{1000}{s+1000}\bigg|_{s=\frac{2}{T_s}\frac{z-1}{z+1}} = \frac{1000}{\frac{2}{T_s}\frac{z-1}{z+1}+1000}$$
$$= \frac{T_s(z+1)1000}{2(z-1)+1000T_s(z+1)} = \frac{1000T_sz+1000T_s}{2z-2+1000T_sz+1000T_s},$$

and finally

$$H(z) = \frac{1000T_sz+1000T_s}{z(1000T_s+2)+1000T_s-2}.$$

Using the value for $T_s = 0.1\,\text{ms}$ then yields the transfer function

$$H(z) = \frac{0.1z+0.1}{2.1z-1.9} = \frac{0.1+0.1z^{-1}}{2.1-1.9z^{-1}} = \frac{0.0476+0.0476z^{-1}}{1-0.9048z^{-1}}.$$

Here, the last step involved breaking out the factor 2.1 from the denominator in order to normalize the a_0 coefficient to 1.
The filter can then be implemented by deriving the input-output equation in the time domain as follows. First, note that

$$Y(z) = H(z)X(z) = \frac{0.0476+0.0476z^{-1}}{1-0.9048z^{-1}}X(z),$$

which leads to

$$Y(z)(1-0.9048z^{-1}) = (0.0476+0.0476z^{-1})X(z)$$
$$Y(z)-0.9048z^{-1}Y(z) = 0.0476X(z)+0.0476z^{-1}X(z)$$
$$\Downarrow$$
$$Y(z) = 0.9048z^{-1}Y(z)+0.0476X(z)+0.0476z^{-1}X(z).$$

Finally, taking the inverse z-transform yields the difference equation

$$y[k] = 0.9048y[k-1]+0.0476x[k]+0.0476x[k-1],$$

which can be implemented in a digital computer.

Recalling that the frequency responses for continuous and discrete time systems are given by $H(\omega) = H(s)|_{s=\mathrm{j}\,\omega}$ and $H(\Omega) = H(z)|_{z=e^{\mathrm{j}\,\Omega}}$ we obtain the frequency relationship

$$\omega = \frac{2}{T_s}\tan\left(\frac{\Omega}{2}\right)$$

from (10.7). This shows that the relationship between the two frequencies is nonlinear. Furthermore, by replacing the constant $\frac{2}{T_s}$ by a more generic constant C and using the relationship $\Omega = \omega T_s$ for sampled continuous time signals, we can make the frequency transformation match at a specific desired frequency $\omega_\star$ as follows. First, rewriting the frequency relationship yields

$$\omega_\star = C \tan\left(\frac{\omega_\star T_s}{2}\right).$$

Then, solving for C leads to

$$C = \frac{\omega_\star}{\tan\left(\frac{\omega_\star T_s}{2}\right)}. \tag{10.9}$$

This is called *pre-warping* and is used when it has to be ensured that the continuous and discrete time frequency responses have to be equivalent at the pre-warping frequency $\omega_\star$.

The bilinear transform (without pre-warping) is the default IIR filter design method used in SciPy and the design process is illustrated in Example 10.5.

Example 10.5: IIR filter design using Python

Here, we show how the filter in Example 10.4 can be designed using Python. The first step is to include the necessary libraries. These are NumPy (`numpy`) and the signal processing library from SciPy (`scipy.signal`):

```
import numpy as np
from scipy import signal
```

Then, the filter requirements and other parameters are specified:

```
# Pass- and stopband edge frequencies
wpass = 1e3
wstop = 10e3

# Passband ripple and stopband attenuation in dB
Apass = 3
Astop = 20

# Sampling time and frequency
Ts = 0.1e-3
ws = 2*np.pi/Ts
```

Next, the filter order and normalization frequency are determined using the `buttord()` function and the filter coefficients are calculated using `butter()`. Note that for digital filters, the frequencies are specified relative to the Nyquist frequency ω_N, that is, as $\frac{\omega_{\text{pass}}}{\omega_N}$ and $\frac{\omega_{\text{stop}}}{\omega_N}$ for the passband and stopband edge frequencies, respectively:

```
# Determine the filter order and normalization frequency
N, wn = signal.buttord(wpass/(ws/2), wstop/(ws/2), Apass, Astop)

# Determine the filter coefficients
```

```
b, a = signal.butter(N, wn, btype='low')
```

Note that the default for the functions `buttord()` and `butter()` is to design a digital filter and thus, we do not have to specify this explicitly (in contrast to Example 5.5). The resulting filter coefficients are

$$b_0 = 0.0478, b_1 = 0.0478, a_0 = 1, a_1 = -0.9044,$$

which corresponds to the coefficients in Example 10.4 (the slight differences in the coefficients can be attributed to roundoff errors).
The filter's frequency response can then be calculated using

```
# Calculate the frequency response
w, H = signal.freqz(b, a)
```

The steps for designing Chebyshev and elliptic filters as well as high- and bandpass as well as bandstop filters are the same but use the corresponding functions and different parameters, see the SciPy documentation. Finally, note that SciPy also provides the convenience function `iirdesign()` that wraps the above steps into one, simplifying the process somewhat.

10.3.3 Filter Coefficient Quantization and Stability

As discussed above, IIR filters may, if poorly designed, be unstable, in contrast to FIR filters that are always stable. However, even filters that are stable at the design stage may actually become unstable in practice. One reason for this is coefficient quantization due to the computer's or digital signal processors's limited numerical precision. For example, an IIR filter may be designed on a general purpose computer where the filter coefficients are calculated using a 64-bit float representation. If, however, this filter is implemented in a digital signal processor that does not support 64-bit floats, the coefficients have to be converted to the supported format. This can, in turn, cause a loss of precision and render the filter unstable. This is illustrated in Example 10.6.

Example 10.6: Filter coefficient quantization

Consider the lowpass IIR filter with numerator coefficients

$$\{0.0039, 0.0093, 0.0198, 0.0276, 0.0317, 0.0276, 0.0198, 0.0093, 0.0039\},$$

and denominator coefficients

$$\{1.0000, -3.7597, 8.1976, -11.8524, 12.3314, -9.2974, 4.9767, -1.7419, 0.3172\}.$$

Furthermore, assume that the filter coefficients are quantized using 11 fractional bits for the numerator coefficients and 3 fractional bits for the denominator coefficients. This yields the quantized numerator coefficients

$$\{0.0039, 0.0093, 0.020, 0.0273, 0.0317, 0.0273, 0.020, 0.0093, 0.0039\},$$

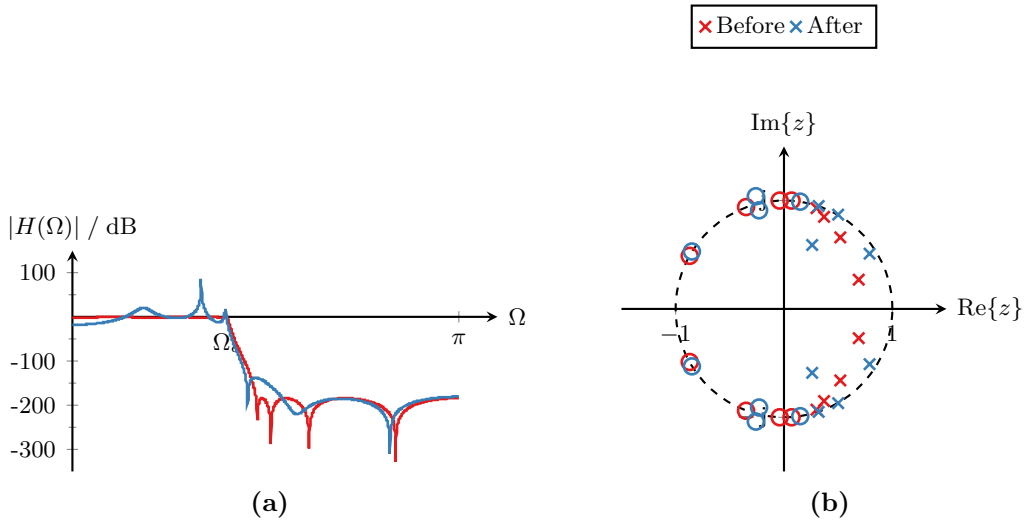

Figure 10.8. Effect of the quantization of IIR filter coefficients. (a) Frequency response and (b) pole-zero map.

and quantized denominator coefficients

$$\{1.00, -3.75, 8.25, -11.875, 12.375, -9.25, 5.00, -1.75, 0.375\}.$$

Figure 10.8 shows the frequency response and the poles and zeros of the filter before and after quantization of the coefficients.

One approach to mitigate problems caused by coefficient quantization and to improve numerical stability is to split the filter into a cascade of several lower-order filters such that

$$H(z) = H_1(z)H_2(z)\dots H_M(z).$$

The typical way of doing this is to split the filter into so-called *second order sections*, that is, filters of order two. In this way, each filter consists of numerically well-conditioned coefficients that are less susceptible to quantization effects (and other numerical issues). Filter design tools can typically automatically calculate the coefficients for each second order section, instead of the coefficients for the overall filter. Figure 10.9 shows the frequency response and pole-zero map for the filter in Example 10.6 when implemented using second order sections.

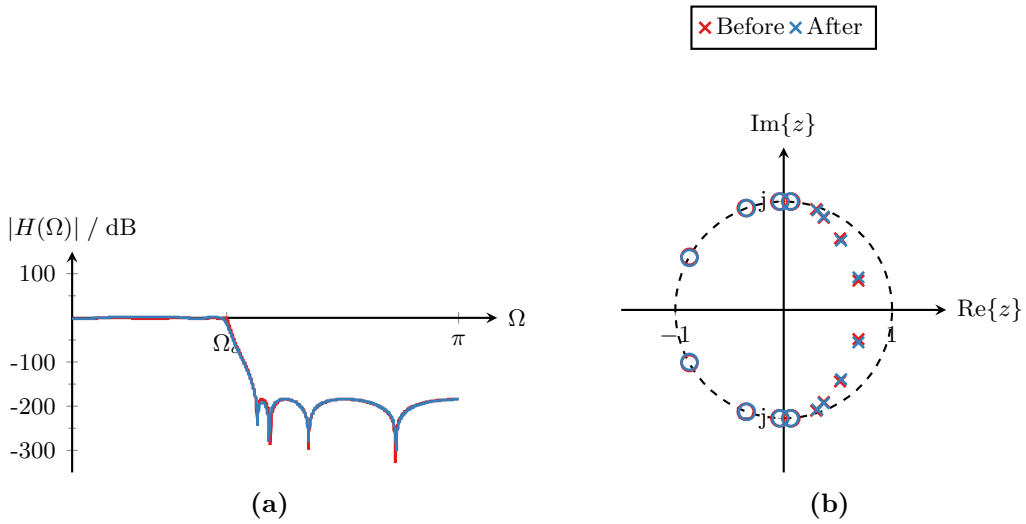

Figure 10.9. Effect of the quantization of IIR filter coefficients when implemented as a cascade of second order sections.(a) Frequency response and (b) pole-zero map.

Appendix A

Mathematical Preliminaries

A.1 Scientific Notation

In science and engineering, quantities are often stated in scientific notation using the list of prefixes in Table A.1.

A.2 Complex Numbers

In electrical engineering, the imaginary unit is denoted as

$$\mathrm{j} \triangleq \sqrt{-1}$$

in contrast to mathematics, where i is used. This is to avoid confusion with the electrical currents that are denoted using i (mostly for alternating current; AC) and I (mostly for direct current; DC).

Complex numbers can be expressed in *rectangular form*

$$z = a + \mathrm{j}\, b$$

where a is the *real part* of the complex number z denoted $\mathrm{Re}\{z\} = a$ and b is the *imaginary part* of z denoted $\mathrm{Im}\{z\} = b$.

Alternatively, complex numbers can be expressed in *polar form*

$$z = re^{\mathrm{j}\,\varphi}$$

Table A.1. Scientific Prefixes

Name	Symbol	Factor
Tera	T	10^{12}
Giga	G	10^{9}
Mega	M	10^{6}
Kilo	k	10^{3}
Milli	m	10^{-3}
Micro	μ	10^{-6}
Nano	n	10^{-9}
Pico	p	10^{-12}

Table A.2. Elementary operations for complex numbers.

Name	Operation
Addition	$z_1 + z_2 = (a + \mathrm{j}\, b) + (c + \mathrm{j}\, d) = (a + c) + \mathrm{j}(b + d)$
Subtraction	$z_1 - z_2 = (a + \mathrm{j}\, b) - (c + \mathrm{j}\, d) = (a - c) + \mathrm{j}(b - d)$
Multiplication (rectangular form)	$z_1 z_2 = (a + \mathrm{j}\, b)(c + \mathrm{j}\, d) = (ac - bd) + \mathrm{j}(bc + ad)$
Multiplication (polar form)	$z_1 z_2 = r_1 e^{\mathrm{j}\,\varphi_1} r_2 e^{\mathrm{j}\,\varphi_2} = (r_1 r_2) e^{\mathrm{j}(\varphi_1 + \varphi_2)}$
Division (rectangular form)	$\dfrac{z_1}{z_2} = \dfrac{a + \mathrm{j}\, b}{c + \mathrm{j}\, d} = \dfrac{(a + \mathrm{j}\, b)(c - \mathrm{j}\, d)}{c^2 + d^2}$
Division (polar form)	$\dfrac{z_1}{z_2} = \dfrac{r_1 e^{\mathrm{j}\,\varphi_1}}{r_2 e^{\mathrm{j}\,\varphi_2}} = \dfrac{r_1}{r_2} e^{\mathrm{j}(\varphi_1 - \varphi_2)}$
Absolute value	$\lvert z_1 \rvert = \lvert a + \mathrm{j}\, b \rvert = \sqrt{a^2 + b^2}$
Complex conjugate	$z_1^* = (a + \mathrm{j}\, b)^* = a - \mathrm{j}\, b = r e^{-\mathrm{j}\,\varphi}$

where r is the absolute value or magnitude of z, that is, $r = |z|$ and φ is the angle or phase of z, that is, $\varphi = \angle z$.

To convert a complex number from rectangular form to polar form, the conversion formulas

$$r = |z| = \sqrt{a^2 + b^2} \quad \text{and} \quad \varphi = \arctan 2\,(b, a)$$

are used. Here, $\arctan 2(b, a)$ is the quadrant-aware arc tangent function. The conversion from polar form to rectangular form is given by

$$a = r\cos(\phi) \quad \text{and} \quad b = r\sin(\phi).$$

The complex conjugate of a complex number $z = a + \mathrm{j}\, b = r e^{\mathrm{j}\,\varphi}$ is denoted by

$$z^* \triangleq a - \mathrm{j}\, b = r e^{-\mathrm{j}\,\varphi}.$$

Finally, some basic operations for complex numbers are given in Table A.2.

A.3 Euler's Identity

Euler's identity states that

$$e^{\mathrm{j}\,\varphi} = \cos(\varphi) + \mathrm{j}\sin(\varphi).$$

From this it follows that the cosine and sine can be written in terms of a pair of complex exponentials given by

$$\cos(\varphi) = \frac{e^{\mathrm{j}\,\varphi} + e^{-\mathrm{j}\,\varphi}}{2}$$

and

$$\sin(\varphi) = \frac{e^{\mathrm{j}\,\varphi} - e^{-\mathrm{j}\,\varphi}}{2\,\mathrm{j}},$$

respectively.

A.4 Integration by Parts

The integral of a product of two functions can be rewritten as

$$\int u(x)\frac{\mathrm{d}v(x)}{\mathrm{d}x}\,\mathrm{d}x = u(x)v(x) - \int v(x)\frac{\mathrm{d}u(x)}{\mathrm{d}x}\,\mathrm{d}x.$$

A.5 Series

An (infinite) series is the sum of terms of an (infinite) sequence:

$$\sum_{n=0}^{\infty} r_n = r_0 + r_1 + r_2 + \ldots.$$

A *necessary* condition for the series to converge, that is, for

$$\sum_{n=0}^{\infty} r_n < \infty$$

is

$$\lim_{n\to\infty} r_n = 0.$$

However, this is *not* sufficient for convergence. For example, the series with $r_n = \frac{1}{n}$ for $n > 0$ diverges,

$$\sum_{n=1}^{\infty} \frac{1}{n} = \infty,$$

while the series with $r_n = \frac{1}{n^2}$ for $n > 0$ converges,

$$\sum_{n=1}^{\infty} \frac{1}{n^2} < 2.$$

An infinite geometric series has coefficients of the form $r_n = rq^n$ such that

$$\sum_{n=0}^{\infty} rq^n.$$

A finite geometric series, also called a geometric progression, is given by

$$\sum_{n=0}^{M-1} rq^n = r\frac{q^M - 1}{q - 1}$$

for $q \neq 1$. If $|q| < 1$, it can be shown that the infinite series converges as

$$\sum_{n=0}^{\infty} rq^n = r\frac{1}{1 - q},$$

while it diverges if $|q| \geq 1$.

A.6 Logarithm and Decibel

The logarithm of a number is the exponent to which another fixed value, the base, must be raised to produce that number. In signal processing, usually the logarithm with base 10 is used and is often denoted $\log_{10}$, log, lg while the logarithm with base e is denoted as ln. Thus, for the logarithm with base 10 it holds that

$$\log(x) = y \quad \Leftrightarrow \quad 10^y = x.$$

An advantage of using logarithm is that the logarithm of a product is simply the sum of the logarithms of the individual factors, that is,

$$\log(xy) = \log(x) + \log(y)$$

and a division turns into a difference,

$$\log\left(\frac{x}{y}\right) = \log(x) - \log(y).$$

Furthermore, exponents become factors in front of the logarithm such that

$$\log\left(x^y\right) = y\log(x).$$

Due to the advantages of using the logarithm, the logarithmic scale *decibel* (dB) is widely used in signal processing. It is defined as 20 times the logarithm with base 10 such that

$$x_{\text{dB}} = 20\log(x) \quad \Leftrightarrow \quad x = 10^{\frac{x_{\text{dB}}}{20}}.$$

A.7 Partial Fraction Expansion

Partial fraction expansion is a way of decomposing a rational fraction

$$H(s) = \frac{b_0 + b_1 s + \cdots + b_M s^M}{1 + a_1 s + \cdots + a_N s^N} \tag{A.1}$$

into a sum of rational fractions of first and second order polynomials

$$H(s) = \frac{c_1}{s - p_1} + \frac{c_2}{s - p_2} + \cdots + \frac{d_1 s + e_1}{s^2 + q_1 s + r_1} + \frac{d_2 s + e_2}{s^2 + q_2 s + r_2} + \ldots. \tag{A.2}$$

This is done by first calculating the roots of the denominator of (A.1) (poles) and gathering the complex conjugate pairs to obtain a product of first and second order terms in the denominator such that

$$H(s) = \frac{b_0 + b_1 s + \cdots + b_M s^M}{(s - p_1)(s - p_2)\ldots(s^2 + q_1 s + r_1)(s^2 + q_2 s + r_2)\ldots}. \tag{A.3}$$

Next, (A.2) is extended

$$H(s) = \frac{c_1(s - p_2)\cdots + c_2(s - p_1)\cdots + (d_1 s + e_1)(s - p_1)\cdots + (d_2 s + e_2)(s - p_1)\ldots}{(s - p_1)(s - p_2)\ldots(s^2 + q_1 s + r_1)(s^2 + q_2 s + r_2)\ldots}$$

and the resulting numerator polynomial is matched with the numerator polynomial in (A.1).

Example A.1: Partial fraction expansion

Consider the transfer function

$$H(s) = \frac{s+3}{s^2+3s+2}.$$

It can be seen that the denominator can be factorized as

$$s^2 + 3s + 2 = (s+1)(s+2),$$

that is, the system has poles in $p_1 = -1$ and $p_2 = -2$. This yields

$$\begin{aligned} H(s) &= \frac{s+3}{(s+1)(s+2)} \\ &= \frac{c_1}{s+1} + \frac{c_2}{s+2}. \end{aligned}$$

To determine the constants c_1 and c_2, the second line above is expanded, which yields

$$H(s) = \frac{c_1(s+2) + c_2(s+1)}{(s+1)(s+2)}.$$

The final step is to match the numerator polynomials such that

$$\begin{aligned} c_1(s+2) + c_2(s+1) &= s+3 \\ c_1 s + 2c_1 + c_2 s + c_2 &= s+3 \\ s(c_1+c_2) + 2c_1 + c_2 &= s+3. \end{aligned}$$

Comparing the coefficients of the polynomials on the left and right hand side yields that

$$\begin{aligned} c_1 + c_2 &= 1 \\ 2c_1 + c_2 &= 3 \end{aligned}$$

From the first equality, it follows that

$$c_2 = -c_1.$$

Substitutiong that into the second equality yields

$$\begin{aligned} 2c_1 - c_1 &= 3 \\ c_1 &= 3 \end{aligned}$$

and thus,

$$c_2 = -3.$$

Thus, the partial fraction expansion of $H(s)$ is

$$H(s) = \frac{3}{s+1} - \frac{3}{s+2}.$$

Bibliography

Knorn, S. (2019). Signals and systems. Lecture Notes.

Mandal, M. and Asif, A. (2007). *Continuous and discrete time signals and systems*. Cambridge University Press, Cambridge, UK.

McClellan, J. H., Schafer, R. W., and Yoder, M. A. (2003). *Signal Processing First*. Pearson.

von Grünigen, D. C. (2002). *Digitale Signalverarbeitung*. Fachbuchverlag Leipzig, 2 edition.